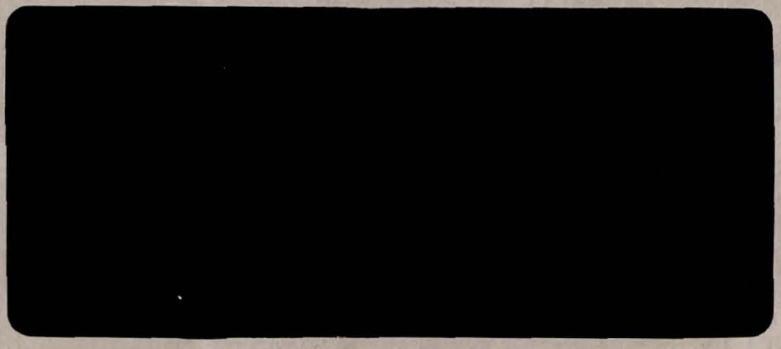

JET PROPULSION LABORATORY
CALIFORNIA INSTITUTE OF TECHNOLOGY
PASADENA, CALIFORNIA

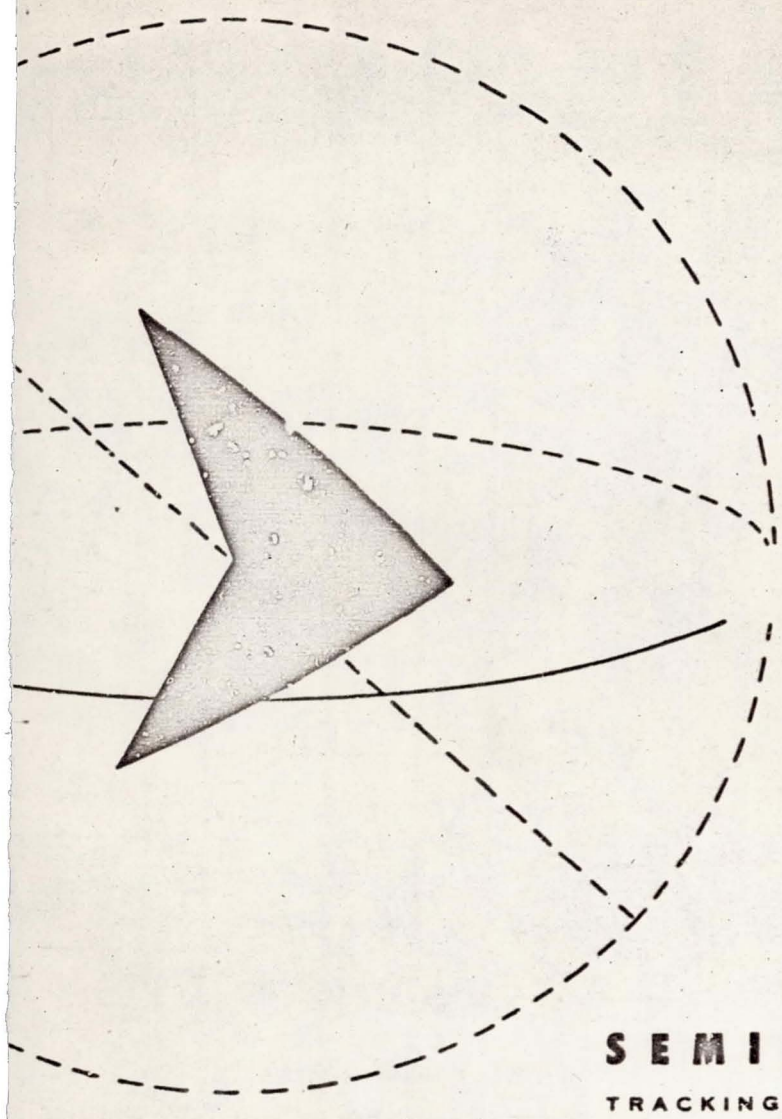

SEMINAR PROCEEDINGS

TRACKING PROGRAMS AND ORBIT DETERMINATION

FEBRUARY 23—26, 1960

JET PROPULSION LABORATORY
CALIFORNIA INSTITUTE OF TECHNOLOGY

National Aeronautics and Space Administration
Contract No. NASw-6

SEMINAR PROCEEDINGS

TRACKING PROGRAMS AND ORBIT DETERMINATION

February 23–26, 1960

JET PROPULSION LABORATORY
California Institute of Technology
Pasadena, California

FOREWORD

In February 1960, the Jet Propulsion Laboratory of the California Institute of Technology sponsored a Seminar on "Tracking Programs and Orbit Determination," the purposes of which were to pool information, to stimulate discussion, and to unify notation related to these rapidly evolving areas. Attendance at the seminar (see Addendum A) was limited to individuals representing organizations actively working in the tracking field, and seminar subject material was precisely defined in advance. It was hoped thus to foster pertinent discussion, to avoid excursions into other technical areas (such as trajectory computation), and to obviate the presentation of background material.

The seminar program was divided into two main parts: deep-space-probe tracking and satellite tracking. This division was natural since the organizations involved have, for the most part, specialized in one of these two areas and since tracking and orbit determination procedures vary considerably between the two. For example, in satellite tracking it is often convenient to use computing methods based on the perturbation schemes of classical celestial mechanics, with data comprising small samples from many passes over the observation station. In contrast, deep-space tracking can effectively use less sophisticated integration methods, with data comprising large samples (except for the initial phase) taken during passes that last many hours.

These Proceedings comprise all but a few of the papers presented at the seminar. (Titles and authors of papers not available for publication are given in Addendum B.) Because of printing schedule requirements, many authors did not have an opportunity to review their material following seminar presentation and prior to publication herein. However, the intention of the co-chairmen has been to maintain the various papers in their original form and to minimize changes and modifications. It is hoped that technical errors or inaccuracies have not crept in during the publication process.

In addition to the papers presented, two business items of general interest were brought before the meeting: (1) the standardization of ephemeris tapes (of the Moon and planets) for use in computer programs, and (2) the standardization of coordinate systems for use in tracking. Proposals made concerning item (1) have been acted upon, and results are presented in Addendum C. Material relating to item (2) is presently being integrated.

Much of the credit for the success of the seminar belongs to the session chairmen: J. W. Siry (NASA), S. D. Conte (STL), S. Herrick (Aeronutronic), C. A. Lundquist (ABMA), J. V. Breakwell (Lockheed), and M. Eimer (JPL).

J. Lorell
F. Yagi
Co-chairmen

CONTENTS

Blank VII

CONTENTS (Cont'd)

Methods for Nonlinear Least Squares Problems and Convergence Proofs[1]

DAVID D. MORRISON

Space Technology Laboratories, Inc., Los Angeles, Calif.

ABSTRACT

The STL tracking programs are designed to compute by least squares the most probable trajectory of a missile, from observed radar or optical data. These data can be any combination of range, azimuth, elevation, range rate, hour angle and declination, or direction cosines, with respect to a given location.

A differential correction method is used, starting from an initial estimate, and the iteration continues until the residuals (observed minus computed values, weighted according to the relative accuracies of the types of data) are either all within specified limits, or until there is no further improvement. Errors above a certain absolute value are automatically eliminated.

One program has been prepared primarily for lunar and interplanetary flights. In this, Cowell's method of trajectory computation is used. The partial derivatives used in the least squares solution are found by solving the related variational equations. Here the trajectory elements, to which the corrections are applied, are the components of position and velocity of the missile at a particular point in the trajectory (expressed in spherical coordinates).

For Earth satellite tracking, the elliptical elements of the osculating ellipse are used to specify the trajectory. Herrick's "variation of elements" method is used to compute the trajectory, and the partial derivatives are computed analytically.

For these two programs a special least squares subroutine has been prepared in which convergence can be assured by limiting the amount any variable can change in one iteration. The standard deviation of each variable is printed out. After a trajectory has been fitted to a certain set of data, additional data can be added without the necessity of reprocessing the original set, a feature which is especially valuable in regard to computing time.

[1]This paper presents one phase of the work involved in the STL tracking programs. Other STL papers presented at the seminar are not available for publication.

I. INTRODUCTION

The present report is a study of techniques for solving nonlinear least squares problems of the sort which arise in orbit determination. Since the results are not limited to the orbit determination problem, they are discussed in a general framework.

The first section gives a general description of some methods which have been used or suggested. The last method described in the section is believed to be new and has been used with good results for a number of orbit determination problems. The second section is more rigorous; it contains theorems which provide sufficient conditions so that each iteration of a method produces an improvement, i.e., decreases the sum of squares. The final section deals with a connection between the orbit determination problem and the two point boundary value problem of differential equations. This connection suggests some interesting new techniques for solving the orbit determination problem. The techniques have not yet been investigated.

II. METHODS

Consider the problem of minimizing

$$F(\mathbf{a}) = \| \mathbf{f}(\mathbf{a}) \|^2$$

where $\mathbf{f}(\mathbf{a})$ is a nonlinear vector function of the vector $\mathbf{a}$. Let $\mathbf{a}_0$ be an approximate solution.

For the methods under consideration, the first step is to replace $F(\mathbf{a})$ by a quadratic form which approximates $F(\mathbf{a})$ in the neighborhood of $\mathbf{a}_0$. To this end, we expand $\mathbf{f}(\mathbf{a})$ in a Taylor series and ignore terms which are higher than second order:

$$\mathbf{f}(\mathbf{a}) \cong \mathbf{f}(\mathbf{a}_0) + A\mathbf{x} + \tfrac{1}{2}\mathbf{E}$$

Here $\mathbf{x} = \mathbf{a} - \mathbf{a}_0$, A is the matrix

$$A = \left(\frac{\partial f_i(\mathbf{a}_0)}{\partial a_j} \right)$$

and $\mathbf{E}$ is a vector with components

$$E_i = (B_i \mathbf{x}, \mathbf{x})$$

where B_i is the matrix

$$B_i = \left(\frac{\partial^2 f_i(\mathbf{a}_0)}{\partial a_k a_j} \right)$$

We now compute the approximation to $F(\mathbf{a})$:

$$F(\mathbf{a}) \cong \| \mathbf{f}_0 + A\mathbf{x} + \tfrac{1}{2}\mathbf{E} \|^2$$
$$\cong (A^* A\mathbf{x}, \mathbf{x}) + (\mathbf{f}_0, \mathbf{E}) + 2(A^* \mathbf{f}_0, \mathbf{x}) + \| \mathbf{f}_0 \|^2$$

again ignoring terms higher than second order. Letting

$$B = \sum f_i(\mathbf{a}_0) B_i$$

we have

$$F(\mathbf{a}) \cong [(A^* A + B)\mathbf{x}, \mathbf{x}] + 2(A^* \mathbf{f}_0, \mathbf{x}) + \|\mathbf{f}_0\|^2$$

Now it is customary to ignore the matrix B. The reason is that if the second derivatives of the components of $\mathbf{f}$ are small, or if the components of $\mathbf{f}(\mathbf{a}_0)$ are small (which usually means that $\mathbf{a}_0$ is a good approximation) then B will be small. Since it is also hard to compute, it is usually omitted.

In any case, if $\mathbf{a}_0 + \mathbf{x}$ is "near" $\mathbf{a}_0$, then F is approximated by a quadratic form

$$F_1(\mathbf{a}_0 + \mathbf{x}) = F_2(\mathbf{x}) = (C\mathbf{x}, \mathbf{x}) + 2(\mathbf{d}, \mathbf{x}) + F_0$$

where

$$C = A^* A + B \text{ (or } C = A^* A), \mathbf{d} = A^* \mathbf{f}_0, F_0 = F(\mathbf{a}_0) = \| \mathbf{f}_0 \|^2$$

Next we wish to choose $\mathbf{x}$ so that $\mathbf{a}_0 + \mathbf{x}$ is a better approximation to the minimum of F; the criterion for a "better" approximation is that $F(\mathbf{a}_0 + \mathbf{x}) \leqslant F(\mathbf{a}_0)$.

One possibility is to choose $\mathbf{x}$ so as to minimize the approximate quadratic form $F_1(\mathbf{a}_0 + \mathbf{x})$. It is easy to show that the minimum of $F_1(\mathbf{a}_0 + \mathbf{x})$ is attained when $\mathbf{x}$ satisfies the system of equations

$$C\mathbf{x} = -\mathbf{d} \tag{1}$$

and so, if C is nonsingular, $\mathbf{x}$ can be found by solving a system of linear equations.

Now this method, when it works, usually works very well. It does, however, "blow up" in some problems. The basic trouble is that the solution $\mathbf{x}$ to (1) may be very large. This makes $F_1(\mathbf{a}_0 + \mathbf{x})$ a poor approximation to $F(\mathbf{a}_0 + \mathbf{x})$, and while $F_1(\mathbf{a}_0 + \mathbf{x})$ may be small, $F(\mathbf{a}_0 + \mathbf{x})$ can be very large.

A heuristic description of sufficient conditions for the method to work is the following. If the problem is well represented by a quadratic form over a large range, then a fairly large value of $\mathbf{x}$ can be tolerated. On the other hand, if $\mathbf{a}_0$ is a good approximation to the minimum ($\mathbf{d} = \frac{1}{2}\nabla F$ is small) and C is "well conditioned," then $\mathbf{x}$ will tend to be small. A small $\mathbf{x}$ means that $F_1(\mathbf{a}_0 + \mathbf{x})$ is a good approximation to $F(\mathbf{a}_0 + \mathbf{x})$. Since $F_1(\mathbf{a}_0 + \mathbf{x}) < F(\mathbf{a}_0)$ it is reasonable to hope that $F(\mathbf{a}_0 + \mathbf{x}) < F(\mathbf{a}_0)$. The three requirements that the method should work are then that (a) F is nearly quadratic, (b) C is well conditioned, and (c) $\mathbf{a}_0$ is a good approximation to the solution.

If, however, the above conditions are not met, the new approximation $\mathbf{a}_0 + \mathbf{x}$ might be worse than $\mathbf{x}$. This suggests that we modify the method by taking the value of $\mathbf{x}$ which minimizes $F_1(\mathbf{a}_0 + \mathbf{x})$ under the constraint that $\mathbf{a}_0 + \mathbf{x}$ lies in a given neighborhood of $\mathbf{a}_0$. The neighborhood is chosen so that F_1 is a good approximation to F in the neighborhood.

Now, depending on the size and shape of the neighborhood chosen, we get a number of methods. For example, it is reasonable to require that $\mathbf{x}$ lie inside of a given ellipse; i.e., that

$$\left(\frac{x_1}{k_1}\right)^2 + \cdots + \left(\frac{x_n}{k_n}\right)^2 \leqslant k^2$$

Now it is possible to rescale the problem so that this ellipse is the unit circle. [Let $x_j' = k(x_j/k_j)$.] We assume that this has been done, so that the problem is to minimize $F_2(\mathbf{x})$ under the constraint that $\|\mathbf{x}\|^2 \leqslant 1$.

Before describing a means of solving this problem, we need two theorems.

Theorem 1. Let $\lambda \geqslant 0$ be arbitrary, and let $\mathbf{x}_0$ satisfy the equation

$$(C + \lambda I)\mathbf{x}_0 = -\mathbf{d} \tag{2}$$

Then $\mathbf{x}_0$ minimizes $F_2(\mathbf{x})$ on the circle $\|\mathbf{x}\|^2 = \|\mathbf{x}_0\|^2$; i.e., if $\|\mathbf{x}\|^2 = \|\mathbf{x}_0\|^2$ then $F_2(\mathbf{x}) \geqslant F_2(\mathbf{x}_0)$.

Proof. Let $\|\mathbf{x}\|^2 = \|\mathbf{x}_0\|^2$, and let $\boldsymbol{\eta} = \mathbf{x} - \mathbf{x}_0$. Then $\|\mathbf{x}_0 + \boldsymbol{\eta}\|^2 = \|\mathbf{x}_0\|^2$, whence $2(\mathbf{x}_0, \boldsymbol{\eta}) = -\|\boldsymbol{\eta}\|^2$. Also,

$$\begin{aligned} F_2(\mathbf{x}) &= F_2(\mathbf{x}_0 + \boldsymbol{\eta}) \\ &= (C\mathbf{x}_0, \mathbf{x}_0) + 2(\mathbf{d}, \mathbf{x}_0) + F_0 \\ &\quad + 2(C\mathbf{x}_0, \boldsymbol{\eta}) + 2(\mathbf{d}, \boldsymbol{\eta}) + (C\boldsymbol{\eta}, \boldsymbol{\eta}) \\ &= F_2(\mathbf{x}_0) - 2\lambda(\mathbf{x}_0, \boldsymbol{\eta}) + (C\boldsymbol{\eta}, \boldsymbol{\eta}) \\ &= F_2(\mathbf{x}_0) + \lambda\|\boldsymbol{\eta}\|^2 + (C\boldsymbol{\eta}, \boldsymbol{\eta}) \\ &\geqslant F_2(\mathbf{x}_0). \end{aligned}$$

This completes the proof.

We define $\mathbf{x}(\lambda)$ to be the solution of (2) for any value of λ. Then we have the following:

Theorem 2. (a) $\|\mathbf{x}(\lambda)\|^2$ is a continuous decreasing function of λ. As $\lambda \to \infty$, $\|\mathbf{x}(\lambda)\|^2 \to 0$.

(b) $F_2[\mathbf{x}(\lambda)]$ is an increasing function of λ.

Proof. We may assume that C is a diagonal matrix with diagonal elements $C_i > 0$. This involves no loss of generality since it is always possible to transform the problem via an orthogonal (i.e., norm preserving) transformation so that C is diagonal. The exact details of the transformation will be given later. Then the solution to (2) is given by

$$x_i(\lambda) = \frac{-d_i}{(C_i + \lambda)}$$

whence

$$\|\mathbf{x}(\lambda)\|^2 = \sum \frac{d_i^2}{(C_i + \lambda)^2}$$

which is clearly a decreasing function of λ (for $\lambda \geqslant 0$). It is also clear that $\|\mathbf{x}(\lambda)\|^2$ is continuous and that $\|\mathbf{x}(\lambda)\|^2 \to 0$ as $\lambda \to \infty$. Also,

$$\begin{aligned} F_2[\mathbf{x}(\lambda)] &= \sum C_i x_i^2 + 2\sum d_i x_i + F_0 \\ &= \sum d_i^2 \left[\frac{C_i}{(\lambda + C_i)^2} - \frac{2}{\lambda + C_i}\right] + F_0 \end{aligned}$$

It is decidedly verified by differentiation that the terms inside the bracket are a monotone increasing function of λ (for $\lambda \geqslant 0$), whence F_2 is an increasing function of λ, and the proof is complete.

Now we return to the problem of minimizing F_2 with the side condition $\|\mathbf{x}\|^2 \leqslant 1$. To solve this, we first find $\mathbf{x}(0)$. If $\|\mathbf{x}(0)\|^2 \leqslant 1$, we are done, for $\mathbf{x}(0)$ gives the

absolute minimum of F_2 and hence the solution to the constrained minimum problem.

Suppose that $\|\mathbf{x}(0)\|^2 > 1$. We then find a value λ_0 for which $\|\mathbf{x}(\lambda_0)\|^2 = 1$. The exact technique used to find λ_0 need not concern us here. The main point is that it can be done because $\|\mathbf{x}(\lambda)\|^2$ is a continuous decreasing function which is greater than one at $\lambda = 0$ and tends to zero as λ tends to infinity. To prove that $\|\mathbf{x}(\lambda_0)\|^2$ is the solution to the problem, let $\|\mathbf{x}\|^2 \leqslant 1$. We must show that $F_2(\mathbf{x}) \geqslant F_2[\mathbf{x}(\lambda_0)]$. By Theorem 2a, since $\|\mathbf{x}\|^2 \leqslant \|\mathbf{x}(\lambda_0)\|^2$, it is possible to find a value $\lambda_1 \geqslant \lambda_0$ such that $\|\mathbf{x}(\lambda_1)\|^2 = \|\mathbf{x}\|^2$. By Theorem 2b, we have $F_2[\mathbf{x}(\lambda_0)] \leqslant F_2[\mathbf{x}(\lambda_1)]$. By Theorem 1, we have $F_2[\mathbf{x}(\lambda_1)] \leqslant F(\mathbf{x})$. Combining these inequalities we have $F[\mathbf{x}(\lambda_0)] \leqslant F(\mathbf{x})$.

We now summarize the method just described. From previous knowledge of how linear the functions involved are, one prescribes a set of constants k_j so that it is safe to assume that $F_2(\mathbf{x})$ is a good approximation to $F(\mathbf{a}_0 + \mathbf{x})$ provided that

$$\sum \left(\frac{x_j}{k_j}\right)^2 < k^2 \tag{3}$$

We evaluate C and $\mathbf{d}$; this involves the evaluation of first and, possibly, second derivatives of the functions $\mathbf{f}$. These derivative evaluations may be done analytically or by differences, depending on the problem. We next scale the problem by setting $\mathbf{x}' = K^{-1}\mathbf{x}$, where K is a diagonal matrix with diagonal elements k_j/k. Then C and $\mathbf{d}$ are scaled: $C' = K^{-1}CK^{-1}$, $\mathbf{d}' = K^{-1}\mathbf{d}$. Now $F_2(\mathbf{x})$ becomes

$$\begin{aligned} F_2(\mathbf{x}) &= (C\mathbf{x}, \mathbf{x}) + 2(\mathbf{d}, \mathbf{x}) + F_0 \\ &= (C'\mathbf{x}', \mathbf{x}') + 2(\mathbf{d}', \mathbf{x}') + F_0 \end{aligned}$$

and (3) becomes $\|\mathbf{x}'\|^2 \leqslant 1$. Next the system

$$(C' + \lambda I)\mathbf{x}' = \mathbf{d}' \tag{4}$$

is solved for $\lambda = 0$. If the resulting solution $\mathbf{x}'(0)$ satisfies $\|\mathbf{x}'(0)\|^2 \leqslant 1$, we let $\lambda_0 = 0$. Otherwise λ is systematically changed until a value λ_0 is found with the property that the solution $\mathbf{x}'(\lambda_0)$ of (4) satisfies $\|\mathbf{x}'(\lambda_0)\|^2 = 1$. Finally, having found $\mathbf{x}' = \mathbf{x}'(\lambda_0)$, we rescale ($\mathbf{x} = K\mathbf{x}'$) and let $\mathbf{a}_0 + \mathbf{x}$ be the new approximation.

We have used, with good results, the following variant of the method just described. As in the proof of Theorem 2, suppose the problem has been transformed so that C is diagonal. We now replace the constraint $\|\mathbf{x}\|^2 \leqslant 1$ by the constraints $|x_j| \leqslant 1$, $j = 1, \cdots, n$, and seek a solution under the new constraints. (We have simply replaced the requirement that $\mathbf{x}$ lie in a sphere by the requirement that $\mathbf{x}$ lie inside a hypercube. Since the main idea is just to keep the solution small, the shape of the region used is not particularly important.) Using a previous formula for F_2 we have

$$F_2(\mathbf{x}) = \sum (C_i x_i^2 + 2 d_i x_i) + F_0 \tag{5}$$

To minimize F_2 under the new constraints, we may clearly look at each term of the sum individually. We thus seek a minimum of

$$C_i x_i^2 + 2 d_i x_i \; (C_i > 0)$$

under the constraint that $|x_i| \leqslant 1$. The solution is simply

$$x_i = \begin{cases} -\dfrac{d_i}{C_i} & \text{if } \left|\dfrac{d_i}{C_i}\right| \leqslant 1 \\ -\operatorname{sgn} d_i & \text{if } \left|\dfrac{d_i}{C_i}\right| > 1 \end{cases} \tag{6}$$

(In case $C_i = 0$, we should take $x_i = 0$.)

We now summarize this method, keeping track of the transformations involved. We rescale as before, getting $C' = K^{-1}CK^{-1}$, $\mathbf{d}' = K^{-1}\mathbf{d}$. We next find the eigenvalues λ_i and orthonormalized eigenvectors $\mathbf{u}_i$ of the matrix C'. Then

$$C' = U^* C'' U$$

where U is the matrix whose columns are $\mathbf{u}_i$ and C'' is a diagonal matrix with diagonal elements λ_i. We let $\mathbf{x}'' = U\mathbf{x}'$, $\mathbf{d}'' = U^*\mathbf{d}'$. Then, since $U^*U = I$,

$$\begin{aligned} F_2(\mathbf{x}) &= (C'\mathbf{x}', \mathbf{x}') + 2(\mathbf{d}', \mathbf{x}') + F_0 \\ &= (U^*C''U\mathbf{x}', \mathbf{x}') + 2(\mathbf{d}', U^*\mathbf{x}'') + F_0 \\ &= (C''\mathbf{x}'', \mathbf{x}'') + 2(\mathbf{d}'', \mathbf{x}'') + F_0 \end{aligned}$$

Since the matrix C'' is now diagonal, we may minimize F_2 under the constraint $|x_j''| \leqslant 1$. The result is (6) with x_i'', C_i'' and d_i'' replacing x_i, C_i and d_i. We then get $\mathbf{x}'$ by computing $\mathbf{x}' = U^*\mathbf{x}''$ and get $\mathbf{x}$ by computing $\mathbf{x} = K\mathbf{x}'$. Then $\mathbf{a}_0 + \mathbf{x}$ is the new approximation.

III. MONOTONICITY THEOREMS

A proposed method for solving iteratively the problem of minimizing $F(\mathbf{a})$ should have the property that, if $\mathbf{a}_0$ is the current value of the parameter and $\mathbf{x}$ is the correction added at this iteration, then $F(\mathbf{a}_0 + \mathbf{x}) < F(\mathbf{a}_0)$. If the method has this property, the iterative method will produce a sequence of approximations $\mathbf{a}_1, \mathbf{a}_2, \cdots$, such that $F(\mathbf{a}_1) > F(\mathbf{a}_2) > \cdots$. We call such a method "monotone." We will investigate in this section the conditions that a method be monotone.

A. General Theorem

We shall give in this section a proof of a theorem from which we may derive monotonicity theorems for particular methods. According to the mean value theorem we may write

$$\mathbf{f}(\mathbf{a} + \mathbf{x}) = \mathbf{f}(\mathbf{a}) + A\mathbf{x} + \tfrac{1}{2}\mathbf{E}$$

where $\mathbf{E}$ is a vector with components

$$E_k = \sum_{i,j} \frac{\partial^2 f_k(\xi_{ij}^{(k)})}{\partial a_i \partial a_j} x_i x_j$$

Here the points $\xi_{ij}^{(k)}$ lie in a region determined by the points $\mathbf{a}$ and $\mathbf{x}$. The exact shape of this region does not concern us. For brevity we let

$$b_{ij} = \frac{\partial^2 f_k(\xi_{ij}^{(k)})}{\partial a_i \partial a_j}$$

Then, using the Schwarz inequality,

$$\begin{aligned} E_k^2 &= \{\sum_i x_i \sum_j b_{ij} x_j\}^2 \\ &\leqslant \sum_i x_i^2 \{\sum_j b_{ij} x_j\}^2 \\ &\leqslant \sum_i x_i^2 \{\sum_j b_{ij}^2\} \{\sum_j x_j^2\} \\ &= \|\mathbf{x}\|^2 \sum_i x_i^2 \{\sum_j b_{ij}^2\} \\ &\leqslant \|\mathbf{x}\|^4 \max_i \sum_j b_{ij}^2 \\ &\leqslant \|\mathbf{x}\|^4 \max_i \sum_j \max_{\mathbf{a}} \left(\frac{\partial^2 f_K(\mathbf{a})}{\partial a_i \partial a_j}\right)^2 \end{aligned}$$

Now letting

$$M^2 = \sum_K \max_i \sum_j \max_{\mathbf{a}} \left(\frac{\partial^2 f_K(\mathbf{a})}{\partial a_i \partial a_j}\right)^2$$

we have

$$\|\mathbf{E}\|^2 = \sum E_k^2 \leqslant \|\mathbf{x}\|^4 M^2$$

or

$$\|\mathbf{E}\| \leqslant \|\mathbf{x}\|^2 M$$

It is convenient to introduce $\boldsymbol{\varepsilon} = \frac{1}{2}\mathbf{E}/\|\mathbf{x}\|^2$. Then

$$\|\boldsymbol{\varepsilon}\| \leqslant \tfrac{1}{2}M$$

Now the linear approximation to $\mathbf{f}(\mathbf{a})$ is denoted by $\tilde{\mathbf{f}}(\mathbf{a})$:

$$\tilde{\mathbf{f}}(\mathbf{a}) = \mathbf{f}(\mathbf{a}_0) + A(\mathbf{a} - \mathbf{a}_0)$$

and the corresponding approximation to $F(\mathbf{a})$ is denoted by $\tilde{F}(\mathbf{a})$:

$$\tilde{F}(\mathbf{a}) = \|\tilde{\mathbf{f}}(\mathbf{a})\|^2$$

Note that $F(\mathbf{a}_0) = \tilde{F}(\mathbf{a}_0)$.
The solution $\mathbf{a}_0 + \mathbf{x}$ is better than $\mathbf{x}$ if $F(\mathbf{a}_0 + \mathbf{x}) < F(\mathbf{a}_0)$.

Theorem. The method is monotone if

$$\tilde{F}(\mathbf{a}_0) - \tilde{F}(\mathbf{a}_0 + \mathbf{x}) > \|\mathbf{x}\|^2 M [2\sqrt{F(\mathbf{a}_0)} + \tfrac{1}{4}M\|\mathbf{x}\|^2] \qquad (1)$$

Proof. We compute $F(\mathbf{a}_0 + \mathbf{x})$:

$$\begin{aligned} F(\mathbf{a}_0 + \mathbf{x}) &= \|\tilde{\mathbf{f}}(\mathbf{a}_0 + \mathbf{x}) + \boldsymbol{\varepsilon}\|\mathbf{x}\|^2\|^2 \\ &= F(\mathbf{a}_0) - [\tilde{F}(\mathbf{a}_0) - \tilde{F}(\mathbf{a}_0 + \mathbf{x})] \\ &\quad + \|\mathbf{x}\|^2 \{2[\tilde{\mathbf{f}}(\mathbf{a}_0 + \mathbf{x}), \boldsymbol{\varepsilon}] + \|\boldsymbol{\varepsilon}\|^2 \|\mathbf{x}\|^2\} \end{aligned}$$

Now under the hypothesis of the theorem

$$\tilde{F}(\mathbf{a}_0) > \tilde{F}(\mathbf{a}_0 + \mathbf{x}), \qquad \text{or } \|\tilde{\mathbf{f}}(\mathbf{a}_0 + \mathbf{x})\| < \sqrt{F(\mathbf{a}_0)}$$

Then

$$\begin{aligned} &\|\mathbf{x}\|^2 \{2[\tilde{\mathbf{f}}(\mathbf{a}_0 + \mathbf{x}), \boldsymbol{\varepsilon}] + \|\boldsymbol{\varepsilon}\|^2 \|\mathbf{x}\|^2\} \\ &\leqslant \|\mathbf{x}\|^2 [2\|\tilde{\mathbf{f}}(\mathbf{a}_0 + \mathbf{x})\| \|\boldsymbol{\varepsilon}\| + \|\boldsymbol{\varepsilon}\|^2 \|\mathbf{x}\|^2] \\ &\leqslant \|\mathbf{x}\|^2 M [2\sqrt{F(\mathbf{a}_0)} + \tfrac{1}{4}M^2 \|\mathbf{x}\|^2] \\ &< \tilde{F}(\mathbf{a}_0) - \tilde{F}(\mathbf{a}_0 + \mathbf{x}) \end{aligned}$$

again using the hypothesis.

Then

$$-[\tilde{F}(\mathbf{a}_0) - \tilde{F}(\mathbf{a}_0 + \mathbf{x})] + \|\mathbf{x}\|^2 \{2[\tilde{\mathbf{f}}(\mathbf{a}_0 + \mathbf{x}), \boldsymbol{\varepsilon}] + \|\boldsymbol{\varepsilon}\|^2 \|\mathbf{x}\|^2\} < 0$$

whence

$$F(\mathbf{a}_0 + \mathbf{x}) < F(\mathbf{a}_0)$$

which completes the proof.

B. The Method of Gauss

This method consists of choosing $\mathbf{x}$ so as to minimize the expression

$$\tilde{F}(\mathbf{a}_0 + \mathbf{x}) = \|\mathbf{f}(\mathbf{a}_0) + A\mathbf{x}\|^2$$

This is a linear least squares problem, and the minimum is found by solving the systems of linear equations

$$A'Ax + A'f_0 = 0$$

[We let $f_0 = f(a_0)$.] $A'A$ is assumed to be nonsingular for convenience.

To test the inequality (1), we first compute the left-hand side

$$\begin{aligned}\tilde{F}(a_0) - \tilde{F}(a_0 + x) &= -2(Ax, f_0) - \|Ax\|^2 \qquad (2)\\ &= -2(x, A'f_0) - (x, A'Ax)\\ &= -2(x, A'f_0) + (x, A'f_0)\\ &= -(x, A'f_0)\end{aligned}$$

To evaluate this more exactly, we consider the (positive) eigenvalues λ_j and the corresponding normalized eigenvectors u_j of $A'A$. We assume that $\lambda_1 < \lambda_2 <, \cdots, < \lambda_n$. Both x and $A'f_0$ may be expressed in terms of the eigenvectors u_j:

$$x = \sum_{j=1}^{n} y_j u_j$$

$$A'f_0 = \sum_{j=1}^{n} d_j u_j$$

Then since $A'Ax + A'f_0 = 0$, we have

$$\sum \lambda_j y_j u_j + \sum d_j u_j = 0$$

or

$$y_j = -\frac{d_j}{\lambda_j}$$

Now

$$\begin{aligned}-(x, A'f_0) &= -(\sum y_j u_j, \sum d_j u_j) \qquad (3)\\ &= -\sum y_j d_j\\ &= -\sum \frac{d_j^2}{\lambda_j}\\ &\geqslant \frac{1}{\lambda_n}\sum d_j^2\\ &= \frac{1}{\lambda_n}\|A'f_0\|^2\end{aligned}$$

Next $\|x\|^2$ is bounded by noting that

$$\begin{aligned}\|x\|^2 &= \sum y_j^2 \qquad (4)\\ &= \sum \frac{d_j^2}{\lambda_j^2}\\ &\leqslant \frac{1}{\lambda_1^2}\sum d_j^2\\ &= \frac{1}{\lambda_1^2}\|A'f_0\|^2\end{aligned}$$

Thus we have a lower bound for the right-hand side of (1) and an upper bound for the left-hand side. Using Theorem 1, we thus have the result that this method will result in improvement at each iteration provided

$$\frac{1}{\lambda_n}\|A'f_0\|^2 > \frac{\|A'f_0\|^2 M}{\lambda_1^2}\left(2\sqrt{F_0} + M\frac{\|A'f_0\|^2}{\lambda_1^2}\right)$$

or

$$\frac{\lambda_1^2}{\lambda_n} > M\left(2\sqrt{F_0} + M\frac{\|A'f_0\|^2}{\lambda_1^2}\right)$$

This inequality demonstrates some facts about the method which are well known from experience. If the matrix $A'A$ is sufficiently well conditioned (λ_1^2/λ_n is large), the problem is not too nonlinear (M is small), and the starting guess is good enough (F_0 is small), then the method of Gauss will work.

We assumed that $\|A'f_0\|^2 \neq 0$. If this is not true then $x = 0$. Since $\nabla F(a_0) = 2A'f_0$, this means that the method of Gauss will fail if a_0 is at a maximum or saddle point of F.

C. Modified Gauss Method

This method starts by solving $A'Ax_0 + f_0 = 0$, and then lets $x = \rho x_0$, where ρ is some scalar. If $\rho = 1$, this reduces to the previous method. We assume that $\rho < 2$.

As before, we compute

$$\begin{aligned}\tilde{F}(a_0) - \tilde{F}(a_0 + x) &= -(2\rho - \rho^2)(A'f_0, x_0)\\ &\geqslant +(2\rho - \rho^2)\|A'f_0\|^2/\lambda_n\end{aligned}$$

Also,

$$\begin{aligned}\|x\|^2 &= \rho^2\|x_0\|^2\\ &\leqslant (\rho^2/\lambda_1^2)\|A'f_0\|^2\end{aligned}$$

Hence the requirement for improvement at each iteration is

$$\frac{2\rho - \rho^2}{\lambda_n} > \frac{\rho^2}{\lambda_1^2}M\left(2\sqrt{F_0} + M\frac{\rho^2}{\lambda_1^2}\|A'f_0\|^2\right)$$

or

$$\frac{2}{\lambda_n} > \rho\left(\frac{2M\sqrt{F_0}}{\lambda_1^2} + \frac{1}{\lambda_n}\right) + \frac{\rho^3}{\lambda_1^4}M^2\|A'f_0\|^2$$

By choosing ρ sufficiently small, the right-hand side can be made arbitrarily small and the method will work. We have again assumed only the existence of the bound M, the nonvanishing of $A'f_0$, and the nonsingularity of $A'A$. The last assumption could be easily dropped.

The same sort of analysis can be carried out for other methods, including those described in Section I. The details are omitted here.

IV. CONNECTIONS WITH BOUNDARY VALUE PROBLEMS

The object of this section is to describe a connection between the orbit determination problem and the two-point boundary value problem of ordinary differential equations.

We shall show that if the data are given continuously, the orbit determination problem is a two-point boundary value differential equations problem. If the data are given at discrete times then the orbit determination problem is a two-point boundary value differential-difference equations problem.

We will also show that the Gauss method usually used to solve the orbit determination problem is exactly the same as a favorite method for solving boundary value problems. The method is called an "initial value technique for a boundary value problem" or a "shooting" technique. The basic idea is to vary the solution at one end point until the conditions at the other end are met. Now this is not the only way of solving a two-point boundary value problem—there are other techniques in which one starts with an approximate function which satisfies the boundary conditions and varies this function until it satisfies the differential equation. This suggests that one might try such a technique to solve the orbit determination problem.

Thus the connection between the two problems suggests a class of new methods for the orbit determination problems. These methods may be promising since they involve solving for an entire trajectory at once, rather than solving for the initial conditions; one thereby avoids some of the problems which arise from the fact that, because of numerical difficulties, the initial conditions may not determine the trajectory with sufficient accuracy.

We will not propose in this note any particularly new methods. We will only give the details of the connection between the two problems both for its independent mathematical interest and in the hope that it may furnish a foundation for future developments of new methods.

Consider a space vehicle in free flight with equations of motion given by

$$\dot{\mathbf{x}} = \mathbf{f}(\mathbf{x})$$

Here $\mathbf{x} = \mathbf{x}(t)$ is the vector which gives the position and velocity of the vehicle at time t.

Now suppose that the vehicle is being observed by N radar stations. At any given time t, and for any given vehicle position and velocity $\mathbf{x}$, the noise-free radar observations from the ith station can be computed and are denoted by $R_i(\mathbf{x},t)$, $A_i(\mathbf{x},t)$, $E_i(\mathbf{x},t)$ and $\dot{R}_i(\mathbf{x},t)$. (R, A, E, and $\dot{R}$ stand for range, azimuth, elevation and range rate.) The actual observations reported by the ith station at time t are denoted by $\hat{R}_i(t)$, $\hat{A}_i(t)$, $\hat{E}_i(t)$, and $\hat{\dot{R}}_i(t)$. If there are no radar observations reported from the ith station at time t, we set $\hat{R}_i(t) = \hat{A}_i(t) = \hat{E}_i(t) = \hat{\dot{R}}_i(t) = 0$. Then the vectors $\mathbf{r}(\mathbf{x},t)$ and $\hat{\mathbf{r}}(t)$ are defined by

$$\mathbf{r}(\mathbf{x},t) = \begin{pmatrix} R_1(\mathbf{x},t) \\ A_1(\mathbf{x},t) \\ E_1(\mathbf{x},t) \\ \dot{R}_1(\mathbf{x},t) \\ \cdot \\ \cdot \\ \cdot \\ \dot{R}_N(\mathbf{x},t) \end{pmatrix} \qquad \hat{\mathbf{r}}(t) = \begin{pmatrix} \hat{R}_1(t) \\ \hat{A}_1(t) \\ \hat{E}_1(t) \\ \hat{\dot{R}}_1(t) \\ \cdot \\ \cdot \\ \cdot \\ \hat{\dot{R}}_N(t) \end{pmatrix}$$

A diagonal matrix $W(t)$ is also assumed to be given:

$$W(t) = \begin{pmatrix} W_{R_1}(t) & & & & \mathbf{0} \\ & W_{A_1}(t) & & & \\ & & \cdot & & \\ & & & \cdot & \\ & & & & \cdot \\ \mathbf{0} & & & & W_{\dot{R}_N}(t) \end{pmatrix}$$

Here $W_{R_1}(t)$, for example, is the weight assigned to the radar observation R_1 at time t. If the noise in R_1 has standard deviation $\sigma_{R_1}(t)$ we would set $W_{R_1}(t) = 1/\sigma_{R_1}(t)$. If the data R_1 is given only for a discrete set of points $t_1, \cdots, t_K$, we would set

$$W_{R_1}(t) = \sum_{j=1}^{K} \frac{\delta(t - t_j)}{\sigma_{R_1}(t_j)}$$

where $\delta(t)$ is the Dirac delta function.

The problem is then to minimize the integral

$$I = \int_a^b [\mathbf{r}(\mathbf{x},t) - \hat{\mathbf{r}}(t)]' W(t) [\mathbf{r}(\mathbf{x},t) - \hat{\mathbf{r}}(t)]\, dt \qquad (2)$$

under the constraint that $\mathbf{x} = \mathbf{x}(t)$ satisfies the equations of motion (1). (The integral I is simply the usual weighted sum of squares of the radar errors.) Here $t = a$ and $t = b$ are the times of the first and last radar observations.

A vector $\lambda(t)$ of Lagrange multipliers is now introduced and we then seek a minimum of

$$I_1 = \int_a^b (\mathbf{r} - \hat{\mathbf{r}})' W (\mathbf{r} - \hat{\mathbf{r}})\, dt - 2 \int_a^b \lambda'(t) [\dot{\mathbf{x}} - \mathbf{f}(\mathbf{x})]\, dt \qquad (3)$$

Now let F denote the matrix $(\partial f_i/\partial x_j)$ of partial derivatives of the components of $\mathbf{f}$ with respect to the components of $\mathbf{x}$, and let A denote the matrix $(\partial r_i/\partial x_j)$ with respect to the components of $\mathbf{x}$. Then the first variation of I_1 is

$$\delta I_1 = 2\int_a^b (\mathbf{r}-\hat{\mathbf{r}})' W A \delta \mathbf{x} dt - 2\int_a^b \boldsymbol{\lambda}'(t)\left[\frac{d}{dt}(\delta \mathbf{x}) - F\delta \mathbf{x}\right] dt$$

$$= 2\int_a^b \left[(\mathbf{r}-\hat{\mathbf{r}})' WA + \dot{\boldsymbol{\lambda}}' + \boldsymbol{\lambda}' F\right] \delta \mathbf{x} dt - \left[2\boldsymbol{\lambda}'(t)\,\delta \mathbf{x}\right]_a^b$$

Now δI_1 must vanish for all continuously differentiable variations $\delta \mathbf{x}$ if I_1 is to be extremized. By considering functions $\delta \mathbf{x}$ such that $\delta \mathbf{x}(a) = 1$ and such that $\delta \mathbf{x}$ drops off arbitrarily fast to zero and remains zero for the rest of the interval (a, b) we see that $\boldsymbol{\lambda}(a) = 0$. Similarly, $\boldsymbol{\lambda}(b) = 0$. Also, in the usual way, we have

$$\dot{\boldsymbol{\lambda}}' + \boldsymbol{\lambda}' F + (\mathbf{r}-\hat{\mathbf{r}})' WA = 0$$

This gives rise to the following boundary value problem:

$$\begin{cases} \dot{\boldsymbol{\lambda}} + F\boldsymbol{\lambda} = -A'W(\mathbf{r}-\hat{\mathbf{r}}) \\ \dot{\mathbf{x}} = \mathbf{f}(\mathbf{x}) \\ \boldsymbol{\lambda}(a) = \boldsymbol{\lambda}(b) = 0 \end{cases} \tag{4}$$

This is a system of twelve first-order differential equations with twelve functions (six components each of $\boldsymbol{\lambda}$ and $\mathbf{x}$) and twelve boundary conditions (six on each end). The "forcing functions" $-(AW)'(\mathbf{r}-\hat{\mathbf{r}})$ will contain delta functions if the data are given at discrete times. (Those who object to delta functions could convert the differential equations for $\boldsymbol{\lambda}$ into difference equations if the data are given at discrete times.)

Now define the 6×6 matrix U as the solution of the "variational equation"

$$\dot{U} = FU \qquad U(a) = I$$

and the 6×6 matrix V as the solution of the "adjoint equations"

$$\dot{V} = -VF \qquad V(a) = I$$

Then it is quickly verified that $(VU)^{\cdot} = 0$, whence $V(t) = U^{-1}(t)$. If $\boldsymbol{\alpha} = \mathbf{x}(0)$, then U is the matrix of partial derivatives of the components of $\mathbf{x}(t)$ with respect to the components of $\boldsymbol{\alpha}$. It follows that

$$B = AU \tag{5}$$

is the matrix of partial derivatives of the components of $\mathbf{r}(t)$ with respect to $\boldsymbol{\alpha}$.

We now multiply the first equation of (4) on the left by U':

$$U'\dot{\boldsymbol{\lambda}} + U'F\boldsymbol{\lambda} = -U'A'W(\mathbf{r}-\hat{\mathbf{r}})$$

$$U'\dot{\boldsymbol{\lambda}} + \dot{U}'\boldsymbol{\lambda} = -B'W(\mathbf{r}-\hat{\mathbf{r}})$$

$$\frac{d}{dt}(U'\boldsymbol{\lambda}) = -B'W(\mathbf{r}-\hat{\mathbf{r}})$$

Integrating, and using the fact that $\boldsymbol{\lambda}(a) = 0$.

$$U'(b)\boldsymbol{\lambda}(b) = -\int_a^b B'W(\mathbf{r}-\hat{\mathbf{r}})\,dt \tag{6}$$

We will now show that the same equation results from considering the orbit determination problem from another (more common) approach. In this approach, I is regarded as a function of the six initial conditions $\boldsymbol{\alpha} = \mathbf{x}(a)$. The matrix B is simply the matrix of partial derivatives of the components of $\mathbf{x}$ with respect to the components of $\boldsymbol{\alpha}$. It follows that a small perturbation $\delta\boldsymbol{\alpha}$ in $\boldsymbol{\alpha}$ will result in a perturbation δI in I given by

$$\delta I = 2\int_a^b (\mathbf{r}-\hat{\mathbf{r}})' WB\delta\boldsymbol{\alpha} dt$$

$$= 2\left[\int_a^b (\mathbf{r}-\hat{\mathbf{r}})' WB dt\right]\delta\boldsymbol{\alpha}$$

Since we wish to minimize I, we wish to have $\delta I = 0$ for all $\delta\boldsymbol{\alpha}$; it follows that

$$\int_a^b (\mathbf{r}-\hat{\mathbf{r}})' WB dt = 0$$

But this is just the transpose of Eq. (5).

Thus we have arrived at the same equation by starting with the boundary value problem (4) and by starting with the problem of minimizing I considered as a function of $\boldsymbol{\alpha}$. Now the idea is that it may be better to consider techniques for solving (4) directly rather than by solving (5). By applying various boundary value techniques to the solution of (4), one arrives at a whole class of possible techniques for determining the trajectory.

We will next show that one popular technique for solving the boundary value problem (4) is exactly the same as the usual method for solving the orbit determination problem.

Let $\mathbf{x}_0, \boldsymbol{\lambda}_0$ be an approximate solution to the boundary value problem (4) in the sense that everything is satisfied except $\boldsymbol{\lambda}_0(b) = 0$. Thus we assume that

$$\begin{cases} \dot{\boldsymbol{\lambda}}_0 + F'\boldsymbol{\lambda}_0 = -A'W[\mathbf{r}(\mathbf{x}_0) - \hat{\mathbf{r}}] \\ \dot{\mathbf{x}}_0 = \mathbf{f}(\mathbf{x}_0) \\ \boldsymbol{\lambda}_0(a) = 0 \end{cases} \tag{8}$$

We now wish to perturb the solution $(\mathbf{x}_0, \lambda_0)$ by an amount $(\mathbf{v}, \mu)$ so that the perturbed solution satisfies the differential equations and also the end condition at $t = b$. Ignoring second-order effects, a perturbation $\mathbf{v}$ in $\mathbf{x}_0$ results in a perturbation $A\mathbf{v}$ in $\mathbf{r}(\mathbf{x})$ and $F\mathbf{v}$ in $\mathbf{f}(\mathbf{x})$. Thus

$$\frac{d}{dt}(\lambda_0 + \mu) + F'(\lambda_0 + \mu) = -A'W[\mathbf{r}(\mathbf{x}_0) + A\mathbf{v} - \hat{\mathbf{r}}]$$

$$\frac{d}{dt}(\mathbf{x}_0 + \mathbf{v}) = \mathbf{f}(\mathbf{x}_0) + F\mathbf{v}$$

$$\lambda_0(a) + \mu(a) = 0$$

$$\lambda_0(b) + \mu(b) = 0$$

whence the perturbations satisfy

$$\begin{cases} \dot{\mu} + F'\mu = -A'WA\mathbf{v} \\ \dot{\mathbf{v}} = F\mathbf{v} \\ \mu(a) = 0 \\ \mu(b) = -\lambda_0(b) \end{cases} \tag{9}$$

Now the general solution of $\dot{\mathbf{v}} = F\mathbf{v}$ is $\mathbf{v} = U\mathbf{v}_0$, where $\mathbf{v}_0 = \mathbf{v}(a)$. We will choose $\mathbf{v}_0$ so as to satisfy the other equation. Multiplying the first equation on the right by U' and integrating as before yields

$$\begin{aligned} U'(b)\mu(b) &= -\int_a^b U'(t)A(t)W(t)A(t)\mathbf{v}(t)\,dt \\ &= -\left(\int_a^b U'AWAU\,dt\right)\mathbf{v}_0 \\ &= -\left(\int_a^b B'WB\,dt\right)\mathbf{v}_0 \end{aligned} \tag{10}$$

Multiplying the last equation of (9) by $U'(b)$ and then using (6) and (10) yields

$$U'(b)\mu(b) = U'(b)\lambda_0(b)$$

$$\left[\int_a^b B'WB\,dt\right]\mathbf{v}_0 = -\int_a^b B'W(\mathbf{r} - \hat{\mathbf{r}})\,dt \tag{11}$$

The method now involves solving (11) for $\mathbf{v}_0$. Then the perturbation $\mathbf{v}$ defined by $\mathbf{v} = U\mathbf{v}_0$ and the perturbation μ defined by the equations $\dot{\mu} + F'\mu = -A'WA\mathbf{v}$, $\mu(b) = 0$ will be such that $\mathbf{x}_0 + \mathbf{v}$ and $\lambda_0 + \mu$ will satisfy the boundary value problem (4) (ignoring second-order effects).

We next show that (11) can be derived also from the other approach. We begin with a set of initial conditions $\alpha_0 = \mathbf{x}(t_0)$ and try to perturb α_0 by an amount $\mathbf{v}_0$ so as to satisfy (7). If α_0 is perturbed by $\mathbf{v}_0$, then $\mathbf{r}$ is perturbed by $B\mathbf{v}_0$. We thus wish to satisfy

$$\int_a^b B'W(\mathbf{r} + B\mathbf{v}_0 - \hat{\mathbf{r}})\,dt = 0$$

which gives Eq. (11) again.

The situation may be summarized as follows. The usual method involves considering I as a function of the initial position α. A sufficient condition for the minimization of I is that the "nonlinear normal equations" (6) are satisfied. The usual method for solving this problem is to solve the "linearized normal equations" (11) for a small perturbation $\mathbf{v}_0$ in α. We have seen that equation (6) may be derived also from the boundary value problem (4) and that one method of solving (4) is to solve (6) for a small perturbation $\mathbf{v}_0$ in α. However, one may start with the boundary value problem (4) and consider other methods for solving it; this could give rise to some interesting new technique for solving the problem.

Tracking and Orbit Determination Program of the Jet Propulsion Laboratory

RUSSELL E. CARR AND R. HENRY HUDSON

Jet Propulsion Laboratory, Pasadena, Calif.

ABSTRACT

The lunar-probe tracking program at the Jet Propulsion Laboratory has two prime objectives: (1) provide real-time predictions of the direction of the probe from various observation stations; (2) establish a reliable trajectory corresponding to the actual flight path of the probe. The tracking program, although developed for use with lunar probes, can be used for interplanetary probes if certain modifications are made.

The program, as developed for the IBM 704 digital computer, has two distinct phases. First, the equations of motion and the variational equations are integrated to each observation time where the elements of the equation $Au = b$ are computed. The second phase is concerned with the solution of a specified subset of $Au = b$.

Flexibility and ease of operation have been major objectives in writing the 704 program. The number of data points and tracking stations that may be used is limited only by computing time and core storage. Input formats and operating instructions are presented for utilizing the various computational options available in the program.

I. INTRODUCTION

The lunar-probe tracking program of the Jet Propulsion Laboratory (JPL) has been developed using the maximum likelihood approach for correction of estimated values of the parameters defining the coasting trajectory. The correction of the estimate is obtained by correlating predicted values of certain quantities with the corresponding observed values.

The tracking program has two prime objectives: (1) provide real-time predictions of the direction of the probe from various observation stations in order that the antennas may acquire the signals being transmitted; (2) establish a reliable trajectory corresponding to the actual flight path of the probe.

The tracking program currently available at the IBM 704 digital-computer installation at JPL was developed for use with lunar probes. Although this tracking program can be used for interplanetary probes, certain modifications should be made to account for approximations which, though appropriate for flight paths of short duration, are unsuitable for interplanetary flights.

II. THEORETICAL BASIS FOR THE PROGRAM

The tracking program is assumed to be effective during the coasting portion of the flight. The parameters chosen to define the calculated trajectory are the injection conditions

$$R_0, \phi_0, \theta_0, v_0, \gamma_0, \sigma_0 \tag{1}$$

at time t_0, where

$R \equiv$ distance from center of Earth, meters

$\phi \equiv$ geocentric latitude (positive north)

$\theta \equiv$ longitude from Greenwich (measured east)

$v \equiv$ magnitude of velocity relative to Earth, m/sec

$\gamma \equiv$ elevation angle of velocity relative to Earth (positive up from the local geocentric horizontal)

$\sigma \equiv$ azimuth angle of velocity relative to Earth (measured clockwise from north in local geocentric horizontal as viewed looking toward the center of the Earth)

at Greenwich Mean Time (GMT) t. (The time is actually measured in seconds from some reference time t_{ref}.)

It is assumed that the following quantities can be observed from the ith observation station:

$$r_i^{***}, f_i^{***}, \gamma_i^{***}, \sigma_i^{***}, \delta_i^{***}, \alpha_i^{***} \tag{2}$$

$( )^{***} \equiv$ the effect of station aberrations have been included

$r_i \equiv$ distance from ith station to probe

$f_i \equiv$ doppler signal from probe at ith station

$\gamma_i \equiv$ local elevation angle of probe relative to ith station (geocentric horizontal)

$\sigma_i \equiv$ local azimuth angle of probe relative to ith station (geocentric horizontal)

$\delta_i \equiv$ local declination of probe relative to ith station

$\alpha_i \equiv$ local hour angle of probe relative to ith station

It is convenient to introduce the notation F^{ik} to designate the kth type of observation from the ith observation station:

$$F^{i1} \equiv r_i^{***}$$
$$F^{i2} \equiv f_i^{***}$$
$$F^{i3} \equiv \gamma_i^{***}$$
$$F^{i4} \equiv \sigma_i^{***}$$
$$F^{i5} \equiv \delta_i^{***}$$
$$F^{i6} \equiv \alpha_i^{***}$$

The quantity of the kth type which is actually observed from the ith observation station at time t_j will be denoted by $\hat{F}_j^{ik}$ which will differ from the true value of the observable F_j^{ik} by the observational error e_j^{ik}; therefore,

$$\hat{F}_j^{ik} = F_j^{ik} + e_j^{ik} \tag{3}$$

It is assumed that the observational error consists of two parts,

$$e_j^{ik} = E^{ik} + \varepsilon_j^{ik} \tag{4}$$

where E^{ik} is a constant, referred to as a bias, and ε_j^{ik} is a random error from a normal distribution with mean zero and standard deviation σ_j^{ik}. Thus,

$$\hat{F}_j^{ik} = \tilde{F}_j^{ik} + \varepsilon_j^{ik} \tag{5}$$

where

$$\tilde{F}_j^{ik} \equiv F_j^{ik} + E^{ik} \tag{6}$$

Identity (6) might be written more completely as

$$\tilde{F}_j^{ik}(q_1, q_2, \cdots, q_6, E^{ik}) \equiv F_j^{ik}(q_1, q_2, \cdots, q_6) + E^{ik} \tag{7}$$

where

$$q_1 \equiv R_0$$
$$q_2 \equiv \phi_0$$
$$q_3 \equiv \theta_0$$
$$q_4 \equiv v_0$$
$$q_5 \equiv \gamma_0$$
$$q_6 \equiv \sigma_0$$

From identity (7), it is evident that

$$\frac{\partial F_j^{ik}}{\partial q_l} = \frac{\partial \tilde{F}_j^{ik}}{\partial q_l} \tag{8}$$

for $l = 1, 2, \cdots, 6$.

If $q_l^{(r)}$ $(l = 1, 2, \cdots, 6)$ represents the rth estimate of the injection conditions (1), and if E^{ikr} represents the rth estimate of the bias E^{ik}, then

$$\varepsilon_j^{ik} = (\hat{F}_j^{ik} - \tilde{F}_j^{ikr}) - \sum_{l=1}^{6} \frac{\partial F_j^{ikr}}{\partial q_l} \delta q_l^{(r)} - \delta E^{ikr} - \cdots \tag{9}$$

where

$$\tilde{F}_j^{ikr} \equiv \tilde{F}_j^{ik}[q_1^{(r)}, q_2^{(r)}, \cdots, q_6^{(r)}, E^{ikr}]$$

$$\frac{\partial F_j^{ikr}}{\partial q_l} \equiv \left.\frac{\partial F_j^{ik}}{\partial q_l}\right|_{q_1 = q_1^{(r)}, \cdots, q_6 = q_6^{(r)}}$$

$$\delta q_l^{(r)} \equiv q_l - q_l^{(r)}$$

$$\delta E^{ikr} \equiv E^{ik} - E^{ikr}$$

The assumptions made thus far on ϵ_j^{ik} imply the frequency function

$$\frac{1}{\sqrt{2\pi}\,\sigma_j^{ik}} \exp\left[-\frac{1}{2}\left(\frac{\hat{F}_j^{ik} - \tilde{F}_j^{ik}}{\sigma_j^{ik}}\right)^2\right] \qquad (10)$$

In setting up the likelihood function for the set of random observational errors $\{\epsilon_j^{ik}\}$ associated with a set of observations $\{F_j^{ik}\}$, two additional assumptions have been made:

1. The errors ϵ_j^{ik} are independent with regard to time as well as to observational type and observation station.
2. The standard deviations σ_j^{ik} are not known, but for fixed i and k, the ratio of any two of the σ_j^{ik} is known; therefore

$$\sigma_j^{ik} = \frac{\sigma^{ik}}{w_j^{ik}} \qquad (11)$$

where w_j^{ik} is known, may be written.

With these assumptions, the likelihood function associated with a set of observations $\{\hat{F}_j^{ik}\}$ has the form

$$\prod_{i,k}\left\{\left[\left(\frac{1}{\sqrt{2\pi}}\right)^{N^{ik}}\right]\left(\prod_j \frac{w_j^{ik}}{\sigma^{ik}}\right)\right\}$$

$$\exp\left\{-\frac{1}{2}\sum\left[\sum_j\left(\frac{w_j^{ik}\hat{F}_j^{ik} - w_j^{ik}\tilde{F}_j^{ik}}{\sigma^{ik}}\right)^2\right]\right\} \qquad (12)$$

where the products and the summations on j are understood to take place only on values of j corresponding to times t_j at which observations of the kth type have been made from the ith station. The number N^{ik} is the number of observations of the kth type from the ith observation station.

In addition, it is assumed that there is a frequency function, associated with the injection conditions and with the biases E^{ik}, of the form

$$\prod_{l=1}^{6}\left(\frac{1}{\sqrt{2\pi}\,\sigma_{q_l}}\right)\prod_{i,k}\left(\frac{1}{\sqrt{2\pi}\,\sigma_{E^{ik}}}\right)$$

$$\exp\left[-\frac{1}{2}\sum_{l=1}^{6}\left(\frac{q_l^{(r)} - q_l}{\sigma_{q_l}}\right)^2 - \frac{1}{2}\Sigma\left(\frac{E^{ikr} - E^{ik}}{\sigma_{E^{ik}}}\right)^2\right]\Bigg\} \qquad (13)$$

where σ_{q_l} and $\sigma_{E^{ik}}$ are *a priori* estimates, based on engineering knowledge, of the standard deviations of q_l and E^{ik} from their nominal values.

The resulting likelihood function L is merely the product of functions (12 and (13). The maximization of L with respect to the differences, $\delta q_l^{(r)}$ and δE^{ikr} leads to a set of nonlinear equations in these differences. The numerical solution of the nonlinear system is obtained by linearizing, replacing $q_l - q_l^{(r)}$ and $E^{ik} - E^{ikr}$ by $q_l^{(r+1)} - q_l^{(r)}$ and $E^{ik(r+1)} - E^{ikr}$, respectively, and iterating until the linear system coverages. The inclusion of the function (13) as a factor improves the conditioning of the linear system and, thus, accelerates convergence. The *a priori* estimates of the standard deviations enter in as reciprocal squares; therefore, setting the reciprocal squares to zero in the linear system corresponds to deletion of factor (13).

The tacit assumptions in any application using the procedure of iterating on the linear system to solve the nonlinear system are:

1. The initial estimate of the injection conditions and biases must be sufficiently close to the maximum likelihood estimate of the injection conditions and biases.
2. Sufficient data to determine the solutions must be used.

III. THE SYSTEM OF EQUATIONS

The system of equations resulting from linearization of the maximum likelihood equations may be written in the matrix form

$$Au = b \tag{14}$$

where the column matrix is partitioned

$$u = \begin{pmatrix} u_l \\ u_s \end{pmatrix} \tag{15}$$

$$l = 1, 2, \cdots, 6$$

$$s = 7, 8, 9, \cdots.$$

The sequence on s represents some well ordering of the biases E^{ik}. The elements of u, then, are

$$u_l = q_l^{(r+1)} - q_l^{(r)} \tag{16}$$

$$u_s = E^{ik(r+1)} - E^{ikr}$$

The corresponding elements of the column matrix b are

$$b_l = \sum_{i,k}\left[\frac{1}{(\sigma^{ikr})^2}\sum_j\left(w_j^{ik}\right)^2\frac{\partial F_j^{ikr}}{\partial q_l}(\hat{F}_j^{ik} - \tilde{F}_j^{ikr})\right]$$

$$b_s = \frac{1}{(\sigma^{ikr})^2}\sum_j\left(w_j^{ik}\right)^2\left(\hat{F}_j^{ik} - \tilde{F}_j^{ikr}\right) \tag{17}$$

and the elements of the symmetric matrix A are given by

$$A_{lm} = \sum_{ik}\left\{\frac{1}{(\sigma^{ikr})^2}\sum_j\left[\left(w_j^{ik}\right)^2\frac{\partial F_j^{ikr}}{\partial q_l}\frac{\partial F_j^{ikr}}{\partial q_m}\right]\right\} + \frac{\delta_{lm}}{(\sigma_{q_l})^2}$$

$$A_{lt} = \frac{1}{(\sigma^{ikr})^2}\sum_j\left(w_j^{ik}\right)^2\frac{\partial F_j^{ikr}}{\partial q_l}$$

$$A_{st} = \delta_{st}\left[\frac{1}{(\sigma^{ikr})^2}\sum_j\left(w_j^{ik}\right)^2 + \frac{1}{(\sigma_{E^{ik}})^2}\right] \tag{18}$$

where δ_{pq} is Kronecker's delta, and

$$l, m = 1, 2, \cdots, 6$$

$$s, t = 7, 8, 9, \cdots.$$

The quantity σ^{ikr} is the rth estimate of σ^{ik} and is given by

$$(\sigma^{ikr})^2 = \frac{1}{N^{ik}}\sum_j\left(w_j^{ik}\right)^2\left(\hat{F}_j^{ik} - \tilde{F}_j^{ikr}\right)^2 \tag{19}$$

In addition to σ^{ikr}, it is also desirable to have the quantity σ^{*ikr}, defined by

$$(\sigma^{*ikr})^2 = \frac{1}{N^{ik}}\sum_j\left(w_j^{ik}\right)^2$$

$$\times\left[\left(\hat{F}_j^{ik} - \tilde{F}_j^{ikr}\right) - \left(\sum_l\frac{\partial F_j^{ikr}}{\partial q_l}\Delta^r q_l + \Delta^r E^{ik}\right)\right]^2 \tag{20}$$

where

$$w = \begin{pmatrix} \Delta^r q_l \\ \Delta^r E^{ik} \end{pmatrix} \tag{21}$$

is the solution to the matrix equation

$$Bw = c \tag{22}$$

with the elements of the 7×7 symmetric matrix B given by

$$B_{lm} = \sum_j\left(w_j^{ik}\right)^2\frac{\partial F_j^{ikr}}{\partial q_l}\frac{\partial F_j^{ikr}}{\partial q_m}$$

$$B_{lt} = \sum_j\left(w_j^{ik}\right)^2\frac{\partial F_j^{ikr}}{\partial q_l}$$

$$B_{tt} = \sum_j\left(w_j^{ik}\right)^2 \tag{23}$$

and the elements of c given by

$$c_l = \sum_j\left(w_j^{ik}\right)^2\frac{\partial F_j^{ikr}}{\partial q_l}\left(\hat{F}_j^{ik} - \tilde{F}_j^{ikr}\right)$$

$$c_t = \sum_j\left(w_j^{ik}\right)^2\left(\hat{F}_j^{ik} - \tilde{F}_j^{ikr}\right) \tag{24}$$

The quantity σ^{*ikr} serves as a measure of the noise on the data of the corresponding type.

IV. THE ITERATIVE PROCEDURE

At the beginning of the determination of the $(r+1)$st estimate of the injection conditions $q_l (l = 1, 2, \cdots, 6)$ and the biases E^{ik} it is necessary to have the set of observations $\{\hat{F}_j^{ik}\}$ and the rth estimate of q_l and E^{ik}.

As corrections may not be made to the estimates of all injection conditions or estimates of biases, those which are to be corrected must be specified in order that the elements of column matrices (15) and (21) corresponding to those injection conditions and biases not being corrected may be set equal to zero, and the order of the matrix equations (Eqs. 14 and 22) may be correspondingly reduced. In the remainder of this section, it is assumed that the reduced systems are being used when any reference is made to Eqs. (14) and (22). It should be added that, for simplification of the machine programming, biases are corrected for only one observation station at a time. Thus, the system of Eq. (14) is, at most, of 12th order.

The following steps indicate the iterative procedure, although they do not describe the sequence actually programmed for the computer.

1. Calculate the set of $\tilde{F}_j^{ikr}$.
2. Calculate σ^{ikr} from Eq. (19).
3. Calculate the set of $\partial F_j^{ikr}/\partial q_l$.
4. Form the coefficients of $Au = b$.
5. Solve $Au = b$ for $q_l^{(r+1)} - q_l^{(r)}$ and $E^{ik(r+1)} - E^{ikr}$, where any difference not explicitly solved for is assumed to be zero.
6. Calculate

$$D_p^{(r)} = \sqrt{(\text{cofactor of } A_{pp})/(\text{determinant of } A)} \quad (25)$$

for $p = 1, 2, \cdots$

7. Form the coefficients of $Bw = c$.
8. Solve $Bw = c$ for $\Delta^r q_l$ and $\Delta^r E^{ik}$, where any quantity not explicitly solved for is assumed to be zero.
9. Calculate σ^{*ikr} from Eq. (20).
10. Replace $q_l^{(r)}$ and E^{ikr} with $q_l^{(r+1)}$ and $E^{ik(r+1)}$, respectively, and repeat the procedure.

One of the options available at the end of each iteration is that of predicting the value of one of the observables at some later time t_μ. The prediction is accomplished by calculating

$$\tilde{F}_\mu^{ik(r+1)} \equiv \tilde{F}_\mu^{ik}[(q_1^{(r+1)}, q_2^{(r+1)}, \cdots, q_6^{(r+1)}, E^{ik(r+1)}, t_\mu] \quad (26)$$

as well as the quantity

$$\left\{\left[\frac{\partial F_\mu^{ik(r+1)}}{\partial q_1} D_1^{(r)}\right] + \cdots + \left[\frac{\partial F_\mu^{ik(r+1)}}{\partial q_6} D_6^{(r)}\right]^2\right\}^{\frac{1}{2}} \quad (27)$$

(referred to as the "standard deviation of the prediction") where p indicates the particular member of (25) corresponding to the choice of i and k.

Another of the available options is that of putting the F_j^{ik} observations to the test of a rejection procedure; the observation is rejected if

$$\left|\frac{w^{ik}[\hat{F}_j^{ik} - \tilde{F}_j^{ik(r+1)}]}{\sigma^{ik}}\right| \geq K \quad (28)$$

where the denominator is inserted as an external constant for each data type, and K is a prescribed constant. Additional observations may be added to the original set of $\hat{F}_j^{ik}$ in conjunction with this procedure.

The method of calculating $\tilde{F}_j^{ikr}$ and $\partial F_j^{ikr}/\partial q_l$ is discussed in the following section.

V. CALCULATED VALUES OF THE OBSERVABLES AND PARTIALS

The quantities $\tilde{F}_j^{ikr}$ and the partial derivatives $\partial F_j^{ikr}/\partial q_l$ are obtained numerically as a result of integrating a system of differential equations. This system may be divided into two parts: (1) an independent system which leads to the quantities $\tilde{F}_j^{ikr}$, and (2) a system dependent on the solution of the independent system and leading to the partial derivatives $\partial F_j^{ikr}/\partial q_l$. Both systems are integrated numerically relative to a rectangular coordinate system; transformations from the rth estimate of injection conditions (1) to the injection conditions

$$X_0^{(r)},\ Y_0^{(r)},\ Z_0^{(r)},\ \dot{X}_0^{(r)},\ \dot{Y}_0^{(r)},\ \dot{Z}_0^{(r)} \tag{29}$$

are made by using the following equations at time t_0:

$$\begin{aligned}
x &= R\cos\phi\cos\theta \\
y &= R\cos\phi\sin\theta \\
z &= R\sin\phi \\
\dot{x} &= v\sin\gamma\cos\phi\cos\theta - v\cos\gamma\sin\theta\sin\sigma - v\cos\gamma\sin\phi\cos\theta\cos\sigma \\
\dot{y} &= v\sin\gamma\cos\phi\sin\theta + v\cos\gamma\cos\theta\sin\sigma - v\cos\gamma\sin\phi\sin\theta\cos\sigma \\
\dot{z} &= v\sin\gamma\sin\phi + v\cos\gamma\cos\phi\cos\sigma
\end{aligned} \tag{30}$$

$$\Theta = [\theta + \text{GHA}\ \Omega\ (t)] \bmod 2\pi \tag{31}$$

where GHA Ω (t) is the Greenwich Hour Angle of the first point of Aries (i.e., vernal equinox) at time t,

$$\begin{aligned}
X &= R\cos\phi\cos\Theta \\
Y &= R\cos\phi\sin\Theta \\
Z &= z \\
\dot{X} &= (\dot{x} - \omega y)\cos[\text{GHA}\ \Omega\ (t)] - (\dot{y} + \omega x)\sin[\text{GHA}\ \Omega\ (t)] \\
\dot{Y} &= (\dot{x} - \omega y)\sin[\text{GHA}\ \Omega\ (t)] + (\dot{y} + \omega x)\cos[\text{GHA}\ \Omega\ (t)] \\
\dot{Z} &= z
\end{aligned} \tag{32}$$

where ω is the angular rate of the Earth's rotation.

It is convenient to introduce the notation

$$\begin{aligned}
X_1 &= X \\
X_2 &= Y \\
X_3 &= Z \\
X_4 &= \dot{X} \\
X_5 &= \dot{Y} \\
X_6 &= \dot{Z} \\
X_1^{(0)} &= X_0^{(r)} \\
X_2^{(0)} &= Y_0^{(r)} \\
X_3^{(0)} &= Z_0^{(r)} \\
X_4^{(0)} &= \dot{X}_0^{(r)} \\
X_5^{(0)} &= \dot{Y}_0^{(r)} \\
X_6^{(0)} &= \dot{Z}_0^{(r)}
\end{aligned}$$

The aforementioned independent system of differential equations may then be written

$$\frac{dX_p}{dt} = f_p(X_1, X_2, \cdots, X_6, t) \tag{34}$$

with initial conditions

$$X_p = X_p^{(0)} \text{ at } t = t_0$$

for $p = 1, 2, \cdots, 6$.

The dependent system of differential equations then may be written

$$\frac{d}{dt}\left[\frac{\partial X_p}{\partial X_q^{(0)}}\right] = \sum_{m=1}^{6} \frac{\partial f_p}{\partial X_m}\left[\frac{\partial X_m}{\partial X_q^{(0)}}\right] \tag{35}$$

with initial conditions

$$\left[\frac{\partial X_p}{\partial X_q^{(0)}}\right] = \delta_{pq} \text{ at } t = t_0$$

for $p, q = 1, 2, \cdots, 6$, where δ_{pq} is Kronecker's delta.

It is noted that the unknowns being solved for in Eq. (35) are the partial derivatives $[\partial X_p/\partial X_q^{(0)}]$.

The functions f_p are given explicitly in the prior terminology by

$$\begin{aligned}
f_1 &= \dot{X} \\
f_2 &= \dot{Y} \\
f_3 &= \dot{Z} \\
f_4 &= -\frac{K_E X}{R^3} g_1 - \sum_n K_n\left[\frac{X - X^{(n)}}{r_n^3} + \frac{X^{(n)}}{R_n^3}\right] \\
f_5 &= -\frac{K_E Y}{R^3} g_1 - \sum_n K_n\left[\frac{Y - Y^{(n)}}{r_n^3} + \frac{Y^{(n)}}{R_n^3}\right] \\
f_6 &= -\frac{K_E Z}{R^3} g_2 - \sum_n K_n\left[\frac{Z - Z^{(n)}}{r_n^3} + \frac{Z^{(n)}}{R_n^3}\right]
\end{aligned} \tag{36}$$

where

$$\begin{aligned}
g_1 &= 1 + \frac{Ja^2}{R^2}\left(1 - \frac{5Z^2}{R^2}\right) + \frac{Da^4}{7R^4}\left(\frac{63Z^4}{R^4} - \frac{42Z^2}{R^2} + 3\right) \\
g_2 &= 1 + \frac{Ja^2}{R^2}\left(3 - \frac{5Z^2}{R^2}\right) + \frac{Da^4}{7R^4}\left(\frac{63Z^4}{R^4} - \frac{70Z^2}{R^2} + 15\right)
\end{aligned} \tag{37}$$

where

$$r_n = \{[X - X^{(n)}]^2 + [Y - Y^{(n)}]^2 + [Z - Z^{(n)}]^2\}^{\frac{1}{2}}$$
$$R_n = \{[X^{(n)}]^2 + [Y^{(n)}]^2 + [Z^{(n)}]^2\}^{\frac{1}{2}}$$

a is the Earth's equatorial radius; J and D are the Earth's coupling constants; K_E is the product of the universal gravitational constant and the mass of the Earth, $K_E = GM_E$; K_n is the product of the universal gravitational constant and the mass of the nth body whose potential is being taken into account, $K_n = GM_n$; and $X^{(n)}$, $Y^{(n)}$, $Z^{(n)}$ are the rectangular coordinates of the nth body at time t.

For the system of Eq. (35), it is assumed that the terms associated with J and D may be omitted, and that the explicit formulas used for the partial derivatives of the f_p are obtained by setting $g_1 = g_2 = 1$ in Eq. (36) and performing the respective differentiations with respect to X, Y, Z, $\dot{X}$, $\dot{Y}$, $\dot{Z}$. The following examples are typical of the twelve formulas which do not yield zero:

$$\frac{\partial f_1}{\partial \dot{X}} = 1$$

$$\frac{\partial f_4}{\partial X} = -K_E\left(\frac{1}{R^3} - \frac{3X^2}{R^5}\right) - \sum_n K_n\left\{\frac{1}{r_n^3} - \frac{3[X - X^{(n)}]^2}{r_n^5}\right\}$$

$$\frac{\partial f_4}{\partial Y} = \frac{\partial f_5}{\partial X} = K_E\left(\frac{3XY}{R^5}\right) + \sum_n K_n\left\{\frac{3[X - X^{(n)}][Y - Y^{(n)}]}{r_n^5}\right\}$$

(The remaining eight nonvanishing formulas are permutations of these four.)

The values used for $\partial F_j^{ikr}/\partial q_l$ are obtained from

$$\frac{\partial F_j^{ikr}}{\partial q_l} = \sum_{m,p}^{6} \frac{\partial F_j^{ikr}}{\partial X_p} \frac{\partial X_p}{\partial X_m^{(0)}} \frac{\partial X_m^{(0)}}{\partial q_l} \tag{38}$$

It is assumed that, so far as the partial derivatives $\partial F_j^{ikr}/\partial q_l$ are concerned, one can use the calculated values of the partial derivatives of the functions F_j^{ik} which are not corrected for station aberrations or atmosphere. With this assumption, analytical formulas can be given for $\partial F_j^{ikr}/\partial X_p$ and for $\partial X_m^{(0)}/\partial q_l$. These formulas are given explicitly in App. A. The middle factor in each term of the right side of Eq. (38) is given by the numerical solution of system (35) at time t_j.

The transformations from the numerical solution of system (34) at time t_j to $\tilde{F}_j^{ikr}$ are made as follows:

The location of the ith observation station is given by

$$R_i, \phi_i, \theta_i \tag{39}$$

Then,

$$x_i = R_i \cos\phi_i \cos\theta_i$$
$$y_i = R_i \cos\phi_i \sin\theta_i$$
$$z_i = R_i \sin\phi_i \tag{40}$$

$$r_i = [(x - x_i)^2 + (y - y_i)^2 + (z - z_i)^2]^{\frac{1}{2}} \tag{41}$$

$$\dot{r}_i = \frac{(x - x_i)\dot{x} + (y - y_i)\dot{y} + (z - z_i)\dot{z}}{r_i} \tag{42}$$

$$\gamma_i = \arcsin\left[\frac{(x - x_i)x_i + (y - y_i)y_i + (z - z_i)z_i}{R_i r_i}\right] \tag{43}$$

$$\dot{\gamma}_i = \frac{x\dot{x} + y_i\dot{y} + z_i\dot{z} - R_i\dot{r}_i \sin\gamma_i}{R_i r_i \cos\gamma_i} \tag{44}$$

The value of σ_i is given by

$$\sigma_i = \sigma_i' \quad \text{if } [-(x - x_i)\sin\theta_i + (y - y_i)\cos\theta_i] \geq 0$$
$$= 2\pi - \sigma_i' \quad \text{if } [-(x - x_i)\sin\theta_i + (y - y_i)\cos\theta_i] < 0 \tag{45}$$

where, using principal values in the range $0 \leq \sigma_i' \leq \pi$,

$$\sigma_i' = \arccos\left[\frac{-(x - x_i)\sin\phi_i\cos\theta_i - (y - y_i)\sin\phi_i\sin\theta_i + (z - z_i)\cos\phi_i}{r_i\cos\gamma_i}\right] \tag{46}$$

Also,

$$\dot{\sigma}_i = \frac{\dot{x}\sin\phi_i\cos\theta_i + \dot{y}\sin\phi_i\sin\theta_i - \dot{z}\cos\phi_i + \cos\sigma_i(\dot{r}_i\cos\gamma_i - r_i\dot{\gamma}_i\sin\gamma_i)}{r_i\sin\sigma_i\cos\gamma_i} \tag{47}$$

$$\delta_i = \arcsin[(z - z_i)/r_i] \tag{48}$$

$$\dot{\delta}_i = (\dot{z} - \dot{r}_i\sin\delta_i)/r_i\cos\delta_i \tag{49}$$

$$\alpha_i = (\theta_i - \bar{\theta}_i) \bmod 2\pi \tag{50}$$

where, using values from the range $0 \leq \bar{\theta}_i < 2\pi$

$$\bar{\theta}_i = \arctan[(y - y_i)/(x - x_i)] \tag{51}$$

(Ambiguities are resolved by observing the signs of numerator and denominator.)

$$\dot{\alpha}_i = \frac{(y - y_i)\dot{x} - (x - x_i)\dot{y}}{(x - x_i)^2 + (y - y_i)^2} \tag{52}$$

The values of δ_i and α_i may also be computed from the values of γ_i and σ_i by using the formulas

$$u_x = -\cos\gamma_i \sin\sigma_i \sin\theta_i - \cos\gamma_i \cos\sigma_i \sin\phi_i \cos\theta_i + \sin\gamma_i \cos\phi_i \cos\theta_i \quad (53)$$

$$u_y = \cos\gamma_i \sin\sigma_i \cos\theta_i - \cos\gamma_i \cos\sigma_i \sin\phi_i \sin\theta_i + \sin\gamma_i \cos\phi_i \sin\theta_i \quad (54)$$

$$u_z = \cos\gamma_i \cos\sigma_i \cos\phi_i + \sin\gamma_i \sin\phi_i \quad (55)$$

$$\delta_i = \arcsin u_z \quad (56)$$

$$\alpha_i = (\theta_i - \alpha_i') \bmod 2\pi \quad (57)$$

where the elevation angle and azimuth angle of the bubble vertical at the ith station (relative to the geocentric horizontal) are given by γ_I and σ_I.

The second equation of (60) is obtained by using the small angle approximations

$$\sin\gamma_I = 1$$

$$\cos\gamma_I = \frac{\pi}{2} - \gamma_I$$

$$\cos^2\gamma_I = 0$$

in

$$\sigma_i^{**} = \arctan\left[\frac{(\sin\sigma_i^* \sin\gamma_I \cos\gamma_i^* - \sin\gamma_i^* \sin\sigma_I \cos\gamma_I)\sin\gamma_I - \cos\gamma_i^* \cos\sigma_I \cos^2\gamma_I \sin(\sigma_I - \sigma_i^*)}{\cos\sigma_i^* \cos\gamma_i^* \sin\gamma_I - \sin\gamma_i^* \cos\sigma_I \cos\gamma_I}\right]$$

where, using values from the range $0 \leq \alpha_i' < 2\pi$

$$\alpha_i' = \arctan(u_y/u_x) \quad (58)$$

(Ambiguities are resolved by observing the signs of numerator and denominator.)

The angles γ_i, σ_i, α_i, δ_i are subjected to a number of corrections:

1. The following correction is made for refraction:

$$\left.\begin{aligned}\gamma_i^* &= \gamma_i + \Delta\gamma_i(\gamma_i, R) \quad \text{if } 0 \leq \gamma_i \leq 15 \text{ deg}\\ &= \gamma_i + N_i \cot\gamma_i \quad \text{if } 15 \text{ deg} < \gamma_i \leq 90 \text{ deg}\end{aligned}\right\} \quad (59)$$

$$\sigma_i^* = \sigma_i$$

The basis for this correction is given in App. B. The increment $\Delta\gamma_i$ is a function of γ_i, the elevation angle, and R, the probe's distance from the center of the Earth. The form suggested for $\gamma_i > 15$ deg is a result of fitting the numerical results.

The corresponding values of δ_i^* and α_i^* are found by applying formulas (53) through (58) to γ_i^* and σ_i^*.

2. The following correction is made for the bubble vertical deviation from the radial vertical:

$$\left.\begin{aligned}\gamma_i^{**} &= \arcsin[\sin\gamma_i^* \sin\gamma_I + \cos\gamma_i^* \cos\gamma_I \cos(\sigma_I - \sigma_i^*)]\\ \sigma_i^{**} &= \arctan\left[\frac{\sin\sigma_i^* \cos\gamma_i^* - \left(\frac{\pi}{2} - \gamma_I\right)\sin\gamma_i^* \sin\sigma_I}{\cos\sigma_i^* \cos\gamma_i^* - \left(\frac{\pi}{2} - \gamma_I\right)\sin\gamma_i^* \cos\sigma_I}\right]\end{aligned}\right\} \quad (60)$$

(the exact formula). The ambiguity in the second equation of (60) is resolved by choosing that value of σ_i^* which differs the least from σ_i.

It is assumed that the bubble vertical deviation occurs only with observations made using a radio telescope having an azimuth-elevation angle mounting; therefore, no corresponding changes are made in δ_i^* and α_i^*.

Finally, bore-sight corrections are made:

$$\left.\begin{aligned}\gamma_i^{***} &= \gamma_i^{**} + \Delta\gamma_i\\ \sigma_i^{***} &= \sigma_i^{**} + \Delta\sigma_i\\ \delta_i^{***} &= \delta_i^* + \Delta\delta_i\\ \alpha_i^{***} &= \alpha_i^* + \Delta\alpha_i\end{aligned}\right\} \quad (61)$$

where $\Delta\gamma_i$, $\Delta\sigma_i$, $\Delta\delta_i$, $\Delta\alpha_i$ are simply additive constants which must be provided.

The quantity f_i^{***} is assumed to be a linear function of r_i, the coefficients depending on the frequency transmitted as well as the manner in which the circuits are built for determining the doppler shift in frequency.

The formula presently being used for f_i^{***} has the form

$$f_i^{***} = \frac{f_{co} + B_i + C_i + \frac{f_{co}}{c} r_i}{A_i} - F_i \quad (62)$$

where

f_{co} is the transmitted frequency, cps

B_i, C_i, F_i are reference frequencies for the ith station, cps

A_i is a multiplicative factor in the circuitry used at the ith station

c is the velocity of light in a vacuum

Currently, no correction in $\dot{r}_i$ is made for the effects of refraction. The coefficient of $\dot{r}_i$ in the linear function must also multiply the partial derivative of $\dot{r}_i^{***}$ in order to obtain the partial derivative of f_i^{***}. The range r_i is treated in a similar manner.

It is assumed that the time derivatives of γ_i^{***}, σ_i^{***}, δ_i^{***}, and α_i^{***} are the same as those of γ_i, σ_i, δ_i, and α_i. The values of these time derivatives are useful in determining tracking rates required of the observing instruments.

VI. AUXILIARY OUTPUT FROM THE PROGRAM

A number of quantities are calculated as auxiliary outputs of the program.

The transformations for obtaining

$$R, \phi, \theta, v, \gamma, \sigma \tag{63}$$

at time t from

$$X, Y, Z, \dot{X}, \dot{Y}, \dot{Z} \tag{64}$$

are given by

$$R = (X^2 + Y^2 + Z^2)^{1/2} \tag{65}$$

$$\phi = \arcsin\left(\frac{Z}{R}\right) \tag{66}$$

$$\Theta = \arctan\left(\frac{Y}{X}\right) \tag{67}$$

(Ambiguities are resolved by observing the signs of numerator and denominator.)

$$\theta = [\Theta - \mathrm{GHA}\,\Omega\,(t)] \bmod 2\pi \tag{68}$$

$$\dot{x} = (\dot{X} + \omega Y)\cos[\mathrm{GHA}\,\Omega\,(t)] + (\dot{Y} - \omega X)\sin[\mathrm{GHA}\,\Omega\,(t)]$$
$$\dot{y} = -(\dot{X} + \omega Y)\sin[\mathrm{GHA}\,\Omega\,(t)] + (\dot{Y} - \omega X)\cos[\mathrm{GHA}\,\Omega\,(t)]$$
$$\dot{z} = \dot{Z} \tag{69}$$

$$v = [\dot{x}^2 + \dot{y}^2 + \dot{z}^2]^{1/2} \tag{70}$$

$$\gamma = \arcsin\left(\frac{x\dot{x} + y\dot{y} + z\dot{z}}{Rv}\right) \tag{71}$$

$$\sigma = \sigma' \quad \text{if } (-\dot{x}\sin\theta + \dot{y}\cos\theta) \geqq 0$$
$$= 2\pi - \sigma' \quad \text{if } (-\dot{x}\sin\theta + \dot{y}\cos\theta) < 0 \tag{72}$$

where, using principal values in the range $0 \leqq \sigma' \leqq \pi$

$$\sigma' = \arccos\left[(-\dot{x}\sin\phi\cos\theta - \dot{y}\sin\phi\sin\theta + \dot{z}\cos\phi)/v\cos\gamma\right] \tag{73}$$

A number of the auxiliary quantities calculated are related to the attitude of the probe. The equations of motion (Eq. 34) are those of the center of mass only, and their solution gives no information regarding the attitude. Although it is conceivable that dynamic equations may be added which would account for the calculation of the attitude of the probe at any time, the current assumption is that the attitude is known in terms of a unit vector $\mathbf{e}$ in the direction of the probe axis.

The following quantities are also available as output from the program:

$$\measuredangle \mathbf{c}, \mathbf{R}_{ip} = \arccos \left[\frac{C_1 (X - X_i) + C_2 (Y - Y_i) + C_3 (Z - Z_i)}{r_i} \right] \quad (74)$$

where C_1, C_2, C_3 are the components of $\mathbf{c}$ in the X, Y, Z system and where $\measuredangle \mathbf{c}, \mathbf{R}_{ip}$ means the angle between $\mathbf{c}$ and the vector from the ith station to the probe,

$$\measuredangle \mathbf{c}, \mathbf{R}_{pn} = \arccos \left\{ \frac{C_1 [X^{(n)} - X] + C_2 [Y^{(n)} - Y] + C_3 [Z^{(n)} - Z]}{r_n} \right\} \quad (75)$$

where the time derivatives on the right are obtained from differencing ephemeris data for the nth body,

$$|\mathbf{V} - \mathbf{V}_n| = \{ [\dot{X} - \dot{X}^{(n)}]^2 + [\dot{Y} - \dot{Y}^{(n)}]^2 + [\dot{Z} - \dot{Z}^{(n)}]^2 \}^{1/2} \quad (78)$$

$$\measuredangle (\mathbf{c}, \mathbf{V} - \mathbf{V}_n) = \arccos \left\{ \frac{C_1 [\dot{X} - \dot{X}^{(n)}] + C_2 [\dot{Y} - \dot{Y}^{(n)}] + C_3 [\dot{Z} - \dot{Z}^{(n)}]}{|\mathbf{V} - \mathbf{V}_n|} \right\} \quad (79)$$

where $\mathbf{V} - \mathbf{V}_n$ is the velocity of the probe relative to the nth body

$$\measuredangle \mathbf{R}_{pn}, \mathbf{R}_{ns} = \arccos \left\{ \frac{[X^{(n)} - X][X_s - X^{(n)}] + [Y^{(n)} - Y][Y_s - Y^{(n)}] + [Z^{(n)} - Z][Z_s - Z^{(n)}]}{r_n |\mathbf{R}_{ns}|} \right\} \quad (80)$$

where $\mathbf{R}_{pn}$ and $\mathbf{R}_{ns}$ are, respectively, the vectors from the probe to the nth body and from the nth body to the Sun,

$$\dot{r}_n = \frac{[X - X^{(n)}][\dot{X} - \dot{X}^{(n)}] + [Y - Y^{(n)}][\dot{Y} - \dot{Y}^{(n)}][Z - Z^{(n)}][\dot{Z} - \dot{Z}^{(n)}]}{r_n} \quad (81)$$

where $\mathbf{R}_{pn}$ is the vector from the probe to the nth body whose potential is included,

$$\measuredangle \mathbf{c}, \mathbf{R} = \arccos \left[\frac{C_1 X + C_2 Y + C_3 Z}{R} \right] \quad (76)$$

$$\measuredangle \mathbf{R}_{En}, \mathbf{R}_{Ep} = \arccos \left[\frac{X^{(n)} X + Y^{(n)} Y + Z^{(n)} Z}{R_n R} \right] \quad (82)$$

where $\mathbf{R}_{En}$ and $\mathbf{R}_{Ep}$ are the vectors from the center of the Earth to the nth body and the probe, respectively,

$$\measuredangle \mathbf{R}_{ip}, \mathbf{R}_{is} = \arccos \left[\frac{(X - X_i)(X_s - X_i) + (Y - Y_i)(Y_s - Y_i) + (Z - Z_i)(Z_s - Z_i)}{r_i |\mathbf{R}_{is}|} \right] \quad (83)$$

where $\mathbf{R}$ is the vector from the center of the Earth to the probe,

$$V_n = |\mathbf{V}_n| = \{ [\dot{X}^{(n)}]^2 + [\dot{Y}^{(n)}]^2 + [\dot{Z}^{(n)}]^2 \}^{1/2} \quad (77)$$

where $\mathbf{R}_{ip}$ and $\mathbf{R}_{is}$ are the vectors from the ith station to the probe and to the Sun, respectively, and

$$r_n = \{ [X - X^{(n)}]^2 + [Y - Y^{(n)}]^2 + [Z - Z^{(n)}]^2 \}^{1/2} \quad (84)$$

VII. THE IBM 704 COMPUTER PROGRAM

As mechanized for the 704 digital computer, the tracking program can be considered as having two distinct phases. In the first phase, the equations of motion and the variational equations are integrated to each observation time where the elements of Eq. (14) are computed and stored. The second phase is concerned with the solution of a specified subset of Eq. (14). Figures 1 to 3 present block diagrams of the procedure.

The normal mode of operation is the iterative procedure where Eq. (14) is generated, solved, and the corrections are added to the prior estimate of the probe's injection coordinates. For increased flexibility, several alternatives are under operator control during this sequence of operations. The major options are as follows:

1. The composition of Eq. (14) may be specified as to (a) number of stations and data types to include

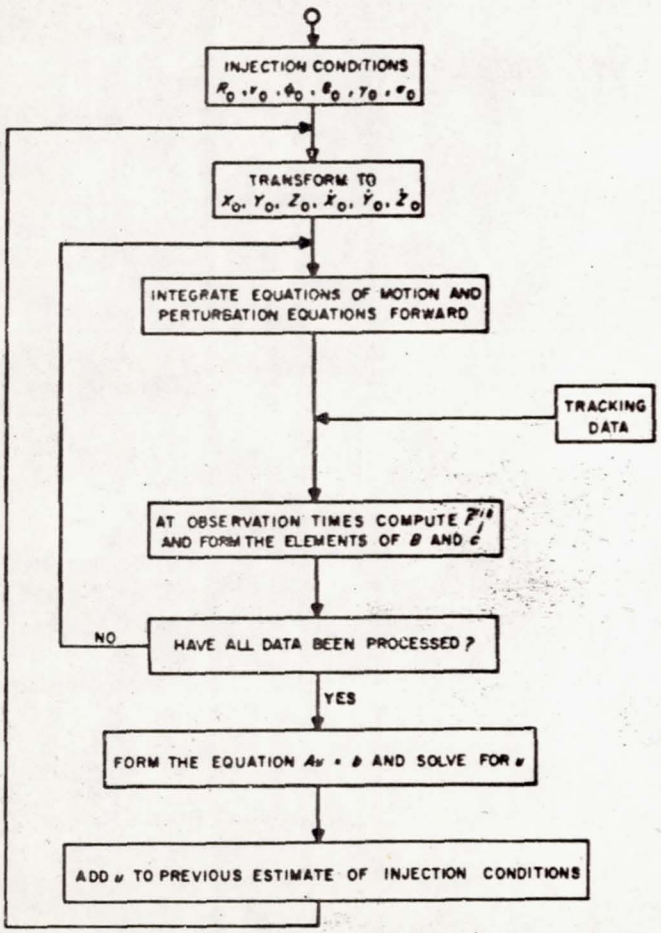

Fig. 1. The basic computer program

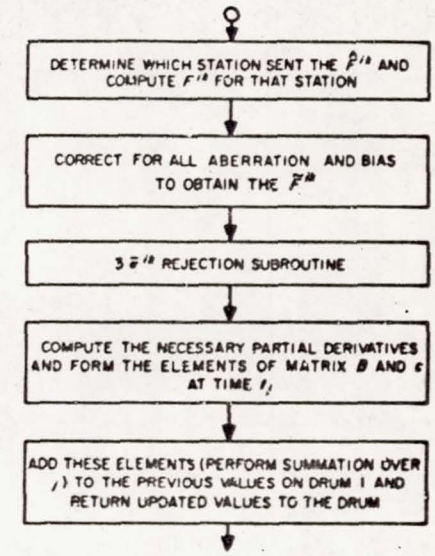

Fig. 2. Procedure at data times

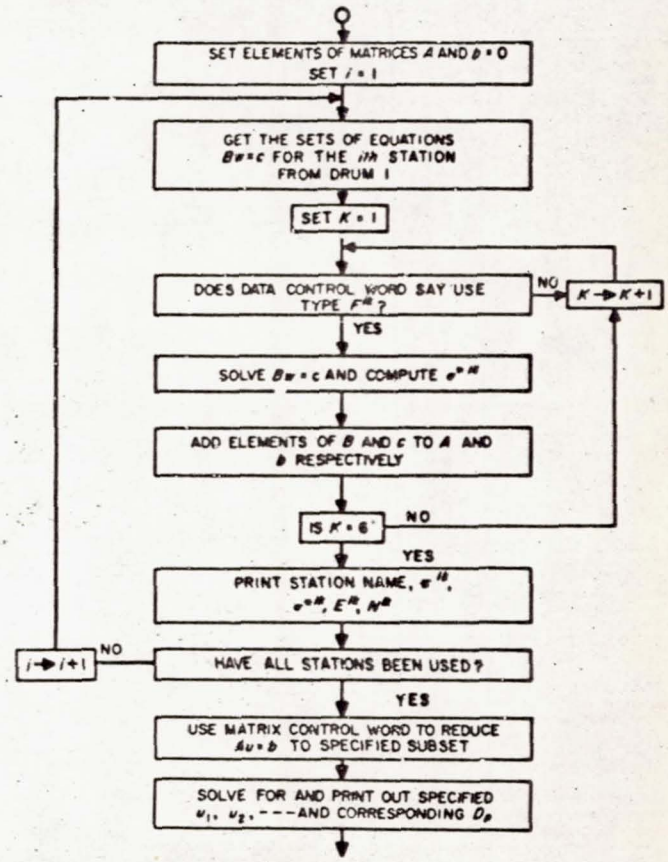

Fig. 3. Generation and solution of the normal equations

(b) order of the matrix (c) weighting of the data types.

2. The data can be ignored if they fall $3\sigma^{ik}$ or more outside the predicted value. (a) Data which fail the test are left out on subsequent iterations except that (b) all data may be re-examined at any time.
3. Pointing predictions for the tracking stations may be obtained at specified times using the latest values of the probe's injection coordinates. The "standard deviations of the predictions" may be computed.
4. During any iteration, the $\hat{F}_j^{ik}, \tilde{F}_j^{ik}$ and the partial derivatives $\partial F_j^{ik}/\partial q_l$ may be printed off-line.

VIII. INTERNAL PROGRAM CONTROL

The input required by the program during any tracking operation may be divided into four groups:

a. An estimate of the injection coordinates

b. Data from tracking stations

c. Internal constants

d. Internal program control

Groups a, b, and c are defined by listing all the pertinent quantities in Section IX on input format.

The group d input is used primarily to specify the order and composition of the matrix equation (Eq. 14). In forming this equation, the program must ask the following questions:

a. What data did the ith station send?

b. Which data types are to be used?

c. What subset of Eq. (14) is to be solved?

The control words to answer these questions are termed format control, data control, and matrix control, respectively.

A. Format Control

The first word on each tracking data card is assumed to be the station identification number i. The format control must identify the rest of the data on the cards. It should be noted that these control words are fixed in the sense that they are determined solely by the data sent from the tracking stations. The format control is an octal number associated with each tracking station of the form $CCCCCCCOOOON$. The C digits specify the type of data and the N specifies the amount. The first digit corresponds to the second word on the data card (remembering that the first word is i), the second digit corresponds to the third word, etc. The amount, N, is the number of C digits used. The following tabulation gives the possible data types:

C	DATA TYPE
0	data condition
1	time (t_j)
2	slant range ($\hat{F}^{i1}$)
3	frequency ($\hat{F}^{i2}$)
4	elevation ($\hat{F}^{i3}$)
5	azimuth ($\hat{F}^{i4}$)
6	declination ($\hat{F}^{i5}$)
7	hour angle ($\hat{F}^{i6}$)

The data condition is a digit on the data card indicating the quality of the observations. The program accepts only data with a zero data condition. The minimum information that a card may contain is i, t_j, and one observation. The maximum is i and the eight quantities above.

B. Data Control

The situation may occur in which the operator desires to omit a particular data type even though it appeared on the data cards. In order to accomplish this, another list of control words is kept by the program to specify the data types to be used in Eq. (14).

The data control words are octal numbers having the form *ABABABABABAB* where each pair *AB* represents a station. Six stations may be specified by one word; the left pair *AB* is associated with station 1, the right pair with station 6.

DIGIT A	DIGIT B
elevation = 1	hour angle = 1
frequency = 2	declination = 2
slant range = 4	azimuth = 4

In order to determine *A* and *B*, add the numbers corresponding to the data type desired. For example, in Eq. (14), use only slant range, frequency, hour angle, and declination from station 2. The data control word would be 006300000000.

C. Matrix Control

Thus far, only the type of data has been specified. The order of Eq. (14) must also be entered as must the choice of weighting factors 1 or $1/[(\sigma^{ik})^2]$. This is accomplished by one control word which is constructed as follows: If bit 2 equals 1, set $\sigma^{ik} = 1$. If the program is to solve for a bias from the ith station, i must be entered in the decrement of the control word. The right-most 12 bits of the address are used to specify which quantities are to be solved for.

BIT NUMBER	SOLVE FOR CORRECTION TO:
24	R_0
25	ϕ_0
26	θ_0
27	v_0
28	γ_0
29	σ_0
30	bias in r_i
31	bias in f_i
32	bias in γ_i
33	bias in σ_i
34	bias in δ_i
35	bias in α_i

The control word is checked for the two allowable cases,

1. decrement $\neq 0$, one or more of the bits 30-35 $\neq 0$
2. decrement = 0, bits 30-35 = 0

The program will stop on a divide check if it is asked to solve for a bias in an F^{ik} which either did not appear in the tracking data or was omitted by means of the data control word.

D. The Rejection Sigmas

A table of $\bar{\sigma}^{ik}$ is kept by the program for the purpose of rejecting bad data points. During any iteration, the observation $\hat{F}^{ik}_j$ will not be used, by sense switch option, if $|\hat{F}^{ik}_j - \hat{F}^{ik}_j| \geq 3\bar{\sigma}^{ik}$. In order to conserve storage the $\bar{\sigma}^{ik}$ is packed in a pseudo-floating point form, three per word. As a station is allowed six types of observations, two words per station are required. The two words are decimal numbers of the form *ExxExxExx*, *ExxExxExx*, where each triplet *Exx* represents a $\bar{\sigma}^{ik}$ and the order, left to right, is elevation, frequency, slant range, hour angle, declination, and azimuth. The decimal point is assumed at the right of *xx* and *E* is the exponent plus five; e.g., 815 = 15000., 515 = 15., 111 = .0011. If the rejection option is being used and a triplet *Exx* = 0, it is interpreted as an instruction to keep that data type. Hence, rejection sigmas need be entered only for the data types which are suspected of containing bad points.

IX. GENERAL INPUT

The input subroutine used by the program is *NYINP*1, which will accept data in the standard SAP form. Each card has a location field, an operation field, and a variable field. The location field, if needed, must contain the decimal address of the first word of data on the card. The operation field must contain *BCD*, *DEC*, *OCT*, or *TRA* specifying *BCD* information, decimal data, octal data, or a transfer. Floating point information is recognized by a decimal point or the letter *E* denoting multiplication by a power of 10; e.g., $1.88 = .188E1 = 18.8E-1$. As with SAP, if data are to be stored sequentially in core, more than one word of data may be put on a card, each word being separated by a comma. A blank in the variable field indicates that information to the right of the blank is a comment and is not to be used.

A. Format

The following tabulation gives the location and form of input data needed by the program. All *DEC* information is in floating point decimal form unless the identifying symbol is followed by an asterisk, in which event the information is a decimal integer. All storage locations are referred to by their symbolic locations, though decimal addresses must appear on the cards. A decimal symbol table is provided with the program listing.

The following dimensional units are used throughout the program:

length, meters;
velocity, m/sec; angular rates, deg/hr;
angles, deg; frequency, cps.

COLUMNS	LOCATION FIELD 1-6	OPERATION FIELD 8-11	VARIABLE FIELD 12-72	
GROUP 1	*R*1	*DEC*	R_0	
	*R*1 + 1	*DEC*	v_0	
	*R*1 + 2	*DEC*	ϕ_0	
	*R*1 + 3	*DEC*	θ_0	
	*R*1 + 4	*DEC*	γ_0	
	*R*1 + 5	*DEC*	σ_0	
	*R*1 + 6	*DEC*	γ_{c0}	
	*R*1 + 7	*DEC*	σ_{c0}	1
	*R*1 + 8	*DEC*	t^*	1
GROUP 2	(none)	*DEC*	$t^*, D^*, t^*, r_i, f_i, \gamma_i, \sigma_i, \alpha_i, \delta_i$	
GROUP 3	*RI* − *i*	*DEC*	R_i	
	PHII − *i*	*DEC*	ϕ_i	
	THETAI − *i*	*DEC*	θ_i	
	GI − *i*	*DEC*	γ_i	2
	SI − *i*	*DEC*	σ_i	2
	RBIAS − *i*	*DEC*	$\Delta r_i \equiv E^{11}$	3
	FBIAS − *i*	*DEC*	$\Delta f_i \equiv E^{12}$	3
	DIG − *i*	*DEC*	$\Delta\gamma_i \equiv E^{13}$	3
	DIS − *i*	*DEC*	$\Delta\sigma_i \equiv E^{14}$	3
	DID − *i*	*DEC*	$\Delta\delta_i \equiv E^{15}$	3
	DIA − *i*	*DEC*	$\Delta\alpha_i \equiv E^{16}$	3
	ASUBI − *i*	*DEC*	A_i	4
	BSUBI − *i*	*DEC*	B_i	4
	CSUBI − *i*	*DEC*	C_i	4
	FSUBI − *i*	*DEC*	F_i	4

COLUMNS	LOCATION FIELD 1-6	OPERATION FIELD 8-11	VARIABLE FIELD 12-72	
	HOLL1 − *i*	*BCD*	1xxxxxx	
	HOLL2 − *i*	*BCD*	1xxxxxx	
	FCOO	*DEC*	f_{co}	4
	NOS	*DEC*	m^*	
GROUP 4	*CODEWD* − *i*	*OCT*	*CCCCCCCOOOON*	
	DTYPE	*OCT*	*ABABABABABAB*	
	REJSIG + 2(*i* − 1)	*DEC*	*ExxExxExx*, ExxExxExx**	5

In the preceding tabulation, the numbered input is not needed under the following assumptions:

1. Spin axis orientation is immaterial.
2. No station misalignment (nominal values $\gamma_i = 90.$, $\sigma_i = 0$ should be entered).
3. There are no constant biases to be subtracted from the data.
4. The frequency computation is immaterial.
5. The rejection option is not used.

In group 1, t_0 is a 10-digit decimal number giving GMT of injection. The word in pairs of digits is month, day, hour, minutes and seconds; e.g., 0113051648 is January 13, 5h, 16m, 48s. In group 2, *D* is the data condition and *t* is the GMT of the observation; *t* is a 6-digit number giving hours, minutes, and seconds. In order to specify the day of the year, the number of days since 0 hr January 1, 1959 must be punched in columns 70 through 72 on the first card of each day's data. As it reads the tracking data, *NYINP*1 is modified in order that this number is not interpreted as a comment. It should be recalled that by means of the format control the amount of data following the *i* on each group 2 card is flexible and the data may be in any order. In group 3, the two *BCD* words are the first and last 6 letters of the station name, and *m* is the number of stations.

B. The Input Deck

All input from groups 1 and 4 (and group 3, if it was not written on the program tape) is stacked together and followed by the card *TRA* 3, 4. This card is followed by all the group 2 data.

Although the program sorts the group 2 data, with respect to time, in groups of 15 cards, the operator should take care that the data cards are not seriously out of time sequence. The group 2 cards are written on tape 2 as soon as they have been read. These cards are read only once, unless the operator decides to merge additional data with previously read cards. In this event, the operator will have to merge the cards and start over. Other than considerations of computing time, there is no limit on the number of group 2 cards that many be entered.

The group 2 input procedure is illustrated in Fig. 4.

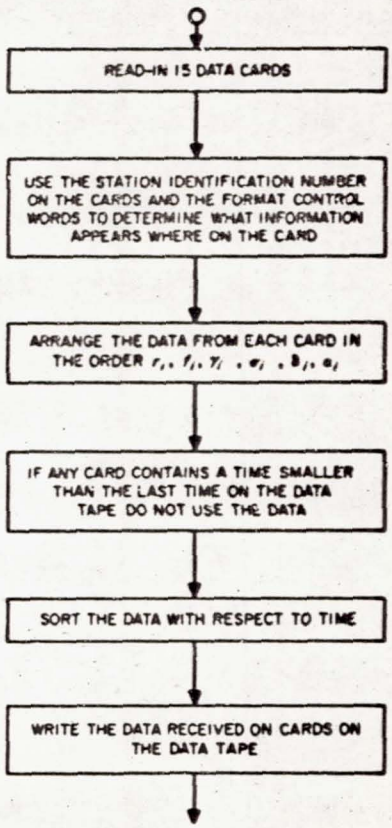

Fig. 4. Transcription of data card to data tape

X. MISCELLANEOUS INFORMATION

A. The Prediction Option

If sense switch 6 is down, the program will integrate past the last group 2 time and print the normal output at intervals specified by the operator. The prediction times may be specified in one of two ways:

PREDT DEC t', Δt, n or *PREDT DEC* t'', Δt, n

where $t', \Delta t, n$ are floating point numbers, and t'' is a decimal integer.

In the first case, t' is the number of seconds beyond the last group 2 card, Δt is the print interval in seconds, and n is the number of prediction points. In the second case, t'' is the GMT of the first prediction with the same form as t_0 in the group 1 cards; Δt and n mean the same as in the first case. Nominal values of 900., 1., 1. are currently assembled. This instructs the program to make one prediction 15 min after the last group 2 card. If sense switch 2 is down along with sense switch 6, Eq. (27) is evaluated and printed out at each prediction time.

B. The Use of the Sense Switches

In the following tabulation, sense switch 2 is additionally tested as the program is loaded in core for on-line (down) or off-line output. Output is usually taken on-line as the operator must make decisions such as which data to use, when to reject bad points, and whether or not convergence has occurred.

SENSE SWITCH	UP	DOWN
1	no operation	a. select card reader to read data while program is running
		b. if put down at *LS*1 + 2 stop, program returns to *LS*1 + 2 after solution of Eq. (14)
2	stop to enter matrix control word	a. if matrix control word ≠ 0, do not stop
		b. if SSW6 down, do standard deviations of the predictions.
3	no operation	print $\hat{F}_j^k$, $\tilde{F}_j^k$, and $\partial F_j^k / \partial q_l$ on tape 4
4	no operation	do $3\bar{\sigma}^{jk}$ rejection
5	all data on tape 2	more tracking data in card reader
6	no operation	predict

Sense switch 1 is tested at each integration step and merely selects the card reader, which is used to read in constants or control words which the operator may wish to change. Sense switches 3 and 4 are tested at each observation time. Sense switches 2, 5, and 6 are tested after the final observation is read from the data tape. Sense switch 5 should be up if there is no tracking data in the card reader.

C. Program Halts and Error Indications

1. Error Stops (should not occur).

LOCATION	DESCRIPTION
INP + 60$_8$	Illegal operation in data card.
INP + 376$_8$	Out of range decimal data.
INP + 657$_8$	Illegal punch in data card.
BSTP − 5	Check sum error on tape 5 after 3 tries.
LOOKD − 10$_8$	Time out of range of ephemerides, check input.
LOOKD − 1	Time out of range of ephemerides, check input
D 2 + 7	Check sum error on tape 1, rewrite program tape.
START + 2	*EOF* return for card reader, input error if in tracking mode.

2. Error Indications.

If a 5-digit number appears on-line in columns 1 to 5, the octal location of an error return is indicated. These usually occur in the output transformations and do not affect the program; e.g., if $\gamma = 90$ deg, σ is not defined and will give an error return. If there is a check sum error in reading the data tape, CHECK SUM ERROR ON DATA TAPE will be printed on-line.

3. Normal Stops.

LOCATION	DESCRIPTION
START − 3	Occurs after program deck or tape is loaded. If tracking, hit *Start*. If running single trajectory enter S, 1, 2 in *MQ*, hit *Start*.
*LS*1 + 2	Enter matrix control word in *MQ*. If SSW 1 is down, program will return to this location to solve a different matrix. If the control word is zero or illegal, the program will remain at this stop.
*TS*4	Program stops here after a prediction. If further iteration is desired, put SSW 6 up and hit *Start*.

D. Restart Feature

If the matrix A is ill-conditioned, the solution may be meaningless. The initial conditions from the previous iteration are saved; thus, if meaningless corrections are added to the injection conditions, they may be removed by hitting *Reset*, then *Start*. The program will return to the previous initial conditions and the operator can solve for a lower order matrix at the *LS*1 + 2 stop.

E. Single Trajectories

It is possible to run the tracking program to obtain "single" trajectories. The variational equations are not integrated and computations pertinent only to tracking are ignored. The input consists of groups 1 and 3 followed by cards which specify the amount of printing to be done. These cards have the form

$$TSTOP + 6 \quad DEC\ t_1, \Delta t_1, 1, t_2, 1, \cdots, t_f, 0, 0$$
$$TRA\ 3, 4$$

This instructs the program to begin printing at t_1 with a print interval of Δt_1 seconds. At t_2 switch to Δt_2 seconds for the print interval, etc. As many as 18 time triplets may be entered. The triplet $t_f, 0, 0$ instructs the program to select the card reader for another case at time t_f. The t's are GMT and have the same format as t_0 in group 1, whereas the Δt's are entered as floating point numbers. As many cases as desired may be stacked together, separated by *TRA* 3, 4 cards. Only those parameters which change need be input on succeeding cases. After the program tape is loaded, enter bits S, 1, 2 in the *MQ* at the stop in location START − 3. Put the input deck in the card reader and hit *Start*. Output will be off-line on tape 3.

F. The Program Tape

Clear and load the binary deck. After the final card is read, the program will be written on tape 1. The operator may, at this time, write the group 3 data on the program tape. At the program halt in START − 3, put the group 3 data in the card reader, followed by the card *TRA DUMP*, and hit *Start*. The group 3 data will be written on the program tape. This may be done with any of the data but that of group 2. However, groups 1 and 4 are usually entered each time on cards as they are likely to change.

G. Atmospheric Refraction

In the present program a correction is added to the elevation angle to account for refraction effects. A two-parameter table look-up is made to determine this correction. As the current table in the program is for a transmitter frequency of 960 mc, the user may want to remove the atmospheric refractions correction. This may be done by putting the instruction *TRA STR* in location *SXD* + 7.

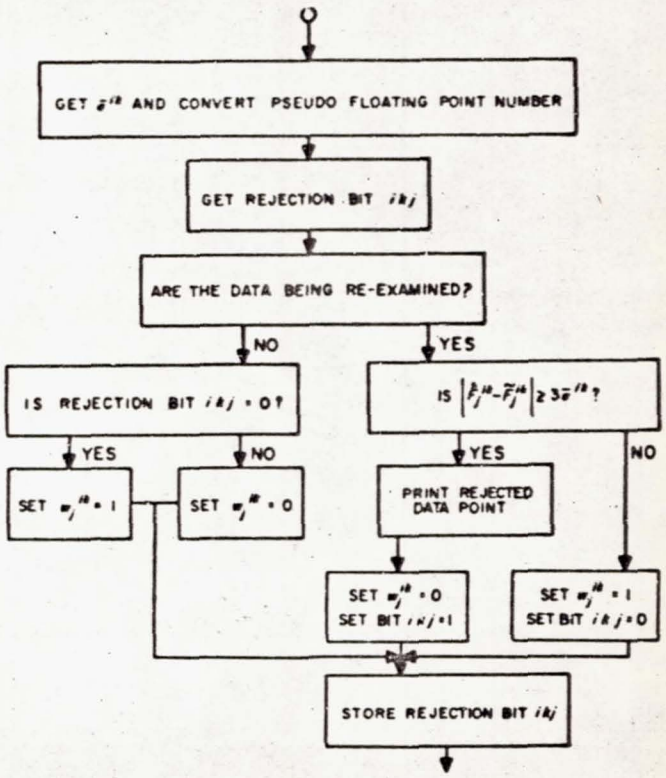

Fig. 5. The $3\bar{\sigma}^{ik}$ rejection test

H. Rejection Logic

The program keeps a table of *ikj* binary bits corresponding to each observation $\hat{F}_j^k$. If an observed value is rejected, the *ikj*th bit is set to 1 to indicate a bad data point. On subsequent iterations, instead of re-examining the data, this table is scanned to determine whether or not to use the $\hat{F}_j^k$ in the least-squares fit. Each time the sense switch option to reject bad points is used, the table is cleared and all data are re-examined for $3\bar{\sigma}^{ik}$ rejection (see Fig. 5).

I. Storage Allocation

The current JPL program has been written for a 704 computer with an 8K core, an 8K drum, and 5 tape units. Memory is distributed as follows: The program, tracking data, and Sun–Moon ephemerides are kept on separate tapes, leaving two units for off-line output. The *ik* normal matrixes and the *ikj* rejection bits are stored on the magnetic drums. All other data are kept in core memory. Although coded for M tracking stations, the current 8K core restricts the program to a maximum of five stations. A maximum on the order of 50 stations is anticipated for a 32K core with no magnetic drums.

UNIT	FUNCTION
tape 1	program
tape 2	tracking data
tape 3	if SSW2; output
tape 4	if SSW3; $\hat{F}_j^k$, $\tilde{F}_j^k$ and $\partial F_j^k/\partial q_l$
tape 5	Sun–Moon ephemerides
drum 1	*ik* normal matrixes
drum 4	*ikj* rejection bits

XI. NUMERICAL METHODS

A fourth-order Runge-Kutta method is used to integrate the equations of motion. This method was chosen primarily for the convenience of using a variable integration step which, as the tracking data may come in at any interval, is an important feature.

The matrix equations which appear in the least-squares method are often ill-conditioned, a situation which can cause serious loss of significant digits in the process of solving the equations. The program reduces this source of error as much as possible by using a Gauss-Jordan reduction method which interchanges rows and columns in order to obtain the largest pivotal element while developing the inverse matrix.

The current program uses a tape which contains the Cartesian coordinates of the Moon and Sun at ½-day intervals for the years 1959 through 1962. A fourth-order interpolating polynomial is used to find positions at any GMT. Efforts are currently under way to include an ephemeris of all the planets for the years 1960 through 1970.

As set up for tracking satellites and lunar probes, the program uses the following criteria for choosing integration step size:

$$\bar{R} = \min(R, R_s)$$

$0 \leq \bar{R} < 16000$ km	$\Delta t =$ 30 sec
$16000 \leq \bar{R} < 86400$	360
$86400 \leq \bar{R}$	1800

These values have been determined empirically in order to ensure a small truncation error while, at the same time, giving relatively small computing times. A 35-hr trajectory to the Moon requires about 3 min computing time with a truncation error of less than 5 km at the Moon.

The computing time is severely increased when the program is in the tracking mode. The 36 variational equations must now be integrated and matrix computation must be made at each observation time. Further, the program is usually restricted from taking an optimum step size by the group 2 data rate. In the tracking mode, the computing time is on the order of 2 sec per observation time.

APPENDIX A

Analytical Formulas for Partials

$$\frac{\partial X_0}{\partial R_0} = \cos\phi_0 \cos\Theta_0 \tag{A-1}$$

where

$$\Theta_0 = [\theta_0 + \mathrm{GHA}\,\Omega\,(t_0)] \bmod 2\pi$$

$$\frac{\partial X_0}{\partial \phi_0} = -R_0 \sin\phi_0 \cos\Theta_0 \tag{A-2}$$

$$\frac{\partial X_0}{\partial \theta_0} = -R_0 \cos\phi_0 \sin\Theta_0 \tag{A-3}$$

$$\frac{\partial X_0}{\partial v_0} = 0 \tag{A-4}$$

$$\frac{\partial X_0}{\partial \gamma_0} = 0 \tag{A-5}$$

$$\frac{\partial X_0}{\partial \sigma_0} = 0 \tag{A-6}$$

$$\frac{\partial Y_0}{\partial R_0} = \cos\phi_0 \sin\Theta_0 \tag{A-7}$$

$$\frac{\partial Y_0}{\partial \phi_0} = -R_0 \sin\phi_0 \sin\Theta_0 \tag{A-8}$$

$$\frac{\partial Y_0}{\partial \theta_0} = R_0 \cos\phi_0 \cos\Theta_0 \tag{A-9}$$

$$\frac{\partial Y_0}{\partial v_0} = 0 \tag{A-10}$$

$$\frac{\partial Y_0}{\partial \gamma_0} = 0 \tag{A-11}$$

$$\frac{\partial Y_0}{\partial \sigma_0} = 0 \tag{A-12}$$

$$\frac{\partial Z_0}{\partial R_0} = \sin\phi \tag{A-13}$$

$$\frac{\partial Z_0}{\partial \phi_0} = R_0 \cos\phi_0 \tag{A-14}$$

$$\frac{\partial Z_0}{\partial \theta_0} = 0 \tag{A-15}$$

$$\frac{\partial Z_0}{\partial v_0} = 0 \tag{A-16}$$

$$\frac{\partial Z_0}{\partial \gamma_0} = 0 \tag{A-17}$$

$$\frac{\partial Z_0}{\partial \sigma_0} = 0 \tag{A-18}$$

$$\frac{\partial \dot{X}_0}{\partial R_0} = -\omega \cos\phi_0 \sin\Theta_0 \tag{A-19}$$

$$\frac{\partial \dot{X}_0}{\partial \phi_0} = -v_0 \cos\gamma_0 \cos\phi_0 \cos\sigma_0 \cos\Theta_0 - v_0 \sin\gamma_0 \sin\phi_0 \cos\Theta_0 + \omega R_0 \sin\phi_0 \sin\Theta_0 \tag{A-20}$$

$$\frac{\partial \dot{X}_0}{\partial \theta_0} = -v_0 \cos\gamma_0 \sin\sigma_0 \cos\Theta_0 + v_0 \cos\gamma_0 \sin\phi_0 \cos\sigma_0 \sin\Theta_0 - v_0 \sin\gamma_0 \cos\phi_0 \sin\Theta_0 - \omega R_0 \cos\phi_0 \cos\Theta_0 \tag{A-21}$$

$$\frac{\partial \dot{X}_0}{\partial v_0} = -\cos\gamma_0 \sin\sigma_0 \sin\Theta_0 - \cos\gamma_0 \sin\phi_0 \cos\sigma_0 \cos\Theta_0 + \sin\gamma_0 \cos\phi_0 \cos\Theta_0 \tag{A-22}$$

$$\frac{\partial \dot{X}_0}{\partial \gamma_0} = v_0 \sin\gamma_0 \sin\sigma_0 \sin\Theta_0 + v_0 \sin\gamma_0 \sin\phi_0 \cos\sigma_0 \cos\Theta_0 + v_0 \cos\gamma_0 \cos\phi_0 \cos\Theta_0 \tag{A-23}$$

$$\frac{\partial \dot{X}_0}{\partial \sigma_0} = -v_0 \cos\gamma_0 \cos\sigma_0 \sin\Theta_0 + v_0 \cos\gamma_0 \sin\phi_0 \sin\sigma_0 \cos\Theta_0 \tag{A-24}$$

$$\frac{\partial \dot{Y}_0}{\partial R_0} = \omega \cos\phi_0 \cos\Theta_0 \tag{A-25}$$

$$\frac{\partial \dot{Y}_0}{\partial \phi_0} = -v_0 \cos\gamma_0 \cos\phi_0 \cos\sigma_0 \sin\Theta_0 - v_0 \sin\gamma_0 \sin\phi_0 \sin\Theta_0 - \omega R_0 \sin\phi_0 \cos\Theta_0 \tag{A-26}$$

$$\frac{\partial \dot{Y}_0}{\partial \theta_0} = -v_0 \cos\gamma_0 \sin\sigma_0 \sin\Theta_0 - v_0 \cos\gamma_0 \sin\phi_0 \cos\sigma_0 \cos\Theta_0 + v_0 \sin\gamma_0 \cos\phi_0 \cos\Theta_0 - \omega R_0 \cos\phi_0 \sin\Theta_0 \tag{A-27}$$

$$\frac{\partial \dot{Y}_0}{\partial v_0} = \cos\gamma_0 \sin\sigma_0 \cos\Theta_0 - \cos\gamma_0 \sin\phi_0 \cos\sigma_0 \sin\Theta_0 + \sin\gamma_0 \cos\phi_0 \sin\Theta_0 \tag{A-28}$$

$$\frac{\partial \dot{Y}_0}{\partial \gamma_0} = -v_0 \sin\gamma_0 \sin\sigma_0 \cos\Theta_0 + v_0 \sin\gamma_0 \sin\phi_0 \cos\sigma_0 \sin\Theta_0 + v_0 \cos\gamma_0 \cos\phi_0 \sin\Theta_0 \tag{A-29}$$

$$\frac{\partial \dot{Y}_0}{\partial \sigma_0} = v_0 \cos\gamma_0 \cos\sigma_0 \cos\Theta_0 + v_0 \cos\gamma_0 \sin\phi_0 \sin\sigma_0 \sin\Theta_0 \tag{A-30}$$

$$\frac{\partial \dot{Z}_0}{\partial R_0} = 0 \tag{A-31}$$

$$\frac{\partial \dot{Z}_0}{\partial \phi_0} = v_0 \sin\gamma_0 \cos\phi_0 - v_0 \cos\gamma_0 \sin\phi_0 \cos\sigma_0 \tag{A-32}$$

$$\frac{\partial \dot{Z}_0}{\partial \theta_0} = 0 \tag{A-33}$$

$$\frac{\partial \dot{Z}_0}{\partial v_0} = \sin\gamma_0 \sin\phi_0 + \cos\gamma_0 \cos\phi_0 \cos\sigma_0 \tag{A-34}$$

$$\frac{\partial \dot{Z}_0}{\partial \gamma_0} = v_0 \cos\gamma_0 \sin\phi_0 - v_0 \sin\gamma_0 \cos\phi_0 \cos\sigma_0 \tag{A-35}$$

$$\frac{\partial \dot{Z}_0}{\partial \sigma_0} = -v_0 \cos\gamma_0 \cos\phi_0 \sin\sigma_0 \tag{A-36}$$

$$\frac{\partial r_i}{\partial X} = \frac{X - R_i \cos\phi_i \cos\Theta_i}{r_i} \tag{A-37}$$

where

$$\Theta_i = [\theta_i + \mathrm{GHA}\,\Omega\,(t)] \bmod 2\pi$$

$$\frac{\partial r_i}{\partial Y} = \frac{Y - R_i \cos\phi_i \sin\Theta_i}{r_i} \tag{A-38}$$

$$\frac{\partial r_i}{\partial Z} = \frac{Z - R_i \sin\phi_i}{r_i} \tag{A-39}$$

$$\frac{\partial r_i}{\partial \dot{X}} = 0 \tag{A-40}$$

$$\frac{\partial r_i}{\partial \dot{Y}} = 0 \tag{A-41}$$

$$\frac{\partial r_i}{\partial \dot{Z}} = 0 \tag{A-42}$$

$$\frac{\partial \dot{r}_i}{\partial X} = \frac{1}{r_i}(\dot{X} + \omega R_i \cos\phi_i \sin\Theta_i) - \frac{1}{r_i}\left(\dot{r}_i \frac{\partial r_i}{\partial X}\right) \tag{A-43}$$

$$\frac{\partial \dot{r}_i}{\partial Y} = \frac{1}{r_i}(\dot{Y} - \omega R_i \cos\phi_i \cos\Theta_i) - \frac{1}{r_i}\left(\dot{r}_i \frac{\partial r_i}{\partial Y}\right) \tag{A-44}$$

$$\frac{\partial \dot{r}_i}{\partial Z} = \frac{1}{r_i}\left(\dot{Z} - \dot{r}_i \frac{\partial r_i}{\partial Z}\right) \tag{A-45}$$

$$\frac{\partial \dot{r}_i}{\partial \dot{X}} = \frac{\partial r_i}{\partial X} \tag{A-46}$$

$$\frac{\partial \dot{r}_i}{\partial \dot{Y}} = \frac{\partial r_i}{\partial Y} \tag{A-47}$$

$$\frac{\partial \dot{r}_i}{\partial \dot{Z}} = \frac{\partial r_i}{\partial Z} \tag{A-48}$$

$$\frac{\partial \gamma_i}{\partial X} = \frac{1}{r_i \cos\gamma_i}\left(\cos\phi_i \cos\Theta_i - \sin\gamma_i \frac{\partial r_i}{\partial X}\right) \tag{A-49}$$

$$\frac{\partial \gamma_i}{\partial Y} = \frac{1}{r_i \cos\gamma_i}\left(\cos\phi_i \sin\Theta_i - \sin\gamma_i \frac{\partial r_i}{\partial Y}\right) \tag{A-50}$$

$$\frac{\partial \gamma_i}{\partial Z} = \frac{1}{r_i \cos\gamma_i}\left(\sin\phi_i - \sin\gamma_i \frac{\partial r_i}{\partial Z}\right) \tag{A-51}$$

$$\frac{\partial \gamma_i}{\partial \dot{X}} = 0 \tag{A-52}$$

$$\frac{\partial \gamma_i}{\partial \dot{Y}} = 0 \tag{A-53}$$

$$\frac{\partial \gamma_i}{\partial \dot{Z}} = 0 \tag{A-54}$$

$$\frac{\partial \sigma_i}{\partial X} = \frac{1}{r_i \cos\gamma_i}(\sin\sigma_i \sin\phi_i \cos\Theta_i - \cos\sigma_i \sin\Theta_i) \tag{A-55}$$

$$\frac{\partial \sigma_i}{\partial Y} = \frac{1}{r_i \cos\gamma_i}(\sin\sigma_i \sin\phi_i \sin\Theta_i + \cos\sigma_i \cos\Theta_i) \tag{A-56}$$

$$\frac{\partial \sigma_i}{\partial Z} = \frac{1}{r_i \cos\gamma_i}(-\sin\sigma_i \cos\phi_i) \tag{A-57}$$

$$\frac{\partial \sigma_i}{\partial \dot{X}} = 0 \tag{A-58}$$

$$\frac{\partial \sigma_i}{\partial \dot{Y}} = 0 \tag{A-59}$$

$$\frac{\partial \sigma_i}{\partial \dot{Z}} = 0 \tag{A-60}$$

$$\frac{\partial \delta_i}{\partial X} = \frac{1}{r_i \cos\delta_i}\left[\frac{\partial r_i}{\partial X}\ \frac{\partial r_i}{\partial Z}\right] \tag{A-61}$$

$$\frac{\partial \delta_i}{\partial Y} = \frac{1}{r_i \cos\delta_i}\left[\frac{\partial r_i}{\partial Y}\ \frac{\partial r_i}{\partial Z}\right] \tag{A-62}$$

$$\frac{\partial \delta_i}{\partial Z} = \frac{1}{r_i \cos\delta_i}\left[1 - \left(\frac{\partial r_i}{\partial Z}\right)^2\right] \tag{A-63}$$

$$\frac{\partial \delta_i}{\partial \dot{X}} = 0 \tag{A-64}$$

$$\frac{\partial \delta_i}{\partial \dot{Y}} = 0 \tag{A-65}$$

$$\frac{\partial \delta_i}{\partial \dot{Z}} = 0 \tag{A-66}$$

$$\frac{\partial \alpha_i}{\partial X} = +\frac{1}{r_i \cos\delta_i}[\sin(\Theta_i - \alpha_i)] \tag{A-67}$$

$$\frac{\partial \alpha_i}{\partial Y} = -\frac{1}{r_i \cos\delta_i}[\cos(\Theta_i - \alpha_i)] \tag{A-68}$$

$$\frac{\partial \alpha_i}{\partial Z} = 0 \tag{A-69}$$

$$\frac{\partial \alpha_i}{\partial \dot{X}} = 0 \tag{A-70}$$

$$\frac{\partial \alpha_i}{\partial \dot{Y}} = 0 \tag{A-71}$$

$$\frac{\partial \alpha_i}{\partial \dot{Z}} = 0 \tag{A-72}$$

APPENDIX B

Basis for Corrections for Refraction

Consider an electromagnetic signal of given frequency sent from a probe to a receiving station fixed on the surface of the Earth. Assume an index of refraction

$$n = n(h) \tag{B-1}$$

where $h = R - R_i$. Suppose that the position of the probe (in the azimuth plane) at time t, relative to the observation station, is given by $R(t)$, $\gamma_i(t)$, where $R(t)$ is the distance to the probe from the center of the Earth and $\gamma_i(t)$ is the elevation angle relative to the station (see Fig. B-1).

Because of an index of refraction which varies with increasing h, the path taken by the signal will not, in general, be a straight line but rather some curve such as C. The path C can be determined by using Fermat's principle and applying the calculus of variations.

Suppose one considers a variety of paths between the probe and the observation station. Fermat's principle states that the path taken will be that path C for which

$$\delta \int_C dt = 0 \tag{B-2}$$

Multiplying by the velocity of light in vacuum, c, replacing dt by ds/c' where c' is the velocity of light in the medium, and using the definition

$$n = c/c' \tag{B-3}$$

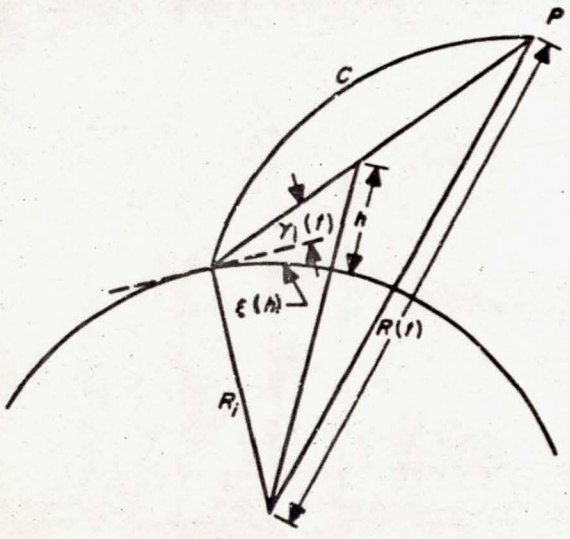

Fig. B-1. Path of electromagnetic signal

the relation (B-2) is replaced by

$$\delta \int_C n ds = 0 \tag{B-4}$$

Using the metric

$$ds^2 = |h^2 + (R_i + h)^2 (d\tau^*)^2 \tag{B-5}$$

where τ^* is the central angle (see Fig. B-2), (B-5) becomes

$$\delta \int_C n \sqrt{1 + (R_i + h)^2 \left(\frac{d\tau^*}{dh}\right)^2}\, dh = 0 \tag{B-6}$$

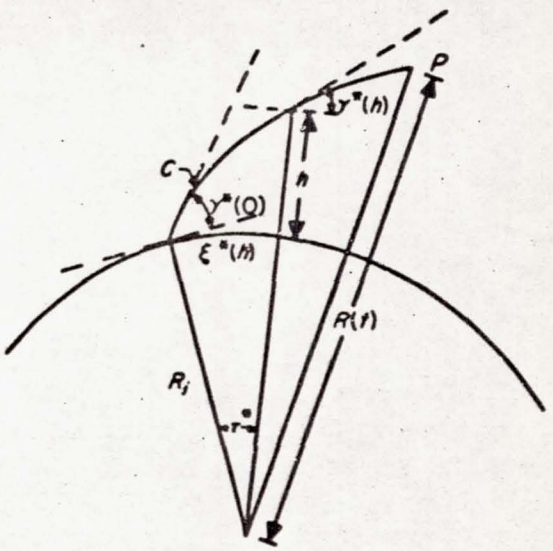

Fig. B-2. Apparent elevation angle

Applying the calculus of variations to (B-6), the result is

$$\frac{d}{dh}\left\{\frac{n(R_i + h)^2 \left(\frac{d\tau^*}{dh}\right)}{\left[1 + (R_i + h)^2 \left(\frac{d\tau^*}{dh}\right)^2\right]^{1/2}}\right\} = 0 \tag{B-7}$$

Substituting

$$\gamma^*(h) = \operatorname{arc\,cot}\left[(R_i + h)\frac{d\tau^*}{dh}\right] \tag{B-8}$$

the result is

$$\frac{d}{dh}\left[n(R_i + h)\cos\gamma^*\right] = 0 \tag{B-9}$$

or

$$n(\dot{\rho}) \cdot (R_i + h) \cdot \cos\gamma^*(h) = n(0) \cdot R_i \cdot \cos\gamma^*(0) \qquad \text{(B-10)}$$

If the variable $\xi^* = R_i\,\tau^*$ is introduced, Eq. (B-9) is replaced by

$$\frac{d\xi^*}{dh} = \frac{R_i}{R_i + h} \cot\gamma^*(h) \qquad \text{(B-11)}$$

where

$$\cos\gamma^*(h) = \frac{n(0)}{n(h)} \frac{R_i}{R_i + h} \cos\gamma^*(0)$$

If there were no atmosphere, $n(h)$ would always equal 1, and in this case, omitting the asterisk,

$$\frac{d\xi}{dh} = \frac{R_i}{R_i + h} \cot\gamma(h) \qquad \text{(B-12)}$$

where

$$\cos\gamma(h) = \frac{R_i}{R_i + h} \cos\gamma(0)$$

Since at time t,

$$\left.\begin{aligned} \gamma(0) &= \gamma_i(t) \\ \gamma^*(0) &= \gamma_i^*(t) \end{aligned}\right\} \qquad \text{(B-13)}$$

the determination of the apparent elevation angle $\gamma_i^*(t)$ from given $R(t)$ and $\gamma_i(t)$ consists of finding the initial condition $\gamma^*(0)$ which is needed in order that the integration of (B-11) gives a value of

$$\xi_p^* = \int_0^{R(t)-R_i} \frac{R_i}{R_i + h} \cot\gamma^*(h)\,dh \qquad \text{(B-14)}$$

equal to the value obtained by integration of (B-12),

$$\xi_p = \int_0^{R(t)-R_i} \frac{R_i}{R_i + h} \cot\gamma(h)\,dh \qquad \text{(B-15)}$$

wherein the initial condition $\gamma(0) = \gamma_i(t)$ is used.

In terms of the variables ξ^* and ξ, it is evident from Fig. B-1 and B-2 that the above determination is equivalent to requiring

$$\xi^*|_{h=R(t)-R_i}| = \xi_{h=R(t)-R_i} \qquad \text{(B-16)}$$

a condition which must hold if C intersects the straight line path to the probe at the probe.

The numerical accomplishment of the determination can be done in the following manner:

A sequence of angles

$$\gamma^{*(1)}(0), \gamma^{*(2)}(0), \gamma^{*(3)}(0), \cdots, \gamma^{*(k)}, \cdots \qquad \text{(B-17)}$$

is built up by using

$$\left.\begin{aligned} \gamma^{*(1)}(0) &= \gamma_i(t), \text{ in degrees} \\ \gamma^{*(2)}(0) &= \left(1.5 + \frac{88.5}{90}\gamma_i(t)\right), \text{ in degrees} \end{aligned}\right\} \qquad \text{(B-18)}$$

Integrals of type (B-14) are obtained with each of these initial conditions, giving, respectively,

$$\xi_p^{*(1)} \qquad \text{(B-19)}$$

and

$$\xi_p^{*(2)} \qquad \text{(B-20)}$$

Using the integral (B-15), the differences

$$\xi_p - \xi_p^{*(1)} \leq 0 \qquad \text{(B-21)}$$

and

$$\xi_p - \xi_p^{*(2)} \geq 0 \qquad \text{(B-22)}$$

are formed.

If $\xi_p - \xi_p^{*(1)} = \xi_p - \xi_p^{*(2)} = 0$, $\gamma_i^*(t) = \gamma_i(t) = 90$ deg. Otherwise, with $k = 3$, use

$$\gamma^{*(k)}(0) = \frac{|\xi_p - \xi_p^{*(2)}|\,\gamma^{*(1)}(0) + |\xi_p - \xi_p^{*(1)}|\,\gamma^{*(2)}(0)}{|\xi_p - \xi_p^{*(1)}| + |\xi_p - \xi_p^{*(2)}|} \qquad \text{(B-23)}$$

Evaluate the integral of type (B-14) with initial condition $\gamma^{*(k)}(0)$, to obtain $\xi^{*(k)}$. If

$$|\xi_p - \xi_p^{*(k)}| > \epsilon \qquad \text{(B-24)}$$

where ϵ is some preassigned small non-negative number (in practice ϵ is usually not chosen equal to zero), then, on the right side of (B-23), substitute the difference $\xi_p - \xi_p^{*(k)}$ for the previous difference having the same sign and substitute $\gamma^{*(k)}(0)$ for the corresponding angle. On the left side of (B-23), increase k by one, and repeat the process until a value of $\xi_p^{*(k)}$ is obtained such that

$$|\xi_p - \xi_p^{*(k)}| \leq \epsilon \qquad \text{(B-25)}$$

The corresponding value of $\gamma^{*(k)}(0)$ is then used as $\gamma_i^*(t)$.

It is evident that the value of $n(h)$ must be provided. For the current program, the assumption has been made that $n(h)$ is of the form

$$n(h) = 1 + 10^{-6} G_i\, e^{-Ah} \qquad \text{(B-26)}$$

where, if h is measured in statute miles,

$$A = 0.22$$

and G_i represents the surface refractivity for the ith observation station.

APPENDIX C

Output Format

The output is composed of three groups; the formats are given in this appendix. Group 1 is the normal trajectory output; group 2 is the output obtained from the least-squares fit; group 3 is the off-line output obtained from the sense-switch 3 option. In group 1, the last line of output is obtained only if the option to compute the "standard deviations of the predictions" is used (see quantity 27). In group 2, A^{-1} is printed as a 6×6 matrix if the rightmost 6 bits of the matrix control word are zero. Otherwise, A^{-1} is printed as a 12×12 matrix with each two lines of printing representing one row of matrix.

GROUP 1

GMT		GMT-t_0			Year
R	v	ϕ	θ	γ	σ
γ_c	σ_c	$\measuredangle c, R$	GHA $\Omega(t)$	Θ	V
X	$\dot{X}$	X	x	$\dot{x}$	C_1
Y	$\dot{Y}$	Y	y	$\dot{y}$	C_2
Z	$\dot{Z}$	Z	z	$\dot{z}$	C_3
Name of *N*th Body					
X_n	$\dot{X}_n$	R_n	r_n	$\measuredangle c, R_{pn}$	$\measuredangle \mathbf{R}_{pn}, \mathbf{R}_{ns}$
Y_n	$\dot{Y}_n$	ϕn	$\dot{r}_n$	$\measuredangle (c, \mathbf{V} - \mathbf{V}_n)$	V_n
Z_n	$\dot{Z}_n$	θ_n	$\lvert \mathbf{V} - \mathbf{V}_n \rvert$	$\measuredangle \mathbf{R}_{En}, \mathbf{R}_{Ep}$	0
Name of *i*th Station					
	α_i	δ_i	σ_i	γ_i	f_i
	$\dot{\alpha}_i$	$\dot{\delta}_i$	$\dot{\sigma}_i$	$\dot{\gamma}_i$	$\dot{r}_i$
	$\measuredangle c, \mathbf{R}_{ip}$	$\measuredangle \mathbf{R}_{ip}, \mathbf{R}_{is}$	ϕ_i	θ_i	r_i
Name of *i*th Station					
D_1	D_2	D_3	D_4	D_5	D_6

GROUP 2

Normalization with Sigma

Name of *i*th Station	Sigma 1	Sigma 2	Bias	N
R	σ^{i1}	σ^{*i1}	Δr_i	N^{i1}
F	σ^{i2}	σ^{*i2}	Δf_i	N^{i2}
EL	σ^{i3}	σ^{*i3}	$\Delta\gamma_i$	N^{i3}
AZ	σ^{i4}	σ^{*i4}	$\Delta\sigma_i$	N^{i4}
DEC	σ^{i5}	σ^{*i5}	$\Delta\delta_i$	N^{i5}
HA	σ^{i6}	σ^{*i6}	$\Delta\alpha_i$	N^{i6}

Noise Moment Matrix

A^{-1}

Corrections to Initial Conditions

N_1	N_4	N_2	N_3	N_5	N_6
N_7	N_8	N_9	N_{10}	N_{11}	N_{12}
D_1	D_4	D_2	D_3	D_5	D_6
D_7	D_8	D_9	D_{10}	D_{11}	D_{12}

GROUP 3

GMT

$i \quad w^{ik} \quad \hat{F}^{ik} \quad \hat{F}^{ik} - \tilde{F}^{ik} \quad \tilde{F}^{ik} \quad \partial F^{ik}/\partial R_0$

$\partial F^{ik}/\partial \phi_0 \quad \partial F^{ik}/\partial \theta_0 \quad \partial F^{ik}/\partial \nu_0 \quad \partial F^{ik}/\partial \gamma_0 \quad \partial F^{ik}/\partial \sigma_0$

For each GMT and each i, these three lines will be repeated K times, where K is the number of data types from the ith station. Samples of the output are presented in Fig. C.

```
03 MAR 05 15 25          00 00 00                                  1959

 7 659009     5 106401    2 281818    3 285774    2 120342    2 934874
-6 543389     3 360000    2 900000    3 239093    3 164867    5 110540

 7-560743     4-499837    1 780841    7 157913    5 106086      455894
 7 151645     4-964715    1-211167    7-559010    3 654199     -123290
 7 311231     3 489722    1-434727    7 311231    3 489722      881453

MOON

 8-255926     4 103874    9 375142    9 377229    3 101052    3 104880
 9-355025     3-107687    2-184081    4-936332    2 955477    4 104438
 9-118463     2-124912    2 267840    5 114698    3 107990      000000

SUN

 12 140862    4 975523   12 148210   12 148216    2 689367      000000
 11-422834    5 260537    1-710677    4 244244    3 107071    5 300271
 11-183364    5 112990    3 104199    5 402912    3 158872      000000

HAWAII        3 227999    1 777193    2 650915   2-357255    9 960020
              3-129698    2-209660   2-566588    3-121810    4 943169
              3 100264    3 128348    2 188235    3 204315    7 780168

JODRELL BANK  3 110121    3 341444    3 274454   2-267660    9 960065
              3-335187    2-337859    3-299684    3 174695   4-456593
              3 129223    3 135691    2 530510    3 357694    7 620343

CANAVERAL     3 284134    1 786064    2 896566    2 161304    5 104550
              3-470765    3-292280    2 478928    3-548468    5 104892
              2 924771    3 109543    2 282954    3 279420    6 669041

GOLDSTONE     3 256667    3 352092    2 888032   2-154199    5 105907
              3-158956    2 951701    3-173784   2-760349    4 999798
              3 110494    3 116107    2 352070    3 243152    7 408132

PUERTO RICO   3 111951    2 556770    3 328410    1 329563    5 122655
              3 151360    4 135059    4 123029    3 567065   4-561316
              2 371607    2 881727    2 180650    3 292911    7 137767
```

Fig. C-1. Samples of format

NORMALIZATION WITH SIGMA

PUERTO RICO	SIGMA1	SIGMA2	BIAS	N
R	.0000	.0000	.0000	
F	.0000	.0000	.0000	
EL	2.1686	.0248	.0000	30
AZ	.5713	.0211	.0000	30
DEC	.0000	.0000	.0000	
HA	.0000	.0000	.0000	

GOLDSTONE	SIGMA1	SIGMA2	BIAS	N
R	.0000	.0000	.0000	
F	.0000	.0000	.0000	
EL	.0000	.0000	.0000	
AZ	.0000	.0000	.0000	
DEC	4.2864	.0041	.0000	10
HA	6.3258	.0055	.0000	10

NOISE MOMENT MATRIX

9 453242	4 146721	3-825884	6 696876	5-148040	3-922859
4 146721	-1 217607	-2-792041	1 804976	-1-653040	-1 308419
3-825884	-2-792041	-2 683842	1-597993	-1 454346	-2 168771
6 696876	1 804976	1-597993	4 687693	2-348524	1-215197
5-148040	-1-653040	-1 454346	2-348524	634947	-1 571974
3-922859	-1 308419	-2 168771	1-215197	-1 571974	.145895

CORRECTIONS TO INITIAL CONDITIONS

6 126241	3-121620	555782	-101311	1-431624	1 123789
000000	000000	000000	000000	000000	000000
5 212895	2 829272	147515	-1 826947	796836	381963
000000	000000	000000	000000	000000	000000

Fig. C-1. Samples of format (cont'd)

```
03 MAR 05 17 11
 1  1 10000   5 11435000   3 15050000   5 11284500  -3 74873738
 3-32386463   3 80175083   1 12017831   2 29025449   3-10357997

03 MAR 05 17 11
 1  1 10000   2 19500000   1 12094400   2 16290560  -4 44734961
 1-25922729    81205436  -2 15734382    83152147     42405450

03 MAR 05 17 11
 1  1 10000   2 17508000    -84399700   2 18351997  -5-81731311
 1-15683623   1 52092538  -2 48278849    -44148571     21275023

03 MAR 05 17 21
 1  1 10000   5 11355000   3 15025000   5 11204750  -3 40256253
 3-36546930   3 72706720   1 12620384   2 19458219   2-86128892

03 MAR 05 17 21
 1  1 10000   2 20252000    84741807   2 19404582  -4 43198870
 1-25565827   1-10298101  -2 14982958    88608335     45780827

03 MAR 05 17 21
 1  1 10000   2 22324000    -85982084   2 23183621  -5-84777583
 1-20039277   1 49194936  -2 49916649    -47395046     31075049

03 MAR 05 17 31
 1  1 10000   5 11282000   3 14850000   5 11133500  -3 11683992
 3-39027717   3 65036476   1 12974494   2 10769599   2-70157784

03 MAR 05 17 31
 1  1 10000   2 20816000    51687098   2 20299129  -4 41615510
 1-24781614   1-12205844  -2 14011162    93448831     48221737

03 MAR 05 17 31
 1  1 10000   2 26908000    -82308936   2 27731089  -5-86320892
 1-23647999   1 45882686  -2 50647464    -49873461     40777286

03 MAR 05 17 41
 1  1 10000   5 11217000   3 14575000   5 11071250  -3-10820597
 3-40096569   3 57591097   1 13135474   1 31410656   2-56113612

03 MAR 05 17 41
 1  1 10000   2 21204000    21026969   2 20993730  -4 40030438
 1-23693790   1-13801022  -2 12944934    97697803     49789397

03 MAR 05 17 41
 1  1 10000   2 31196000    -77243805   2 31966438  -5-86572025
 1-26501107   1 42358952  -2 50603247    -51623899     50020243
```

Fig. C-1. Samples of format (cont'd)

Evaluation of *Pioneer IV* Orbit-Determination Program[1]

M. EIMER AND Y. HIROSHIGE
Jet Propulsion Laboratory, Pasadena, Calif.

ABSTRACT

The orbit-determination computing program is evaluated in terms of its effectiveness on the *Pioneer IV* shot. The tracking net used for *Pioneers III* and *IV*, including details of the Goldstone antenna, is described briefly. Then the real time operation of the system is analyzed with regard to the time and effort required to produce predictions and the accuracy thereof. Causes of trouble (particularly biases in the antenna alignment equipment) are diagnosed and remedies are proposed.

I. INTRODUCTION

In December of 1958 and again in March of 1959, NASA employed the *Juno II* rocket system for the third and fourth attempts on the part of the U.S. to place a scientific payload on an escape trajectory in the vicinity of the Moon. The missile used in the December firing failed to achieve escape velocity, and the payload, *Pioneer III*, achieved a maximum distance from the center of the Earth of a little over 100,000 km. The cosmic-ray data from *Pioneer III* revealed the existence of a second Van Allen radiation belt at a higher altitude than that discovered by the satellite *Explorer I*.

The later attempt, the following March, was more successful. The payload *Pioneer IV* passed the Moon at a distance of approximately 60,000 km and continued on to an interplanetary orbit with a period around the Sun of 395 days.

[1]This paper presents the results of one phase of research carried out at the Jet Propulsion Laboratory, California Institute of Technology, under Contract No. NASw-6, sponsored by the National Aeronautics and Space Administration.

During the 80 hr of its battery life, this payload transmitted to Earth new information on the extent and nature of cosmic radiation in space, indicating variations on both the extent and intensity of the high-altitude Van Allen radiation belt. Data were received to a range of 650,000 km.

Information on the position and speed of the probe and the telemetered scientific data were received and processed by a tracking and data handling network. The major requirements placed upon this network were:

1. To provide continuous reception of telemetering data to approximately 100,000 km from the Earth in order to receive cosmic-ray data from the outer radiation bands.
2. To provide at least intermittent reception of telemetering information to distances beyond the Moon.
3. To make precision angular measurements required for accurate determination of the flight paths of the probes.

In addition, the concepts and the basic hardware of the system could be utilized in the future evolution of a deep-space network which would meet the tracking, data handling, and computational requirements of more sophisticated deep-space experiments.

The deep-space tracking network being developed by the Jet Propulsion Laboratory (JPL) for the National Aeronautics and Space Administration (NASA) in cooperation with other countries around the world will make use of installations similar to those described in this paper. This network and the elements of which it is composed are being designed for the primary purpose of obtaining radioed data on position and telemetered measurements from lunar, interplanetary, and planetary flights.

II. NETWORK CONFIGURATION

The primary data-acquisition and tracking network consisted of a set of receiving stations, which were connected to a data-processing center by teletype and voice communications, and a number of cooperating tracking stations and computing centers. The primary net was established by JPL and utilized (Fig. 1):

1. Tracking stations at the launch site at Cape Canaveral, Florida, at Mayaguez, Puerto Rico, and at Goldstone Lake, California.
2. A data-processing and computing center at Pasadena, California.
3. Message centers at Pasadena and Cape Canaveral.

The function of the launch-site station was to check out the payload radio equipment prior to launch and to provide telemetry reception and one-way doppler during the first 10 to 15 min of flight. This station utilized a narrow-band phase-locked receiver with a manually directed relatively broad-beam antenna. For the *Pioneer IV* trajectory, the vehicle disappeared below the horizon 10 to 15 min after launching. Shortly before the time of loss at the

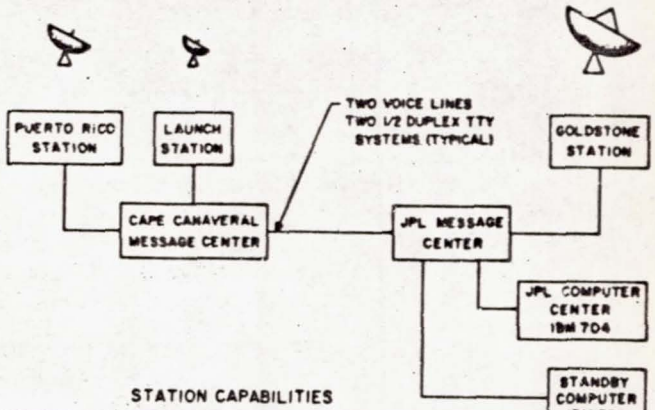

STATION CAPABILITIES

STATION	RANGE CAPABILITY (FOR 200 mw)	FUNCTIONS
LAUNCH	10^6 km	TELEMETRY, DOPPLER
PUERTO RICO	1.6×10^7 km	TELEMETRY, DOPPLER ANGLES 0.1-1° ACCURACY
GOLDSTONE	1.8×10^8 km	TELEMETRY, DOPPLER ANGLES .01-.1 ACCURACY

Fig. 1. Basic tracking network for *Pioneers III and IV*

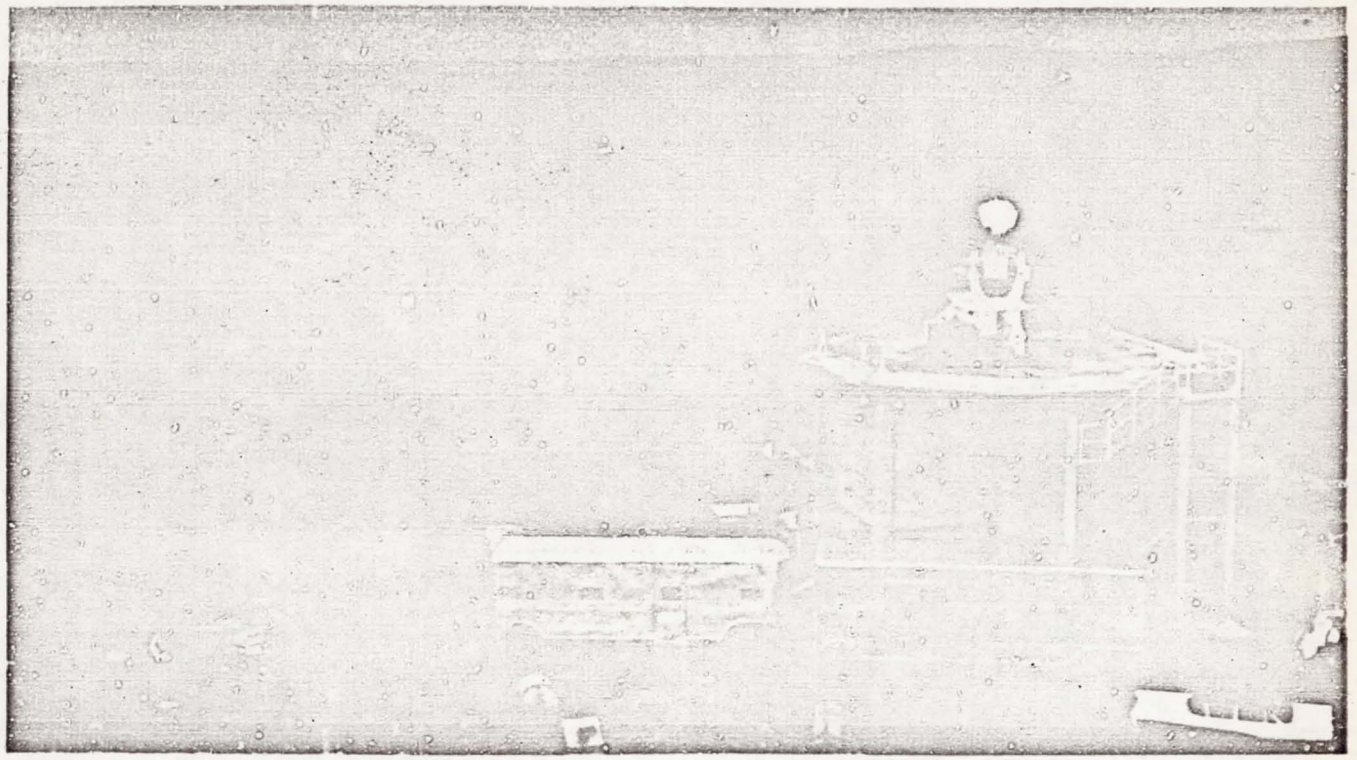

Fig. 2. Puerto Rico downrange tracking station

launch site, approximately 6 min after liftoff, the vehicle appeared on the northwest horizon at the Puerto Rico station and that station acquired the signal.

The Puerto Rico station has a narrow-band phase-locked receiver which is used in conjunction with a 10-ft-diameter automatic tracking antenna mounted on a modified Nike az-el antenna pedestal (Fig. 2). Data provided by the station include vehicle coordinates (az-el), one-way doppler, and telemetry.

After approximately 6½ hr of tracking by the Puerto Rico station, the vehicle appeared on the southeast horizon at Goldstone Lake and that station acquired the signal (Fig. 3). At that time, the probe was approximately 80,000 km from the Earth, still high in the sky at Puerto Rico, and providing a signal considerably above the threshold of the Puerto Rico station receiver.

The Goldstone station, which will be described in some detail, has a phase-locked receiver used in conjunction with an 85-ft-diameter polar-mounted tracking antenna. Basic data provided by the Goldstone installation are the same as provided by Puerto Rico: angular position, one-way doppler, and telemetry. The Goldstone station tracked the *Pioneer* probe from horizon to horizon, a period of about 9 hr. After the probe set in the west at Goldstone, it was not visible to that station for about 15 hr, after which time it was again acquired and tracked for another 9-hr period. This sequence was repeated for the life of the probe transmitter.

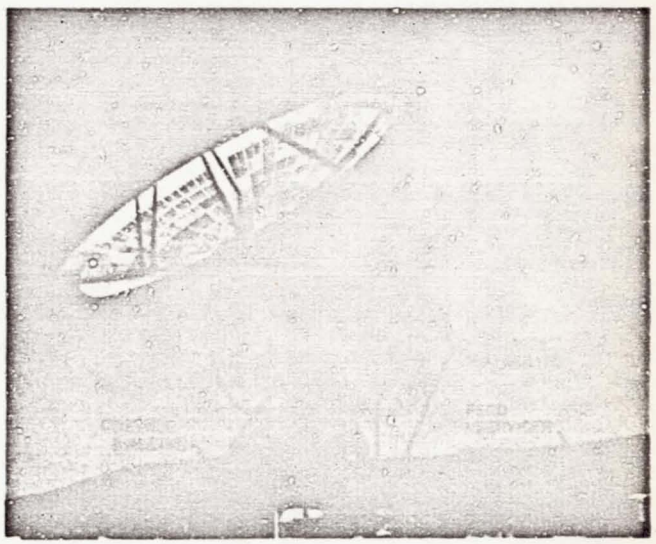

Fig. 3. Goldstone Lake tracking station

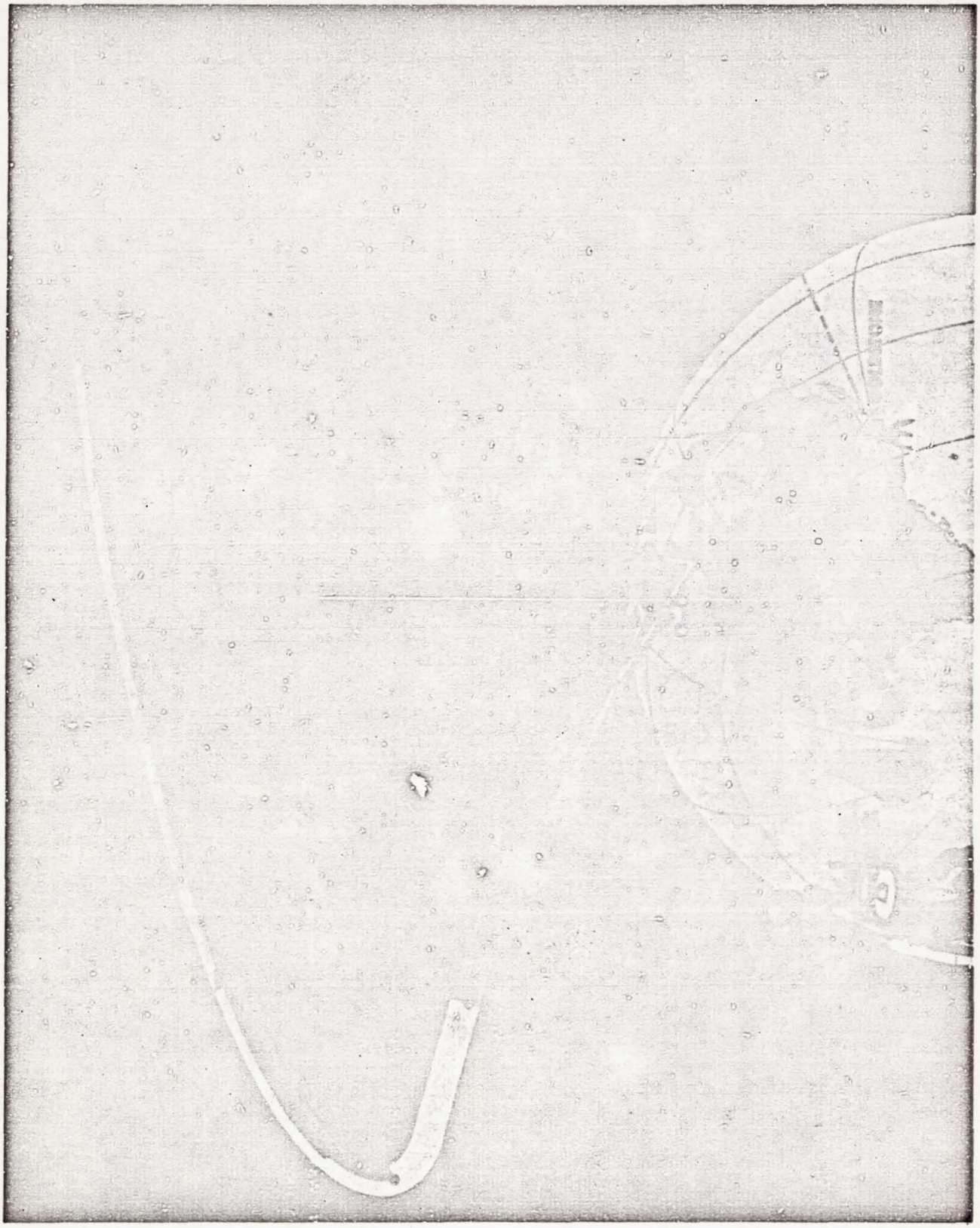

Fig. 4. Initial path of Pioneer Moon probe (Earth-fixed)

The tracking station coverage is shown pictorially in Fig. 4. Coverage by one of the major cooperating stations, the 250-ft-diameter Jodrell Bank radio telescope of the University of Manchester, in England, is indicated on this drawing. A less artistic but more technically factual representation of the coverage by the network is shown in Fig. 5.

The doppler data from all stations and the angular information from the Puerto Rico and Goldstone stations, tagged with the exact Greenwich Mean Time, were automatically encoded into standard teletype format and transmitted to the Computing Center in California (Fig. 6). Automatic teletype to IBM-card converters were used to put the received data into the proper machine input format.

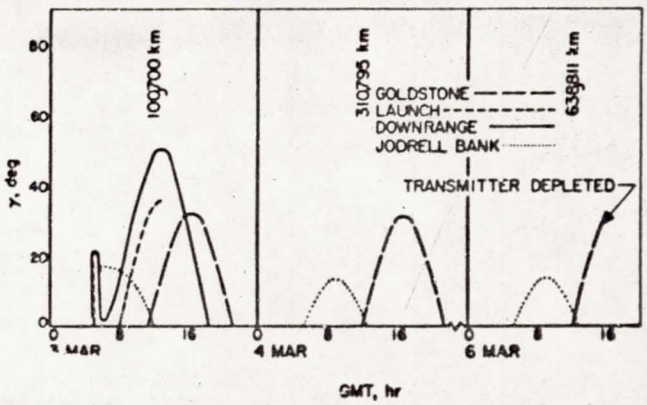

Fig. 5. Plot of elevation angle vs time for *Pioneer IV*

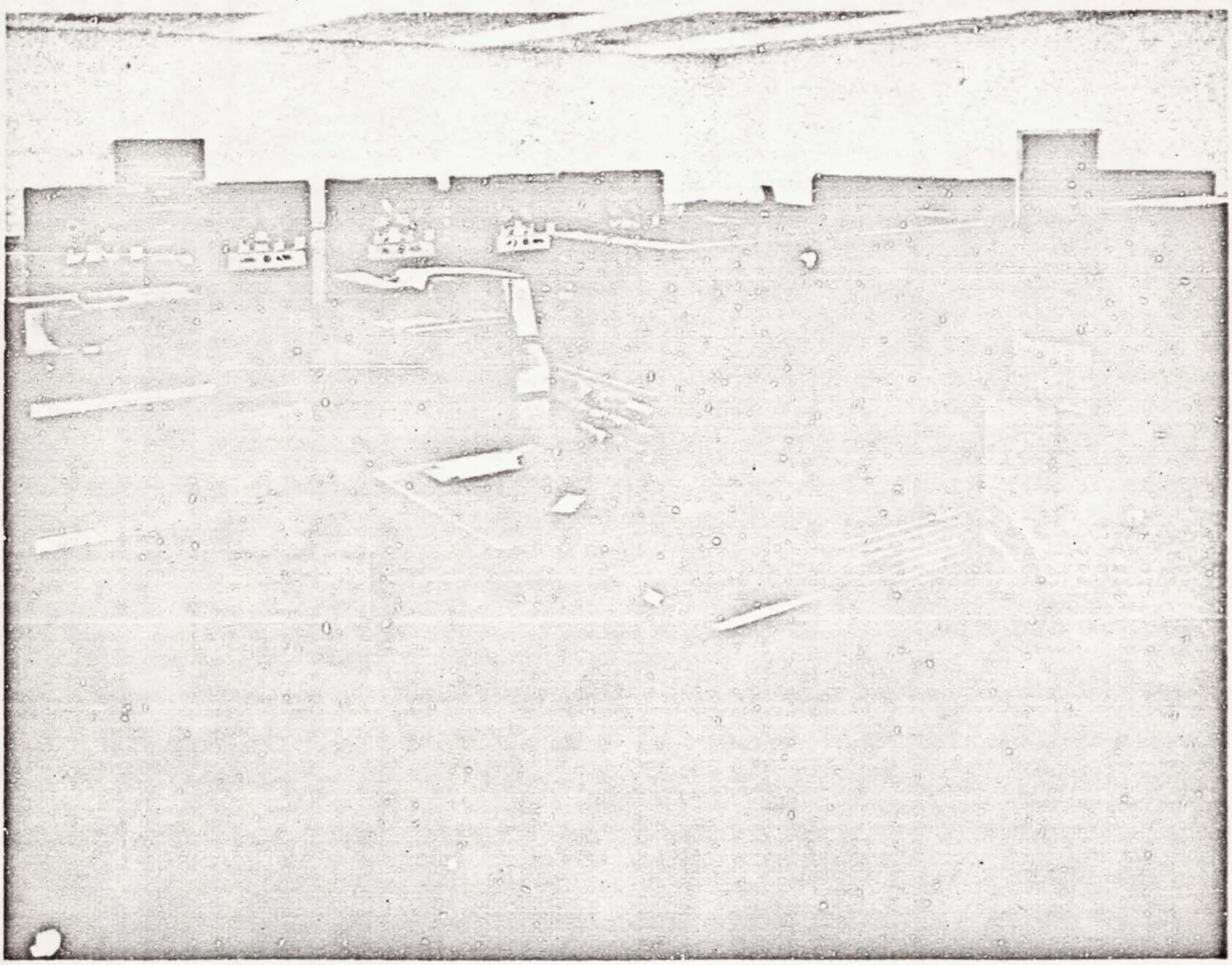

Fig. 6. Computing center for *Pioneers III* and *IV*

A sample of a data message received at the Computing Center from the Goldstone station is shown in Fig. 7. With machines adjusted for a transmission rate of 60 words/min, a single teletype line of data was transmitted in 7 sec. To facilitate the statistical evaluation of station performance after the completion of tracking, the comparatively high data-sampling rate of 6 samples/min was used throughout the *Pioneer IV* operation.

The Computing Center in Pasadena utilized primarily an IBM 704 computer. The computer results were monitored with several independent procedures using smaller electronic computers, desk calculators, and precomputed charts. The IBM 704 computer at the Rand Corporation in Santa Monica, California, served as backup. In the Computing Center the data were analyzed to provide rapid and precise acquisition pointing information for the tracking stations and accurate determination of the vehicle paths. The results of these computations were provided on IBM cards which were fed into a card-to-tape converter and transmitted to the appropriate tracking stations by teletype (Fig. 8).

STATION IDENTIFICATION	DATA CONDITION	GMT hr, min sec	GOLDSTONE HOUR ANGLE deg $\times 10^{-3}$	GOLDSTONE DECLINATION ANGLE deg $\times 10^{-3}$	COUNTED DOPPLER FREQUENCY, cps
2	0	151401	335476	336524	11337
2	0	151411	335508	336524	11336
2	0	151421	335556	336524	11336
2	0	151431	335648	336524	11337
2	0	151441	335736	336524	11338
2	0	151451	335828	336524	11336
2	0	151501	335848	336524	11337

Fig. 7. Sample of Goldstone data message

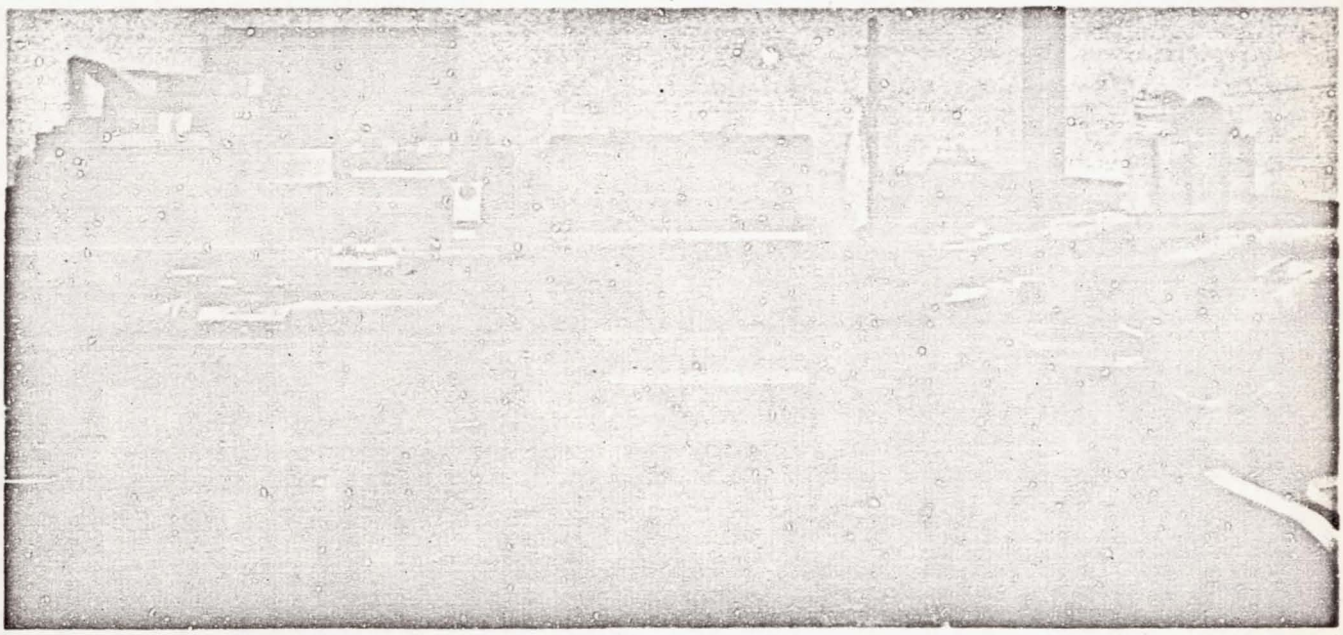

Fig. 8. Data handling facility

The standard acquisition message provides data in 1-min intervals. For long-range predictions less frequent intervals were used.

Figure 9 shows a sample of a standard message sent from the Computing Center to the Goldstone tracking station. The first four columns represent time, local hour angle, local declination angle, and counted doppler frequency in the same format and in the same coordinate system (including refraction corrections, etc.) as the expected data message. The remaining three columns represent local hour angle and local declination angle rates in thousandths of degrees per hour and range in kilometers.

The flow of data into and out of the Computing Center was regulated from a communications net control center located in the computer area which directed the switching of communications lines actually carried out by the two message centers located on the east and west coasts of the United States.

The primary tracking network was thus an almost completely automatic system which, when receiving a probe signal, would automatically count, encode, transmit, and convert tracking data, and then compute, convert, transmit, and display acquisition data. The only nonautomatic function in the system was the carrying of data cards the 25 ft between converters and machine input and output.

GMT hr, min sec	GOLDSTONE HOUR ANGLE deg $\times 10^{-3}$	GOLDSTONE DECLINATION ANGLE deg $\times 10^{-3}$	COUNTED DOPPLER FREQUENCY, cps	GOLDSTONE HOUR ANGLE RATE, deg $\times 10^{-3}$/hr	GOLDSTONE DECLINATION ANGLE RATE, deg $\times 10^{-3}$/hr	RANGE, km
131201	304776	336507	11329	015102	-00048	492858
131301	305027	336506	11329	015102	-00048	492954
131401	305277	336504	11329	015103	-00048	493050
131601	305779	336501	11329	015104	-00048	493242
131701	306029	336500	11329	015105	-00048	493338
131801	306280	336498	11329	015105	-00047	493435
131901	306531	336497	11329	015106	-00047	493531

Fig. 9. Sample of Goldstone acquisition message

III. GOLDSTONE TRACKING STATION

A description of the Goldstone facility will illustrate the degree of complexity of the stations in the *Pioneer III* and *Pioneer IV* network. Except for the larger antenna size and the greater permanency of the Goldstone station, the Puerto Rico and Goldstone installations are very similar. In particular, identical electronic equipment was installed at the two stations whenever feasible.

The Goldstone tracking antenna is 85 ft in diameter and is equatorially mounted. Significant parameters of the structure are:

1. Maximum tracking rate, 1 deg/sec in both axes.
2. Maximum acceleration, 5 deg/sec^2.
3. Accuracy of structure (constancy of axes alignment, etc.), on the order of 1 min of arc.

The drive system has two speeds of operation: a high speed of 1 deg/sec for satellite tracking and a low speed capable of tracking the range which might be encountered with a space vehicle—0.1 to 0.005 deg/sec.

The feed for the 85-ft-diameter antenna was a simultaneous-lobing type, using four circularly polarized turnstile radiators located in front of a ground plane. The outputs of the individual radiators are combined in coaxial hybrids to derive the hour-angle and declination error patterns and the reference channel pattern. The electrical performance of the antenna is as follows:

1. Gain, 41 db above linearly polarized isotrope.
2. Half-power beam width of reference channel, 0.9 to 1.3 deg.

The radio receiver utilized with the 960-mc tracking system is a narrow-band phase-coherent double-conversion superheterodyne. It has three separate channels: a reference channel for detection of the carrier and telemetry signals and derivation of the coherent automatic gain control (AGC) and two similar error channels for the hour-angle and declination error signals from the simultaneous-lobing antenna. Parameters of the receiving systems can be adjusted to provide best performance for a particular mission. For the *Pioneer IV* tracking mission the significant characteristics of the receiver were:

1. Noise bandwidth at UHF, 20 cps.
2. Noise temperature of receiver, 1330°K.
3. Approximate receiver threshold, -154 dbm $= 4 \times 10^{-16}$ watts.

For the above parameters, the maximum range for the *Pioneer IV* transmitter of 200-mw transmitted power was approximately 1.6×10^6 km for a unity S/N on the carrier signal and about 20-db S/N in the angle track and AGC loops. During the last phase of the *Pioneer IV* transmission, as the radiated power of the vehicle transmitter fell off because of depletion of the batteries, the bandwidth of the receiver was changed to a 10-cps value which increased the receiver sensitivity to about -157 dbm. This is equivalent to a range capability of 2.2×10^6 km for a 200-mw transmitted power.

IV. DATA TRANSMISSION NETWORK

A communications system made up of voice and teletype facilities was established early in November 1958 to provide a reliable, rapid, and flexible means of transmission of digital data, technical information, and administrative messages between the various tracking stations, computing centers, and communications centers. This network provided full-time voice and 60-word/min teletype communication between stations at JPL, the Goldstone Lake tracking station, and the Atlantic Missile Range by means of trunk tielines with existing administrative exchanges at these areas. The Mayaguez tracking station was linked to the net through the submarine cable which extends from Cape Canaveral to the southeastern range stations.

The overall network, illustrated in Fig. 10, provided for at least two half-duplex teletype circuits and two voice circuits between all points, with switching capabilities at the two message centers to provide for any makeup from a single point-to-point connection to a full party line.

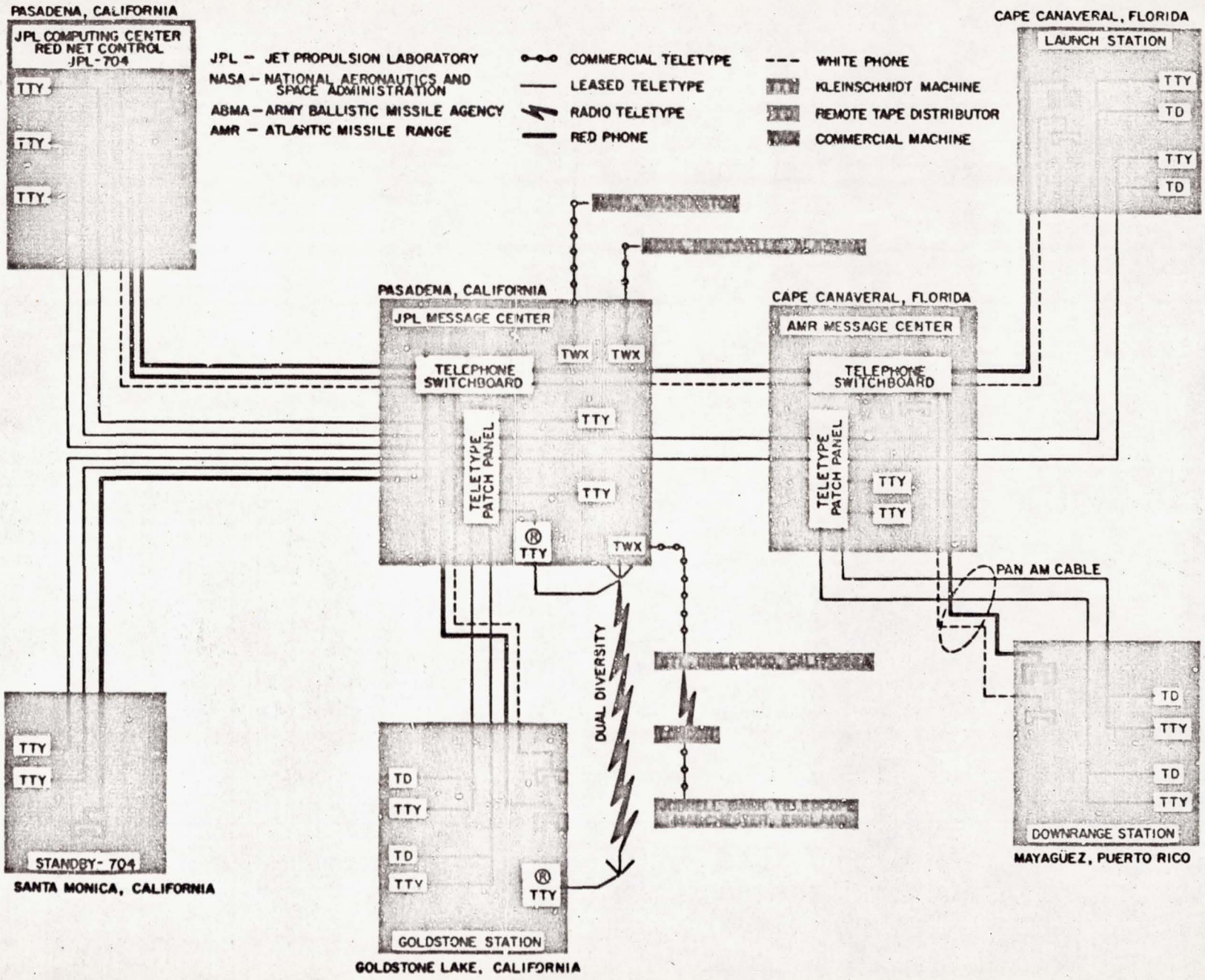

Fig. 10. Communications network for *Pioneers III and IV*

V. ANALYSIS OF THE TRACKING PROGRAM

The computing program was first constructed at JPL for the tracking of *Pioneer III*. Although the December 1958 *Pioneer III* firing date was only 2 months after the acceptance at the Laboratory of an IBM 704 computer, the program used contained most of the essential principles. During the period between the firings of *Pioneer III* and *Pioneer IV* (less than 3 months), the method of combining data from the various sources and the methods of relative weighting of the data were significantly altered. The recently completed program, described in the preceding paper (Carr–Hudson), is the result of major reorganization of the computing procedure and incorporation of extensions in the types and quantity of data to be handled.

During the flight of *Pioneer IV*, the tracking program gave excellent results. The first 15 min of data after last-stage burnout were used to make pointing predictions for the Puerto Rico station for a time 1 hr later than the last data point used. These predictions and all later predictions for Puerto Rico were subsequently found to agree with the observations to within less than 0.2 deg. The initial conditions, obtained with 15 min of data, differ from the present best estimate by 12 km in injection altitude and 30 m/sec in velocity.

With 3½ hours of data from Puerto Rico, an acquisition prediction was transmitted to the Goldstone station which agreed with subsequent observations to within 0.1 deg. The initial conditions obtained at that time differ from the present best estimates by 2 km in altitude, 0.05 deg in latitude and longitude, 5 m/sec in velocity, and 0.1 deg in the velocity angles. All predictions made after the first day of tracking, for periods 1 day later, were found to agree with the observations to within 0.05 deg. At the distance of the Moon, the accuracy of the probe position as determined by the tracking and computation network was estimated to be 100 km.

The fundamental assumptions made in the design of the tracking program relate to the statistical properties of the errors in the data. It was assumed that (1) the errors in the data are normally distributed, (2) the errors are not correlated in time, (3) the errors in the two angular coordinates at a station are not correlated, and (4) bias is a constant over any sampling interval.

Figures 11 and 12 show the errors in actual samples of data with respect to the computed trajectory for the flight of *Pioneer IV* at ranges of 100,000 and 500,000 km, respectively. At close tracking ranges several characteristics of the tracking system are discernible (see Fig. 11). The declination-angle error graph clearly shows the sawtooth form with slopes proportional to the angular rates which are caused by roundoff in the digital encoding system. The hour-angle graph (Fig. 11) shows a sinusoidal form with a period of 25 min which, it was subsequently found, was caused by an out-of-round component in the angular readout system. At the larger ranges, the dominant feature of the error graphs is the indication of a substantial increase in noise in the system (see Fig. 12). It is evident that not all the fundamental assumptions as to the statistical nature of the tracking data were completely justified.

A. Methods of Analysis

An analysis of angular tracking data from the Goldstone station consisted of (1) separating noise from bias, (2) computing the root-mean-square error, (3) determining the noise autocorrelation functions, (4) computing the power spectral densities, (5) determining the form of the error-distribution function, and (6) determining the correlation between the errors in the declination and the hour angles.

Items (1) through (5) were computed for the declination angle using the IBM 704 computer routine developed by R. Mosher and R. Southworth[3] assuming that the data were stationary over 2-hr periods for the entire duration of the tracking period. The data were then analyzed in groups of 2-hr periods.

The one-dimensional distribution function is computed in the usual manner by counting the number of samples in each of the preselected intervals of width ½ σ, where σ is the standard deviation from the mean, or

$$\sigma = \frac{1}{N}\left\{\sum_{i=1}^{N}\left[\Delta\delta_i - E(\Delta\delta_i)\right]^2\right\}^{\frac{1}{2}} \qquad (1)$$

where

$\Delta\delta_i$ = residuals, or the difference between the observed declination angle and that obtained from the fitted trajectory. (The fitted trajectory is the best fit through all the data points in the least-mean-squares sense.)

[3] *Auto-Correlation and Power Spectrum Analysis*, NYCP2, 704 Program Library, SBC NY Data Processing Center (IBM), April 25, 1957.

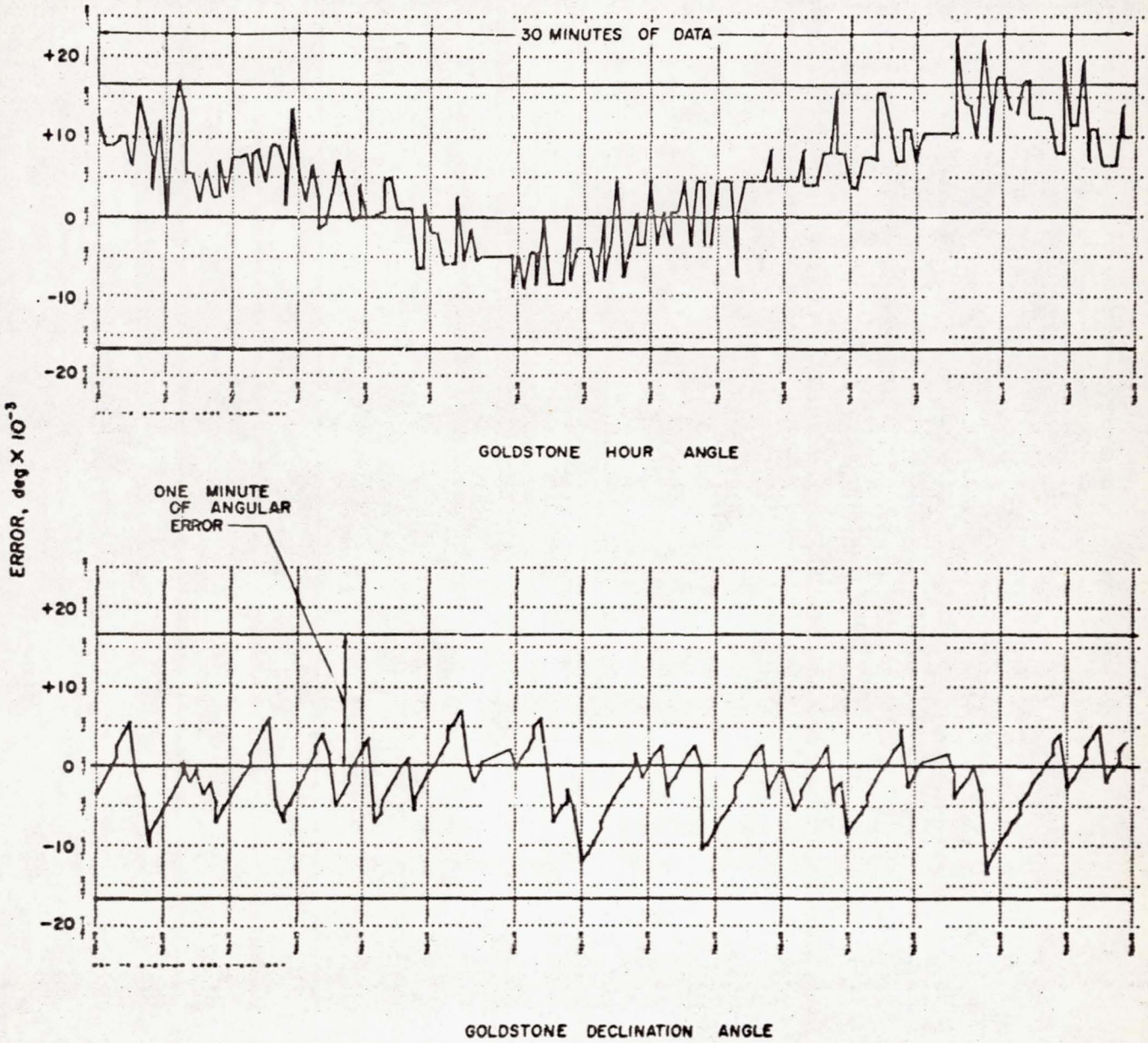

Fig. 11. Goldstone angular errors (100,000-km range)

$E(\Delta\delta_i)$ = average of the residuals.

N = number of samples.

The autocorrelation function R_p is computed from the following equation:

$$R_p = \frac{1}{N-p} \sum_{i=1}^{N-p} [\Delta\delta_i - E(\Delta\delta_i)]\,[\Delta\delta_{i+p} - E(\Delta\delta_i)]$$

$$p = 0, 1, \cdots, M \qquad (2)$$

where

M = number of lags.

The power spectrum, L_h, is computed from

$$L_h = \frac{2}{M}\left(R_0 + 2\sum_{p=1}^{M-1} R_p \cos\frac{\pi p b}{M} + R_m \cos \pi b\right)$$

$$b = 0, 1, \cdots, M \qquad (3)$$

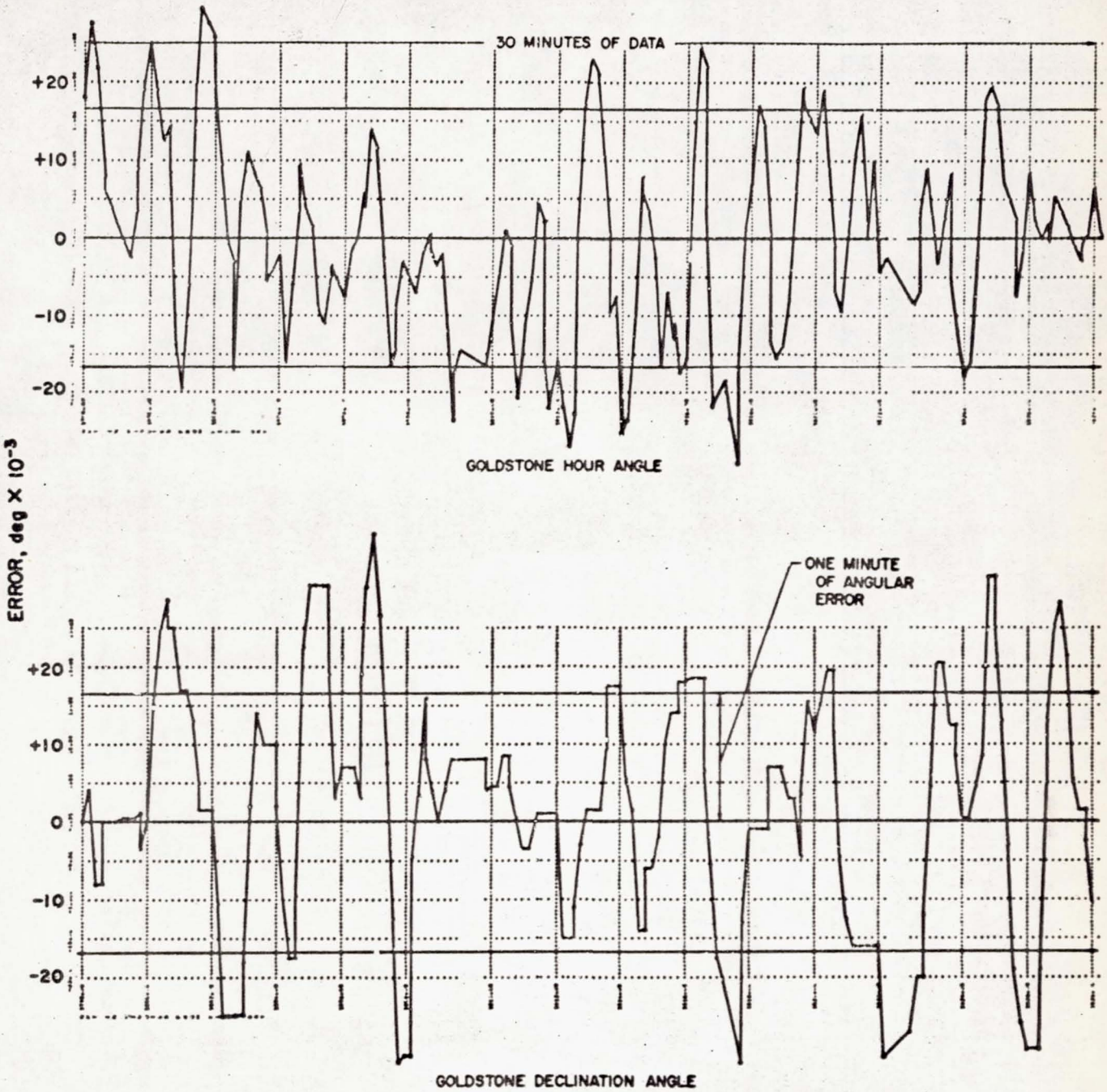

Fig. 12. Goldstone angular errors (500,000-km range)

The cross-correlation functions were computed for the residuals in the declination and the hour angles using the following equations:

$$R_{\Delta\alpha,\,\Delta\delta(p)} = \frac{1}{N-p}\sum_{i=1}^{N-p}\Delta\alpha_i\,\Delta\delta_{i+p} \qquad p = 0, 1, \cdots, M \tag{4}$$

$$R_{\Delta\delta,\,\Delta\alpha(p)} = \frac{1}{N-p}\sum_{i=1}^{N-p}\Delta\delta_i\,\Delta\alpha_{i+p} \qquad p = 0, 1, \cdots, M \tag{5}$$

where

$\Delta\alpha_i$ = residual in the local hour angle.

$\Delta\delta_i$ = residual in the declination angle.

The number of samples N were taken over time periods greater than 5 hr.

A linear relationship between the residuals may be obtained by passing a straight line through the $\Delta\alpha - \Delta\delta$ scatter diagram in the least-mean-square sense. Such a line is termed the "mean-square linear-regression line." In terms of normalized variables (ξ_i, η_i), the regression line is

$$\eta_i = \rho\xi_i \tag{6}$$

where

$$\eta_i = \frac{\Delta\delta_i - E(\Delta\delta_i)}{[E(\Delta\delta_i^2) - E(\Delta\delta_i)^2]^{1/2}} \tag{7}$$

$$\xi_i = \frac{\Delta\alpha_i - E(\Delta\alpha_i)}{[E(\Delta\alpha_i^2) - E(\Delta\alpha_i)^2]^{1/2}} \tag{8}$$

$$\rho = \frac{E(\Delta\delta_i\,\Delta\alpha_i) - E(\Delta\delta_i)\,E(\Delta\alpha_i)}{[E(\Delta\alpha_i^2) - E(\Delta\alpha_i)^2]\,[E(\Delta\delta_i^2) - E(\Delta\delta_i)^2]} \tag{9}$$

and $E(\ )$ denotes average of the quantity in parentheses. The numerical value of the correlation coefficient ρ is a measure of coherence between the two residuals of the angles and lies in the range

$$-1 \leq \rho \leq 1$$

For monotonically related samples, the coefficient of correlation generally gives a good measure of correlation.

B. Results of Analysis

1. The plot of average values of the residuals over each of the 2-hr intervals (see Fig. 13) shows that, over an entire day, the slope is nearly constant, and from day to day the slopes are nearly equal. The plot further shows that the curves are translated up or down in a random fashion from day to day.
2. The root-mean-square values of the errors over each of the 2-hr intervals computed from Eq. (1) are plotted in Fig. 14 as a function of time.
3. The power spectral-density plots computed from Eq. (3) show that about one-half of the noise power is concentrated in the frequency range of from 1/15 to 1/2 cpm for the first 1½ days, and from 1/5 to 1/2 cpm for the remainder of the record. A typical plot is presented in Fig. 15.
4. The autocorrelation function further reveals a harmonic component having a period of approximately 25 min. If it is assumed that this component can be taken out, the autocorrelation function can be represented approximately by an exponential func-

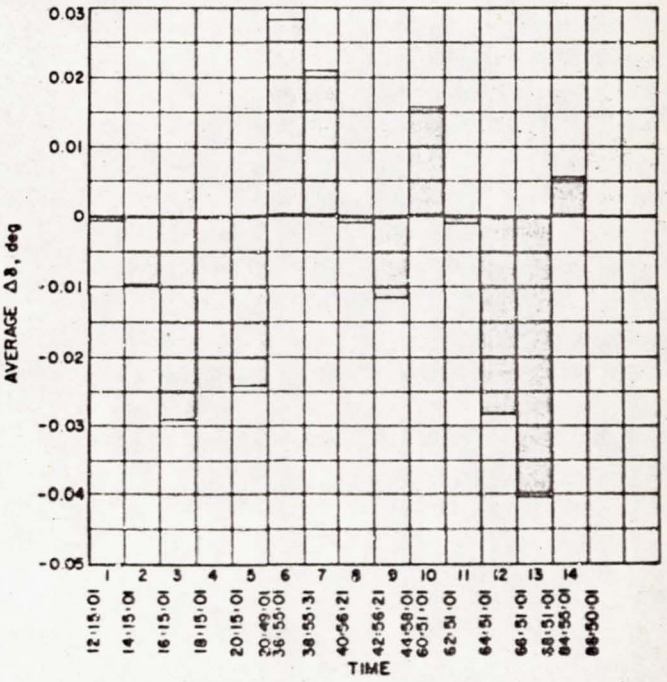

Fig. 13. Goldstone Δδ-average over 2-hr intervals

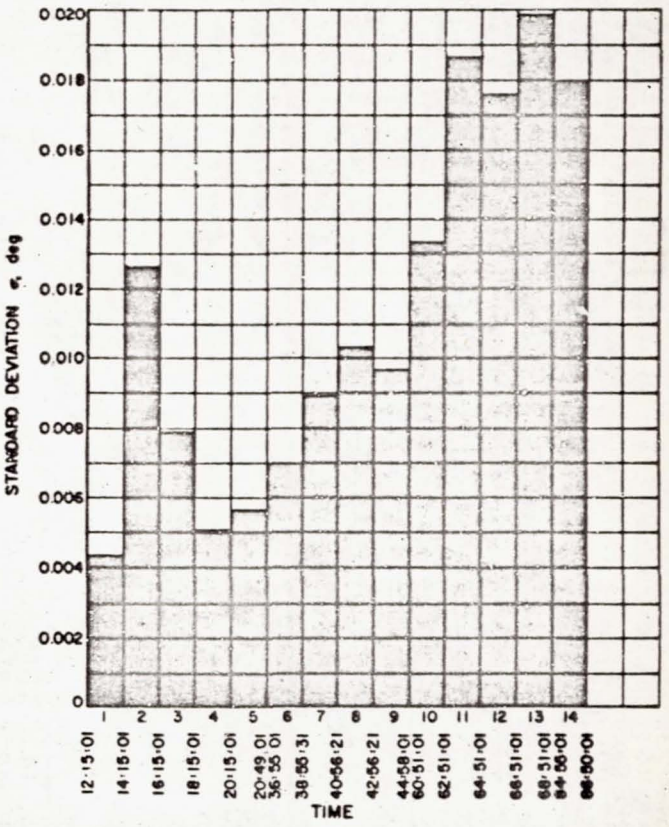

Fig. 14. Goldstone Δδ standard deviation

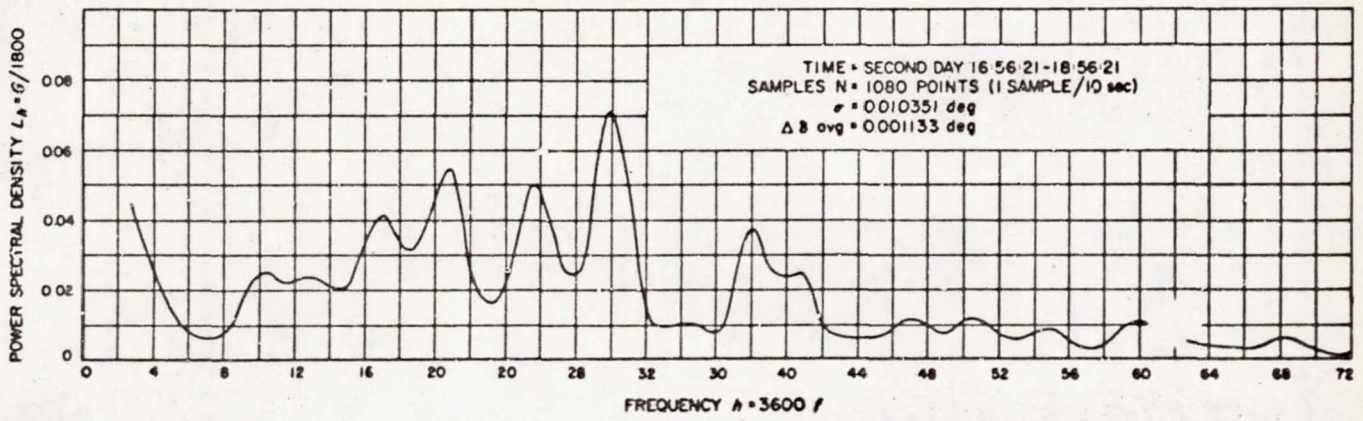

Fig. 15. Goldstone Δδ normalized power spectral density

tion having a time constant of 50 sec. Figure 16 shows a typical plot.

5. Table 1 is a summary of the correlation coefficient ρ, which is computed from Eq. (9), for the 3 days of tracking. It is noted that the linear correlation between the residuals of the declination and the hour angles is less than 10%. A typical plot of the cross-correlation function is presented in Fig. 17.
6. A study of the one-dimensional distribution functions (see Fig. 18 for a typical plot) and autocorrelation functions reveals that the errors in the angular data may be represented by a multivariate Gaussian distribution over each of the 2-hr intervals, or

$$p(y) = \frac{1}{[(2\pi)^N |M|]^{1/2}} e^{-\frac{1}{2}y^T M^{-1} y} \tag{10}$$

where

$$y = \begin{bmatrix} \Delta\delta_1 - E(\Delta\delta_i) \\ \Delta\delta_2 - E(\Delta\delta_i) \\ \cdot \\ \cdot \\ \cdot \\ \Delta\delta_N - E(\Delta\delta_i) \end{bmatrix} = \text{errors} \tag{11}$$

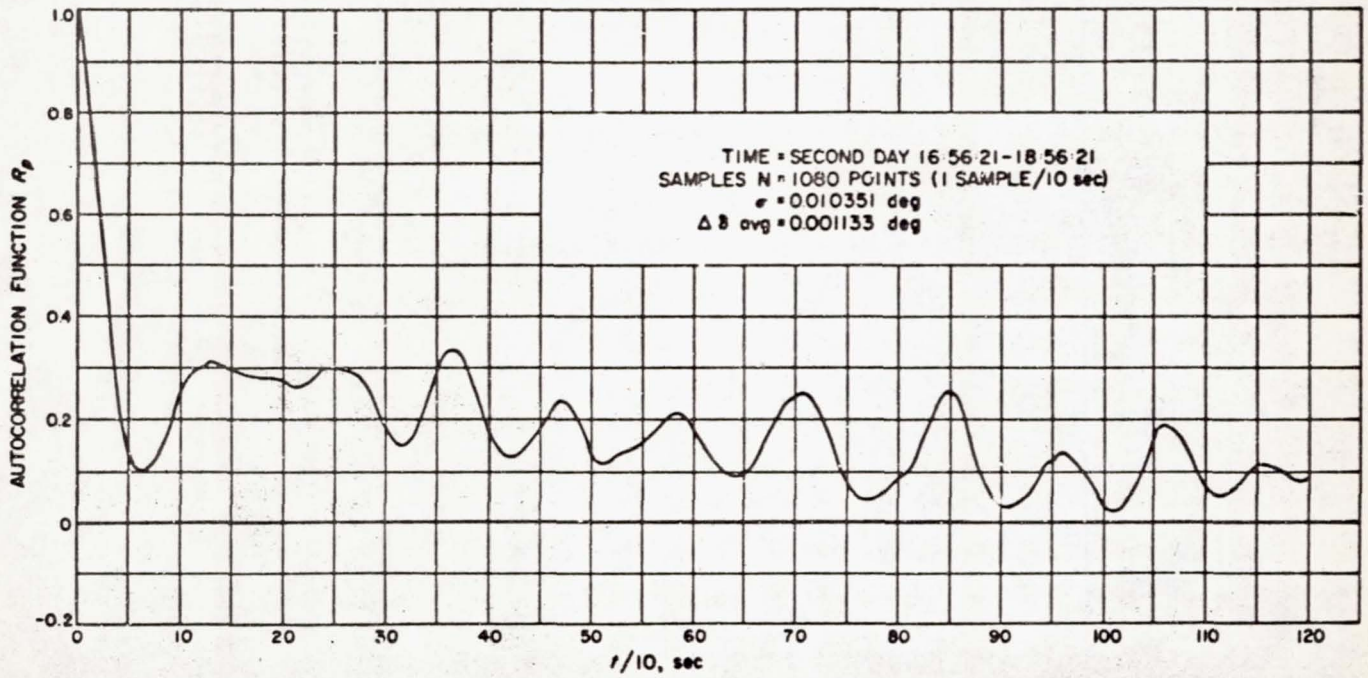

Fig. 16. Goldstone Δδ normalized autocorrelation function

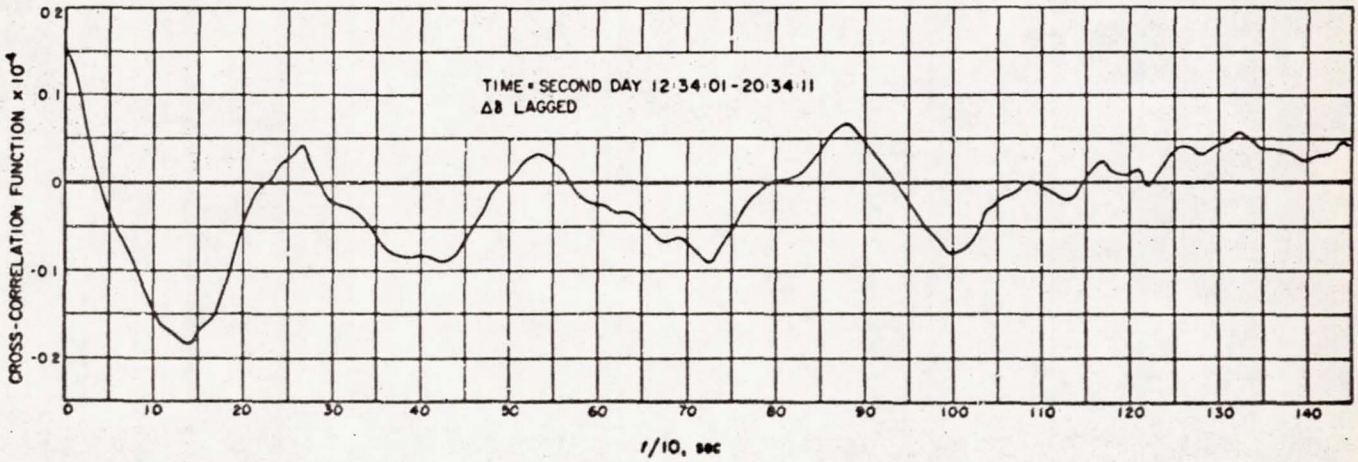

Fig. 17. Cross-correlation between $\Delta\alpha$ and $\Delta\delta$ *Pioneer IV* data from Goldstone

and M = moment matrix of the error which is obtained from the autocorrelation function.

For example, M may have the following form for the first two hours of tracking from the second day:

$$M = 10^{-4} \begin{vmatrix} 1 & 0.4 & 0.2 & 0.1 & 0 \cdots 0 \\ 0.4 & 1 & 0.4 & \diagdown & \diagdown \\ 0.2 & 0.4 & 1 & \diagdown & \diagdown \\ 0.1 & \diagdown & \diagdown & \diagdown & \diagdown \\ 0 & \diagdown & \diagdown & \diagdown & \diagdown \\ \vdots & & & & \\ 0 & \diagdown & \diagdown & \diagdown & 1 \end{vmatrix} \qquad (12)$$

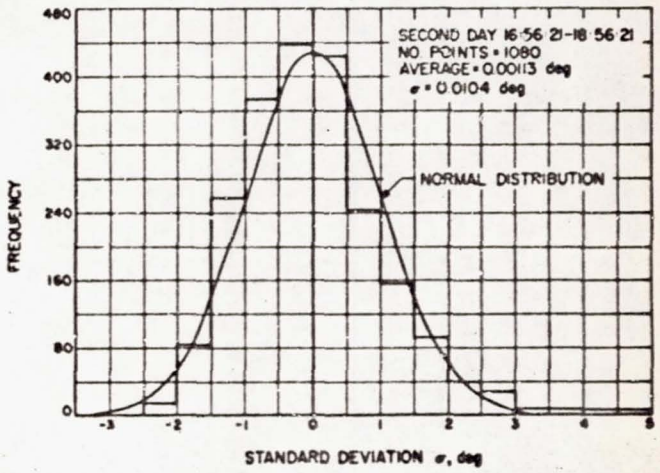

Fig. 18. Normalized distribution, Goldstone

C. Conclusions

From the analysis just described, it can be concluded that none of the four basic assumptions made with respect to the statistical nature of the data is completely justified. Although the errors appear to be normally distributed for data representing relatively short periods of time, a corollary to that assumption is that the data can be made homoscedastic by a proper selection of weighting factors.

The weighting factors which were used for *Pioneer IV* were those determined *a priori* from calibrated characteristics of the tracking stations. It is evident, however, that the deterioration in data expected from preflight calibrations did not correspond exactly to that observed in *Pioneer IV*. The weighting factors used were expressed as polynomials in range and elevation angle from the stations in question. The coefficients in the polynomial were, however, unfortunately different in flight than had been predicted.

Although it is evident that data sampled at the rate of one every 10 sec are correlated in time, during the flight of *Pioneer IV* the least-squares-fitting routines were applied to samples generally of not more than 1-min frequency. Thus, for the relatively slow data rates actually used, time correlation was apparently not a major problem.

Table 1 shows that a correlation actually did exist between the errors in declination angles and hour angles. However, the relatively small correlation factor of one tenth apparently did not affect the assumptions made.

The assumption of constancy of bias appears to have been violated in two major ways. On any one of the track-

Table 1. Correlation coefficients and expected values

Day	$E[\Delta\alpha_i]$	$E[\Delta\delta_i]$	$E[\Delta\alpha_i \cdot \Delta\delta_i]^{\frac{1}{2}}$	$E[\Delta\alpha_i^2]^{\frac{1}{2}}$	$E[\Delta\delta_i^2]^{\frac{1}{2}}$	ρ
1	−0.00187	−0.0103	0.0051	0.0086	0.0140	0.086
2	−0.00182	0.0098	0.0040	0.0117	0.0182	−0.012
3	−0.0021	−0.0093	0.0069	0.0170	0.0170	0.068

ing days, the bias appears to be representable by a constant plus a term which varies approximately linearly with hour angle. Preflight calibration of the Goldstone antenna, made by observing stars at various declinations through the boresight telescope, also shows angular errors which vary with local hour angle. As the biases must, in part, be the result of deflections in the dish structure, errors in the biases with respect to preflight calibrations may be the result of relative deflections between the RF and optical axes. The RF and optical axes are aligned using a collimation tower approximately 1 mile from the Goldstone dish. A further calibration of the RF axis is accomplished by tracking a helicopter-borne RF and optical target by means of the primary antenna and a precision optical theodolite.

The hour-angle dependent bias appears to be the result, in part, of dimensional discrepancies in the encoding system which will be removed by an improved position pickoff system. The dependent bias appears to be repeatable from day to day and amenable to preflight calibration.

The reason for the day-to-day variation of the numerically much larger constant-bias term is not presently known. The uncertainty in the determination of the magnitude of the constant bias using the tracking program during the flight of *Pioneer IV* is estimated to have been of the order of 1 min of arc.

In order to improve the reduction to homoscedasticity and facilitate the handling of ever greater quantities of tracking data, special data-handling techniques are presently being programmed for the computer. It is hoped that, in the future, all tracking data transmitted from the stations will be stored directly in the computer; that is, be independent of tape-to-card conversion.

In the simplest method of data compression presently being programmed, specified subsets of the total data stored can be selected and inserted into the tracking program. A second data-compression method, which utilizes least-mean-square polynomial fits to the raw data over predetermined time intervals, is used to insert one smoothed point per interval, as well as the standard deviation over that interval, into the orbit-determination program. The degree of the polynomials used and the intervals taken are determined, prior to flight, by matching the standard trajectory. The lower bound on length of time interval used is determined by the lowest expected noise frequency. For example, for *Pioneer IV*, a second- or third-degree polynomial would require time intervals greater than 11 or 22 min, respectively, as the lowest undesired frequency component was ½ cpm.

The third and most complex method of data compression presently being programmed also makes use of least-squares-fit polynomials to sections of the raw data. However, in this case, the polynomials used are determined by first fitting to the current best estimate of the flight trajectory, and then determining the constant of translation of this polynomial necessary to optimize the fit with respect to the raw data.

It is evident that in the first of the three methods of data compression a maximum amount of information is discarded for a specified rate of data insertion into the standard tracking program. Although the third method extracts a relatively large amount of information from the data received, it represents a significant complication in the machine computing program. It is not yet clear which method of data compression will yield the best results for a specified machine computing time.

The standard deviations obtained by polynomial fitting data-compression routines can be used to produce an essentially homoscedastic set. The standard deviation required to give the property correct relative weighting between data of various types and from various sources can be obtained in two ways: (1) It is assumed that the quality of a set of data is inversely related to its noise content. (2) It is assumed that the quality of the data is inversely related to the deviation of a set of points of one type from one station from the mean of all types of data from all stations.

It should be noted that, for *Pioneer III*, the noise standard deviation was used for the raw data weighting, and for *Pioneer IV* the standard deviation from the mean was used as a relative weighting. It is evident that occasions may arise when neither of these standard deviations should be used. In the first method, if the data

is smooth but biased, it is weighted too heavily. The second method represents the majority rule, which is not always right.

In order to minimize the expected difficulties with the relative weighting method used for *Pioneer IV*, a special subroutine was provided which, on command by means of a sense switch, would change all relative weightings to unity. Thus, if during the tracking procedure one data type is erroneously completely misfitted such that its standard deviation from the mean is much larger than all the other data types, the least-squares-fitting routine will only slowly converge to include the misfitted data type. In order to accelerate this convergence, the reduction of the relative weighting to unity is used for one or two iterations and then removed to complete the convergence using the proper relative weighting. It should be noted that close agreement between the standard deviations from the mean and the noise standard deviations obtained by fitting separately to each data type is a good indication of convergence of the iteration process.

The most serious unresolved problem in the tracking program is a proper determination of the degree of degeneracy of the matrix involved in the solution for the changes in initial conditions. Such degeneracy occurs either because of inadequacies in the calculation of the partial derivatives or a partial or complete degeneracy in the tracking geometry. It is evident that both of these sources of difficulties are related in the sense that it is more difficult to compute partial derivatives when the tracking geometry becomes weak or degenerate. For example, with the probe far from the center of the Earth, angle data alone cannot be used to compute distance from the station. Similarly, range rate or range data cannot be used to compute the angular position.

For *Pioneer IV*, difficulties with degenerate matrices were avoided primarily by applying the experience gained during preflight practice runs on the computer using simulated tracking data. In the procedure evolved during these practice runs, the order of the matrix used varied from 3 to 8 as a function of quality and quantity of data. During the early part of the flight, when the data were primarily from Puerto Rico, the maximum number of initial conditions solved for at any one time was three. The particular set of coordinates used was alternated essentially between the position and velocity coordinates. During the later portions of the flight, when substantial quantities of Goldstone data were available, the changes in all six of the initial conditions could be solved for in addition to two of the biases.

With the increasingly complex geometries and the increasing quantities of data to be expected in future flights, analytical procedures must be made available for determining the size of the largest nondegenerate matrix. It is in this area that the present tracking program has its greatest weakness and would most benefit from improvement of the program.

Satellite Orbit Determination and Prediction Utilizing JPL Goldstone 85-ft Antenna and the JPL Tracking Program[1]

DUANE MUHLEMAN

Jet Propulsion Laboratory, Pasadena, Calif.

ABSTRACT

Three successive passes of the satellite 1958 β 2 over Goldstone, California, were angle-tracked with the JPL Goldstone 85-ft antenna at 108 mc/s. Local hour angle and declination angle data were then used to compute injection conditions arbitrarily chosen to be at the time of the first horizon crossing on the first pass. The injection conditions were computed utilizing the first pass only, then utilizing the data from the first and second passes, and, finally, utilizing the data from all three passes. The three sets of injection conditions were then used to predict the hour angle and declination at several points during the third pass. These predictions were compared to the definitive orbit supplied by the Goddard Space Flight Center. Agreement to 0.1 to 0.2 deg was found for the predictions generated from the two- and three-pass orbit. A time slippage was observed in the predictions from the one-pass orbit.

Osculating orbital elements were also computed from the injection conditions and compared with the elements from the definitive orbit. The agreement was very satisfactory for the two- and three-pass orbits. The improvement in the orbit determination with one pass was systematically studied by combining velocity and range data generated from the known orbit with the angle data in the tracking program.

I. INTRODUCTION

As a part of the research and development effort in the area of tracking and communications, 108-mc tracking equipment was designed and built for the Goldstone 85-ft parabolic antenna. This system has been utilized to track several satellites. The satellite 1958 β 2 has been tracked many times, since it served as an excellent reference for the determination of systematic errors in the antenna system, e.g., servo errors and boresight errors. In each case, prediction information was supplied by the Goddard Space Flight Center, Washington, D.C. Definitive orbital information was also supplied by that agency

[1]This paper presents the results of one phase of research carried out at the Jet Propulsion Laboratory, California Institute of Technology, under Contract No. NASw-6, sponsored by the National Aeronautics and Space Administration.

for purposes of comparison. This work has been extended to the computation of the orbit itself, utilizing the JPL lunar tracking program.

It should be emphasized that the Goldstone antenna was designed for operation at frequencies much higher than 108 mc. The beamwidth at this frequency is 8 deg. A theoretical rms angle error greater than 0.1 deg should be expected at the signal levels available from 1958 β 2.

The orbit determination and prediction procedures should be considered as an integral part of the radio tracking system. This tracking program was described in detail in the previous paper (Eimer-Hiroshige). It is of interest to compute the orbit for the following reasons:

1. To determine the feasibility of orbit determination from one station with one pass, two successive passes, and three successive passes.
2. To study the effects of correlated errors in the angle information due to antenna deformation, wind, etc., on orbit determination and to acquire some insight into the removal of such errors.
3. To study the application of the JPL lunar tracking program to the satellite orbit determination problem.
4. To study the problem of orbit determination in real time on a pass-to-pass basis.
5. To determine the accuracy with which predictions can be computed from an orbit so determined.
6. To study the effect of combining angle observations with doppler velocity observations and with range observations.
7. To study the combination of angle data and velocity or range data in the orbit program and to determine the required accuracy of doppler and range measurement systems.
8. To compare the results of satellite orbit computations to the results of lunar tracking experiments such as *Pioneer IV* so as to better determine the overall specifications and design changes of the tracking net.
9. To add to the general understanding of the JPL tracking program.

The JPL tracking program is essentially a least squares fitting of observations to the equations of motion. At a specified time, injection coordinates, which include position of the probe and magnitude and direction of the velocity vector, are computed from the observations. The Cowell's integration was used to predict the station coordinates at any future time. The program was able to use angle, range, and range rate observations from several stations. The refraction corrections are made utilizing a standard atmosphere. Known systematic errors are removed with appropriate biasing, etc.

II. ORBIT DETERMINATION FROM ANGLE OBSERVATIONS ONLY

Three successive passes of 1958 β 2 were tracked at Goldstone on April 24, 1959. These observations were selected for orbit computation. The portions of the orbit covered by each successive pass are indicated in Fig. 1. The wide bar indicates the first pass; the medium-size bar indicates the coverage for the second pass; and the smallest bar indicates the coverage for the third pass. It can be seen from this that about a fourth of the orbit was covered with the three passes. The local hour angle and the declination angle of the satellite were measured from horizon to horizon for each pass. A time at the beginning of the first pass over Goldstone was selected as the injection epoch for all the computations. The injection conditions determined for each case were integrated for about 4 hr; this corresponded to approximately 2 complete revolutions of the satellite about the Earth. The local hour angle and declination angle were computed from this integration at selected times when the satellite was visible over Goldstone, i.e., times during the third pass. These coordinates were compared with true coordinates supplied by the Goddard Space Flight Center from the orbit determined from the Minitrack System. This refer-

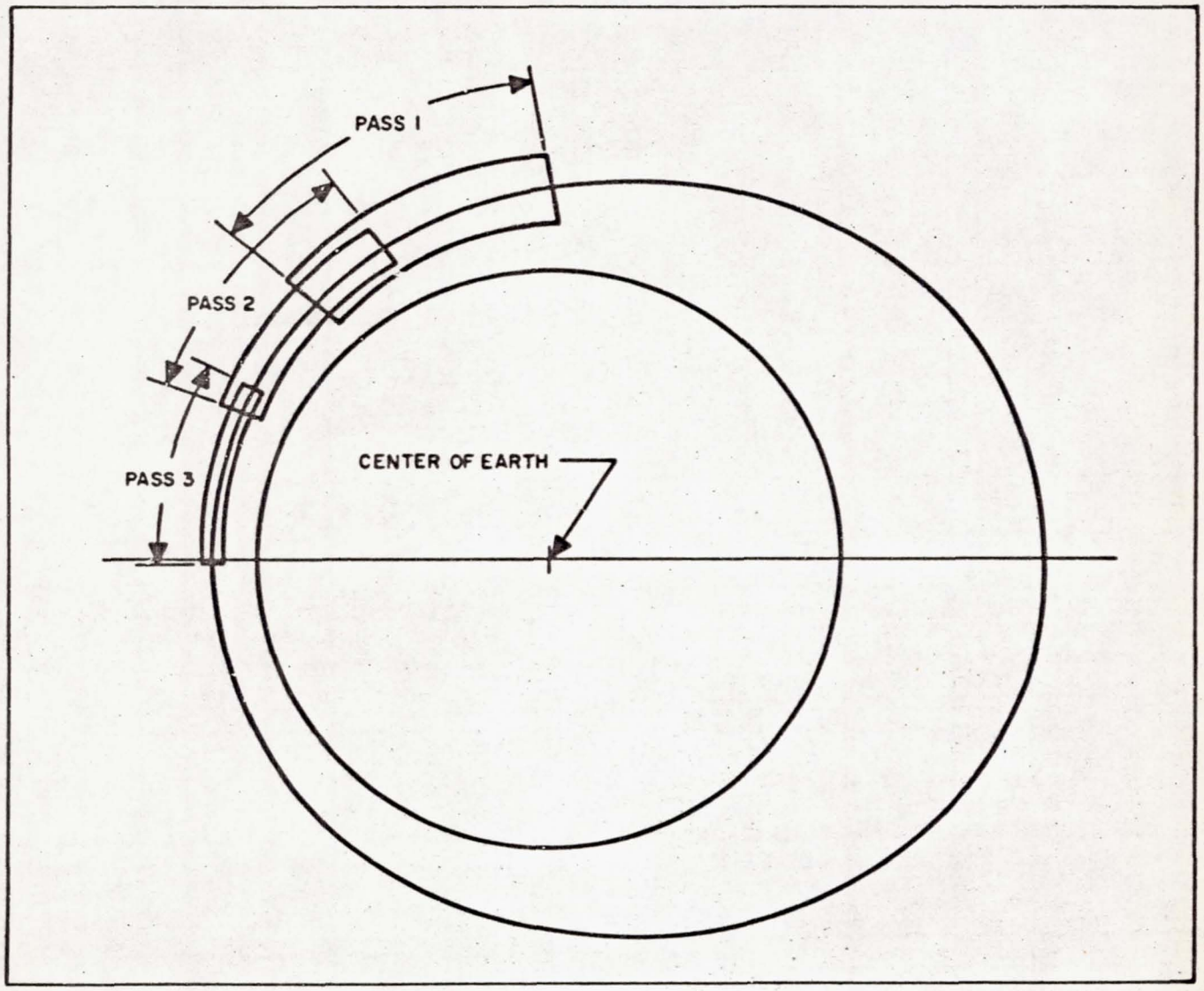

Fig. 1. Orbit of 1958 β 2

ence orbit was considered to be accurate to about 1 min of arc for the 1958 β 2.

An orbit was determined with the first pass observations only (414 points). The resulting orbit fit the data with an rms error in hour angle of 0.268 deg and 0.160 deg in declination angle. These numbers are due mainly to the noise on the raw data. The orbit so determined was poor, and the comparison with the reference orbit indicated that the probe's position had slipped about 12 min by the time of the third pass. This orbit would be nearly useless for prediction purposes. As will be shown below, the poor orbit is primarily due to the geometry of the problem and the use of angle observations alone and not to noise on the data.

The orbit was then determined by combining the first- and second-pass angular data (about 700 points). The injection conditions so computed were then used to predict points during the third pass. The true hour angle and declination angle from the definitive orbit are presented in Fig. 2. Deviations of the predictions in local hour angle from the true trajectory are presented in Fig. 3 along with the predictions generated with all three passes of angular observations (above 1000 points). The

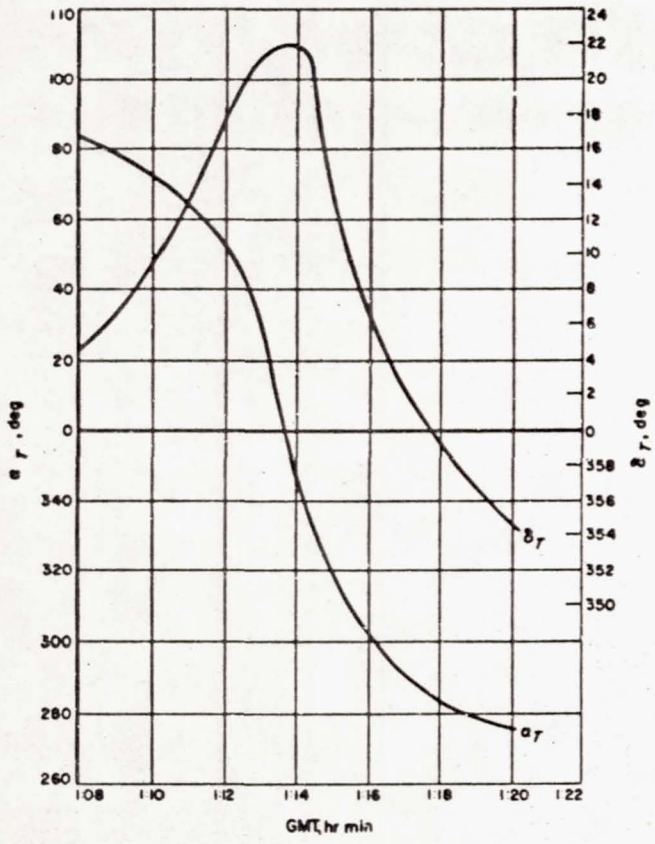

Fig. 2. Hour angle and declination angle of the true orbit of 1958 β 2

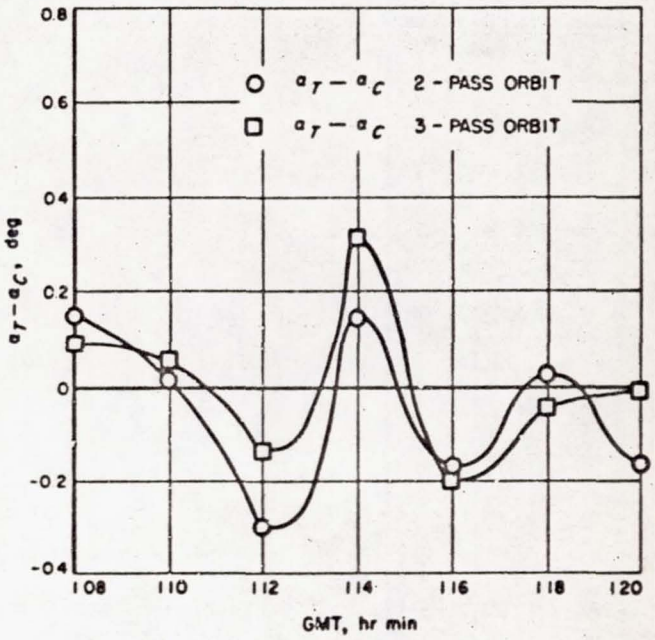

Fig. 3. Prediction error in hour angle; angle data only

deviations of the predictions in declination angle are presented in Fig. 4. These figures indicate that the prediction is accurate to about 0.1 deg or better at the horizon. It can be seen from these curves that excellent predictions can be made on a relatively short time basis from just two passes. The improvement in going to three passes is not remarkably significant. The shape of the curve is due to the complex geometry of the problem. The errors are considerably larger at the middle of the pass because of the angular rates; i.e., the error in the orbits is primarily a time slippage (error in period) of the probe along the orbital path. For these orbits, a slippage of about 1 sec would explain most of the error. The rms deviations of the data for the two-pass orbits are approximately 0.27 deg in local hour angle and 0.35 deg in declination angle. For the third pass, the rms errors are 0.18 deg in local hour angle and 0.29 deg in declination angle. These results seem to indicate that, within reasonable limits, the primary factor in the orbit determination is the geometry and not the noise on the data. The prediction error in slant range for the two cases is presented in Fig. 5 for completeness.

It can be concluded from the above analysis that highly accurate predictions can be generated from the orbit

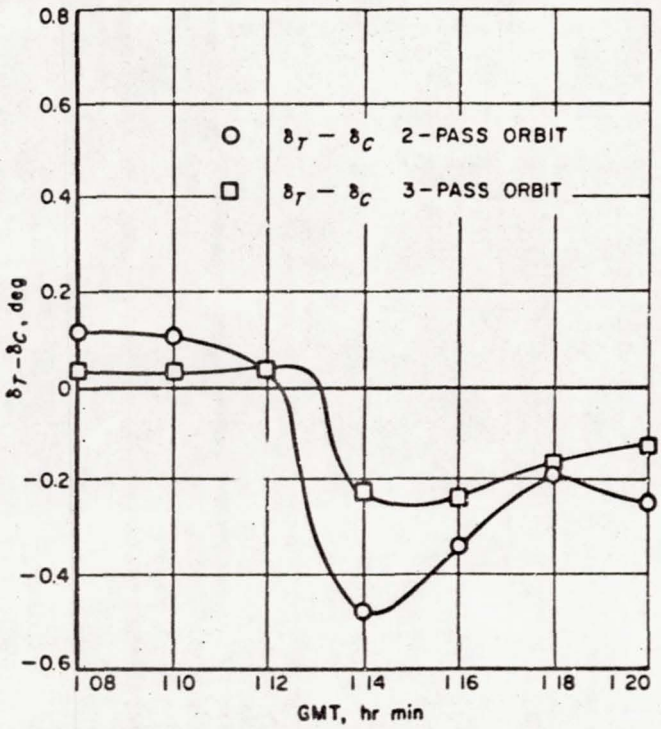

Fig. 4. Prediction error in declination angle; angle data only

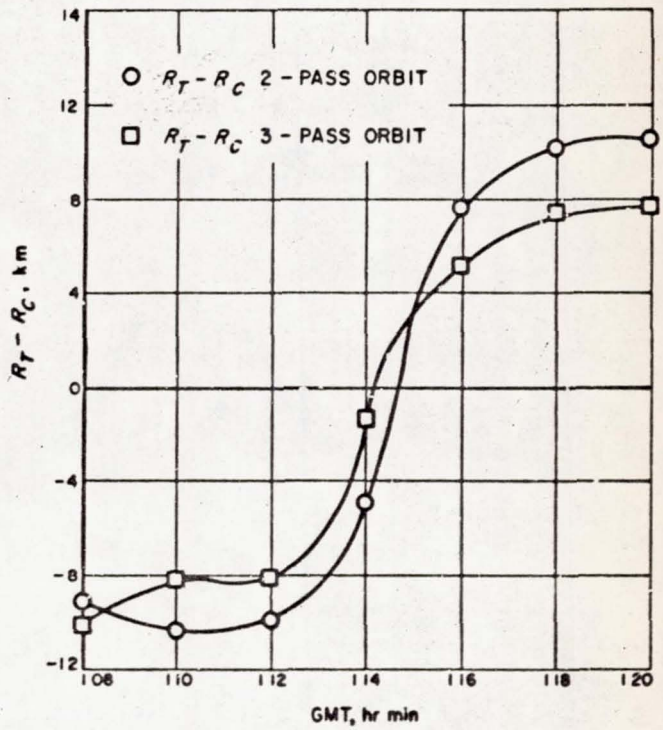

Fig. 5. Prediction error in slant range; angle data only

determined with two successive passes over the one station with angle data alone. It further shows that a poor orbit is found with one pass of angle data alone, and experience with these computations indicates that this is quite unrelated to the rms noise on the observations. It should be pointed out that bias errors or other systematic errors in the observations would have a very serious effect on an orbit determined with one pass.

III. ORBIT DETERMINATION FROM ANGLE OBSERVATIONS COMBINED WITH RANGE OR DOPPLER OBSERVATIONS

The first-pass observations were selected to study systematically the improvement in one-pass, one-station orbit determination by combining slant range or slant-range rates with angle data. Velocity data accurate to 0.01 m/sec was artificially generated with the three-pass orbit injection conditions and added to the angle data. The orbit determined this way probably represents the limit using this particular set of angle data. Orbits were also computed using velocity accurate to 1 m/sec and accurate to 10 m/sec combined with the angular observations. The results are presented in Fig. 6–8. Figure 6 shows the error in hour-angle predictions for the three cases. Figure 7 shows the prediction error in the declination angle for the three cases. The prediction error in slant range for two of the three cases is presented in Fig. 8. The data indicate that velocity observations accurate to 1 m/sec or better combined with the particular angular data available gave predictions for this pass better than 1 deg at the beginning of the pass. This is not an unreasonable angle to search for acquisition purposes. However, the probe must be acquired near the horizon or the errors get very large.

A similar analysis was done with the slant-range data good to the nearest 100 meters and to the nearest 1000 meters. These results are presented in Fig. 9–11. Figure 9 presents the error in the hour angle prediction for the two cases. Figure 10 shows the declination angle prediction error for the two cases. It can be seen that for the errors present in the angle observations there is no significant difference in the two cases. They both serve to give a much improved orbit over that determined by angular observations alone. Apparently, for this particular case, range data accurate to 1 km are nearly equivalent to velocity data accurate to 0.01 m/sec. This graphically indicates the importance of range-measuring systems in

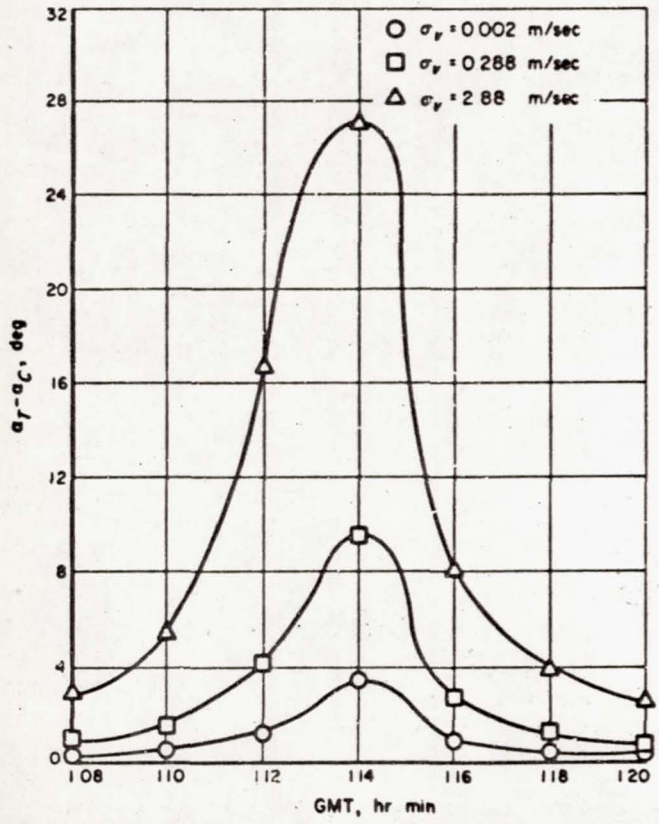

Fig. 6. Prediction error in hour angle; orbit determined with first-pass and computed velocity data

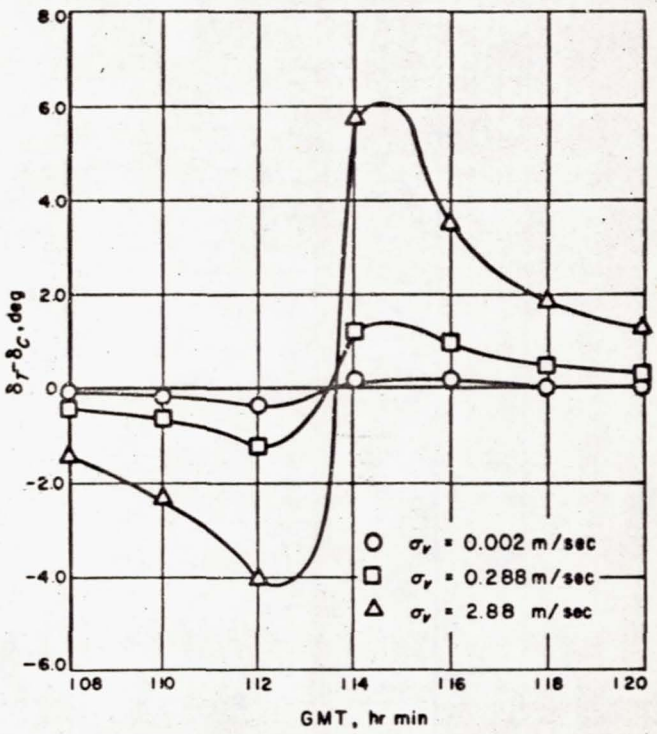

Fig. 7. Prediction error in declination angle; orbit determined with first-pass and computed velocity data

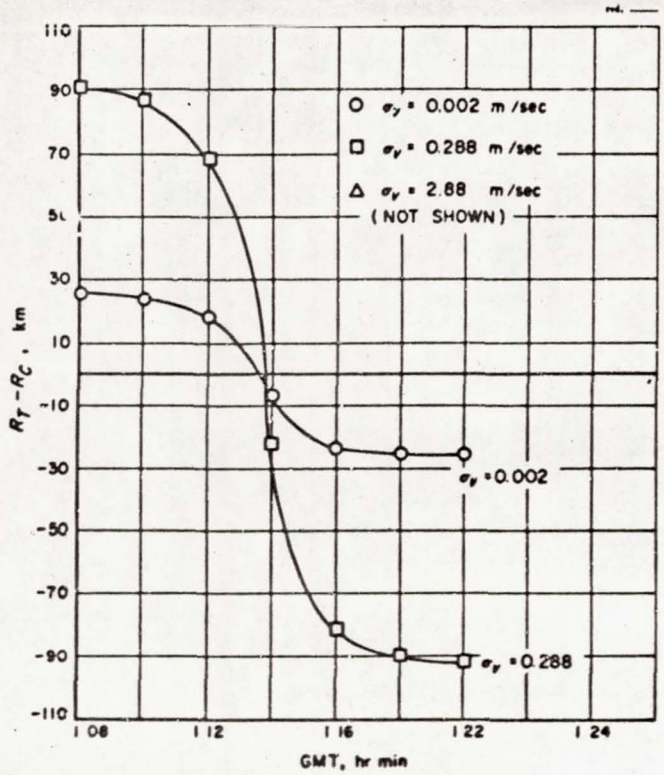

Fig. 8. Prediction error in slant range; orbit determined with first-pass and computed velocity data

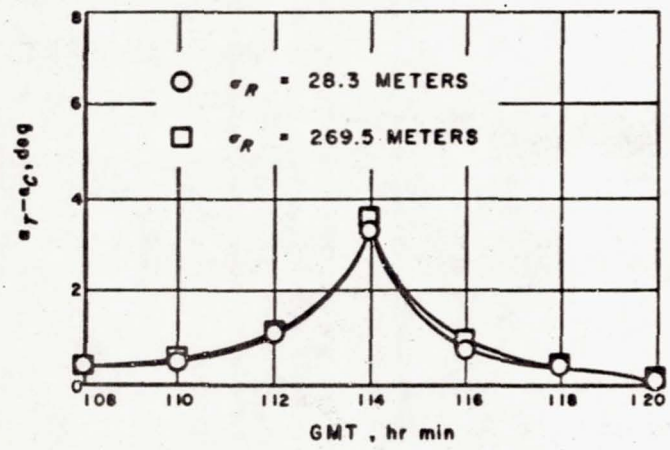

Fig. 9. Prediction error in slant range; orbit determined with first-pass and computed slant-range data

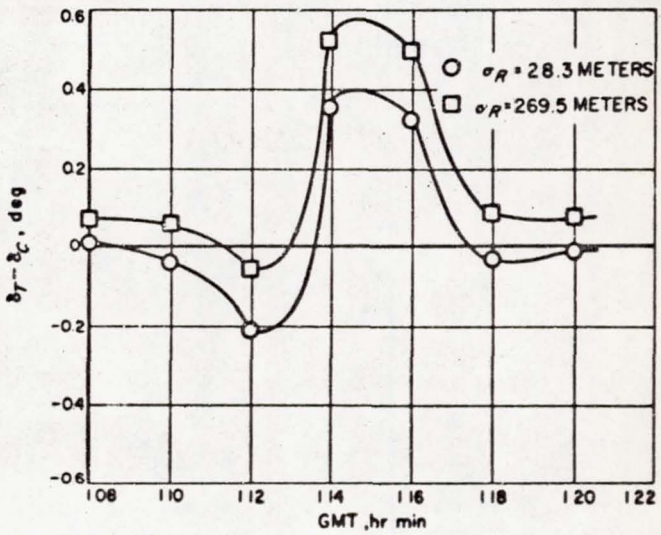

Fig. 10. Prediction error in declination angle; orbit determined with first-pass and computed slant-range data

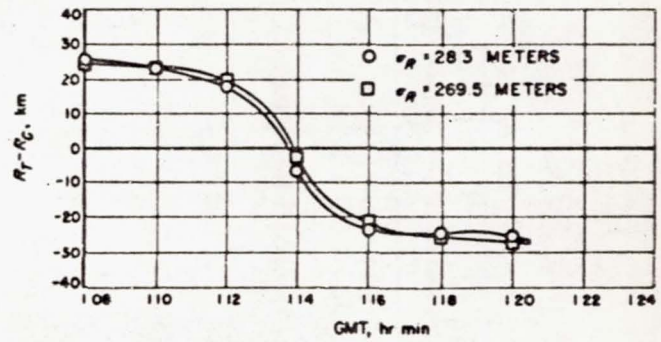

Fig. 11. Prediction error in slant range; orbit determined with first-pass and computed slant-range data

orbit determination. Prediction error in the slant range for the two cases is presented in Fig. 11 for completeness.

In summary, the above analysis indicates that rather excellent predictions over several hours can be computed with angular data for one pass as bad as 0.2 deg rms when combined with velocity data better than 1 m/sec or range data better than 1 km.

IV. ORBITAL ELEMENTS

It is very useful in studying the results reported above to consider the orbital elements of the osculating ellipse at a specific epoch. It was convenient computationally to select an epoch at the beginning of the third pass. First of all, it was necessary to compute the orbital elements of the reference orbit at this epoch. It was necessary to use the tracking program and the data from Fig. 2. Range information to the nearest kilometer was also available. This combination of data resulted in an orbit with an rms error of 0.021 deg in hour angle, 0.005 deg in declination angle, and 280 meters rms in range. This is an excellent fit, but the remarks above concerning orbit determination from one pass certainly apply to this case. Therefore, the orbit so determined cannot be considered as a "true" orbit. This was apparently the best set of orbital elements available to the author.

The orbital elements for the orbits determined from angular observations alone are presented in Table 1. In the first row are the elements computed from the reference orbit. Computations of the probable error for these elements were made from the rms deviations reported above. The orbital elements computed for the orbit from two passes and from three passes are in excellent agreement with the reference orbit. However, it should be noted that the elements from the two-pass orbit and the three-pass orbit are in much closer agreement with each other than with the reference itself. This suggests to me that the computed orbital elements are better than the true elements, as I have defined them. It should be noted that the period computed for the one-pass orbit is high by about 6 min, which essentially explains the time slippage in the prediction data for this case reported above. Also included in the last two columns of this table are the rms deviations of the angular observations from the fit. It can be seen from these that the quality of the orbits is apparently unrelated to the relative sizes of these deviations. This is probably because the rms deviations from the true orbit are basically noise.

Table 2 presents the elements for the one-pass orbits computed from angle plus velocity accurate to 0.01, 1, and 10 m/sec. The three-pass orbit was selected as the reference orbit in this case because the velocity information was generated from the three-pass orbit injection conditions. Table 3 presents the elements for the one-pass range data orbit. These orbital elements are in excellent agreement with the reference orbital elements, reiterating

Table 1. Osculating orbital elements for the satellite 1958 β 2

Epoch: 24 Apr, 1 08 00 GMT

Source of data	a	e	i	ω	Ω	M	P	σ_α	σ_δ
GSFC definitive angles and range	1.36056 ±0.00013	0.190766 ±0.000269	34.2304 ±0.00001	106.028 ±0.023	16.596 ±0.023	−23.354	134.120 ±0.019	0.0206	0.0048
Observations, one pass	1.40187	0.206287	34.2775	100.4161	17.6560	−49.0074	140.243	0.2680	0.1604
Observations, two passes	1.36067	0.190439	34.2633	106.1067	17.3606	−22.6062	134.1064	0.3521	0.2727
Observations, three passes	1.36066	0.190502	34.2272	106.1905	17.2785	−22.6018	134.1043	0.2923	0.1845

Table 2. Osculating orbital elements from one-pass angle observations and computed doppler data

Epoch: 24 Apr, 1 08 00 GMT

Source of data	a	e	i	ω	Ω	M	P	σ_α	σ_δ	$\dot{r}$
Reference orbit from 3 passes	1.36066	0.190502	34.2272	106.1905	17.278	−22.6018	134.1043	0.2923	0.1845	—
$\dot{r}$ accurate to nearest 0.01 m/sec	1.36041	0.190435	34.2329	106.201	17.296	−22.4249	134.068	0.2662	0.1600	0.002
$\dot{r}$ accurate to nearest 1.0 m/sec	1.35990	0.190215	34.2382	106.262	17.290	−22.080	133.9927	0.2654	0.1643	0.288
$\dot{r}$ accurate to nearest 10.0 m/sec	1.35822	0.190170	34.2378	106.651	17.271	−21.015	133.7433	0.2634	0.1642	0.260

Table 3. Osculating orbital elements from one-pass angle observations and computed slant-range data

Epoch: 24 Apr, 1 03 00 GMT

Source of data	a	e	i	ω	Ω	M	P	σ_α	σ_δ	σ_r
Reference orbit 3 passes angle data	1.36066	0.190502	34.2272	106.1905	17.2785	−22.6018	134.1043	0.2923	0.1845	–
r to nearest 100 meters	1.360413	0.190436	34.2334	106.204	17.294	−22.428	134.0679	0.2652	0.1642	33.4
r to nearest 1000 meters	1.360447	0.190954	34.2216	106.333	17.282	−22.498	134.073	0.2654	0.1649	273.4

the value of the range information to the orbit-determination problem.

The above study has been limited to one orbit, of course; and, in particular, all the comparisons were limited to one pass of this one orbit. Future study is required to learn the effects of going to orbits of different eccentricities and semimajor axes. This study will be considered as a foundation on which a theoretical study may be based.

V. CONCLUSIONS

The satellite tracking and orbit-determination experiments have yielded the following results:

1. Analysis shows that highly accurate predictions can be generated from the orbit determined with two successive passes over one station with angular data alone. It shows that a poor orbit is found with one pass of angular data alone, which is due more to the geometry involved than to the rms error on the data.
2. Analysis indicates that excellent predictions can be computed with angular data from one pass as bad as 0.2 deg rms when combined with velocity data better than 1 m/sec or range data better than 1 km for this particular orbit.
3. Further study is required to determine the design specifications for future doppler and range measurement systems.
4. Experience with the computations indicates that sufficiently accurate predictions can be generated for acquisition purposes for satellites, with one pass from one station in real time if an independent measurement of doppler velocity or range is available.
5. The effects of correlated errors due to the deformations of the antenna structure, etc., were found to be negligible in the orbit determination.
6. The orbit for 1958 $\beta 2$ was essentially determined with three passes.

NOMENCLATURE

a semimajor axis in Earth radii

e eccentricity

i inclination, deg

ω argument of perigee, deg

Ω longitude of the node, deg

M mean anomaly at epoch, deg

P period, min

σ_α standard deviation of hour angle from the fit, deg

σ_δ standard deviation of declination angle from the fit, deg

$\sigma_{\dot{r}}$ standard deviation of doppler velocity from fit, m/sec

σ_r standard deviation of slant range from fit, meters

Early Orbit Determination Scheme for the *Juno* Space Vehicle

FLETCHER KURTZ and FRIDTJOF SPEER

Flight Evaluation Branch, Aeroballistics Laboratory,
Army Ballistic Missile Agency, Huntsville, Ala.[1]

ABSTRACT

The present status (1959–60) of the ABMA early orbit determination scheme for the *Juno* space vehicle is described.

The design of the scheme was essentially influenced by three factors: its origin centered around postflight vehicle analysis, the flexibility required for accepting varied kinds of data, and the potential of high-speed computers concentrated in ABMA's Computation Laboratory.

The scheme is outlined, the tracking stations participating are shortly described, and the physical layout and computational equipment are briefly mentioned. The evaluation techniques used for the various steps of the orbit determination are discussed in detail. Appendices describe briefly the principal coordinate systems used and characteristics of the digital computer programs.

[1]The material contained in this document is for information and possible use by other Government activities. It represents the results of work performed at the Army Ballistic Missile Agency and records a significant mark of achievement of the organization or individual whose name appears hereon. Issuance of this document is not intended to indicate that the material has been fully evaluated, tested and accepted by this Agency or the degree to which it has been or may be used in accomplishment of the Agency missions.

I. INTRODUCTION

It is the purpose of this report to describe the Army Ballistic Missile Agency orbit determination scheme in its present state of development. Although varying payload missions, modified tracking instrumentation, and improved techniques are continually changing some feature of the overall scheme, it appears worthwhile to present the basic philosophy and describe the scheme in its present state.

While a number of good and precise methods are available for the orbit determination of artificial satellites and space probes (reference is made especially to the highly advanced but specialized Jet Propulsion Laboratory program, Ref. 1), the ABMA orbit determination has some distinct features which reflect the missions for which it was designed and the facilities directly available to ABMA.

First, this method was primarily intended to analyze the vehicle performance and, therefore, concentrated essentially on the power flight up to and including injection into orbit. Secondly, because ABMA lacked substantial orbital tracking instrumentation, it was mandatory to maintain an extreme degree of flexibility and versatility as to kind and format of tracking data to be accepted from other agencies. A third factor influencing the scheme was the unusual potential of advanced electronic computers and pertaining equipment available in the ABMA Computation Laboratory.

Since for several good reasons it is desirable to know about the vehicle performance approximately in real time, a distinction began to develop between the "quick look" and the precision determination of the injection point. It was realized that the "quick look" fulfills all requirements of an early orbit determination scheme, providing information which could be offered to other agencies as the initial point for long-term tracking and orbit determination.

The present state of the scheme is characterized by the first generation of satellites with payloads between 20 and 100 lb. A single miniaturized radio transmitter is all that can be afforded to make these flights worthwhile scientific experiments. The lack of high-quality tracking has to be compensated for by masses of lower-quality data, which present a problem even to the fastest and most advanced electronic computers.

Most of the incoming tracking data still consist of range rates (one-way doppler frequencies), which have a low specific information content and require a very high transmitter frequency stability.

In all flight tests the programmed flight path is known to a high degree of accuracy. All deviations from this standard flight are due exclusively to unpredictable disturbances. Excluding major failures, these deviations are small enough to permit the application of linear perturbation theory to every step of the orbit determination scheme.

The scheme, consisting of two major phases, the injection phase and the orbital phase, has been successfully applied to five satellite and two lunar probe flights. Four of these flights succeeded in their essential missions.

The responsibilities and efforts in tracking the *Juno* space vehicle were varied. In the beginning, the *Juno I (Explorer)* early orbit determination was carried out as a joint operation of JPL and ABMA, with the former agency primarily responsible. ABMA efforts were directed to postflight analysis of the vehicle performance, in particular that of the cluster (Ref. 2). The early phase of the *Juno II* orbit determination was characterized by the successful operation of the Goldstone tracking station and the JPL mechanized tracking program.

Beginning with *Juno II-16*, however, the orbit determination task was transferred to ABMA. This necessitated the modification of the postflight analysis scheme into a real time orbit determination. The basic philosophy of the ABMA orbit determination scheme may be stated briefly in four points:

1. Utilize tracking during the power flight and the injection phase to the highest possible extent.
2. Accept all available kinds of data from as many stations as possible.
3. Subdivide the data processing and the correction procedure to best utilize all ABMA high-speed computers.
4. Complete the initial orbit determination within approximately two orbits and discontinue the operation when sufficiently precise initial conditions are obtained.

II. EVALUATION SCHEME

The entire orbit determination scheme has been viewed as a continuous process designed to obtain accurate orbital elements and injection conditions at the earliest possible moment. Succeeding phases in the scheme are planned to improve previous results, while remaining as independent as possible of the success or failure of preceding steps.

All steps are designed to yield as much information as possible, whether partial or complete with respect to the orbital elements, as an aid to the interpretation of later data on the following correction phases.

It is convenient to distinguish the following six time periods which are more or less dictated by the launching sequence of the satellite-carrying vehicle: countdown, booster flight, coasting period, cluster flight, early free flight, first orbit. These will be discussed in connection with the orbit determination scheme which is shown graphically in Table 1.

Table 1. ABMA early orbit determination (*Juno II*)

Phase of flight	Source of information	Location	Information received at ABMA	Results obtained by ABMA	Time obtained (after liftoff)
Countdown	Launching operations	AMR	Liftoff time	Orbit 1, based on actual liftoff and precalculated trajectory	5 min
Booster flight	ABMA interferometer	AMR	Cutoff conditions	Booster performance (velocity, attitude)	
	Booster telemetry	AMR Redstone Cape Hatteras			
	FPS-16 radar	AMR			
Coasting flight	FPS-16 radar and IBM-709 computation	AMR	Stage II ignition conditions	Orbit 2, based on actual ignition II and standard cluster flight	15 min
Cluster flight	Microlock stations	AMR Redstone *Cape Hatteras *Bermuda Ft. Monmouth *Van Buren Aberdeen	Cluster slant velocity increments	Orbit 3, based on actual injection conditions from cluster evaluation	Approx 90 min (depending on data)
Early free flight	Northbound Millstone Hill radar	Westford, Mass.	Payload positions	Orbit 4, based on Millstone Hill radar observations	Approx 90 min (depending on data)
	Southbound				
First orbit pass	Microlock stations	Continental U.S. Bermuda	Time of closest approach	Orbit 5, based on period correction from first observed pass	Approx 2 hr (depending on orbit)
	Minitrack stations	San Diego Blossom Point	Time of meridian crossing		
	Goldstone 85-ft dish	Goldstone	Payload tracking angles and doppler	Orbit 6, based on all observations of first orbit	Approx 3 hr
	Millstone Hill radar	Westford	Payload positions		

*Mobile stations, present locations given.

To clarify the six time periods, a brief description of the basic vehicles may be useful (Fig 1). The first stage is a modified *Redstone* or *Jupiter* missile for *Juno I* and *Juno II*, respectively. Both booster vehicles are lengthened from their tactical configurations to permit longer burning times. On top of the booster is an instrumented conical section which houses the flight control equipment, the spatial attitude control and the spin motors for the clustered upper stages. This section separates after booster engine cutoff and coasts to the programmed ignition point of the second stage. It constitutes the attitude-controlled launching platform of the upper stages. The

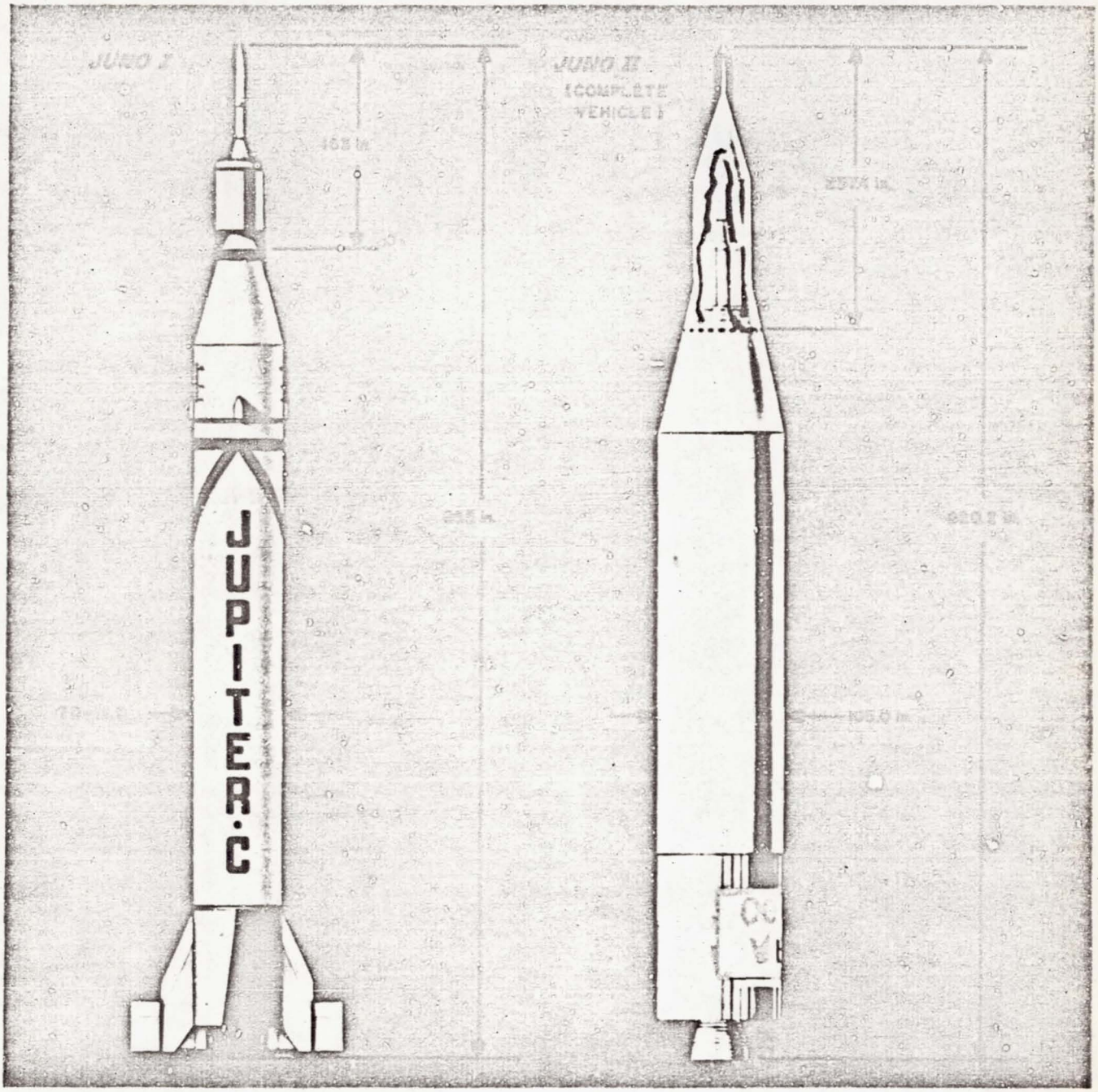

Fig. 1. *Juno I and Juno II* vehicles

flight mechanical events are diagrammed further in Figs. 2 and 3.

The upper stages for both *Juno I* and *Juno II* type vehicles are assemblies of scaled down (1/5) solid-propellant *Sergeant* rockets grouped into a spinning cluster. This cluster contains eleven rockets for stage II, three rockets for stage III, and one rocket for stage IV. The burning time for each stage is about 6 sec, with short coast periods between the stages.

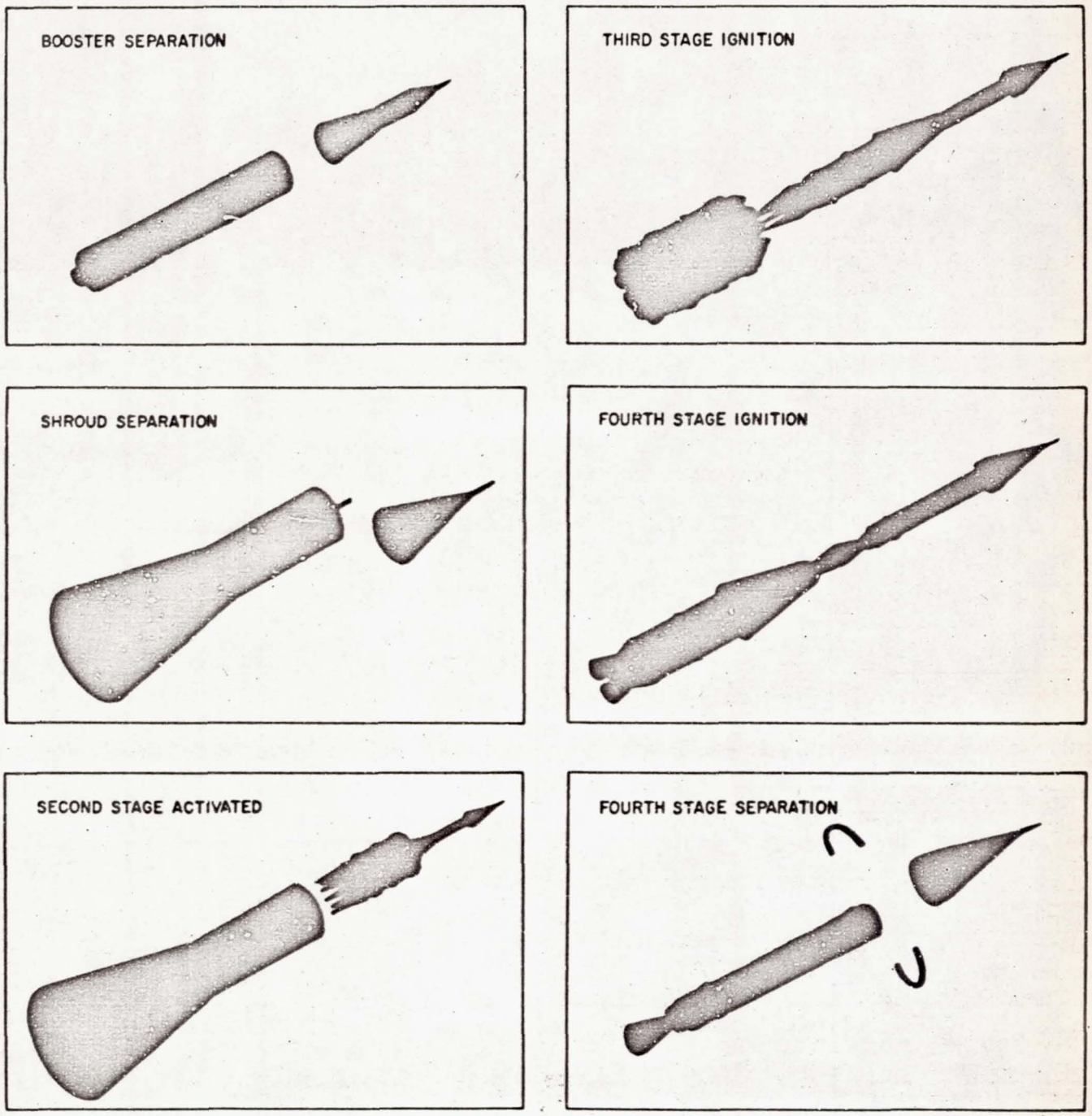

Fig. 2. Sequence *Juno II* space probe launch

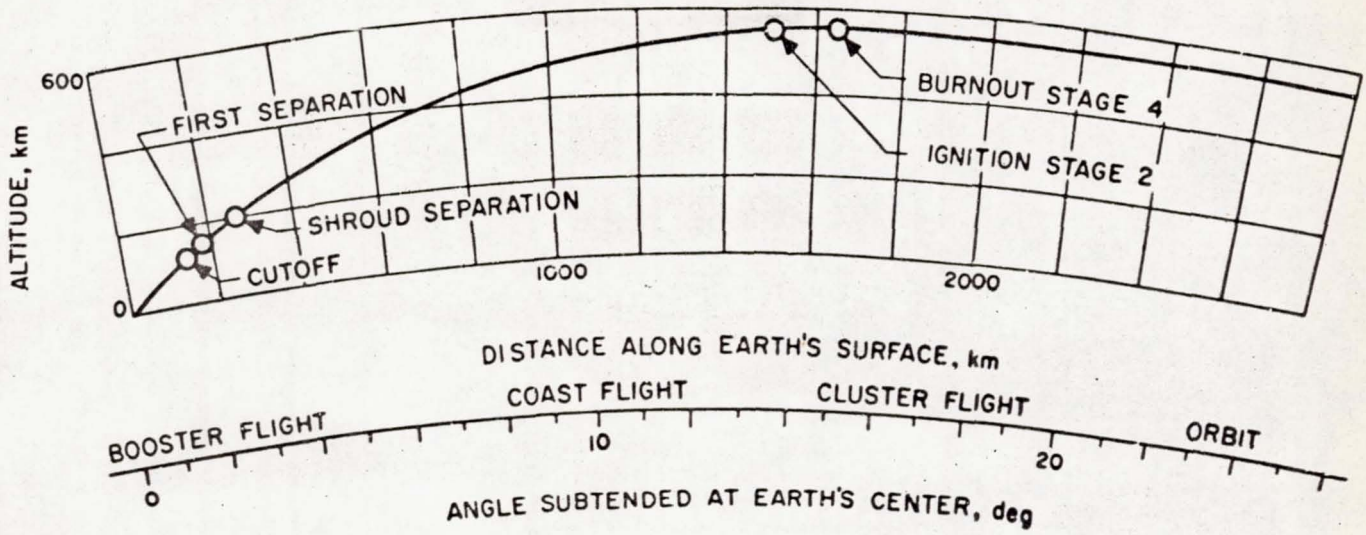

Fig. 3. Vehicle power flight

A. Countdown

During the countdown all necessary communication lines are opened. It is desirable to have one teletype line to each of the key stations. Additional telephone connections are opened temporarily as emergency links in case of teletype failure. The tracking frequency of the payload transmitter is obtained from Missile Firing Laboratory, ABMA, and given to all stations at X − 60 and X − 15 min. All stations within this network have previously received specific tracking instructions based on the predicted flight path. A Microlock station, for instance, is given elevation, azimuth, and frequency increment as a function of time after liftoff. As the liftoff event is communicated to all stations, a first orbit is calculated entirely on the basis of the precalculated flight path. This orbit number one, printed with actual times, is convenient for tracking predictions to the stations in the event of a near-standard flight, and is important as a basis for search patterns in case no further information is obtained from the satellite.

B. Booster Flight

The booster serves as the launching platform for the spin-stabilized upper stages. All the guidance elements are part of this first stage. Regardless of possible performance variations or meteorological influences, the position, velocity, and attitude of the vehicle at the instant of second-stage ignition must be very near the precalculated conditions.

For this reason a real time record of the booster flight performance is important. The first stage is conventionally tracked by FPS-16 (C-band) radar (beacon or skin). The radar output is fed directly into the IBM 709 computer as part of the routine Atlantic Missile Range launch operations. Originally designed for impact prediction, this setup is also capable of computing position and velocity at any time-point after cutoff.

A substantial number of in-flight measurements are telemetered from the instrument compartment of the booster to ground receiving stations at Cape Canaveral, Redstone, and other required locations.

The ground stations have a real time display (brush records) for a dozen or more of the most important telemetry channels. A quick analysis gives answers to the following questions: Did the booster achieve the predicted velocity? Was the booster performance normal? Did separation and other vital mechanical functions occur properly? Was the attitude properly controlled? Did the second stage ignite at the right time?

Knowledge of these facts has no immediate effect on orbit calculation other than to give an indication of whether or not booster errors are present. However, it is of great value for the interpretation of later tracking results.

In addition to the AMR radar tracking, there is, for flight safety purposes, an interferometer-type tracking system using both the dovap beacon (74 mc/s) and the telemeter carrier frequency of the booster. The doppler slant velocity and two angles are compared with the predicted quantities in real time. Should the AMR radar fail, these tracking results are used for first-order corrections of the standard flight to yield approximate conditions at ignition of stage II.

C. Coasting Period

Since the spin-stabilized upper stages are fired into one space-fixed direction, the resulting orbital perigee can never be much higher than the altitude at ignition of stage II. The booster cutoff altitude is much too low to be acceptable as initial perigee. Therefore, a substantial coast period is programmed between booster cutoff and ignition of stage II (Fig. 3).

Shortly after cutoff the instrumented part of the booster is separated from the empty thrust unit (Fig. 2). Essentially, it follows a vacuum ballistic flight and, by means of small control nozzles, maintains the proper attitude of the rotating cluster until ignition of stage II. The length of the coasting period depends on the desired orbital shape and trajectory layout.

The most important part of the FPS-16 radar tracking occurs early after cutoff. In most cases, less than 1 min of tracking is sufficient to establish reliable initial conditions for the free flight. From these initial conditions, the AMR computer calculates the entire ballistic trajectory of the vehicle until impact. Position coordinates and velocity components may be printed at any desired time.

In most cases, ignition of stage II is given by a preset timer. Consequently, the AMR computer can print ignition conditions shortly after cutoff, even before the ignition event occurs. In cases where ignition time is not known beforehand, it has to be evaluated from the real time telemeter display and transmitted to the AMR computer.

As soon as ignition conditions are known and found compatible with the telemetered information received, a cluster trajectory and a second orbit (number two) are computed in the Evaluation Center. In these calculations a standard cluster flight is tied to actual ignition conditions and actual ignition time. Orbit number two is very valuable in conjunction with the cluster analysis which follows. If the observed velocity increments of the cluster flight are close to the calculated values, orbit number two is a good approximation of the actual flight and is obtained in a minimum of time. Depending on the availability of ignition conditions, this orbit is complete about 20 min after launch.

A last important check during this phase concerns the attitude of the entire vehicle immediately prior to ignition of stage II. Noticeable deviations in either pitch or yaw have to be taken into account in the next evaluation phase, the cluster flight.

D. Cluster Flight

The cluster flight is the crucial phase of the entire launch operation. A very substantial velocity contribution is imparted to the payload within a very short time, necessitating high load factors. There is only the open loop control of spin stabilization, and very little on-board instrumentation to monitor the behavior of the cluster stages. Therefore, special efforts have been made to develop a tracking system especially suited for this short but important flight phase. At present, there are seven special Microlock tracking stations available, three of which are mobile. The four permanent stations are located at Cape Canaveral, Florida; Huntsville, Alabama; Fort Monmouth, New Jersey; and Aberdeen, Maryland (Fig. 4).

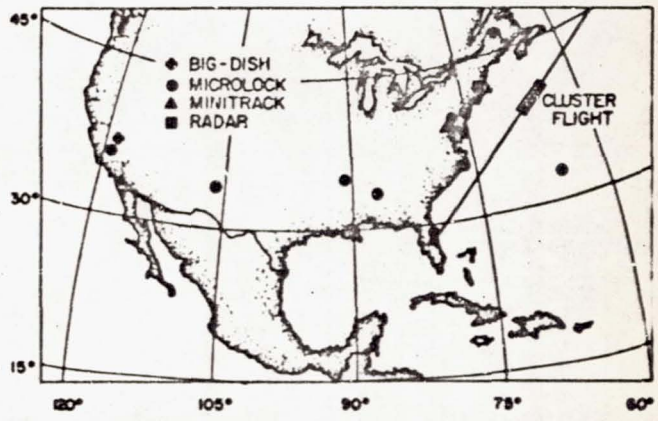

Fig. 4. Tracking stations

The basic tracking principle is spherical velocity tracking (one-way doppler). Main disadvantages are the limited stability of the transmitter frequency and data reduction difficulties; main advantages are simplicity and good tracking geometry (long base lines).

Since the Redstone station is physically close to the Evaluation Center, a real time audio signal reflecting the doppler shift can be displayed within the Evaluation Center from this station. This is the first qualitative information received about the general functioning of the upper stages. Any large deviations from standard flight will be evident on this early record, e.g., failure of one stage to fire.

A corresponding arrangement may be made with some other Microlock tracking station which is closest to the predicted injection point. Her and in Redstone the phase-modulated telemeter signals are displayed in real time to permit immediate conclusions concerning certain

payload functions, e.g., separation and spin reduction. This information is immediately communicated to the Evaluation Center.

The doppler frequencies are received at the Evaluation Center by teletype in 1-sec steps and are automatically plotted in order to find qualitative irregularities, e.g., failure of ignition and gross errors. After determining and defining ignition and injection times, respectively, the frequency difference between these two time points is evaluated and fed into an IBM 704 computer. The computer performs a number of differential correction steps, comparing the predicted frequency increments with those measured and modifying the computed trajectory to minimize the residuals. Since the tracking situation is often marginal with respect to signal strength and elevation angle, the possibility of gross errors exists. As excessive errors would considerably damage the least square solution, an automatic sorting process has been designed which eliminates such gross errors.

The final result of the cluster flight analysis is printed by the IBM 704 in terms of both cluster performance and injection conditions. The latter conditions are immediately utilized for running orbit number three, the first orbit completely based on actual data.

At this point the first major step of the early orbit determination is completed. The results should be available approximately 50 min after launch. About 30 min of this time is required to receive all Microlock data.

E. Early Free Flight

During the early orbit phase after injection, additional Microlock data are obtained by the east coast stations tracking the satellite until loss of signal. This information generally has been insufficient to permit an independent orbit determination. However, large deviations in flight path may be detected and the functioning of the payload telemetry can be monitored during this period.

A truly independent and powerful source of orbital information is the Millstone Hill Radar operated by MIT (described in Section IIIC). This large radar dish possesses the power and receiver sensitivity necessary to skin track even the relatively small target presented by the *Juno II* payloads. Millstone is capable of the accuracy necessary to permit determination of complete injection conditions from a short time period of data, the possible tracking period after injection being normally from 5 to 15 min, depending on the particular mission. The problem of acquisition of the satellite by the radar is a serious one, however, in view of the separation of the missile into several pieces shortly before injection (Fig. 2), the smallest and most rapidly moving piece always being the one desired. For this reason acquisition and tracking predictions are supplied to Millstone before each flight.

The result of the Millstone Hill tracking, orbit number four, should be available approximately 20 min after reception of the complete data message. Therefore, the cluster evaluation and the Millstone Hill determination are processed simultaneously on separate IBM 704 computers. Both results should be available for comparison at approximately the same time, 50 min after liftoff.

If no gross errors are present and the two orbits, numbers three and four, are of comparable quality, the decision as to which one is preferable is postponed until after first-pass data become available.

F. Reacquisition

About 1 hr elapses between completion of the injection phase evaluation and the first appearance of low altitude, low eccentricity orbit satellites over the west coast. Within this time path predictions are prepared and communicated to the stations.

The final adjustment of the initial conditions is done in two steps, which may be called the period correction and full correction, respectively. There are several reasons for this peculiarity. The period correction requires only one exact timing of a closest approach or a median crossing, preferably near completion of one orbital revolution. This time is a fairly accurate measure of the total velocity amount and is comparatively insensitive to position errors and velocity angle deviations. An early time obtained by a west coast station can be received and utilized in a special correction process within a very short time, while the satellite is still passing over the continent.

Also, this simple adjustment provides a better basis for the subsequent full correction than the earlier approximation. If, for example, doppler frequencies as a function of time are used for the corrections, it is important to have predicted and observed inflection points as close together as possible.

Finally, from the standpoint of computer efficiency, it is advantageous to run the period correction first. It requires only one additional variational orbit calculation to generate the partial derivative with respect to the total velocity. Omitting this step would necessitate one to three more iterative steps for the full correction, with at least three additional variational orbit calculations for each iteration.

Thus, the period correction is considered important because it saves valuable time, it improves the linearity

of partial derivatives with respect to doppler frequencies, and it offers a superior computational efficiency. The actual inputs for this special program are the observed times of closest approach or of meridian crossing for any number of stations. The result is a correction coefficient common to all three velocity components at injection (leaving the angles invariable), which is automatically used in a new orbit computation, orbit number five.

At this time sufficient information usually is available to justify an official statement about success or failure of the mission. The main orbital parameters are known within comparatively narrow limits. Good predictions for the following passes can be made to tracking stations all over the world.

The remaining problem is now a more precise determination of injection conditions not only for orbit determination, but for assessment of vehicle performance in terms of deviations from the predicted. This is particularly interesting for the performance analysis of the upper stages. The comparatively crude velocity tracking by the Microlock stations can be improved considerably if start and end points of the cluster flight are precisely known from other sources.

From a computational standpoint the full correction is the most crucial evaluation phase for the following reasons: extreme flexibility in accepting data of all kinds, in every format, and with different weights is required; large amounts of data must be accepted; the highest possible accuracy is required; computational speed is still an important factor.

The full correction normally used at this stage is a differential correction process applied to the velocity and the two velocity angles at injection. The necessary partial derivatives of the actual observations available for the correction process are obtained by variational orbit calculations for each of the three initial parameters.

The magnitude of the variations which generate the partial derivatives is optimized for each particular flight mission. The choice of correction parameters (velocity amount and two angles) represents at least a relative optimum for the correction process. It is superior to the method of correcting Cartesian velocity components in an arbitrary coordinate system.

The restriction to three unknowns was made after it was found in several actual evaluations that the injection position presently is determined better by the AMR range instrumentation than by orbital observations. Of course, this is to be understood only as a general rule. Exceptions are clearly indicated if C-band radar should fail or if very good power flight tracking from Millstone Hill should be available.

The following types of data are used as input for the correction deck:

Range (radar)
Rate of range (Microlock–doppler)
Azimuth and elevation (Millstone Hill)
Hour angle and declination (Goldstone)
Time of doppler inflection (Microlock)
Maximum doppler slope (Microlock)
Time of meridian crossing (Minitrack)

The whole correction process includes the computation of a standard orbit and three variational orbits, the differencing of actual and "standard" observations, the least squares solution, and the printout of the new orbit with all desired orbital parameters. The total time required for this process is 20 min (300 observations).

Provided enough data are available and the previous evaluation steps have at least partially succeeded, only one full correction is needed for the purposes mentioned. To check the accuracy a second correction step is added as a matter of routine. In such a case new partials are always calculated for accuracy, although there is the option to reuse the previously established partials.

III. TRACKING STATIONS

The main tracking systems used for the *Juno* early orbit determination are listed in Table 2.

Table 2. *Juno* early orbit determination tracking systems

Booster flight	FPS-16 radar
Cluster flight	Microlock–doppler
Early orbit	Millstone radar Microlock–doppler Minitrack
Reacquisition	Microlock–doppler Goldstone tracking dish Minitrack

The five different tracking systems are briefly described in the following sections. The locations of all stations normally transmitting data to ABMA are shown in Fig. 4.

A. FPS-16 Radar

This radar dish is becoming increasingly important for all AMR operations. The main advantage is an extremely lightweight (9 lb) beacon and the fact that it suffices for flight safety purposes. Within the *Juno I* and *Juno II* programs the FPS-16 is only used for tracking until ignition of the second stage.

The frequency ranges from 5400 to 5900 mc/s; the peak power amounts to three mw at pulse rates between 341 and 1707 cps. Design accuracy is quoted at 5 yards in range and 0.1 mils for angle measurements. Beacon and skin track may be accomplished by automatic or manual operation. Maximum tracking rates are 8000 yd/sec in range, 40 deg/sec in azimuth, and 30 deg/sec in elevation. (The dishes are azimuth mounted.)

The output is directly fed into the IBM-709 computer for real time impact prediction or computation of any trajectory parameter desired.

B. Microlock

This tracking and communication system was developed by JPL with the goal of minimizing transmitter power and weight (Ref. 3).

The transmitter consists at the present time of a 108 or 960 mc/s radio frequency oscillator which is phase-modulated by subcarriers. The primary unit of the ground station is a phase-locked receiver which is designed to detect the beacon signal and to provide automatic tracking of the doppler shift as the satellite passes the station. Frequency and time standards are obtained from NBS radio station WWV and WWVH.

In the phase-locked loop of the receiver (Fig. 5) the local estimate of the transmitted signal is generated by a voltage-controlled oscillator (VCO). A phase detector provides a dc output voltage which is proportional to the phase difference between the incoming signal and the local estimate generated by the VCO.

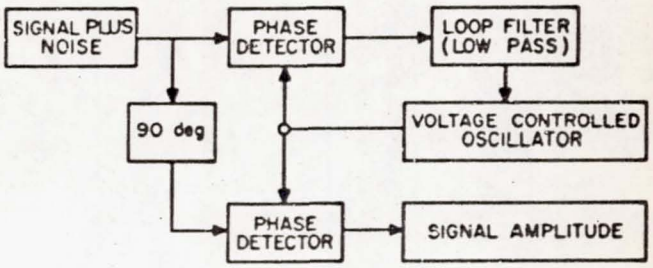

Fig. 5. Microlock receiver diagram

The dc error voltage is separated from noise by the low-pass filter to provide a control voltage to the VCO. In this way the phase-locked loop is an electronic servomechanism which accomplishes signal detection using only linear mixing.

The original design provided for a circularly polarized helical type of antenna in order to insure against loss of signal from polarization effects.

The main disadvantages of this tracking system are twofold: the strong dependence on transmitter frequency stability, and the low information content of a single station measurement. These shortcomings are overcome by reducing the tracking periods to short times with relatively large doppler effects and by combining several stations to a network.

There are now at least ten stations regularly participating in *Juno* space tracking systems; three of them are mobile (*), and the remaining seven are permanently installed.

Cape Canaveral, Florida
Redstone Arsenal, Alabama
Cape Hatteras, North Carolina*
Aberdeen, Maryland
Fort Monmouth, New Jersey
Bermuda*

Van Buren, Maine*
Goldstone, California
White Sands, New Mexico
Forrest City, Arkansas

The mobile stations are placed according to optimization studies performed for each individual flight mission (see Section VA7). The Cape Canaveral, Redstone Arsenal, and Bermuda stations are shown in Fig. 6.

Doppler accuracy depends on the frequency stability of the transmitter within the payload as well as on the stability of the ground receivers. This stability is defined over the length of the observation period. For short time periods such as the 30-sec cluster burning, the overall frequency accuracy observed has been surprisingly good, of the order of 1% of the velocity increment.

In 27 frequency comparisons between observed doppler result and calculated frequency shift from the final trajectory, only three cases exceeded a 3-sigma deviation.

The standard deviation of the remaining 24 samples was 24 m/s or the equivalent of nine cps (based on 108 mc/s). This means a stability of at least 10^{-7}, which is better than laboratory predictions. Over longer time periods, such as for pass observations, the expected frequency drift naturally increases as a function of time.

C. *Millstone Hill Radar*

This 84-ft parabolic radar dish (Fig. 7) in Westford, Massachusetts, was built and is operated by the Lincoln Laboratory of the Massachusetts Institute of Technology (Ref. 4).

At the operating frequency of 440 mc/s, the half-power beam width is 2 deg. Dual receiving and remotely adjustable transmitting polarizations are available. The antenna feed is rotated to provide a conically scanned beam which has automatic tracking capability.

The antenna gain is 37 db, the nominal peak radiated power 333 kw, and the pulse length 2 millisec. The nominal pulse repetition rate amounts to 30 per sec.

The digitized information describing a single received echo is simultaneously recorded and fed into a computer. The information contains time, azimuth, elevation, range, and doppler. Complete tracking results after application of smoothing are automatically fed into the teletype communication net and obtained in 6-sec steps. The estimated accuracies quoted are ±0.2 deg for angle determination, ±8 km in range, and a doppler error of ±27 m/s.

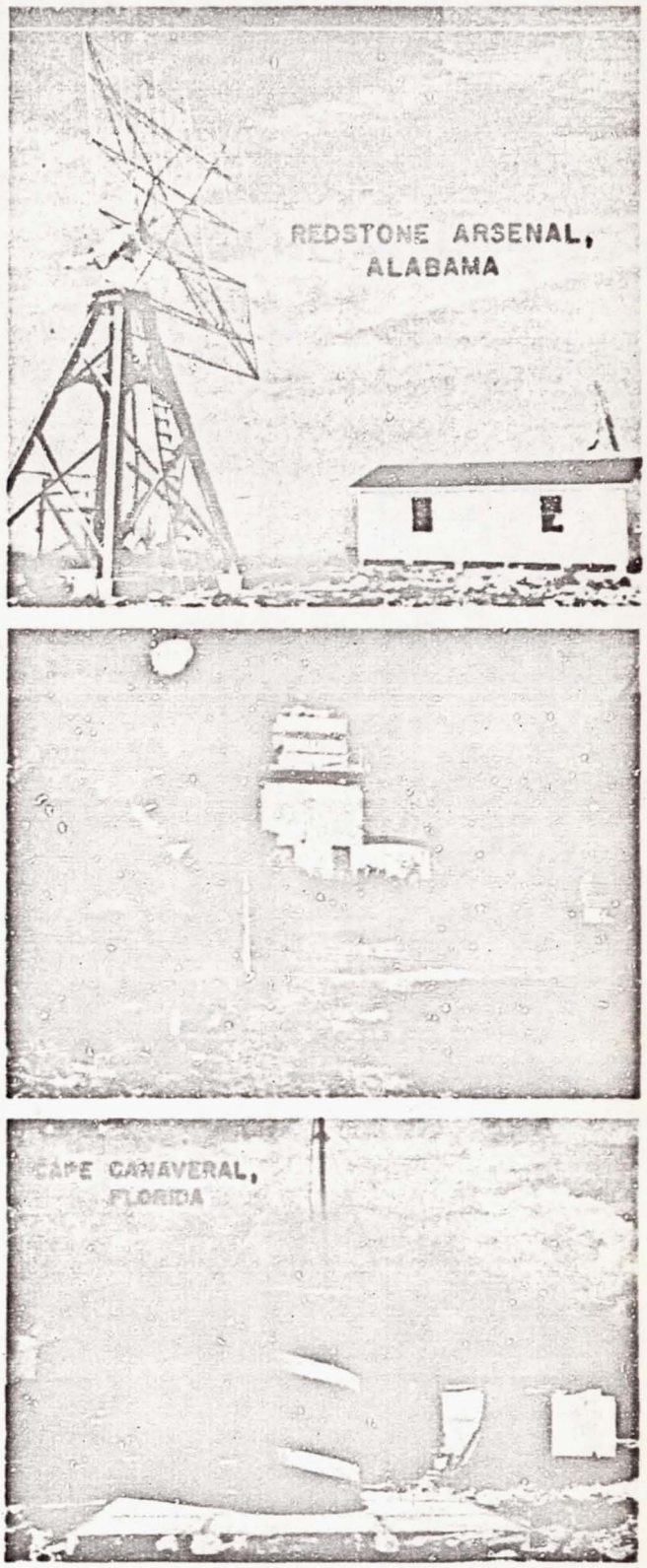

Fig. 6. Microlock stations

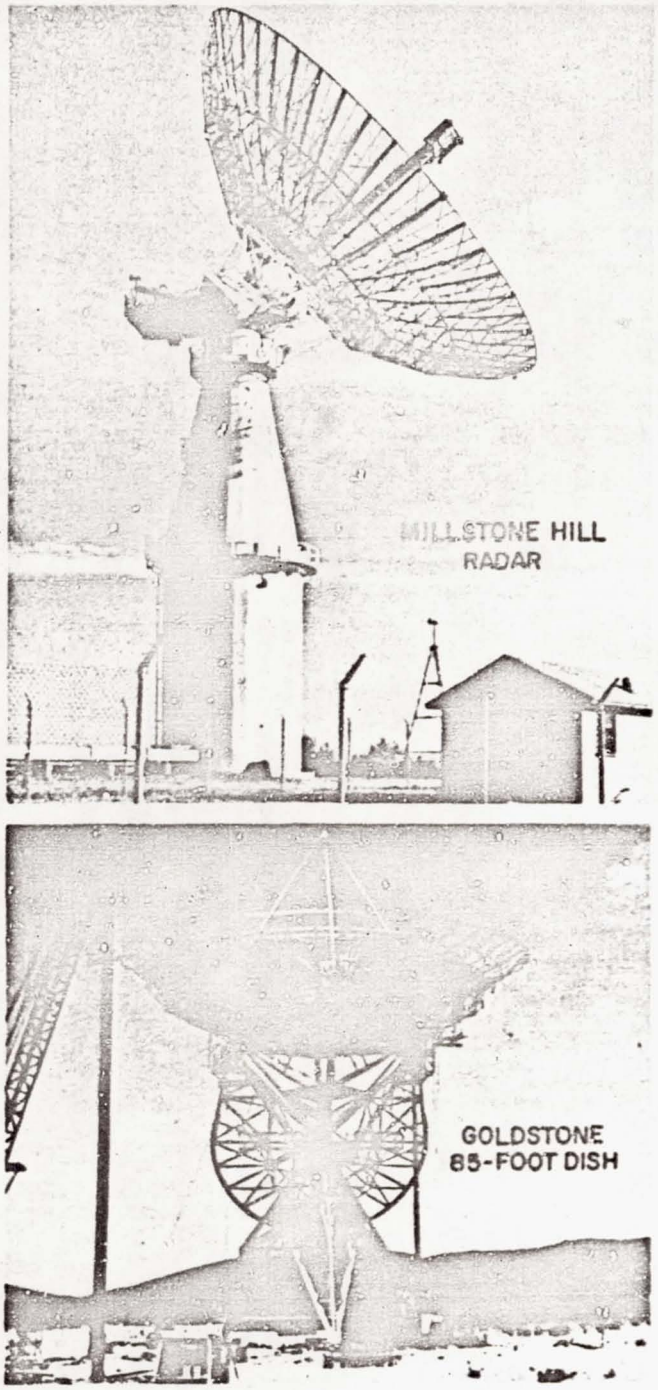

Fig. 7. Millstone Hill radar; Goldstone dish

D. Minitrack

Minitrack, a radio system for tracking an Earth satellite, has been developed at the Naval Research Laboratory as a part of Project Vanguard. It is a radio phase-comparison system employing a low-power, lightweight, 108-mc/s transmitter in the satellite to illuminate a total of eight antennas arranged in five pairs along two orthogonal baselines.

From the five phase comparisons made with these antenna pairs, two direction cosines of the line connecting the center of the antenna system (Fig. 8) and the satellite are determined as a function of time as the satellite passes through the pattern of the receiving antennas. The five phase comparisons made to determine the two direction cosines are: north–south fine, north–south medium, north–south coarse, east–west fine, and east–west medium. The actual measurements are made from the fine baselines; the medium and coarse baselines are used for ambiguity resolution. A single result which is sometimes of importance for the orbital correction process and which may be obtained quite simply and fast is the time of meridian crossing (north–south direction cosine equals one). Important stations are located at Cape Canaveral, Florida, and San Diego, California.

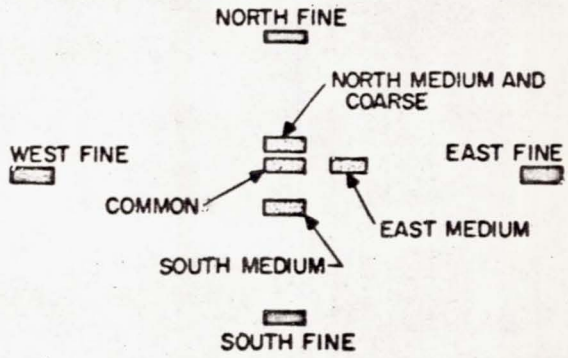

Fig. 8. Minitrack antenna system

E. Goldstone Tracking Dish

The Goldstone 85-ft-diameter dish (Fig. 7) was developed by JPL for long-range tracking of lunar and interplanetary space vehicles, in particular the two moon probes *Pioneer III* and *Pioneer IV* (Ref. 5).

For this purpose the station was operated on a frequency of 960.05 mc/s. The antenna gain on this frequency is 43.1 db, the beam width 0.8 deg. The receiver noise is as low as 7 db, while the threshold lies at −149 db.

The antenna feed is simultaneous-lobing. The automatic tracking is achieved by a servomechanism in connection with a coherent angle error detection system. The mechanical angle accuracy amounts to 2 mils under normal weather conditions.

The dish is equatorially mounted. Output data are local hour angle, declination, and doppler frequency. The maximum angular tracking rate amounts to 1.7×10^{-2} rad/sec.

Goldstone was recently modified to successfully track *Explorer VII* on the 108 mc/s frequency.

The absolute angle accuracies obtained are in the order of 0.01 and 0.1 deg for 960 mc/s and 108 mc/s, respectively. The accuracy of angle tracking has the general advantage of not depending on transmitter frequency shifts, although refraction errors have to be considered for low frequencies and low elevation angles.

F. Summary of Tracking Results

1. FPS-16 Radar

Table 3 details participation of FPS-16 radar in *Juno I* and *II* flights.

Table 3. FPS-16 radar tracking results

Test	Juno	Errors in real time determination		Remarks
		Position (km)	Velocity (m/s)	
C-44	I	–	–	Failed to track
C-47	I	2	31	
AM-11	II	1	37	
AM-14	II	43	54	Essentially time error
AM-19B	II	1	4	
AM-19A	II	1	3	

2. Millstone Hill Radar

MHR participated only in *Juno II* flight 19B. The vehicle was successfully tracked through ignition of stage II. Excessive deviations of the payload from the predicted flight path occurred. MHR reacquired the first stage but not the payload.

3. Minitrack

The Minitrack stations attached to Goddard Space Flight Center attempted to participate in two *Juno II* flights, 19B and 19A. Flight 19B experienced excessive flight deviations and did not orbit. Flight 19A was not acquired during initial reacquisition phase. Only meridian crossing times are used in real time from this tracking network.

4. Goldstone 85-ft Dish

The Goldstone 85-ft dish has proved a reliable and precise tracking instrument. The data obtained on tests AM-11 and AM-14 (*Pioneers III* and *IV*) on a 960-mc/s frequency were of excellent quality (Ref. 1, 5, and 6).

A more recent use of the dish on test AM-19A (*Explorer VII*) was also successful. Operating at 108 mc/s, an accuracy in the vicinity of 0.1 deg was obtained on several favorable orbital passes. The use of the dish is somewhat handicapped for low-altitude orbits by the low elevation angles and short duration of all but overhead passes. The polar mount of the dish imposes a further disadvantage for passes which cross north of the dish, since a region of positive elevation angle in this area is beyond the mechanical limits of the mount.

5. Microlock

Table 4 details participation of Microlock tracking in *Juno I* and *II* flights.[1]

[1]See also Table 5.

Table 4. Microlock tracking results

Test	Juno	Frequency, mc/s	Number of stations participating		Number of stations receiving usable results		Remarks
			Cluster	Orbital	Cluster	Orbital	
C-29	I	108	2	–	2	–	
C-26	I	108	2	–	1	–	No real time performed orbit determination by ABMA
C-24	I	108	4	–	3	–	
C-44	I	108	5	7	4*	7	*One not in real time
C-47	I	108	5	6	2	5	
AM-11	II	960	5	–	3	–	Lunar flights, orbital data not applicable
AM-14	II	960	5	–	2	–	
AM-19B	II	108	7	9	7*	9	*Shifts prevented real time evaluation
AM-19A	II	108	7	7	2*	7	*Strong external interference

IV. LAYOUT AND EQUIPMENT OF EVALUATION COMPLEX

The large computation and reduction facilities of the Computation Laboratory, ABMA, as already available have been one of the determining factors of this entire scheme. The facilities are not the result of optimized requirements for an orbit determination, and the physical evaluation layout has had to compromise between the short-term needs of the early orbit determination and the continuous operation of the Computation Laboratory for other urgent missions. The physical space is rather limited and could not be increased for the early orbit determination.

There are three main areas in the physical layout: the Evaluation Center or headquarters of the operation, the Computer Room, where all digital computation and manual data processing is performed, and the Automatic Data Reduction Room (Fig. 9).

An average operation includes approximately 35 persons.

A. Evaluation Center

The Evaluation Center is located in a 36 by 16-ft room, divided into two parts by a folding partition. One end of the Center serves as headquarters for the operation and contains all external telephone communications. Ten telephones are available for external or internal use. The headquarters room is manned during a typical operation by eight persons of the Flight Evaluation Branch of Aeroballistic Laboratory, including the director of the operation.

The second half of the Evaluation Center, isolated by folding doors, contains the teletype facilities used during the operation (Section IV D).

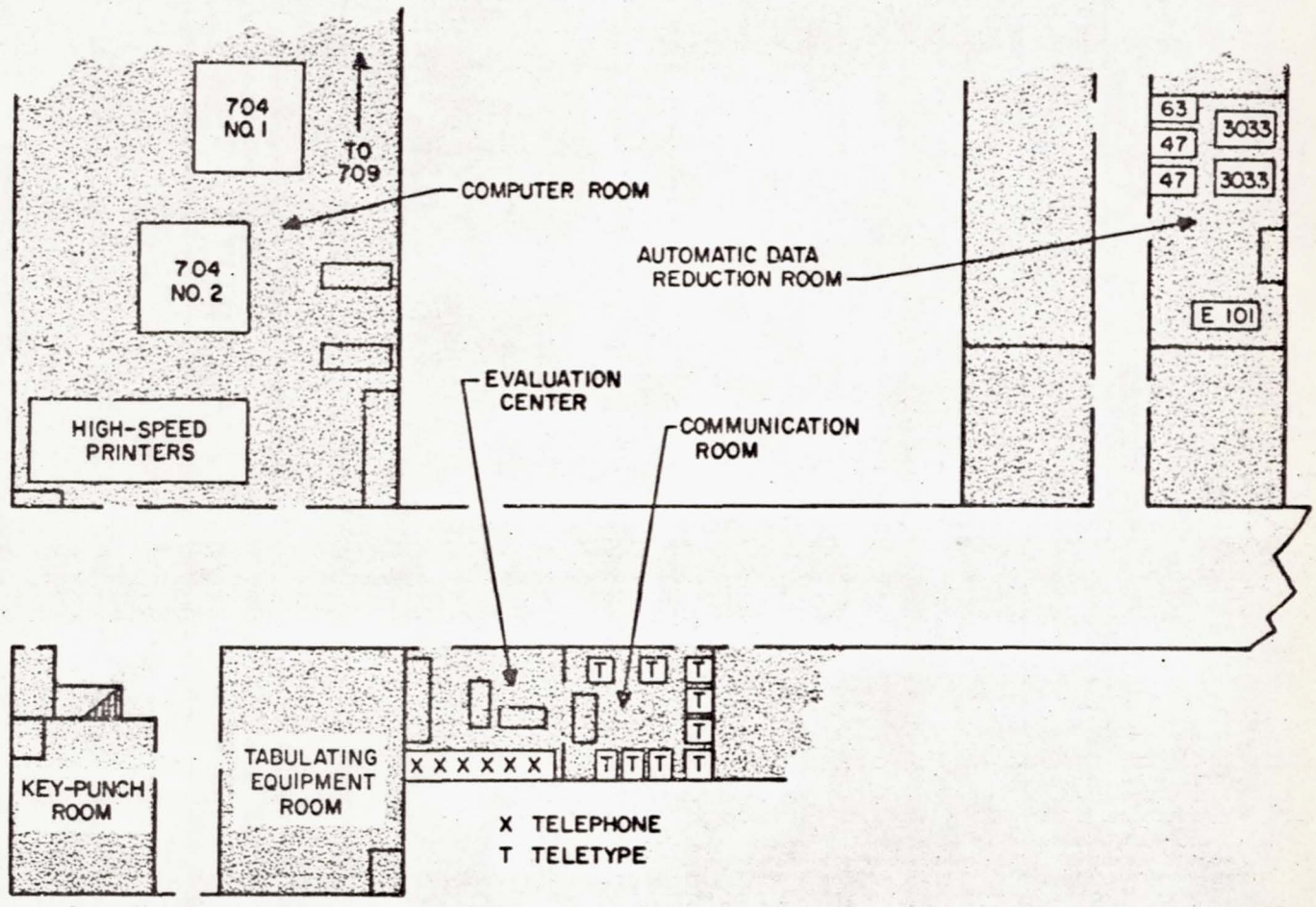

Fig. 9. Evaluation layout

B. Computer Room

The main computation facilities utilized are located immediately across the hall from the Evaluation Center. The computer room contains two IBM 704's and one 709 (Fig. 10). The 704 digital computers are each equipped with 8,192-word core storage, 8,192-word drum storage, seven magnetic tape units, an on-line printer, and a card punch. The 709 has a 32,768-word core storage, ten tape units, an on-line printer and card punches. Two 500-line-per-min and two 1000-line-per-min off-line printers are available for printing from magnetic tape.

One card punch is located in the Computer Room for rapid access. Additional card punches, interpreters, reproducers, and other peripheral equipment are located in rooms immediately adjacent to the Computer Room.

Programming and operating personnel for the evaluation programs generally are three to four members of the Trajectory Studies Unit, General Electric Computer Group, Computation Laboratory. Two key-punch operators and two computer operators from the normal computer operations force are also used.

The Hand Reduction Group, which performs all manual handling and analysis of data required, is also located in the Computer Room. This group comprises four persons from the Flight Evaluation Branch, Aeroballistics Laboratory.

C. Automatic Data Reduction Room

In another wing of the building the Automatic Data Reduction Room is located (Fig.10). In this room all automatic handling of data is performed, including translation of paper teletype tape to punched cards for direct input to the computers and for automatic plotting of data translation of punched cards from the computer to teletype tape for fast transmission of station predictions, automatic plotting of data, and reduction of doppler frequency S-curves for rough inflection time and slope. The personnel staffing this room also process the doppler data (converted from paper tape to cards) on the 704 computers for determination of exact inflection time and slope. The automatic data reduction is performed by four to six persons of the Tracking Section, Data Reduction Branch, Computation Laboratory.

The primary equipment used in the automatic data handling is described below.

1. Two IBM 47 tape-to-card printing punches are used for the conversion of five-channel teletype tape to standard IBM cards. Operating rate is normally eighteen characters per sec. Format control is obtained through a plug-wired control panel.
2. One IBM 63 card-controlled tape punch is used to convert standard IBM cards to perforated five-channel paper tape for teletype transmission. Operating rate is ten characters per sec, and format is controlled by a wired control panel.
3. Two IBM 3033-A-2 data plotters perform the automatic plotting of digital information from punched cards. A 30 by 30-in. plotting surface is available; plotting rate is roughly 1 point per sec.
4. One Burroughs E-101 digital computer is used for the determination of rough inflection time of doppler frequency data. An externally programmed desk-size computer, the E-101 has a memory of 220 twelve-digit numbers.

Adjacent to the Automatic Data Reduction Room are facilities for the reduction and display of missile and payload telemetry data. These facilities are sometimes used in the "quick look" operation for an early check of payload telemetry and performance and for real-time analog displays of data received by the Redstone Arsenal tracking station.

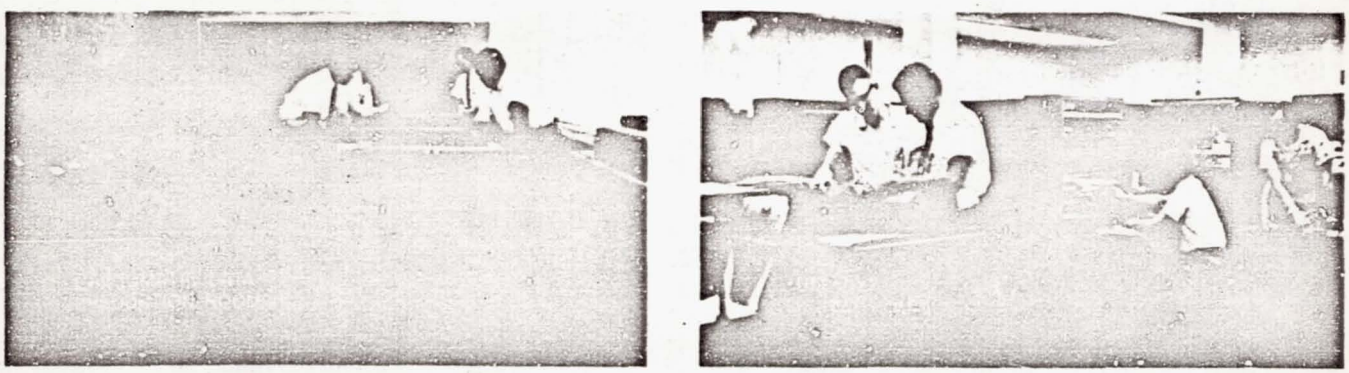

Fig. 10. IBM 709 computer: data reduction room

D. Communications

Primary communications between the Evaluation Center and external sources consist of ten telephones and eight to ten teletypes. Telephone communications are held to a minimum, and primary reliance, especially for all data transmission, is placed on teletype. Teletype is the more reliable transmission medium as it eliminates misunderstanding, particularly of numerical data, and provides firmer control and recording of both incoming and outgoing messages. All teletypes are equipped with paper tape readers and punches.

The available teletype facilities are normally utilized as follows. Direct, single-use lines are maintained to MFL, to the NASA Space Control Center, and to the Central ABMA Communications Center. Remaining lines are allocated to tracking stations. more than one station being placed on a line if necessary and if not detrimental to the success of the mission.

Available telephones are used in the following way. Two lines are opened to a special contact in Hangar D at AMR for close contact with the countdown, the real time telemetry display, and postfiring information. One of the two lines serves as a backup against failure of the other. Other special lines are allocated as required for the particular mission, e.g., to NASA, the blockhouse at AMR, or to JPL.

Remaining phone lines are opened to tracking stations on the following bases: the need for backup to the teletype connections, the transmission of information not easily relayed over teletype, the need for instantaneous transmission of information, etc. A sample communications plan is shown in Fig. 11.

The teletype facility is maintained and operated by the Army Signal Corps; personnel required during an operation generally are one operator per teletype and one supervisor.

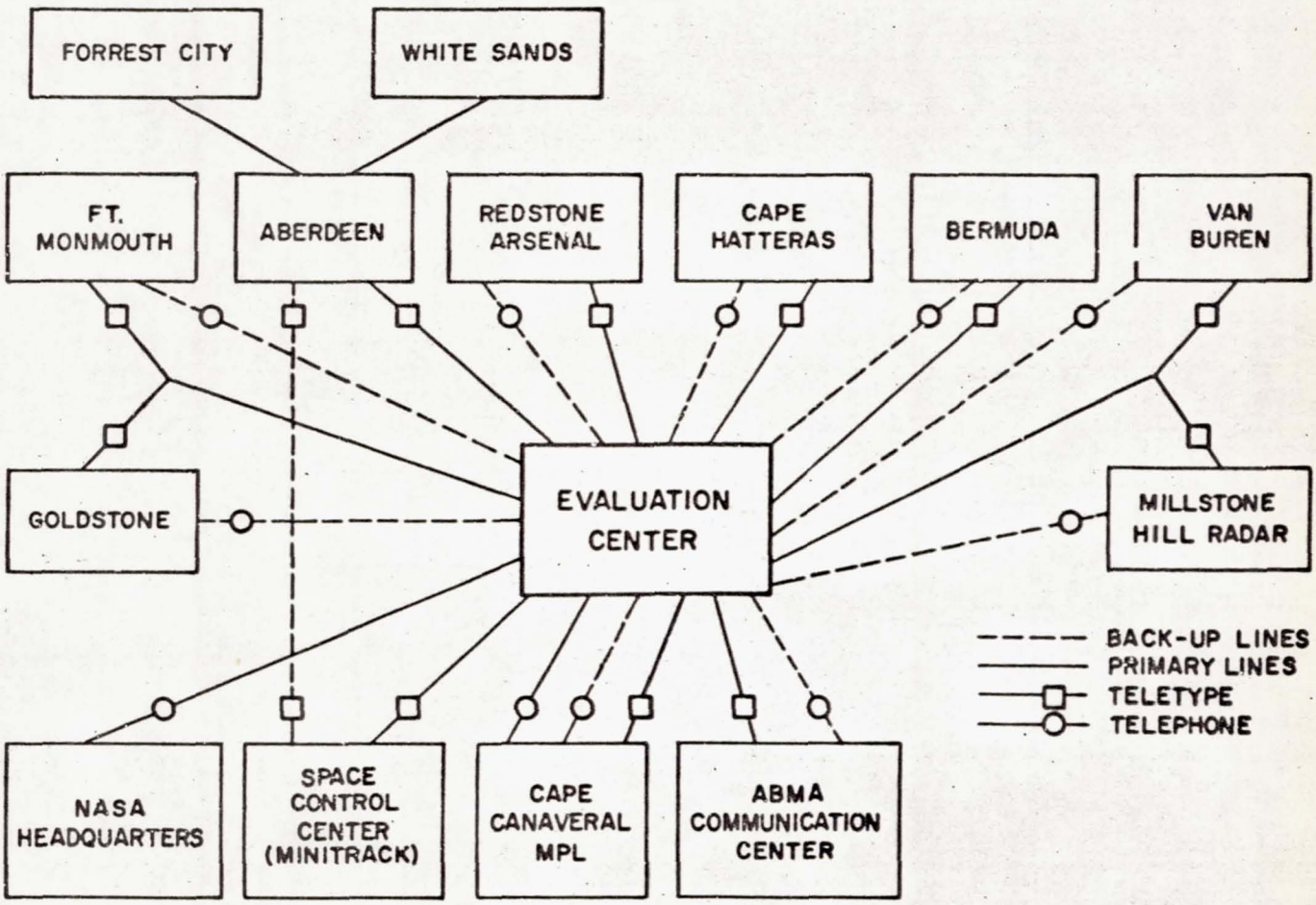

Fig. 11. Communications plan

V. EVALUATION TECHNIQUES

The basic evaluation scheme has been outlined in Section II. In this section the techniques utilized in the scheme will be examined in greater detail. The computation and data handling scheme and its division between manual and machine operations are shown in Fig. 12.

A. Powered Phase—Booster and Cluster Flight

1. Method of Tracking

The evaluation steps performed during power and coast flight of the booster are described in Sections IIB and IIC. In this phase the Evaluation Center serves primarily as the recipient of reduced and interpreted results. The information is important to the orbit scheme, but is not a product of the scheme.

The primary function of the Evaluation Center begins with ignition of the upper stages. The short cluster flight produces a large change in the velocity vector but a relatively small change in position (decreasing the value of angle measurements). It is tracked by utilization of the doppler shift observed in the signal broadcast by the payload transmitter.

2. Cluster Doppler Data

The doppler effect is an apparent shift in the frequency of a signal due to the relative motion between the observer and the source. For all practical purposes the frequency shift Δf measured by an observer is

$$\Delta f = (f_r - f_o) = \frac{f_o}{c}\dot{s}$$
$$f_r = f_o\left(1 + \frac{\dot{s}}{c}\right) \qquad (1)$$

where

f_r is the absolute frequency received by an observer
f_o is the frequency transmitted by the source
c is the propagation velocity of electromagnetic waves
$\dot{s}$ is the relative velocity between observer and source (small compared with c)

The quantity $\dot{s}$ may be called the slant velocity, the rate of change of the path of the radio signal between observer and source. This path would be a straight line were it not for refraction and reflection phenomena.

In the simplest picture, for a transmitter moving with an instantaneous velocity v (Fig. 13), a given receiver measures by the doppler shift only a certain component of v, the component along the line of sight between observer and transmitter.

A schematic plot of received frequency vs time during cluster burning for a typical station is shown in Fig. 14. This plot is typical of the one-way doppler data obtained during cluster flight. The most significant features of these data are the three steps seen. At the ignition time of stage II, the relatively flat frequency function rises steeply as the stage accelerates. The function flattens again during the coast period between burnout of stage II and ignition of stage III, forming the first step. Stage III forms a second step, and stage IV a third step.

3. Data Reduction

In addition to simple qualitative information concerning firing of the three stages (Section IID), a more detailed analysis utilizing the magnitude of the steps in the doppler shift permits a solution for the coordinate and velocity vectors of the payload at burnout of stage IV. For this purpose, the doppler shift is measured by the various tracking stations and recorded digitally as a function of time, normally at 1-sec intervals. This digital information is transmitted via teletype to the Evaluation Center.

At the Center, the doppler shift Δf from ignition of stage II until burnout of stage IV is extracted from the data. This extraction is presently performed by hand because of difficulties involving data quality and transmission problems. About 30 min are normally required for the reduction of all data received. It is anticipated that this problem will be handled on the IBM 709 in the near future. Reduction time should then be less than 5 min.

The problems to be solved for machine reduction are severe. The rapid, irregular change in the doppler frequency during cluster burning, combined with low elevation angles and signal levels, often causes tracking stations to lose signal lock momentarily, creating gaps or bad points in the data. Special smoothing and extrapolation techniques must be developed to fill in such gaps and compensate for variations in data arising from oscillations of the transmitter frequency, shifts in the transmitter frequency, erroneous points, and the normal errors of data transmission.

Further, the doppler increments must be taken between physically corresponding points. Therefore, the ignition point must be determined individually for each station

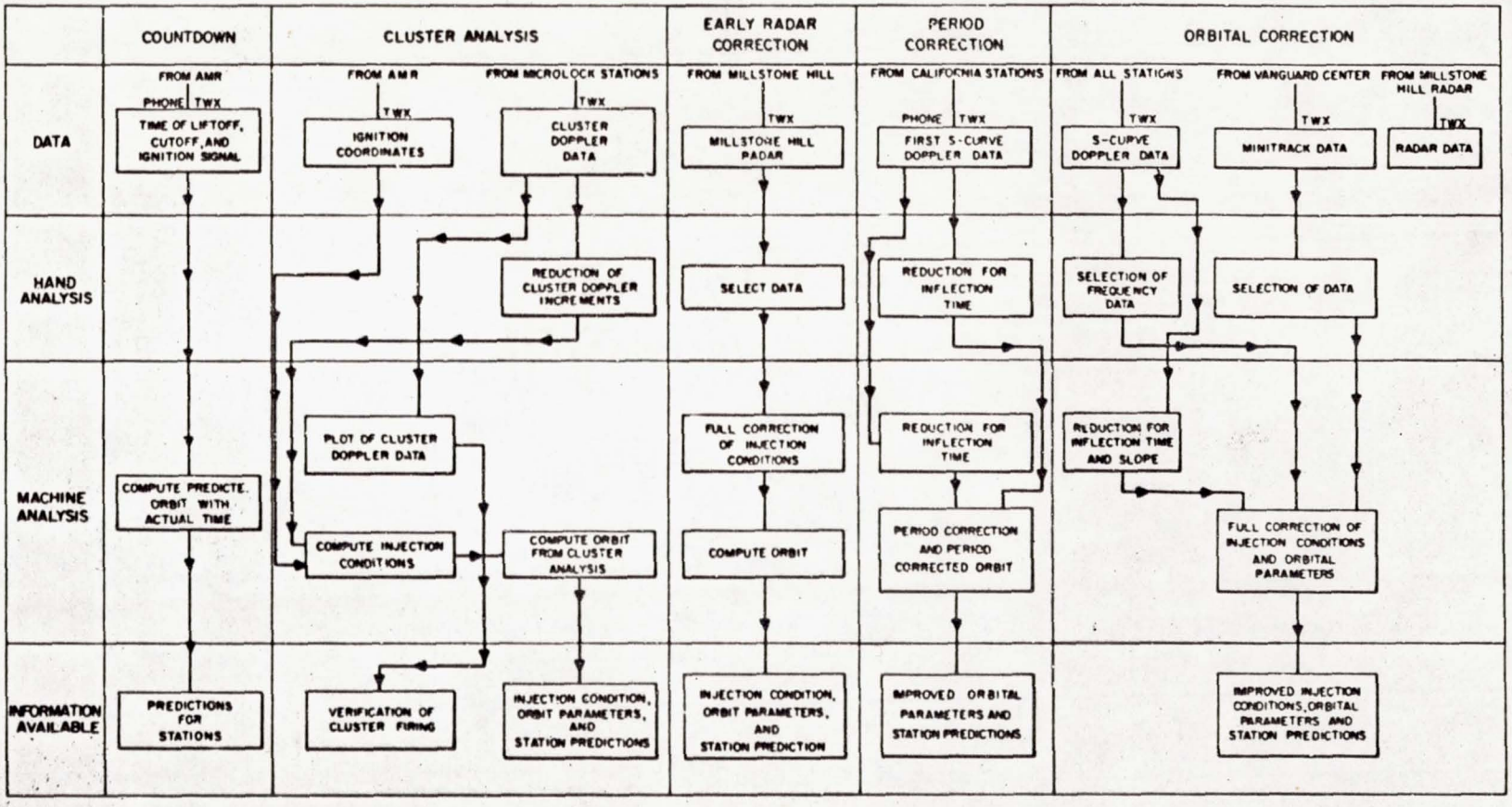

Fig. 12. Cluster and free flight reduction process

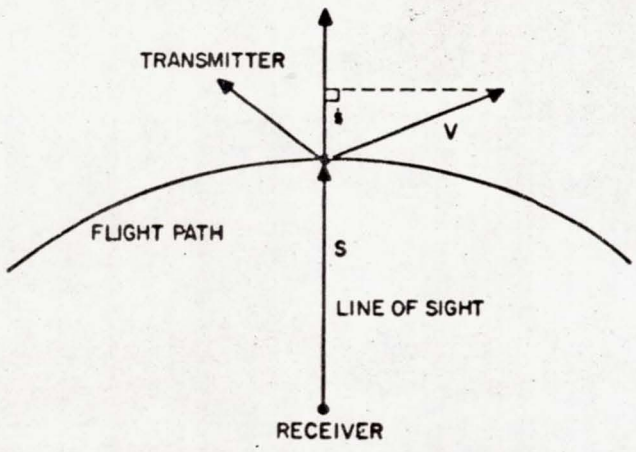

Fig. 13. Doppler velocity diagram

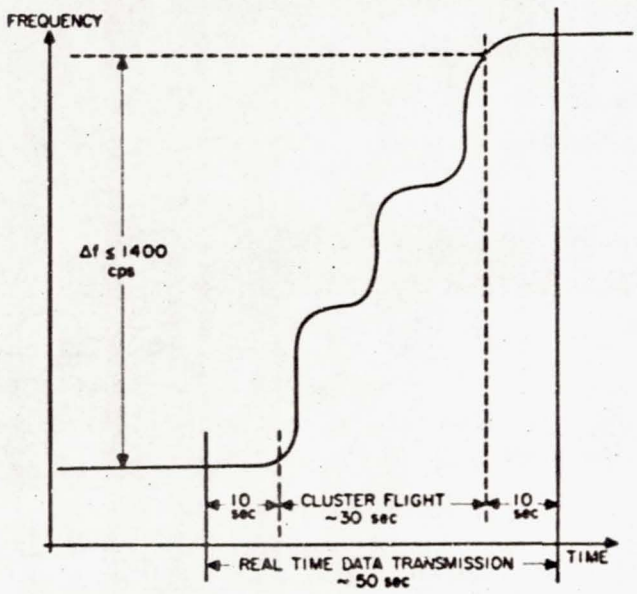

Fig. 14. Cluster doppler data

from the doppler data, since each station measures time increments very accurately, but errors of up to several seconds arise in the digitally coded absolute time.

For detailed postflight analysis of upper stage performance, the doppler increment during burning of each stage is extracted and utilized. However, for the early orbit determination it is only necessary to measure the total increment observed during burning of three stages. The reason for this and the principle of the injection point determination follow.

Neglecting refraction, the doppler shift f observed by a given station at ignition of stage II is:

$$f = \frac{f_0}{c} \dot{s}_{ign} \tag{2}$$

where

$$\dot{s}_{ign} = \frac{\mathbf{r}_{ign} \cdot \dot{\mathbf{r}}_{ign}}{|\mathbf{r}_{ign}|}$$

and $\mathbf{r}_{ign}$ is the line-of-sight vector between the station and transmitter at ignition.

Similarly, the doppler shift f' at injection is

$$f' = \frac{f_0}{c} \dot{s}_{inj} \tag{3}$$

and the doppler increment during burning of the upper stages is

$$\delta f = f' - f = \frac{f_0}{c} (\dot{s}_{inj} - \dot{s}_{ign}) \tag{4}$$

It is seen that

$$\delta f = F(\mathbf{r}_{inj}, \dot{\mathbf{r}}_{inj}) - F(\mathbf{r}_{ign}, \dot{\mathbf{r}}_{ign}) \tag{5}$$

where all other parameters may be considered known. However, since the position and velocity of the missile at ignition of stage II are known from range instrumentation, in terms of unknowns the function δf reduces to

$$\delta f = F(\mathbf{r}_{inj}, \dot{\mathbf{r}}_{inj}) \tag{6}$$

Since $\mathbf{r}_{inj}$ and $\dot{\mathbf{r}}_{inj}$ are each three-component vectors, the function F is known, and the quantity δf is measured, there are six unknowns in Eq. (6). Given accurate δf's observed by six stations, it would be possible to solve for $\mathbf{r}_{inj}$ and $\dot{\mathbf{r}}_{inj}$.

However, an additional restraint is present since the injection conditions are related to the ignition II conditions by the laws of motion. Thus

$$F(\mathbf{r}_{inj}, \dot{\mathbf{r}}_{inj}) = G(\mathbf{r}_{ign}, \dot{\mathbf{r}}_{ign}, I, \alpha, \beta) \tag{7}$$

where I is an average effective thrust magnitude, and α and β are average thrust directions during burning of the stages. The injection conditions are relatively insensitive to the exact time history of α and β, and to small deviations of I from the predicted. Hence only the average effective thrust magnitude and the average thrust directions need be considered unknown, while the nominal time history is used. This is also the reason that only the total doppler increments during cluster burning are needed for determination of injection conditions, rather than the stage-by-stage increments required for a more exact flight history.

Thus, Eq. (6) reduces to

$$\delta f = G(I, \alpha, \beta) \tag{8}$$

Since there are now only three unknowns, only three observed δf's are required for the solution for I, α, and β. The injection conditions may then be computed from $\mathbf{r}_{i_{gn}}$, $\dot{\mathbf{r}}_{i_{gn}}$, I, α, and β.

It should be understood that I, α, and β, while interpretable in terms of mean deviation of the thrust performance of the total cluster stages as an entity, are truly only artificial parameters leading to a close estimate of the injection conditions. They in no way represent the true attitude motion or thrust history of the upper stages.

4. Method of Solution

The method utilized for the solution for injection conditions is the method of linear differential corrections, used in connection with a simplified trajectory computation program. Thus it is assumed that

$$\delta f_{observed} = \delta f_{nominal} + \frac{\partial f}{\partial \alpha}\delta\alpha + \frac{\partial f}{\partial \beta}\delta\beta + \frac{\partial f}{\partial I}\delta I \qquad (9)$$

where δf nominal is the value of δf predicted from a nominal trajectory, and $\delta\alpha$, $\delta\beta$, and δI are corrections to be applied to the nominal trajectory values I, α, and β to produce δf observed.

The partials required are obtained by the method of successive perturbations; that is, δf nominal is calculated from Eq. (8):

$$\delta f_{nominal} = G(I_0, \alpha_0, \beta_0)$$

Then, a perturbed value δf_{pert} is computed as

$$\delta f_\beta = G(I_0, \alpha_0, \beta_0 + \Delta\beta)$$

The desired partial is then taken as

$$\frac{\partial f}{\partial \beta} = \frac{\delta f_\beta - \delta f_{nom}}{\Delta\beta} \qquad (10)$$

Partials are computed similarly for I and α. Thus, Eq. (9) requires the computation of four trajectories, one nominal and three having perturbations in I, α, and β.

The perturbation sizes $\Delta\alpha$, $\Delta\beta$, and ΔI for computation of the partials are optimized to obtain the most accurate partials. They are normally made as small as possible without encountering numerical errors. The perturbation sizes in present use are 0.1 deg for $\Delta\alpha$, 0.1 deg for $\Delta\beta$, and 0.5 % of the nominal thrust for ΔI.

Because the method of differential corrections is based upon the solution of linear equations, and because the doppler increment functions being solved are only linear for small deviations, an iterative process must be used. That is, the solution for I_1, α_1, and β_1 from a set of Eqs. (9) are regarded as new I_0, α_0, and β_0 for an improved trajectory, the partials are recomputed, and the new equations are solved for I_2, α_2, and β_2. This process is repeated until I_n, α_n, β_n are sufficiently close to I_{n-1}, α_{n-1}, β_{n-1}.

It is observed that three observations producing equations of the form of (9) are required to solve for injection conditions. If, in addition, the assumption of a nominal effective impulse I of the upper stages ($\delta I = 0$) is acceptable, only two observations are needed. This is possible if the actual specific impulse of the cluster rockets is nominal and any precessional motion of the cluster is small. It should be noted that even though the actual specific impulse of the upper stage rockets is exactly nominal, the artificial impulse I need not be nominal. This is due to the assumption that I (and α and β) are parameters of a three-stage cluster flight having no change in thrust direction within or between stages. In actual flight, deviations arise generally from precessional motion of the spin-stabilized cluster, causing the true thrust direction to be a complex function of time. This results in a loss of effective thrust, or a change in the quantity I when mean thrust directions α and β are considered .Therefore, as a rule three stations are required.

Although three equations are mathematically sufficient, it is more reliable and accurate to utilize as many observations as are available, solving the equations simultaneously by the method of least squares. At the present time, five or six sets of data are generally available.

5. Elimination of Gross Errors

One major problem is encountered, however, in this application. The method of least squares assumes a normal error distribution and works best for large quantities of data where the normal distribution may perhaps be expected. Even with numerous data points, however, a few gross errors, of perhaps 10 or 15-sigma level, will destroy the least square solution. In the case of the cluster doppler increments where less than 10 observations are available, any large error is sufficient to spoil the solution.

Of the five *Juno I* and *II* missiles to which the method has been fully applied, in all cases a serious error was present in the real time data of at least one station, for reasons not always fully understood. Therefore, it is necessary to provide a fast and simple means of detecting gross errors. The probability of such errors also emphasizes the need for a sufficient redundancy of tracking stations to insure enough good observations for a solution.

The detection of gross errors has been achieved in the following way. All data obtained from n stations are are obtained. The solutions are compared and arranged in groups of solutions which agree within specified limused, and all possible $\binom{n}{3}$ sets of 3-observation solutions

good observations give the same answer within permissible limits, different combinations using a grossly wrong observation usually yield quite different solutions. Thus, the largest group of consistent solutions will normally contain the good data, while the solutions containing bad data fall in small or single-member groups. A least square solution obtained with all stations appearing in the largest group then has a fair degree of reliability.

Because 3-station solutions are normally required, at least 4 good observations must be available for the grouping process to work. The method has been found to require no restrictive time expenditure for up to 10 sets of data.

Another method commonly used for elimination of gross errors is the rejection of all data whose fit to a least square solution exceeds a certain sigma level. This method was found to be less efficient and reliable than the grouping procedure when less than 10 observations were available.

6. Experimental Results

The method of cluster flight analysis described above has proved quite effective in an extended form for the detailed evaluation which follows each space flight, but has experienced certain difficulties as a fast real time method. However, the method is the sole means of tracking the *Juno* upper stages.

The principal difficulties experienced thus far have been: the reliability and quality of data received, partially due to lack of sufficient tracking stations; instability of the satellite transmitter; and data transmission and reduction difficulties. Sufficient tracking stations are now in operation; the stability of the transmitter has been a really serious problem in only one flight, where large frequency shifts were present; rapid data transmission and reduction remain the principal problem.

The problem of data quality may be seen in Table 5 summarizing the final (not real time) data errors experienced on past *Juno* vehicles beginning with the *Juno I* vehicle C-29 (*Explorer I*). The real time method was first applied to C-44 (*Explorer IV*).

7. Optimization of Station Locations

Three Microlock stations are mobile and can be placed for best efficiency according to individual flight missions. The location of tracking stations used in relation to a particular trajectory exhibits strong influence on the results (Ref. 7). Possible station locations are limited by consideration of the altitude and range of the cluster flight with respect to the station. An adequate elevation angle is required to insure acquisition of the payload signal and to minimize refraction effects. New sites for the mobile stations are also limited to existing tracking installations for reasons of support and communication.

Within the restrictions mentioned, however, a wide range of geometrical situations exist which strongly affect the accuracy of the solution. A geometric quality factor

Table 5. Cluster tracking results

Station	Error in observed slant velocity increments, m/s								
	C-29	C-26	C-24	C-44	C-47	AM-11[a]	AM-14	AM-19B	AM-19A
Aberdeen	[b]	[b]	+40	+42	[c]	[c]	[c]	−11	[c]
Cape Canaveral	−20	+67	−46	−5	−2	−36	+8	−22	[d]
Fort Monmouth	[b]	[b]	−2	−33	−621	[b]	[b]	+8	[c]
Redstone Arsenal	[b]	[b]	−29	+38	−3	[c]	−223	+44	[d]
Mobile 1 (V)	[b]	[b]	[b]	[c]	[c]	[b]	[b]	−6	[c]
Mobile 2	[b]	[b]	[b]	[b]	[b]	−54 (M)	+21 (G)	+14 (B)	[c]
Mobile 3	[b]	[b]	[b]	[b]	[b]	−72 (F)	+300 (F)	−12 (C)	[c]

Location Identification ( ): B, Bermuda; C, Cape Hatteras; F, Fort Stewart; G, Grand Bahama Island; M, Miami; V, Van Buren.

[a]Due to conversion from 960-mc frequency, stations actually measured only 1/18 of indicated error.
[b]Station not in operation.
[c]Station failed to track.
[d]Incomplete solution.

may be defined in the following manner: N simultaneous equations of the form of Eq. (9) can be made to yield solutions of the form

$$\delta I = \sum_N \gamma_{IN}\,\delta f_N$$
$$\delta \alpha = \sum_N \gamma_{\alpha N}\,\delta f_N \qquad (11)$$
$$\delta \beta = \sum_N \gamma_{\beta N}\,\delta f_N$$

where δf_N is the observed frequency increment for the Nth station, and the γ's are computed coefficients.

The coefficients γ will be functions such as

$$\gamma_{IN} = \gamma\,(r_{i0}, \dot{r}_{i0}, I_0, \alpha_0, \beta_0, r_{s1}, r_{s2}, \cdots, r_{sN}) \qquad (12)$$

That is, each coefficient is a function of the upper stage trajectory, defined by the ignition and thrust conditions, and of the coordinates of the N stations, $r_{s1}, r_{s2}, \cdots, r_{sN}$.

For a particular trajectory and particular stations, the error ϵ_I in the calculated quantity δ_I is

$$\epsilon_I = \sum_N \gamma_{IN}\,\epsilon_{fN} \qquad (13)$$

where ϵ_{fN} is the error in the observed frequency increment for the Nth station. If the errors ϵ_{fN} are normally distributed with a mean square error σ_{fN}, the mean square error σ_I in δ_I may be taken as

$$\sigma_I = \sigma_{fN}\sqrt{\sum_N \gamma_{IN}^2} = \sigma_{fN}\,\Gamma_I \qquad (14)$$

Similar expressions apply for the errors in α and β.

It is seen, then, that for any given error σ_{fN} in the observed frequency increments, the errors in the desired quantities I, α, and β are directly dependent upon the coefficients γ and hence upon the trajectory parameters and station coordinates. Since satellite trajectories are normally determined by stronger factors than improvement of tracking, the trajectory parameters for a given flight must be considered as fixed. However, tracking accuracy may be improved by proper location of stations.

The quantities Γ_I, Γ_α, and Γ_β may then be taken as geometrical error factors to be minimized by proper selection of station locations. In practice, Γ_I is found to be relatively smaller in physical effect than Γ_α and Γ_β by several orders of magnitude, so for convenience an overall error factor $\bar{\Gamma}$ may be considered where

$$\bar{\Gamma} = \sqrt{\Gamma_\alpha^2 + \Gamma_\beta^2} \qquad (15)$$

It is also found that $\bar{\Gamma}$ is little affected by the number of stations N considered in the solution, being determined essentially by the best 3-station subgroup for N greater than 3. Hence it is necessary only to minimize $\bar{\Gamma}$ for all possible 3-station groups. The consideration of 3-station combinations is further desirable because of the limited number of stations and the possibility of gross errors in the observations, which make the 3- or 4-station solution the most probable in the actual event.

The effect of station geometry may be seen in Table 6, where the relative error factor $\bar{\Gamma}$ is given for various station combinations for the trajectory of the *Juno II* vehicle AM-16. The station locations are shown in Fig. 4. It may be seen that by the inclusion of the Bermuda station, the error factor possible is reduced by a factor of roughly 3. This means that with a given observational error, the results obtained with a Bermuda station may be 3 times as accurate as without; or, to achieve a given accuracy, the observational error may be 3 times as large with a Bermuda station as without.

Table 6. Cluster station optimization for *Explorer VII*

Stations*	$\bar{\Gamma}$**	Stations	$\bar{\Gamma}$
VB-RS-BER	31	CH-RS-BRL	99
VB-BRL-BER	32	AMR-RS-FM	100
AMR-VB-BER	35	AMR-RS-BER	107
AMR-FM-BER	45	AMR-RS-BRL	129
RS-FM-BER	52	AMR-CH-RS	157
AMR-BRL-BER	54	CH-VB-BRL	160
CH-FM-BER	58	CH-BRL-FM	269
RS-BRL-BER	75	AMR-BRL-FM	319
CH-BRL-BER	84	VB-RS-BRL	395
CH-RS-FM	88	VB-BRL-FM	564

*AMR: Atlantic Missile Range, Fla.; BER: Bermuda; BRL: Aberdeen, Md.; CH: Cape Hatteras, N.C.; FM: Fort Monmouth, N.J.; RS: Redstone Arsenal, Ala.; VB: Van Buren, Me.
**For explanation of $\bar{\Gamma}$ see Eq. (15).

No attempt has been made to optimize station locations in the absolute sense; the approach has been rather to choose the best available locations within the limits of other considerations as mentioned previously.

B. Orbital Phase

1. Basic Method

The basic method utilized throughout the orbital analysis is that of differential correction of the orbital parameters (Ref. 8). Beginning with the best orbital characteristics available after the power flight analysis, successive corrections yielding improved parameters are applied, based on the increasing sum of available tracking data.

The corrections are computed as follows: an orbital computation is assumed available which permits the accurate prediction of the value of any desired observation (e.g., range or elevation angle at some time) to some required accuracy, given the parameters of the orbit X_j. The observation α_i is then a function of the orbital parameters X_j.

$$\alpha_i = \alpha_i (X_j, t) \tag{16}$$

Assuming approximate orbital parameters X_j^o, an observed quantity α^{obs} is assumed related to the predicted value α_i^{st}, where

$$\alpha_i^{st} = \alpha_i (X_j^o)$$

by the Taylor expansion

$$\alpha_i^{obs} = \alpha_i^{st} + \sum_j \frac{\partial \alpha_i}{\partial X_j}\Big]_{X_j} \delta X_j \tag{17}$$

where δX_j are the corrections to be applied to the X^o to yield improved parameters X_j' of the true orbit, and higher order terms are neglected.

Because Eq. (17) assumes that the observable function α is linear in each X_j, which is not true, the X_j' are improved but not completely correct parameters, and the correction process must be iterated. The X_j' are used to compute new α_i^{st} and new $\partial \alpha_i / \partial X_j$, and new $\delta X_j'$ are obtained. This process is repeated until the corrections converge (i.e., $\delta X_j \to 0$), the final parameters obtained being

$$X_j' = X_j^o + \Sigma \delta X_j \tag{18}$$

The correction process does converge for most practical cases, assuming observations of sufficient accuracy and information content, and initial parameters of reasonable nearness to the actual parameters.

The minimum number of observations required to solve for the X_j is of course j_{max}, the number of X_j. Because of the quality and type of data normally obtained, overdetermination becomes a necessity, and the number of observations i_{max} used is much larger than j_{max}. The overdetermined set of linear equations of the form (17) is solved by the method of least squares.

The partials $\partial \alpha_j / \partial X_j$ are computed by the method of successive perturbations. That is, in addition to the predicted value

$$\alpha_i^{st} = \alpha_i (X_j^o)$$

j_{max} perturbed values α_i^p are computed for each α_i,

$$\alpha_i^{pj} = \alpha_i(X_1, X_2, \cdots, X_j + \Delta X_j, \cdots, X_{j_{max}})$$

The partials are then approximated as

$$\frac{\partial \alpha_i}{\partial X_j}\Big]_{X_j^o} \cong \frac{\alpha_i^{pj} - \alpha_i^{st}}{\Delta X_j} \tag{19}$$

The size of the perturbations ΔX_j must be chosen carefully to obtain accurate partials. They are normally made as small as possible without encountering numerical difficulties.

The perturbation sizes must be optimized according to the parameters chosen for correction and the data used for the correction. As an example, Fig. 15 shows the relative magnitude of the partial derivative of various observations with respect to the azimuth angle α of the injection velocity vector of an orbit similar to that of *Explorer VII*. For larger perturbation sizes the partials change value rapidly due to the invalidity of Eq. (19). For very small perturbation sizes the partials again change value due to roundoff in the numerical calculations. The optimum perturbation size is chosen as 0.025 deg in the vicinity of which the partials are each almost constant and yield the best approximation to the instantaneous slope of the observation function. The observation curves are not identified in Fig. 15, since they are only a representative few of the many that must be considered.

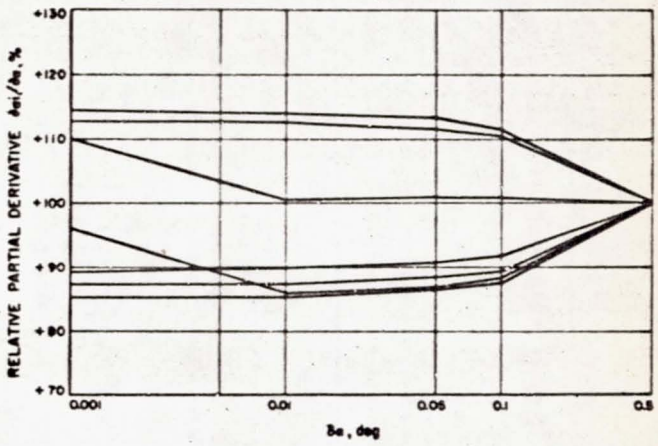

Fig. 15. Relative magnitude of partial derivatives

An alternative method is to obtain approximate analytic expressions for the partials as a function of the time of observation and initial parameters. The method of successive perturbations, while in some cases more time-consuming than the use of analytic expressions (since it requires the computation of $j_{max} + 1$ orbits), was chosen because of its flexibility in accepting varied data types and relative simplicity in development and programming.

2. Orbital Parameters

The orbital parameters chosen for correction are the coordinates and velocity of the satellite at some time after completion of all thrust, defined as the orbital injection point. The reason for this choice lies in the connection of the orbital determination with the power flight analysis and in the mission of evaluation of vehicle performance. The system chosen may be immediately interpreted in terms of missile performance, and this interpretation in turn permits a physical feeling for the reality of results indicated by the orbital correction scheme.

Also, in all cases except the early orbit correction with radar data (Section VB3) it has been found advantageous to solve for only the velocity vector, the injection coordinates being more accurately determined from the power flight analysis than from orbital data. This point is covered more thoroughly in Section VB5, concerning the final orbital phase.

The specific injection quantities chosen are the Cartesian coordinates of the satellite at injection in an Earth-fixed system with origin at the center of the Earth, the magnitude of the Earth-fixed velocity at injection, and the elevation and azimuth angles of this velocity vector. This system of coordinates is denoted as the perturbation system. An error in velocity elevation ε corresponds roughly in missile terminology to an error in the local pitch velocity angle, and an error in the velocity azimuth angle α to the missile yaw velocity angle.

While the above system of coordinates has not been optimized, it has proven convenient, satisfactory, and at least a relative optimum in comparison to some other systems. For instance, if the same correction utilizing doppler data from five stations during one revolution of a satellite in an *Explorer VII* type orbit is made in the perturbation system just described and in a completely Cartesian system (space-fixed ephemeris system), the following results are obtained (Table 7):

The magnitudes of the initial errors to be corrected were 2.8 m/s in V, 1 deg in α, and 1 deg in ε.

Table 7. Comparison of correction convergence (error remaining after one step of correction program)

Correction in perturbation system	Correction in space-fixed ephemeris system	Results in ephemeris system transformed to perturbation system
V 0.1 m/s	$\dot{X}$ 10.8 m/s	V 2.6 m/s
α 0.03 deg	$\dot{Y}$ 20.3 m/s	α 0.22 deg
ε 0.00 deg	$\dot{Z}$ 16.4 m/s	ε 0.03 deg

It may be seen that making the correction in the perturbation system affords a larger initial correction and hence more rapid convergence of the correction process. Ninety-nine percent of the initial injection error is removed in one iteration in the perturbation system, while two or three iterations are required in the ephemeris system.

It should be observed that the final parameter accuracy obtained in the two systems is the same, after proper iteration and convergence of the corrections. However, the correction process performs more efficiently (more rapid convergence) in the perturbation system. The general conclusion is that the relation between orbital parameters and observations is more nearly satisfied by the linear equations used if the coordinate system is properly chosen. Work is now in progress for determining an absolute optimum coordinate system for given circumstances.

3. Early Orbit Phase

During the early orbit phase the doppler data acquired are generally insufficient for a complete orbit determination. When used, the doppler data are treated by the processes described in Section VB5. The data obtained by Millstone Hill Radar, if the acquisition problem is solved, are given special treatment, however. The data are supplied in the form of range, azimuth, and elevation. The data are smoothed by Millstone before transmission to the Evaluation Center, and have an estimated residual error of 8 km in range and 0.2 deg in the angles. From 5 to 15 min of data are usually possible after injection for the 44-deg firing azimuth.

Once the payload is acquired the data processing and transmission via teletype are automatic. The data message is to be expected about 15 min after loss of skin track. At ABMA, the perforated teletype tape is fed into a tape to IBM card converter. The cards are used as input for the orbit correction deck, using orbit number two as an initial estimate. All six parameters of the injection point (position and velocity components) are corrected simultaneously. This is preferable because the complete angle and range data obtained immediately after injection determine both position and velocity. For a typical satellite such as *Explorer VII*, 5.5 min of Millstone data beginning at the injection point will determine the injection point within 2 km in coordinates, 10 m/s in velocity magnitude, and 0.15 deg in the direction of the velocity vector.

After loss of signal by the tracking stations on the western edge of the Atlantic, normally no further information is available to the Evaluation Center until the

satellite again approaches the United States at the completion of its first orbit. The silent period has a duration of approximately 60 to 90 min.

Predictions are computed for the first orbital pass for all stations in the form needed, based on the most accurate and reliable parameters then available from the evaluation scheme. Predictions to Microlock stations equipped with omnidirectional antennas consist of predicted crossover time only and are sent manually. Predictions to stations requiring more detailed information, as, for instance, antenna pointing angles as a function of time, are sent through a mechanized scheme. The 704 computer punches the predicted data required (e.g., time, hour angle, and declination for the Goldstone dish) into IBM cards, which are then converted to punched teletype tape and automatically transmitted.

4. Reacquisition Phase

The end of the silent phase occurs when the signal of the satellite is received by the westernmost station tied into the tracking net, generally located in southern California. This initial reacquisition confirms that the satellite is in orbit and that the transmitter is still functioning properly. The first station to reacquire is followed rapidly by other stations located in the southwestern United States.

In addition to simple verification of orbit, a refinement of orbital parameters may occur immediately during the reacquisition phase. Comparison of actual signal acquisition times with those predicted from the launch and early orbit tracking reveals the accuracy of earlier information. Should early results be in error, considerable improvement may be obtained without awaiting the transmission of complete tracking data. This improvement is obtained by use of the inflection time of the doppler curve recorded by the first Microlock stations, or the time of meridian crossing in the case of Minitrack stations, to determine the injection velocity magnitude. The inflection and meridian crossing times are quantities which may be obtained quickly and simply with fair accuracy at the tracking stations. They require the transmission of one number only, a time, rather than a mass of data. The time lapse between injection into orbit and the inflection time or meridian crossing for a given station is primarily a measure of the injection velocity magnitude, being relatively insensitive to small velocity angle errors.

Thus, for the *Explorer VII* orbit, an error of 3.6 m/s in velocity magnitude would cause a shift of 10 sec in the inflection time for the Goldstone station, while an error of 6.7 deg in velocity pitch angle or 1.3 deg in yaw angle would be required for the same shift.

The correction for the velocity magnitude (called, for historic reasons, a period correction) is accomplished by the differential correction procedure described previously, solving for the one unknown with one or more observed times, inflection or meridian crossings, or a combination of both. The method of averages is used whereby the velocities indicated by each observation are averaged, and the average taken as the result. The methods of averages and of least squares are essentially equivalent in this particular case of few observations and near-identical partials, and the method of averages was chosen only for computational simplicity.

The accuracy of the rough, quickly available observed times varies greatly according to individual circumstances. If, however, one inflection time is used with an accuracy of perhaps 5 sec and the injection velocity angle deviations are small (< 1.0 deg), the velocity magnitude may usually be determined within 5 m/s.

5. Final Orbital Phase

As the orbiting satellite crosses the continental United States, the major portion of the data available for early orbit determination is acquired. One or two revolutions across the United States normally yield sufficient data for an orbit for vehicle evaluation and tracking acquisition purposes, independent of results of the early evaluation phases.

In the final orbital phase, all data available are used in a full differential correction of injection conditions. The parameters corrected are normally chosen as the magnitude and direction of the injection velocity vector. Again, the injection coordinates are not corrected because they are nearly always determined more accurately from the power flight analysis. The velocity vector is less well determined in the power flight analysis, and its determination is more sensitive than that of the coordinates to partial failure of the early phases of the evaluation process. Further, the orbital data obtained two or more hours after injection, particularly the doppler data, are relatively insensitive to variations of injection position of the magnitude of a few kilometers.

Thus, utilizing doppler frequency data from five stations on the first pass, and assuming a standard deviation of 10 cps in the data, the average standard deviation in the resulting injection coordinates is about 10 km. The estimated average error for the injection coordinates from the power flight analysis is only 5 km.

Two practical advantages are also gained by restricting the correction to the velocity vector alone. One is computation time saved by elimination of the calculation of the three orbital trajectories necessary for the partial derivatives in the method of successive perturbations. The second advantage is increased stability and more rapid convergence of the correction due to elimination of the less sensitive parameters.

The majority of the data received in the orbital phase is doppler frequency, although angle data from Goldstone are now available on 108 and 960 mc/s, and radar data (angles and range) are available from Millstone Hill if acquisition is achieved. The techniques used with the doppler data will be treated first.

a. Orbital doppler data. The doppler data received by a tracking station during the passage of an orbiting satellite is commonly known as an S-curve, from the characteristic shape the frequency function takes. Figure 16 shows a plot of a typical set of orbital doppler data.

Two basic approaches exist for utilization of doppler orbital pass data. The first consists of smoothing the doppler S-curve and extracting a few characteristic quantities, usually taken as the inflection time and inflection (maximum) slope of the curve, which are then used in the differential correction process. The second and preferred approach uses the raw doppler frequency as a function of time, smoothed or unsmoothed, directly in the correction program.

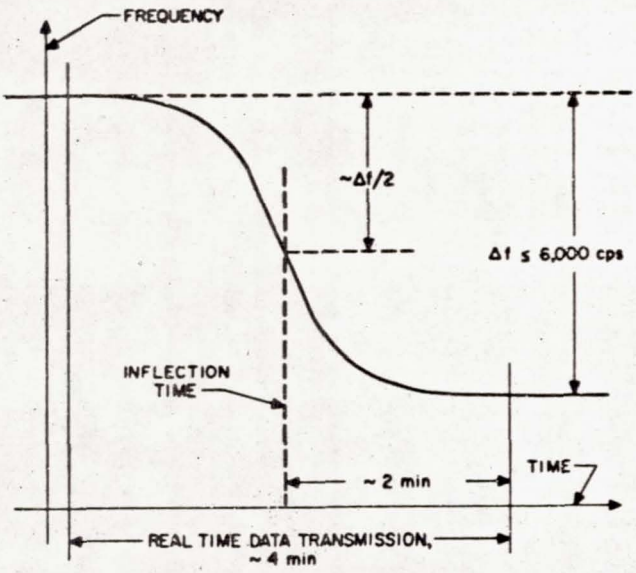

Fig. 16. Orbital doppler data

b. Inflection time and slope. The first approach, extraction of inflection time and slope, has a decided advantage for use in the period correction as described previously (Section VB4). For full correction purposes, the advantages of the use of time and slope lie in part in the convenience of dealing with only two data points per crossing, rather than a larger number of frequencies. Also advantageous is the strong effective smoothing resulting from the extraction of only two quantities from the entire pass, enabling the use of poor data. The disadvantages are the loss of some of the information content of the complete S-curve (discussed below), the length of time required to obtain highly accurate times and slopes, and the requirement of having doppler data both before and after the inflection time in order to achieve accuracy.

The simplest manner of obtaining the inflection time and slope from a doppler curve consists of plotting the first differences of the doppler frequency points (Fig. 17). The first differences, of course, reach a maximum at the inflection time. The inflection slope may then be read as the ordinate of the maximum of the first-difference curve.

The difficulty encountered in this method is also seen in Fig. 17. If the doppler frequencies have much dispersion, the maximum of the first-difference curve becomes difficult to ascertain by inspection, on both the ordinate and abscissa. Also as the sharpness of the first-difference peak is largely a function of the magnitude of the inflection slope, which in turn is largely a measure of the close-approach distance from satellite to tracking station, the inflection time may be read accurately only on data from fairly close passes.

The above difficulties limit the accuracy of this method, particularly under real-time operating conditions; how-

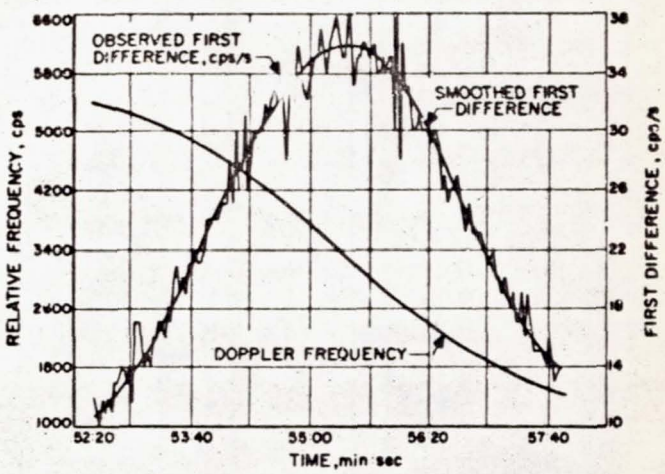

Fig. 17. First difference of orbital doppler data

ever, its simplicity and relative speed are advantages. This method is used for evaluation of the first passes received at initial reacquisition (Section VB4) for period correction purposes, for evaluation of early results, and as a first step for the more exact determination. The accuracy attained under normal conditions is ± 5 sec for inflection time and ± 2 cps/s for inflection slope. The time required for manually processing one S-curve by the first-difference method is approximately 5 min for a two-man team; a similar rough reduction performed by two men utilizing a small E-101 digital computer (Section IVD) is slightly faster.

Other simple methods, e.g., utilizing the approximately skew-symmetric properties of most S-curves to find the symmetry point, have been investigated, but found less reliable and generally less accurate than the first-difference approach.

For accurate early orbit determination with inflection times and slopes, where only a limited number of S-curves are available, it is necessary to extract more exact data from the curves. This is achieved by fitting a least squares polynominal to the raw doppler data, and obtaining the inflection time and slope of the polynominal.

The procedure followed for the polynominal fitting begins with the manual determination of rough inflection time as described above. Simultaneously with the rough determination the punched teletype tape containing the doppler data is converted to punched cards for input to the 704 computer, one time point to the card. Data cards covering a time period of between 90 and 180 sec centered about the rough inflection time are selected, rapidly scanned for gross transmission and punching errors, and fed to the 704 computer. The computer fits an n-degree (usually third-degree) polynominal to the input data in the sense of least squares, yielding as output the smoothed frequency values, the inflection time and slope of the fitted polynominal, and the standard deviation of the raw data from the polynominal. If the standard deviation of the data exceeds a specified input value, raw data points are removed from each end of the S-curve (reducing the length of time coverage). The fitting process is then repeated until the standard deviation of the fit falls below the specified limit, or until the total number of data points being fitted is reduced to a specified minimum. Normally a standard deviation of 15 cps and a minimum of 30 sec of data are required.

The reduction of the number of data points being fitted is desirable for two reasons, one inherent in the method, the other a product of observational inaccuracy. The first and primary reason is brought about by the normal use of a third-degree polynominal. This polynominal has been determined to best approximate the center portion of typical S-curves; however, the total amount of the curve that can be successfully fitted by a third-degree polynominal depends (primarily) upon the steepness or maximum slope; thus for steep curves (close passes), only the central region of the curve can be fitted, while for more moderate slopes, a wider region can be successfully covered. To insure maximum accuracy, the intent is to fit the maximum amount of raw data compatible with the required degree of the polynominal and a required precision of fit.

The secondary reason for the reduction in points fitted is to eliminate points of large dispersion, which normally occur primarily on the outer limbs of the curve.

Through the least squares fitting process, an accuracy of 1 sec in inflection time and ± 0.3 cps/s in inflection slope may be obtained for average data. Five passes on one crossing of the United States, reduced to this accuracy, are sufficient for an injection point determination of 1 m/s in velocity and 0.3 deg in direction, for an orbit like that of *Explorer VII*.

Although accuracy is gained by the least square fitting process, it is at considerable expense of time as well as loss of information. Since only the central portion of the S-curve is fitted, and only two quantities extracted from this fit, any further information content of the total S-curve is discarded.

The possibility of using the third characteristic of the polynominal (second derivative of the frequencies) was discarded because it would involve an impractical amount of computation.

c. Direct use of doppler frequency. The second approach to the use of doppler S-curves requires the use of the raw frequency differences (as defined below) as a function of time directly in the differential correction procedure, and affords a considerable gain in efficiency and accuracy.

Thus the same five passes on one crossing of the United States used as an example above yield an accuracy of 0.2 m/s in velocity magnitude and 0.06 deg in velocity direction when the direct use of frequency is made, assuming a standard deviation of ± 10 cps in all data. This accuracy is 5 times better than that obtained from the same data with inflection times and slopes.

Two difficulties are encountered in the direct use of raw doppler data. Many Microlock stations are not equipped to determine accurately and quickly the true frequency they are receiving, but obtain easily only the

so-called VCO or "beat" frequency (Section IIIB). This frequency exhibits the same shifts as a function of time as the true received frequency (assuming no local equipment shifts), and differs from the received frequency only by some constant additive factor, a function of the reference oscillator frequencies of the station.

While some stations are equipped to accurately determine this factor, little is gained for tracking purposes by doing so because of the following difficulty. The instability of most *Juno* satellite transmitters is such that during injection of the satellite into orbit, when various accelerations and changes in temperature affect the transmitter, the transmitted frequency may exhibit substantial drifts and shifts. These drifts are usually negligible over a short length of time, but the cumulative effect over an orbit is quite significant.

Thus, the absolute frequency f_r received by a tracking station is

$$f_r(t) = f_e + \Delta f(t) + \left(\frac{f_0 + \Delta f(t)}{c}\right) \dot{s}(t) + f_R(t) \quad (20)$$

where

f_0 = nominal transmitter frequency (measured before flight).

$\Delta f(t)$ = any drifts occurring in the transmitter frequency since the measurement f_0.

c = velocity of light.

$f_R(t)$ = any refraction and other effects, expressed for simplicity as additive term.

$\dot{s}$ = radial velocity of satellite from station.

Since $\Delta f(t)$ is an unknown function, this frequency must be compared for the correction process against a computed frequency f_c

$$f_c(t) = f_0 + \left(\frac{f_0}{c}\right) \dot{s}_c(t) + f_{cr}(t) \quad (21)$$

Here f_{cr} is a computed refraction effect, and $\dot{s}_c$ is the calculated radial velocity.

Thus, the direct use of f_r, even if measured by a tracking station, is of little value unless some account is made of the drift term $\Delta f(t)$, which is not negligible.

The above two difficulties are largely eliminated in the following manner. Rather than comparing $f_r(t)$ and $f_c(t)$ in the correction process, the quantities Δf_r and Δf_c are used, where

$$\Delta f_r(t) = f_r(t) - f_r(t')$$
$$= [\Delta f(t) - \Delta f(t')] + \left[\frac{\Delta f(t)\,\dot{s}(t) - \Delta f(t')\,\dot{s}(t')}{c}\right]$$
$$+ \frac{f_0}{c}[\dot{s}(t) - \dot{s}(t')] + [f_R(t) - f_R(t')] \quad (22)$$

$$\Delta f_c(t) = \frac{f_0}{c}[\dot{s}_c(t) - \dot{s}_c(t')] + [f_{cr}(t) - f_{cr}(t')] \quad (23)$$

The first bracket on the right of Eq. (22) is negligible if t' is sufficiently close to t [$\Delta f(t) - \Delta f(t') \to 0$]. The second bracket on the right of (22) is usually negligible in comparison to the third bracket on the right. Neglecting these two brackets in (22), Δf_r and Δf_c are seen to be directly comparable.

Practically, the procedure above amounts to performing the correction not with the true doppler frequency, but with the change in doppler frequency occurring after some arbitrary reference time. In this manner the effect of all drifts in transmitter frequency occurring before the reference time is minimized, and only the VCO frequency need be measured by tracking stations.

One restriction must be placed upon the use of frequencies in this manner. The function of Δf_r is nearly constant for times more than 1 min before or after the inflection time of the S-curve, since the S-curve becomes nearly flat on the outer limbs. The frequency data used are of course centered about the observed inflection time. If the observed and calculated (based on the approximate parameters being corrected) inflection times differ by more than 1 min, the Δf_c function, calculated at the observed times, is almost constant, and the partial derivatives of Δf_c with respect to the parameters are almost zero. The correction process converges slowly and poorly.

This problem is eliminated through use of the period correction, which insures that observed and calculated inflection times agree within a few seconds. Under this condition the observed and calculated S-curves have a close overlap, and the correction process performs efficiently.

Utilizing the above principles, the frequency correction data are utilized in the following manner. From each available S-curve, frequency points are chosen centered about the observed inflection time and covering a total time span of about ± 60 sec. The exact time span used is chosen according to characteristics of the satellite pass over the station, primarily in consideration of refraction effects as discussed in the next paragraph. The data sampling rate during the time span is roughly 1 frequency every 8 to 10 sec, leading to a total number of about 15

frequencies per S-curve. These frequencies are then used as input to the correction deck, where the first time point of each S-curve is regarded as the reference point for the curve and the change in frequency from this time point is utilized for the correction.

The refraction correction f_{cr}, shown for simplicity as an additive term in Eq. (21), is not at present included in the correction process. By using only data received at elevation angles greater than 10 deg, refraction effects are generally small, and are neglected. The time span of the data used from a given S-curve is chosen, therefore, to enforce the condition that the elevation angle at reception of all time points used be greater than 10 deg. Depending upon the relative geometry of station and orbit, this criterion results in the use of data from 1 to 2 min on either side of the inflection point. No more than 2 min is normally used even if the elevation angle is satisfactory. The time span, which may usually be determined in a general manner and within sufficient limits for a given station from the predicted orbit, imposes no large demand on the data handling scheme.

Work is now under way (contract with Aeronutronic Systems, Inc.) on a precise evaluation of refraction effects on various satellite data types, and formulation of efficient schemes for correction when required.

The majority of the doppler frequency data received at the Evaluation Center is not transmitted by automatic electronic readout, but manually by teletype operators. Because of the resulting variations in data and format, automatic data handling equipment is at present used only partially in processing the data. Automatic conversion from teletype tape to punched cards is performed where possible in the curve-fitting procedure for inflection time and slope, since a mass of frequency data must be fed to the computer for fitting. For direct correction with raw frequency data, the desired sampled frequency points (about 15 to an S-curve) are extracted manually from the printed teletype messages, and key punched for input to the computer. Since relatively few points are taken from each set of data, little time is lost by this method in comparison to the time required to extract the desired sampled cards from the mass of cards obtained after complete conversion of the teletype tape.

d. Angle and range data. In the present stage of tracking, experience has shown that angle and range data, when available, are much more powerful than one-way doppler frequency for the purposes of orbit determination. However, the present sources of sufficiently accurate angle (excluding interferometric angles) and range data are limited particularly in real time and at the common satellite frequencies and sizes. For this reason no extensive data scheme is at present in use for these data types. The procedures used are as follows:

Angle and range data are usually received from automatic transmission equipment and hence have uniform format and a minimum of transmission data errors. Thus, the punched teletype tape is converted to punched cards, and the cards used for input to the correction program. The conversion process is monitored for removal of obvious errors. Before use as input, the data cards are sampled at a rate chosen from consideration of the total data available, the total time period covered, the quantity of other data available, and the capacity of the correction program. The minimum of data judged necessary to obtain representative data samples is used in order to reduce the burden of computation.

Refraction corrections are not made, but the data used are limited to data obtained at elevation angles above 10 deg. Corrections will be added to the program where required in accordance with the refraction study mentioned above. Any known observational biases may be removed where significant by input to the correction program.

APPENDIX A

Coordinate Systems

Six coordinate systems are at present in the orbit determination scheme. These systems were chosen because of their convenience in computation and interpretation, and, in some cases, for compatibility with other organizations. Each system is used for the purposes to which it is best adapted. A master transformation deck coded for the IBM-704 and Datatron 205 computers has been found quite useful; this deck accepts input in any one of the six systems and produces output in the other five systems.

1. Earth-Fixed Plumbline System (EFP)

The Earth-Fixed Plumbline System was originated for its convenience in calculation and interpretation of booster trajectories. It is used to provide connection between the orbital and main power flight calculations.

This system is a right-handed Cartesian system with origin at some point upon the surface of the Earth (usually the launch pad). The Y-axis points along the local geodetic vertical (plumbline), making the X-Z plane tangent to the Earth ellipsoid (Clarke ellipsoid of 1866 presently used). The X-axis points in some azimuth direction, usually the vehicle launch azimuth. In this case the X-Y plane is the plane of flight.

2. Space-Fixed Ephemeris System (SFE)

The Space-Fixed Ephemeris System is an often used inertial system, convenient for the numerical integration of satellite orbits. It is a right-handed Cartesian system with origin at the center of the Earth. The Z-axis points along the axis of rotation of the Earth at some time origin, and the X-axis in some other specified direction at the time origin. The time origin is often taken as the instant of the vernal equinox, defined as the crossing of the celestial equator by the Sun. The X-axis is chosen to point toward the Sun at this instant.

Another convenient time origin for orbit calculation during a launch operation (where Sun and Moon effects are neglected) is midnight of the day of launch. The X-axis is chosen to point through the Greenwich meridian at that time.

3. Earth-Fixed Ephemeris System (EFE)

The Earth-Fixed Ephemeris System is convenient for the calculation of Earth-fixed quantities, e.g., tracking observations. The name of the system is obvious from its comparison to the Space-Fixed Ephemeris System.

The EFE system, like the SFE, is a right-handed Cartesian system with origin at the center of the Earth. The Z-axis points along the instantaneous rotational axis of the Earth. The X-axis passes through the Greenwich meridian.

For application in the early orbit scheme the effect of the precession of the Earth's rotational axis upon the EFE system has thus far been neglected. The Z-axes of the EFE and SFE systems have been assumed to coincide. The transformation between the two systems is then a simple rotation in the X-Y (equatorial) plane. This angle of rotation is for convenience taken as $\omega t + \theta$, where ω is the rotational velocity of the Earth, t is Universal Time after some midnight, and θ is the residual rotational angle between the Greenwich meridian at that midnight and the X-axis of the SFE system. For a vernal equinox time origin, θ becomes the sidereal time of the midnight. The rotation may be made as accurate as desired by proper choice of ω and θ.

4. Jet Propulsion Laboratory System (JPL)

The Jet Propulsion Laboratory System was first used by ABMA for convenience in communication with that Laboratory. It has been found convenient for other purposes as well.

The JPL system is Earth-fixed. Position is described by the magnitude R of a position vector from the center of the Earth, and by the geocentric latitude ψ and longitude λ of this vector according to the usual definitions. The Earth-fixed velocity vector is given by its magnitude V and two angles, α and ϵ. The elevation angle ϵ is the angle between the velocity vector and the local geocentric horizontal plane. The azimuth angle α is the angle between the projection of the Earth-fixed velocity vector in the horizontal plane and the north direction in that plane.

5. Perturbation System (Pert)

The Perturbation System was selected for the purpose of orbital differential corrections, and is a hybrid of the EFE and JPL systems. Position is given as in the EFE system, and velocity is given as in the JPL system. This has proved at least a relative optimum system for cor-

rection purposes in the early orbit determination, from the standpoints of computational efficiency and interpretation of correction results.

6. Orbital Element System (OE)

The Orbital Element System is used primarily for communication with other parties and for physical interpretation of results. The instantaneous elements of a simple Keplerian ellipse are taken as

Semimajor axis, a

Eccentricity, e

Inclination to equator, i

Longitude of ascending node, Ω

Argument of perigee, ω

True anomaly of injection point, v

Time of injection, T

APPENDIX B
Computational Programs

This report is not intended to give a detailed description of the computation and coding procedures used in the orbit determination scheme. However, a brief description of the general characteristics of the major programs may be of value. All of the programs described below are coded for the IBM 704 and, to an increasing extent, the 709.

It should be noted that most of the programs are designed and used both for the early orbit determination and for more detailed evaluations and advanced studies. The resulting flexibility of the programs is desirable in view of the varied missions to be performed, but may cause the program to be less than optimum in a specific case.

The gradual development of the early orbit scheme from the first mission of vehicle evaluation, as well as the flexibility required of the programs, is responsible for the coding of the scheme as an integrated library of subprograms for specific purposes rather than one omnibus master program. The system of subprograms also makes more efficient use of the multiple computers available in the Computation Laboratory.

1. Transformation Program

The Transformation Program accepts as input any of the six coordinate systems described in Appendix A. Output is provided in all six, plus related values, e.g., excess circular velocity for orbital flights. The program also optionally punches binary input cards in the input system of the orbit and cluster calculation decks. The deck is coded in single precision floating point arithmetic.

2. Cluster Correction Program

The Cluster Correction Program accepts as primary input the actual coordinates and velocity at ignition of stage II of the *Juno* vehicle, the predicted direction (two angles) and magnitude of thrust during the upper stage flight, and the doppler frequency increments observed by as many as ten tracking stations. Using the method of differential corrections described in Section VA4, corrected effective thrust parameters are computed on the basis of any desired doppler increments. These parameters are used to compute an effective upper stage trajectory which ends with position and velocity at last burnout (injection).

The deck operates in both a manual and automatic mode. In the automatic mode all possible three-station combinations of the input observed doppler increments are obtained, and the solutions grouped, as described in Section VA5. On the basis of the grouping, the operator detects any questionable observed increments and selects those which seem in agreement. Operating the deck then in the manual mode, least square solutions may be obtained with the observations selected as good. The desired observations are selected by console entry to the computer.

The trajectory computation used is a closed solution of the vacuum rocket equation. The brief (30 sec) flight of the upper stages is divided into alternating thrust and coast periods. The assumption is made that during each of these periods the gravity acceleration is equal to that at the first of the period. Assumption of linear mass change during any one period is made. Comparison of this simplified trajectory calculation with a more exact numerical integration of the motion reveals negligible error for trajectory steps of less than 10 sec in length and less than several minutes total time coverage.

Input to the deck is in the EFP system. Calculation of station values (doppler increments) is in the EFE system. Trajectory calculation is in the SFE system. All computation is in floating point.

A modified form of this deck permits more detailed output, such as azimuth, elevation, and range of the vehicle from all tracking stations, and is used as a simplified general trajectory computation.

3. Satellite Prediction Program

The Satellite Prediction Program consists of a numerical integration of the equation of satellite motion, plus the computation of numerous quantities pertinent to tracking stations. The single-precision deck is coded in fixed-point for increased speed and accuracy.

The equations of motion are integrated by Milne numerical integration in the SFE system. Runge-Kutta is used to start the integration. The effects of atmospheric drag and of the first two harmonics of the Earth's oblateness are included. Sun and Moon effects are now being added. The integration step is optimized at 2^{-5} hr for precision work and used as large as 2^{-6} hr when more speed and less accuracy are desired. One minute of integration time on the 704 computer per revolution is required at the 2^{-5} step; 7.5 sec is required at 2^{-6}.

A Runge-Kutta integration was found to require twice as much integration time when maintaining the same accuracy as the Milne method. The Cunningham satellite program requires only 20 sec of integration time per revolution at an optimized integration step of 2^{-4} hr, and achieves an increase in accuracy of at least an order of magnitude with that step in comparison to the Milne at its optimized step. The Cunningham program uses a central-difference method of integration (Ref. 9) and is carefully designed and coded for speed and the maintenance of all possible numerical accuracy. Generation of a difference table requires 20 sec before starting the integration, however, and the Cunningham program was felt to present certain disadvantages with respect to flexibility and complexity for application in regard to station predictions. The Cunningham scheme nevertheless has great advantages in accuracy and speed for integration of orbits over a longer period of time than that considered in the early orbit determination.

Apogee, perigee, and nodal crossings are obtained in the trajectory integration by interpolation for $\dot{R} = 0$ and $Z = 0$ in the SFE system, where R is the distance from the center of the Earth.

The calculation of quantities with respect to tracking stations is performed in the EFE system. As many as twenty Microlock and five Minitrack stations may be accommodated in the program at one time. Input of station coordinates is in geodetic latitude and longitude.

The following values may be calculated for any station at any time interval or any specified time:

Azimuth angle of satellite relative to station.
Elevation angle of satellite with respect to geometric horizon.
Local hour angle of satellite.
Local declination of satellite.
Range of station from satellite.
Doppler frequency shift of signal from satellite.
Rate of change of doppler frequency shift of signal from satellite.

In addition, the program interpolates for the inflection time of the doppler frequency shift of all Microlock stations and prints the above values for the proper station at its inflection time. It also interpolates for the time of north–south meridian crossing for all Minitrack stations. The inflection time is found by interpolation for the maximum of the rate of change of the doppler frequency function. The meridian crossing time is found by interpolation for the longitude of the subsatellite point matching the longitude of a Minitrack station.

The calculation of station values at certain times for certain stations (at the inflection times for Microlock stations and at the meridian crossing times for Mini-

track stations) is independently optional on sense switch control.

A modified form of the satellite prediction deck also prints and punches BCD cards for a given station whenever its elevation angle is greater than a specified minimum. The BCD cards contain the prediction information required by stations and may be teletyped to the stations.

4. Satellite Correction Program

The Satellite Correction Program performs the differential correction of orbital parameters described in Section VB1. It is coded as a sequence of three connected decks.

Data Editing Deck

The Data Editing Deck accepts as input the observed orbital data. These may presently consist of azimuth, elevation, local hour angle, declination angles, range, doppler frequency, doppler inflection time, meridian crossing times, and maximum doppler slope. A maximu of 672 data points is permitted. The data input is by cards, either key-punched or converted from teletype tape. Key-punched cards contain a three-letter station code, two-letter data type code, time in hours, minutes, and seconds, and the observed data. The cards converted from teletype tape contain only a station code, time, and the observed data, the program having been previously informed as to what the data will be from a given station.

The data are checked for format and punching errors as they are read in, and erroneous data rejected. Rejected data points are printed. At this stage all accepted data are also processed for any desired corrections such as conversion of units, correction of refraction errors, removal of known bias and local station errors and smoothing and sampling.

The accepted and processed data are next sorted into time sequence and numbered. All data are then printed, grouped by station and data type, and time sequenced within each group. If desired, a "pull" card is simultaneously punched for each data point for later use in selection of data for the least square solution. The time-sequenced data are written on a master binary tape for further use.

Partial Generation Deck

The Partial Generation Deck at present uses the method of successive variations to compute the required partial derivatives for each data point (Section VB1). The orbit calculation is the same as that described for the satellite prediction program, except that observables are calculated only at times and for stations corresponding to the actual observations on the master data tape (from data editing deck).

Input to the deck is in SFE injection coordinates obtained from the transformation deck. The calculated values from $n + 1$ orbit calculations (n is the number of variables to be solved for) are written on the master data tape, with the observed quantities. The calculated and observed values for each data point now form a data equation.

Least Square Solution Deck

The Least Square Solution Deck selects from the master data tape the observation equations desired for solution. This selection may be made on the basis of individual data points, by use of the pull cards punched by the data editing deck, or on the basis of all observations between given time limits, for given stations, and for given data types. The observation equations may be weighted arbitrarily according to precomputed weights. The complete data equations may be optionally printed.

The selected data equations are solved by the method of least squares through matrix algebra. The solution yields the corrections to be applied to the initial parameters, the standard deviations of the corrections, and the predicted standard deviation of the observations when compared against the corrected trajectory. The corrections are also punched into a binary card, which may be used as input to the transformation deck to produce corrected initial conditions for an orbital prediction run or an iteration of the correction program. If it is desired to reuse the previously computed partials in the iteration, only a standard case is run in the partial generation deck and used to compute revised observational residuals.

The least square solution deck solves simultaneously up to 500 equations for as many as six unknowns. It is coded in single precision floating point arithmetic.

REFERENCES

1. Jet Propulsion Laboratory, California Institute of Technology. Space Programs Summary No. 2. Pasadena, Calif. 1 April 1959. (SPS 2, pp. 2–5) SECRET.

2. Army Ballistic Missile Agency. Summary of Cluster Deviations, by F. Kurtz. Huntsville, Ala. 15 April 1959. (DA-TN-36-59) CONFIDENTIAL.

3. Jet Propulsion Laboratory, California Institute of Technology. Microlock: A Minimum-Weight Radio Instrumentation System for a Satellite, by H. L. Richter, W. F. Sampson, and R. Stevens. Pasadena, Calif. 17 April 1958. (EP 376, Revised).

4. Lincoln Laboratory, Massachusetts Institute of Technology. Earth Satellite Observations Made with the Millstone Hill Radar, by G. H. Pettengill and L. G. Draft, Jr. Pasadena, Calif. 22 June 1959 (Group Report 314-1).

5. Jet Propulsion Laboratory, California Institute of Technology. Space Programs Summary No. 1. Pasadena, Calif. 1 February 1959. (SPS 1, pp. 45–75) SECRET.

6. Jet Propulsion Laboratory, California Institute of Technology. Space Programs Summary No. 3. Pasadena, Calif. 1 June 1959. (SPS 3, pp. 27–53) SECRET.

7. Army Ballistic Missile Agency. Optimization of Microlock Station Locations for Cluster Tracking, by P. Clugston and F. Kurtz. Huntsville, Ala. 30 March 1959. (DA TN-30-59).

8. Zurmuehl, R. Praktische Mathematik fuer Ingenieure und Physiker. Berlin, Springer-Verlag, 1953, pp. 238–260.

9. Watson, J. C. Motion of the Heavenly Bodies. Philadelphia, Penn. J. P. Lippincott, 1868.

Orbital and Rotational Motion of a Rigid Satellite

CHARLES A. LUNDQUIST and ROBERT J. NAUMANN

Research Projects Laboratory, Army Ballistic Missile Agency
Huntsville, Ala.

ABSTRACT

The equations of motion of a rigid body in an orbit around the Earth are usually separated into one set determining the motion of the center of mass of the body and a second set specifying the motion of the body around its center of mass. However, the two sets are intricately coupled.

Computer programs have been developed at ABMA to study the motion about the center of mass, as well as the orbital problem. The coupling between the two sets of equations has been explored with these programs. Particular emphasis has been given to the motions of 1958 ε, *Explorer IV*.

I. DYNAMICAL PRELIMINARIES

If an artificial satellite is assumed to be a rigid body, it possesses six mechanical degrees of freedom. Six generalized coordinates are therefore required to specify its configuration in space. The quantities used as generalized coordinates may be selected in a variety of ways. The usual choice employs three coordinates to specify the location of the center of mass in an inertial system, and three coordinates to specify the orientation of the rigid body about the center of mass.

The form of Lagrange's equations appropriate for nonconservative systems is

$$\frac{d}{dt}\left(\frac{\partial T}{\partial \dot{q}_i}\right) - \frac{\partial T}{\partial q_i} = Q_i \qquad (1)$$

where q_i, $i = 1, 2, 3$ are the generalized coordinates, T the kinetic energy, and Q_i the generalized forces corresponding to the generalized coordinates. General theo-

rems of dynamics prove that the kinetic energy of the system may be expressed as the sum of two parts, one depending only upon the coordinates of the center of mass and their derivatives, the other depending only on the coordinates specifying the orientation and their derivatives (see Ref. 1, Section 63). Therefore, the left sides of three of the equations of set (1) depend only on the coordinates of the center of mass, and the left sides of the other three depend only on the orientation coordinates. However, in general, each generalized force Q_i is a function of all six of the coordinates. Thus, the set (1) does not separate into two sets, one depending upon coordinates of the center of mass and the other upon the orientation coordinates.

An approximation is often made wherein the orientation dependence of the Q_i's corresponding to the coordinates of the center of mass is neglected. This gives a set of three approximate second-order differential equations for the motion of the center of mass in its orbit.

II. MOTIVATION

The orbital equations, in various approximations, have obviously been the subject of many studies by numerous groups. These have many facets. The form of the generalized forces and their relative importance have been studied. Analytical and numerical solutions of the equations have been employed. Methods for utilizing observational data to determine orbits of satellites have been developed and applied.

The corresponding problems with respect to the orientation of a satellite have received much less attention, even though they are part of the same complete problem. With the launching of more sophisticated satellites, the need for knowledge of the orientation as a function of time has become almost as great as the requirements for orbital positions. *Explorer IV* (1958 ϵ) had radiation instrumentation with directional sensitivity (Ref. 2). Thus, orientation as well as positional information is required for the full utilization of data from this satellite. A forthcoming *Juno II*-launched satellite may have an even stronger requirement for orientation information than for a knowledge of its position in orbit.

Further, the state has been reached where a more detailed treatment is needed than the approximation neglecting the orientation dependence of the generalized forces corresponding to coordinates of the center of mass. Clearly, for example, the atmospheric drag of a nonspherical satellite must depend upon the orientation with which it passes through perigee.

These considerations have motivated a re-examination at the Army Ballistic Missile Agency of the full six-degree-of-freedom problem, and particularly the orientation aspects of the full problem. The re-examination is by no means completed. The material to be presented represents the first, perhaps faltering, steps taken so far.

The two principal areas of activity are discussed in chronological order rather than in what might appear to be logical order. The first concerns the methods which have been applied to determine the orientation of satellites from observational data and the methods being developed for future use. The second part of the discussion is concerned with the formulation of the full problem in a form convenient for machine calculation.

A still more difficult problem than the six-degree-of-freedom problem cannot be ignored, although it will not be discussed here. Experience has shown that even satellites without obviously nonrigid components such as flexible antennas may by no means be treated as ideal rigid bodies. The full implication of this observation may not yet be appreciated.

III. METHODS OF ORIENTATION DETERMINATION

The methods used to determine the orientation of a satellite depend primarily upon what provision is made for such determination on board the satellite. On the early *Explorers*, weight limitations precluded the use of special attitude-sensing instruments on the satellite. In these cases indirect methods had to be applied. *Explorer VII* (1959 ι) carried a photocell to facilitate determination of the attitude of the satellite relative to the Sun.

The first satellite on which such a study was carried out at ABMA was *Explorer IV*. A feature in the antenna patterns made it possible to make a crude estimate of the viewing angle, or the angle the line of sight from the station to the satellite makes with the angular momentum vector (Ref. 3).

Explorer IV was cigar-shaped and initially spun about the axis of least moment of inertia. After several days the satellite had undergone a transition to the minimum energy state or rotation about an axis having a maximum moment of inertia. Angular momentum was conserved during this transition. In this state the motion is propeller-like, with the symmetry axis rotating in a plane normal to the angular momentum vector.

The 108.03-mc transmitter was fed across an antenna gap separating the instrument compartment from the last stage casing, forming an electric dipole. This dipole has a cosine radiation pattern with nulls along the body axis in the direction of the nose and tail. If the satellite is viewed by a receiving antenna that is insensitive to polarization, a steady signal will be seen if the line of sight is along the angular momentum vector. As the look angle increases, the voltage output from the receiving antenna fluctuates with twice the tumble frequency of the satellite and with an amplitude ratio roughly equal to the cosine of the look angle.

Having found the look angle, the determination of the space-fixed angular momentum vector is a simple matter. Let R_{space} be the radius vector of the satellite in a space-orientation-fixed system determined from the ephermeris of the satellite. The radius vector of the observer U_{Earth} is known in Earth-fixed coordinates. If the transformation $A(t)$ is the time-dependent rotation matrix that transforms U_{Earth} to U_{space}, the line-of-sight vector S_{space} from the tracking station to the satellite is given by:

$$S_{space} = R_{space} - A(t)\, U_{Earth} \qquad (2)$$

If S is normalized and the look angle ψ is determined from field strength records, the orientation vector Ω, defined as a unit vector along the angular momentum vector, may be found from

$$S \cdot \Omega = \cos\psi \qquad (3)$$

Since there are two independent components of Ω, two observations of ψ must be used with the corresponding values for S. The resulting equations may be solved for the value of the components of Ω.

Some practical difficulties arose when the attempt was made to use this method on *Explorer IV*. Most tracking stations did not use steerable circularly polarized antennas. The Johnston Island station did use the proper antenna, but did not record field strength. Some data were salvaged, however, by examining the telemetered data for periodic fades. The absence of these fades indicated that the look angle was less than about 45 deg. By plotting the S vector in celestial coordinates and noting the points where fading was absent, the region in space containing the angular momentum vector was defined.

It was assumed that fading would be observed for ψ greater than some critical ψ_c and not be observed for ψ less than ψ_c. The locus of lines making angle ψ_c with Ω is a right circular cone. Three values of S where $\psi = \psi_c$ were found from the times indicated on the telemetry where fading either ceased or commenced; Ω was then found by:

$$(S_1 - S_2) \times (S_2 - S_3) = \pm \alpha\, \Omega \qquad (4)$$

where α is some constant.

In the actual analysis, S was calculated each minute from the Smithsonian ephemeris zero results using the IBM 704 (Ref. 4, 5). The ephemeris zero had already been run and the satellite position in latitude, longitude, altitude, and universal time had been recorded on magnetic tapes. These tapes were reread and the observer position vector was subtracted from the satellite vector which had been calculated from the latitude, longitude, and altitude. The resultant S was transformed into the space-orientation-fixed system and normalized. A condition that S be printed only when $S \cdot U > 0$ gave values of S only when the satellite was above the radio horizon for a particular station. The 1-min interval was chosen because the ephemeris zero output available was in 1-min intervals. Interpolation could have been used for finer intervals, but was not deemed necessary because the times that fading ceased or commenced could only be ascertained to the nearest minute. Because of this, the accuracy of the attitude determination is probably not

better than about ± 20 deg. However, even with this accuracy, it could definitely be established that the direction of the satellite angular momentum vector was changing with an average rate of the order of 10 deg per day. This required a torque on the order of 100 dyne-cm to be continually acting on the satellite (Ref. 8).

The nature of these torques is still not completely clear. It appears unlikely that either aerodynamic or magnetic torques could account for the observed precession. Even though the body is slightly asymmetrical, the rapid tumbling (7-sec period) appears to prevent any appreciable net aerodynamic torque. Any magnetic torque which could cause precession should also have a damping component of the same order of magnitude which would increase the tumble period. Such damping was not observed in two months of transmitter lifetime. Gravitational torques should be carefully examined to see if they can account for the observed precession.

Additional evidence of this motion of the angular momentum vector is seen in the temperature and drag measurements. The solar aspect angle determines the average area presented to the Sun. A change in this projected area alters the solar heat input to the satellite and results in a marked change in the equilibrium temperature. The temperature of *Explorer IV* was observed to vary between the maximum and minimum theoretical limits set by the extremes of projected area. When the orientation of the angular momentum vector had been established, the solar aspect angle and the resulting projected area were calculated. Good agreement of this calculated projected area with the area demanded by temperature measurement was obtained.

Variations in the accelerations due to atmospheric drag were observed by Lautman (Ref. 5). Using the satellite orientation previously obtained, the effective drag area at perigee was calculated. Reasonable correlations were obtained between the calculated areas and Lautman's observed variations.

Explorer VII contains an on-board solar aspect photocell. Using the telemetered results of this sensor along with field strength measurements, the orientation history of the spin vector of this satellite may be ascertained. This work is currently in progress.

In future satellites where it is desirable to have complete on-board attitude-sensing equipment, a system used successfully by Kupperian (Ref. 7) in sounding rockets may be employed. This system uses photocells to sense the Earth and Sun. The amplitude of the solar signal, the phase angle between the solar and Earth signals, and the satellite position are the principal inputs for this analysis. If the orientation is not rapidly varying, successive observations may be used to greatly enhance the accuracy of the orientation measurements.

IV. FORMULATION OF THE FULL PROBLEM

The interesting results from the study of the orientation of *Explorer IV* emphasized the need for a detailed and accurate theoretical development. Such a development was undertaken.

The first step in formulating the equations of motion of a rigid body in space is the selection of convenient generalized coordinates. The center of mass of the satellite may be specified by three Cartesian coordinates or many other sets of three generalized coordinates. Cartesian coordinates were selected because they yield equations of a nearly symmetrical form with respect to these coordinates. For the specification of the orientation, two systems are strong competitors, Euler angles and Euler parameters (Ref. 1, Chap. I). The three Euler angles have disadvantages in that the resulting equations of motion lack symmetry with respect to the coordinates, and trigonometric functions occur in the formulation. The four Euler parameters have the disadvantage that they exceed by one the number of degrees of freedom. They have the advantage that they yield symmetrical equations without any trigonometric functions being involved. The latter advantage seemed paramount, and Euler parameters were selected.

The use of more coordinates than degrees of freedom suggests the use of a Lagrange undetermined multiplier. The equations of motion similar to the set (1) in this case are

$$\frac{d}{dt}\left(\frac{\partial T}{\partial \dot{q}_i}\right) - \frac{\partial T}{\partial q_i} = Q_i + \lambda A_i \tag{5}$$

where λ is the undetermined multiplier and A_i are the coefficients of the differential expression

$$\sum_i A_i\, dq_i = 0 \tag{6}$$

which relates the four dependent Euler parameters. To the equations of motion must be appended the differential equations

$$\sum_i A_i\, q_i = 0 \tag{7}$$

thus giving a set of eight equations in eight dependent variables—seven coordinates and the undetermined multiplier. From the relation satisfied by the Euler parameters

$$\xi^2 + \eta^2 + \zeta^2 + \chi^2 = 1 \tag{8}$$

it follows that if $q_1 = \xi, \cdots, q_4 = \chi$, then

$$A_1 = \xi, A_2 = \eta, A_3 = \zeta, A_4 = \chi$$

The Euler parameters specify the orientation of a body-fixed set of Cartesian axes relative to a similar set whose orientation is fixed in space through the transformation exhibited in Ref. 1 (Section 9). The body-fixed axes may be chosen as the principal axes through the center of mass.

If the coordinates of the center of mass are represented by

$$q_5 = X_c, q_6 = Y_c, q_7 = Z_c$$

then the kinetic energy takes the simple form

$$T = \tfrac{1}{2} M (\dot{X}_c^2 + \dot{Y}_c^2 + \dot{Z}_c^2) + \tfrac{1}{2} I_1 \omega_x^2 + \tfrac{1}{2} I_2 \omega_y^2 + \tfrac{1}{2} \omega_z^2 \tag{9}$$

where M is the total mass of the body, I the moment of inertia about the x-axis of the body-fixed system and similarly for I_2 and I_3, and ω_x is the the component of the angular velocity along the body-fixed x-axis. The $\omega_x, \omega_y, \omega_z$ are given in terms of Euler parameters.

$$\begin{aligned}
\omega_x &= 2(\chi\dot{\xi} + \zeta\dot{\eta} - \eta\dot{\zeta} - \xi\dot{\chi}) \\
\omega_y &= 2(-\zeta\dot{\xi} + \chi\dot{\eta} + \xi\dot{\zeta} - \eta\dot{\chi}) \\
\omega_z &= 2(\eta\dot{\xi} - \xi\dot{\eta} + \chi\dot{\zeta} - \zeta\dot{\chi})
\end{aligned} \tag{10}$$

Substituting into Eqs. (5) the equations of motion are easily obtained. These are not yet in a convenient form, since the left sides of the equations involve combinations of derivatives of the coordinates. Combining the ξ, η, ζ, χ equations and (7) appropriately, a form of Euler's equations may be obtained

$$\begin{aligned}
I_1\dot{\omega}_x - \omega_y\omega_z(I_2 - I_3) &= \tfrac{1}{2}(\chi Q_\xi + \zeta Q_\eta - \eta Q_\zeta - \xi Q_\chi) \\
I_2\dot{\omega}_y - \omega_x\omega_z(I_3 - I_1) &= \tfrac{1}{2}(-\zeta Q_\xi + \chi Q_\eta + \xi Q_\zeta - \eta Q_\chi) \\
I_3\dot{\omega}_z - \omega_x\omega_y(I_1 - I_2) &= \tfrac{1}{2}(\eta Q_\xi - \xi Q_\eta + \chi Q_\zeta - \zeta Q_\chi)
\end{aligned} \tag{11}$$

From these and basic definitions, an alternative form may be obtained in terms of the components (L_x, L_y, L_z) along space-orientation-fixed axes of the angular momentum about the center of mass,

$$\begin{aligned}
\dot{L}_x &= \tfrac{1}{2}(\chi Q_\xi - \zeta Q_\eta + \eta Q_\zeta - \xi Q_\chi) \\
\dot{L}_y &= \tfrac{1}{2}(\zeta Q_\xi + \chi Q_\eta - \xi Q_\zeta - \eta Q_\chi) \\
\dot{L}_z &= \tfrac{1}{2}(-\eta Q_\xi + \xi Q_\eta + \chi Q_\zeta - \zeta Q_\chi)
\end{aligned} \tag{12}$$

Differential equations may be obtained for $\dot{\xi}, \dot{\eta}, \dot{\zeta}, \dot{\chi}$. To these must be added the orbital equations for X_c, Y_c, Z_c in a convenient form, for example

$$\begin{aligned}
\dot{P}_{X_c} &= Q_{X_c}, \text{ etc.} \\
\dot{X}_c &= \frac{1}{M} P_{X_c}, \text{ etc.}
\end{aligned} \tag{13}$$

Certain advantages of this formulation may be mentioned, leaving discussion of the Q's until later. None of the equations involve variables in the denominator which may approach zero, producing computational problems. The right sides of the equations involve only additions and subtractions and, in particular, involve no trigonometric functions.

The significant generalized forces arise from three sources: gravitation, aerodynamic effects, and magnetic effects. Only the first two contribute appreciably to Q_{x_c}, Q_{y_c}, Q_{z_c}. Depending upon the satellite orbit, all three sources may contribute appreciably to Q_ξ, Q_η, Q_ζ, Q_χ. In the case of *Explorer IV*, for example, the contribution due to gravitational effects seems most important.

V. GRAVITATIONAL FORCES

In order to explain in detail the orientation observations, the first source of forces considered was gravitation. This question has been discussed by various authors (Doolin, Ref. 8, and Roberson and Tatistcheff, Ref. 9). The objective here is to obtain the Q_i of gravitational origin in the generalized coordinate system of the previous section. Doolin showed that the gravitational effects may be separated into (1) a contribution to Q_{x_c}, Q_{y_c}, Q_{z_c} from the leading term in the Earth's potential, (2) a contribution to Q_{x_c}, Q_{y_c}, Q_{z_c} from the Earth's oblateness, (3) a contribution to $Q_{\xi,\eta,\zeta,\chi}$ from the leading term in the Earth's potential, and (4) a contribution to $Q_{\xi,\eta,\zeta,\chi}$ from the Earth's oblateness. Contribution (4) has been neglected here. If the satellite orientation dependence of (2) is also neglected, (2) corresponds to the usual terms used to specify the effect of oblateness on the motion of the center of mass.

With these simplifications, the problem remaining is the derivation of the Q_i, in the coordinate system selected, for a rigid body in the principal $(1/r)$ contribution to the Earth's gravitational potential. The potential energy of the rigid body is thus

$$V = -m_e k_e^2 \int_{\text{body of satellite}} \frac{dm}{r} \tag{14}$$

where r = radius from the center of the Earth to the element of mass dm. Transforming the integral to a space-orientation-fixed coordinate system X, Y, Z, with origin at the center of mass, expanding $f(r) = 1/r$ in a Taylor's series about the center of mass, and neglecting terms of the third and higher orders, the potential V becomes

$$V = \frac{-m_e M k_e^2}{R_c} - \frac{m_e k_e^2}{2} \sum_{i,j} \frac{\partial^2 f(R_c)}{\partial X_{ci}\,\partial X_{cj}} \int_{\text{body of satellite}} X_i X_j \, dm \tag{15}$$

where

M = total mass of the satellite

$X_{c_1} = X_c, X_{c_2} = Y_c, X_{c_3} = Z_c$

$X_1 = X, X_2 = Y, X_3 = Z$

$f(R_c) = (X_{c_1}^2 + X_{c_2}^2 + X_{c_3}^2)^{-1/2}$

The coordinates X_1, X_2, X_3 and a set of principal body-fixed coordinates χ_1, χ_2, χ_3 are related by the Euler parameters through

$$\begin{pmatrix} X_1 \\ X_2 \\ X_3 \end{pmatrix} = \begin{pmatrix} \xi^2 - \eta^2 - \zeta^2 + \chi^2 & 2(\xi\eta - \zeta\chi) & 2(\xi\zeta + \eta\chi) \\ 2(\xi\eta + \zeta\chi) & -\xi^2 + \eta^2 - \zeta^2 + \chi^2 & 2(\eta\zeta - \xi\chi) \\ 2(\xi\zeta - \eta\chi) & 2(\eta\zeta + \xi\chi) & -\xi^2 - \eta^2 + \zeta^2 + \chi^2 \end{pmatrix} \begin{pmatrix} \chi_1 \\ \chi_2 \\ \chi_3 \end{pmatrix} \tag{16}$$

or

$$X_i = \sum_j a_{ij} x_j$$

Define

$$B_{ij} = \int X_i X_j \, dm = \sum_a a_{ia} a_{ja} J_a \tag{17}$$

where

$$J_a = \int X_a X_a \, dm$$

is a constant depending on the geometry of the body, simply related to principal moments of inertia. The B_{ij} are functions of ξ, η, ζ, χ only.

Define

$$D_{ij} = \frac{\partial^2 f(R_c)}{\partial X_{ci} \partial X_{cj}} \tag{18}$$

The D_{ij} are functions of $X_{c_{1,2,3}}$ only. Thus

$$V = -m_c k_c^2 [M/R_c + \tfrac{1}{2} \sum_{ij} D_{ij} B_{ij}] \tag{19}$$

In this form, the Q_i are easily calculated

$$Q_i = \frac{\partial V}{\partial q_i} \tag{20}$$

Note that these quantities are not particularly involved, since the a_{ij} are simple quadratic functions of the Euler parameters. Again, it is worth noting that no trigonometric functions occur. A further saving in algebraic manipulation occurs if the linear combinations of the Q_i required in Eqs. (12) are computed directly. These operations yield the final set of equations:

$$\dot{L}_i = \frac{3 m_c k_c^2}{R_c^3} \left[\frac{X_{cj}}{R_c} E_k - \frac{X_{ck}}{R_c} E_j \right] \tag{21}$$

where

$$E_k = \sum_{i,j} I_i \frac{X_{cj}}{R_c} a_{ji} a_{ki}$$

and

$$i, j, k \text{ are cyclic}$$

and

$$\dot{\xi} = \chi G_1 - \zeta G_2 + \eta G_3$$
$$\dot{\eta} = \zeta G_1 + \chi G_2 - \xi G_3$$
$$\dot{\zeta} = -\eta G_1 + \xi G_2 + \chi G_3$$
$$\dot{\chi} = -\xi G_1 - \eta G_2 - \zeta G_3$$

where

$$G_i = \frac{1}{2 I_i} \sum_j a_{ji} L_j$$

REFERENCES

1. Whittaker, E. T. A Treatise on the Analytical Dynamics of Particles and Rigid Bodies, New York, Dover, 1944.
2. Van Allen, J. A., C. E. McIlwain, and G. H. Ludwig. "Radiation Observations with Satellite 1958 Epsilon," Journal of Geophysical Research, Vol. 64 (March, 1959).
3. Smithsonian Institution Astrophysical Observatory. "Explorer IV Antennas," by T. A. Barr. Explorer IV—1958 Epsilon Orbital Data Series, Issue 1. Washington, D. C., August, 1958.
4. Smithsonian Institution Astrophysical Observatory. "Ephemeris for Explorer IV—1958 Epsilon," by R. M. Adams. Explorer IV—1958 Epsilon Orbital Data Series, Issue 1. Washington, D. C., October, 1958.
5. Smithsonian Institution Astrophysical Observatory. "Ephemeris for Explorer IV—1958 Epsilon," by D. A. Lautman. Explorer IV—1958 Epsilon Orbital Data Series, Issue 6. Washington, D. C., November, 1959.
6. Naumann, R. J. "Recent Information Gained from Satellite Orientation Measurements," Fourth Symposium on Ballistic Missiles and Space Technology. University of California at Los Angeles. August, 1959.
7. Kupperian, J. E. "Optical Aspect Systems for Rockets," Review of Scientific Instruments, Vol. 28, January, 1957.
8. Ames Research Center, National Aeronautics and Space Administration. Gravity Torque on an Orbiting Vehicle, by Brian F. Doolin. Moffet Field, Calif., Technical Note D-70, August, 1959.
9. Roberson, R. E., and D. Tatistcheff. "The Potential Energy of a Small Rigid Body in the Gravitational Field of an Oblate Spheroid," Journal of the Franklin Institute, Vol. 262, 1956.

Survey of Space Flight Decks Used at ABMA

HANS J. SPERLING

Army Ballistic Missile Agency,
Huntsville, Ala.

ABSTRACT

The method of the varicenter is—in the form it is used here—a generalization of the method of Encke, and it is developed to overcome certain difficulties of Encke's method which arise when the space vehicle does not remain in the neighborhood of one body, i.e., in a prevailing central field. It can be used for all types of space trajectories (orbits of Earth satellites, Moon flight trajectories, and interplanetary flights).

I. INTRODUCTION

The objectives of this paper are (1) to give a short survey of the methods of computation that are used or are being developed at ABMA for space flight calculations, and (2) to explain in detail the concepts of a newly developed method, which at ABMA is called the "varicentric method." All decks discussed deal only with the Newtonian force of attraction; other forces such as drag and thrust are not included.

II. MATHEMATICAL CLASSIFICATION OF THE AVAILABLE METHODS

The differential equations of celestial mechanics are not solvable by known functions except in the case of two bodies, and, for very special configurations, in the case of more than two bodies. Therefore, we are generally restricted to two methods of solution:

1. Closed analytical approximations are obtainable which represent the solution to a certain degree of accuracy within a certain time interval.
2. The equations can be solved by numerical integration.

Here we will consider only methods which include numerical integration. In use are mainly the following three methods:

A. The Method of Cowell

This is the straightforward numerical integration of the differential equations of motion. Any numerical solution involving solely numerical integration will be referred to as the "Method of Cowell," regardless of the particular numerical integration method employed (Runge-Kutta, Nyström, difference methods, etc.).

B. The Method of Encke

Here one uses a "pre-integration" of the function of motion $\mathbf{r}(t)$. In the differential equation $\ddot{\mathbf{r}} = f(\mathbf{r}, t)$ the radius vector $\mathbf{r}$ is replaced by $\mathbf{r} = \mathbf{r}^* + \Delta\mathbf{r}$; $\mathbf{r}^*$ is the pre-integral, a known function of time that approximates the solution of the differential equation. Usually $\mathbf{r}^*$ is the solution of the two body problem, i.e., it represents a conic section. The new differential equation $\Delta\ddot{\mathbf{r}} = -\ddot{\mathbf{r}}^* + f^*(\Delta\mathbf{r}, t)$ is numerically integrated for the small quantity $\Delta\mathbf{r}$.

In some ways the varicentric method will be a generalization of Encke's method.

C. The Method of Variation of Parameters

This method will not be considered in this paper.

III. SPACE FLIGHT DECKS AT ABMA

The following discussion presents a brief survey of the decks we use for space trajectory computations; they are referred to as M-decks. All M-decks are coded for 704 and 709 IBM computers.

The first two are used to a large extent for the computation of moon flight trajectories.

The M-1 deck is coded in fixed point single precision. It is applicable to Earth satellites and lunar probes and takes into account the influences of the Moon and the Sun and the oblateness of the Earth. The coordinates of Moon and Sun are fed in from the tables of the Ephemerides or are taken from analytical formulae. The numerical integration is performed by the method of Runge-Kutta.

The M-2 deck is coded in floating point single precision. Its celestial model is that of the generalized restricted problem of three bodies. This system is primarily provided to make survey studies of Earth satellites and lunar flights. The differential equations are integrated by the method of Runge-Kutta.

While these two decks follow Cowell's method of straightforward integration of the equations, the following two systems (the M-3 and M-4 decks) utilize the varicentric method for pre-integration.

The M-3 deck is identical to the M-4 deck except that it is restricted to a simplified celestial model (that of the M-2 deck).

The M-4 deck is coded in double precision floating point. It is applicable to all kinds of space trajectories. The positions of the celestial bodies are taken from the tables of the Ephemerides or from analytic formulae. The numerical integration is done by a method stemming from Nyström.

The M-5 deck is coded in double precision floating point. It is applicable to Earth satellites and lunar flights and takes into account the influences of Moon and Sun and the oblateness of the Earth. The straightforward numerical integration (Cowell's method) is done by Nyström's method. The main purpose of this deck is the comparison of Cowell's method with the methods employed in M-4 and M-6 regarding speed and accuracy.

The M-6 deck is coded in double precision floating point. It is applicable to Earth satellites; the differential equations are the same as in the M-5 deck, but in this deck Encke's method is used for pre-integration. The numerical integration is performed by Nyström's method.

IV. THE VARICENTRIC METHOD

The varicentric method is, in the form we use it, a generalization of Encke's method, at least in some respects. It is intended to overcome some difficulties which arise in using Encke's method for space flight trajectories.

In Encke's method the true orbit is approximated for a certain interval of time $t_1 - t_0$ by the osculating conic section for t_0 with respect to the main attracting body, and the difference from the approximating conic section to the true orbit is numerically integrated. At the time t_1, when the approximating conic section differs too much from the true orbit, a new osculating conic section is computed, etc. The "main attracting body" is the celestial body whose attraction prevails in the considered interval. This approximation is good only if the gravitational field in the neighborhood of the considered orbit is practically given by the central field of the main body, so that the other celestial bodies only yield small perturbations of that central field. Examples in which Encke's method can be applied successfully are computations of planetary orbits and of orbits of comets, since both are usually in the field of one prevailing celestial body.

Difficulties arise if the body whose orbit we want to compute moves from one central field to another. In this case, for a certain space between the two bodies, the gravitational field is not determined by one body but equally by both of them; then a conic section computed with respect to one of the bodies is not a very close approximation to the true orbit. Besides this, somewhere between the two bodies it would be necessary to shift from the first body as focus of the reference conic section to the second body. The varicentric method, in generalizing the concept of Encke's reference focus, replaces the true celestial reference body by a fictitious body (the "varicenter"), thus generally avoiding any discontinuities.

As in Encke's method, the basic idea is to approximate the true orbit for a certain time interval by a conic sec-

tion and to integrate the differences. For this purpose we approximate the gravitational field in the neighborhood of the space vehicle by a central field. Any central field is completely determined by the generating mass and its location. This means that we must determine a mass m^* and its location $\mathbf{r}^*$. With respect to this fictitious central field, we then compute in the known way, by means of the location vector $\mathbf{r}$ and the velocity vector $\dot{\mathbf{r}}$ of the space ship, the approximating conic section and integrate the deviations from the true orbit.

Generally m^* and $\mathbf{r}^*$ are functions of the time and of the trajectory of the space ship; also the parameters of the approximating conic section are functions of time and trajectory.

The application of the idea of the varicentric method to numerical computations is similar to Encke's method: For a time t_0 we determine m_0^* and $\mathbf{r}_0^*$ and an approximation for $\mathbf{r}^*(t)$, and by the procedure known from the problem of two bodies, we find the approximating conic section. Then we replace $\mathbf{r}$ by $\mathbf{r} = \bar{\mathbf{r}} + \Delta\mathbf{r}$, where $\bar{\mathbf{r}}$ denotes the known values of the conic section, and integrate numerically for $\Delta\mathbf{r}$ from t_0 to t_1. During the numerical integration from t_0 to t_1 the values $m^* = m_0^*$ and the approximating conic section are kept fixed. After the integration we determine at the time t_1 new values of m^*, $\mathbf{r}^*(t)$ and a new reference conic section.

For the determination of m^* and $\mathbf{r}^*$ we have principally several possibilities, since the approximation of an arbitrary gravitational field by a central field is possible in many ways. One of the simplest and most straightforward ways to determine m^* and $\mathbf{r}^*$ is the following, which is used in our first computations:

1. Require that the acceleration $\mathbf{a}$ generated by m_0^* be equal to the true acceleration $\ddot{\mathbf{r}}$ at the location of the probe: $\mathbf{a}(\mathbf{r}_0) = \ddot{\mathbf{r}}(\mathbf{r}_0)$

2. Require that the first derivative of the projection of $\mathbf{a}$ on the straight line given by $\ddot{\mathbf{r}}_0$, taken along this line at the point $\mathbf{r}_0$, be equal to the first derivative of the projection of $\mathbf{r}$ on this line, taken along this line at the same point $\mathbf{r}_0$:

$$\left(\ddot{\mathbf{r}}_0 \operatorname{grad} \frac{(\ddot{\mathbf{r}}_0 \cdot \mathbf{a})}{|\ddot{\mathbf{r}}_0|}\right)_{\mathbf{r}_0} = (\ddot{\mathbf{r}}_0 \operatorname{grad} |\ddot{\mathbf{r}}|)_{\mathbf{r}_0}$$

For the purpose of defining this straight line we consider $\ddot{\mathbf{r}}$ as the constant vector $\ddot{\mathbf{r}}(\mathbf{r}_0) = \ddot{\mathbf{r}}_0$.

More generally we could replace $\mathbf{r}_0$ by any constant vector $\mathbf{b}$, for instance by the velocity vector $\mathbf{r}_0$ of the space ship at the point $\mathbf{r}_0$. We would get then as the second requirement:

2*. Require that the first derivative of the projection of $\mathbf{a}$ on the straight line given by $\mathbf{r}_0$, taken along this line at the point $\mathbf{r}_0$, be equal to the first derivative of the projection of $\ddot{\mathbf{r}}$ on this line, taken along this line at the same point $\mathbf{r}_0$:

$$\left(\mathbf{b} \operatorname{grad} \frac{(\mathbf{b}\,\mathbf{a})}{|\mathbf{b}|}\right)_{\mathbf{r}_0} = \left(\mathbf{b} \operatorname{grad} \frac{(\mathbf{b}\,\ddot{\mathbf{r}})}{|\mathbf{b}|}\right)_{\mathbf{r}_0}$$

In the first models for computations we used barycentric coordinates and, for the sake of simplicity, the constant value $\mathbf{r}^*(t) = \mathbf{r}^*(t_0)$ for the position of the varicenter. Thus the approximate conic section was defined with respect to a space-fixed varicenter. The differential equations of motion with the coordinates referred to a celestial body, as they are used in Encke's method, show that the true orbit generally is very well approximated by a conic section referred to the celestial body in the origin of the moving coordinate system. This fact and the first numerical results indicated that it would be of advantage to take into account the motion of the varicenter. The true values of $\mathbf{r}^*(t)$ and $m^*(t)$ are not known because they depend on the future trajectory of the space vehicle. Therefore, we approximate the future motion of the varicenter; in order to obtain simple formulae, we keep $m^* = m^*(t_0)$ fixed for the time interval $t_1 - t_0$, and approximate the motion of $m^*(t_0)$ by a uniform motion in the following manner:

For t_0 we determine $m^*(t_0)$ and $\mathbf{r}^*(t_0)$; then we assume for the time interval $t_1 - t_0$ a fictitious uniform motion of the space vehicle with the velocity $\dot{\mathbf{r}}_0$ and determine for the time t_1 from the fictitious location $\mathbf{r}_1' = \mathbf{r}_0 + \Delta t\,\dot{\mathbf{r}}_0$ of the space vehicle a new location $\mathbf{r}^{*\prime}$ of the varicenter with the mass $m^*(t_0)$. Then

$$\dot{\mathbf{r}}^{*\prime} = \left(\frac{1}{\Delta t}\mathbf{r}_1^{*\prime} - \mathbf{r}^*(t_0)\right)$$

is the approximate velocity of the varicenter.

In the resulting equations of motion only the positions, not the velocities or accelerations of the celestial bodies, appear.

Interim Definitive Orbits Determined at the NASA Computing Center

ROBERT W. BRYANT

Theoretical Division, Goddard Space Flight Center,
National Aeronautics and Space Administration,
Washington, D. C.

ABSTRACT

Interim definitive orbits for satellites 1958 α, 1958 γ, 1958 ε, 1959 α, 1959 η, and 1959 ι have been determined at the *Vanguard* Computing Center. The ability of the mathematical model to match the observations is indicated by arc length, standard deviations of fit, and the continuity of the various arcs constituting the orbit.

I. GENERAL DISCUSSION

Interim definitive orbits for satellites 1958 α (*Explorer I*), 1958 γ (*Explorer III*), 1958 ε (*Explorer IV*), 1959 α (*Vanguard II*), 1959 η (*Vanguard III*), and 1959 ι (*Heavy IGY*) have been computed at the NASA Computing Center.

The word "definitive" is used to distinguish these orbits from the orbits generated solely for prediction purposes. In orbit determination for prediction purposes, one is governed by the mathematical model being used and the accuracy of prediction required by the observing stations. Specifying accuracy, one can predict only a finite time into the future and maintain this accuracy. Then it is necessary to redetermine orbit elements by differential correction at a later epoch. How long the theory in use (the mathematical model) can be used for prediction is, of course, dependent upon its sophistication. In the paper I will present entitled "NASA Computing Center Predictions," the sophistication of the general oblateness perturbations program of Drs. Herget and Musen (Ref. 1), which is used at the NASA Computing Center, will be evident. Nevertheless, with certain satellites, e.g., 1958 γ (*Explorer III*), whose cylindrical shape and low perigee produced a pronounced drag effect, it was necessary to rectify and differentially correct without having in hand all the observations in existence. This was a result of com-

munications time between the Minitrack station and the Space Operations Control and necessary data processing by Minitrack personnel. "Definitive" means that all Minitrack observations of the satellite have been utilized in the orbit determination.

The word "interim" is utilized for two reasons:

1. The orbits have been determined solely from Minitrack observations.
2. The mathematical model will be changed as a result of knowledge obtained from the study of the orbits and perhaps some of the orbits will be redetermined.

The form of the interim definitive orbits determined at the NASA Computing Center follows that set by agreement of the participants in the Earth Satellite Program of the International Geophysical Year, 1957–58. This orbital information consists of the following: time, longitude, latitude, and height above the surface in kilometers.

The programs used at the Computing Center in this work are the General Oblateness Perturbations Program developed by Drs. Herget and Musen in 1957; the basic Eckert-Brouwer Differential Correction Program (Ref. 2) of 1941; a program to obtain satellite position in inertial coordinates at 1-min intervals; and the World Map Program, which gives the satellites' positions, i.e., longitude, latitude, and height, for each minute of time.

One of the problems which confronted us in the course of the interim definitive work was the length of arc which could be used in the differential correction. By length of arc is meant the time interval covered by the observations. This of course is a function of the model used and the standard deviation of fit tolerable. The first satellite for which an interim definitive orbit was obtained was 1958 γ (*Explorer III*), and the arc length used was 2 days. A longer interval resulted in a standard deviation of fit which we considered too large.

II. RESULTS

Table 1 contains a summary of position information for the interim definitive orbit of 1958 γ. Column 1 contains the arc number, column 2 contains the time interval covered by the particular arc, column 3 contains the standard deviation of fit (root-mean-square measure in radians of the residuals of the observations which were used to determine the arc).[1]

The last four columns of the table give information about the overlapping of the various arcs. Each arc after the first was chosen so that it overlapped the previous arc by about 2 hours. Thus, it is possible that some of the last observations of arc n were the first observations in arc $n + 1$.

In order to obtain a piecewise continuous orbit, it was determined that the time of transfer from one arc to the next should be such that the difference in positions for the same time in the arcs should be a minimum. This time was easily determined from the binary minute vector tapes. The information in the last four columns is this minimum distance in terrestrial coordinates (i.e., the differences in longitude, latitude, and height) and the actual Cartesian coordinate difference.

Tables 2, 3, 4, 5, and 6 contain the same information as the above for the other satellites. It is to be noted that the arc lengths for these satellites are longer than those for 1958 γ. For 1958 α and 1958 ϵ the arc lengths are 4 days, and for 1959 α, 1959 η, and 1959 ι the arc lengths are 1 week.

Perhaps I should comment here on the omission of the satellite 1958 β (*Vanguard I*) from the list of interim

[1] Minitrack observations are phase differences converted to direction cosines and are used in the differential correction program as direction cosines. Since observations are taken near the zenith, one has the approximation to radians; thus speaking of residual in radians is justified.

Table 1. Interim definitive orbit for satellite 1958 γ

Summary of certain position information for arcs extending from 1745 UT 26 March 1958 to 0559 UT 17 June 1958

Arc	Interval (d-h-m) UT	Standard deviation of fit, millirad	Coordinate differences and corresponding distances between points in adjacent books at transfer times			
			Longitude, nm at sea level	Latitude, nm at sea level	Height, nm	Radial distance, nm
1	26-17-45 to 28-23-57	5.5	4.51	0.09	6.42	8.6
2	28-23-57 to 30-23-47	9.8	4.25	0.35	4.25	6.3
3	30-23-47 to 02-01-03	3.4	9.30	6.76	6.16	17.0
4	02-01-03 to 04-01-00	7.0	4.69	0.52	6.33	8.3
5	04-01-00 to 06-00-52	4.6	1.73	3.63	2.44	5.1
6	06-00-52 to 08-01-54	4.5	0.92	1.60	0.01	1.9
7	08-01-54 to 10-02-55	8.4	2.17	3.05	0.25	3.9
8	10-02-55 to 11-21-52	2.4	1.65	0.02	2.05	2.8
9	11-21-52 to 14-02-23	6.4	0.95	1.78	0.22	2.1
10	14-02-23 to 16-02-36	6.2	1.80	4.18	1.48	5.3
11	16-02-36 to 17-23-35	4.6	1.81	2.27	0.19	3.1
12	17-23-35 to 19-21-28	3.6	0.85	0.18	2.10	2.3
13	19-21-28 to 22-01-02	1.4	0.03	0.93	3.25	3.4
14	22-01-02 to 24-02-45	1.3	0.53	1.13	1.01	1.7
15	24-02-45 to 26-00-33	3.4	1.49	1.87	0.61	2.5
16	26-00-33 to 28-01-46	4.1	1.84	1.70	0.05	2.6
17	28-01-46 to 30-04-51	2.0	1.53	2.82	1.09	3.7
18	30-04-51 to 02-04-58	4.8	1.62	0.07	3.77	4.2
19	02-04-58 to 04-00-39	5.9	4.68	4.35	3.87	7.6
20	04-00-39 to 06-01-01	5.1	1.63	1.67	0.96	2.6
21	06-01-01 to 08-04-57	5.7	0.11	1.20	0.90	1.6
22	08-04-57 to 10-01-18	3.0	2.27	1.33	5.86	6.5
23	10-01-18 to 12-04-39	4.9	1.17	0.17	1.16	1.7
24	12-04-39 to 14-02-27	5.6	0.97	0.03	7.59	7.7
25	14-02-27 to 16-04-38	6.4	1.13	1.25	2.30	2.9
26	16-04-38 to 18-05-33	6.1	0.77	1.57	1.74	2.5
27	18-05-33 to 20-04-13	6.7	1.08	1.45	0.69	2.0
28	20-04-13 to 22-4-21	4.0	0.07	0.68	1.48	1.6
29	22-4-21 to 24-00-57	4.5	0.93	1.40	0.86	1.9
30	24-00-57 to 26-00-20	5.6	9.95	2.75	8.28	14.1
31	26-00-20 to 28-00-16	5.6	1.00	1.87	1.86	2.9
32	28-00-16 to 30-00-52	4.9	0.61	1.50	0.75	1.8
33	30-00-52 to 01-04-35	6.7	2.34	2.82	5.45	6.7
34	01-04-35 to 03-00-06	5.9	0.06	2.57	4.73	5.4
35	03-00-06 to 05-04-57	6.2	0.94	0.93	0.49	1.5
36	05-04-57 to 07-01-38	5.0	0.28	0.58	2.03	2.1
37	07-01-38 to 09-01-02	4.3	0.45	2.23	1.30	2.7
38	09-01-02 to 11-05-42	5.1	4.44	1.47	5.08	7.1
39	11-05-42 to 13-04-31	3.9	0.99	0.80	0.50	1.4
40	13-04-31 to 15-05-11	6.0	3.20	0.12	6.44	7.2
41	15-05-11 to 17-05-59	5.6				

definitive orbits. Such a determination has been made on this satellite with the resultant better determination of the Earth's potential. The model in use at the NASA Computing Center has been modified to include the effect of the third harmonic of the Earth's potential, and it is expected that a rerun of the differential corrections using this new model will be made in the near future.

Work is in progress at the moment to combine the various arcs of the interim definitive orbits discussed above into a continuous minute vector tape. The observations will then be compared with the computed values from this continuous tape and the observations, computed values, and residuals will be published as companion volumes to the interim definitive orbits.

Table 2. Interim definitive orbit for satellite 1958 α

Summary of certain position information for arcs extending from 0358 UT 1 February to 1359 UT 23 May 1958

Arc	Interval (d-h-m) UT	Standard deviation of fit, millirad	Coordinate differences and corresponding distances between points in adjacent books at transfer times			
			Longitude, nm at sea level	Latitude, nm at sea level	Height, nm	Radial distance, nm
1	01-03-58 to 05-02-22	6.0	23.04	0.20	1.07	30.35
2	05-02-22 to 09-02-17	4.6	17.92	7.82	0.27	26.85
3	09-02-17 to 13-01-57	2.9	13.49	4.43	0.11	19.17
4	13-01-57 to 17-02-21	3.8	2.13	2.07	2.22	4.39
5	17-02-21 to 21-05-38	4.4	1.17	0.42	1.14	2.05
6	21-05-38 to 25-01-19	4.6	0.29	0.02	0.81	0.91
7	25-01-19 to 01-04-32	3.8	0.12	0.03	0.70	0.73
8	01-04-32 to 05-03-10	2.8	0.04	0.02	1.02	1.02
9	05-03-10 to 09-05-25	5.1	2.18	0.10	0.68	2.83
10	09-05-25 to 13-04-49	4.5	0.32	0.12	0.84	0.93
11	13-04-49 to 17-06-07	4.1	2.32	0.90	0.29	2.78
12	17-06-07 to 21-05-31	5.0	1.13	0.88	0.03	1.52
13	21-05-31 to 25-04-59	4.8	1.84	1.30	0.97	2.57
14	25-04-59 to 29-06-07	5.7	1.56	0.17	2.22	2.82
15	29-06-07 to 02-02-32	5.4	2.26	0.53	1.14	3.22
16	02-02-32 to 06-06-47	4.7	0.00	0.43	0.62	0.79
17	06-06-47 to 10-01-04	4.5	2.02	0.48	0.43	2.46
18	10-01-04 to 14-06-02	3.6	0.09	0.23	0.12	0.31
19	14-06-02 to 18-05-11	5.6	0.00	0.14	0.39	0.39
20	18-05-11 to 22-05-21	3.9	0.13	0.85	1.27	1.75
21	22-05-21 to 26-5-32	4.7	0.18	0.07	0.61	0.64
22	26-5-32 to 30-2-39	5.7	1.08	0.21	0.12	1.26
23	30-2-39 to 4-1-58	5.6	1.81	1.67	1.12	2.89
24	4-1-58 to 8-5-23	3.4	1.29	1.73	1.38	2.82
25	8-5-23 to 12-03-41	5.8	1.83	0.05	0.95	2.55
26	12-03-41 to 16-03-30	2.5	0.56	0.05	0.13	0.15
27	16-03-30 to 20-05-18	5.9	1.13	0.43	0.64	1.80
28	20-05-18 to 23-13-59	3.7				

Table 3. Interim definitive orbit for satellite 1958 ε

Summary of certain position information for arcs extending from 1507 UT 26 July 1958 to 1559 UT 5 October 1958

Arc	Interval (d-h-m) UT	Standard deviation of fit, millirad	Coordinate differences and corresponding distances between points in adjacent books at transfer times			
			Longitude, nm at sea level	Latitude, nm at sea level	Height, nm	Radial distance, nm
1	26-15-07 to 30-15-10	8.2	10.6	2.3	2.9	13.8
2	30-15-10 to 3-17-53	3.5	2.5	0.5	0.5	2.7
3	3-17-53 to 7-16-56	5.0	1.0	2.2	0.2	2.6
4	7-16-56 to 11-12-38	5.0	2.4	0.5	0.9	2.7
5	11-12-38 to 15-17-04	5.7	0.14	0.3	0.99	1.04
6	15-17-04 to 19-17-59	5.0	2.5	0.7	0.8	2.8
7	19-17-59 to 23-17-26	6.8	0.1	1.5	4.5	4.9
8	23-17-26 to 27-12-08	5.4	2.6	.8	0.6	2.9

Table 3. Interim definitive orbit for satellite 1958 ε (Cont'd)

Arc	Interval (d-h-m) UT	Standard deviation of fit, millirad	Coordinate differences and corresponding distances between points in adjacent books at transfer times			
			Longitude, nm at sea level	Latitude, nm at sea level	Height, nm	Radial distance, nm
9	27-12-08 to 31-14-06	5.6	0.3	0.03	0.6	0.7
10	31-14-06 to 4-13-4	3.2	0.7	0.5	1.9	2.2
11	4-13-4 to 8-15-17	4.4	0.8	0.1	1.9	2.2
12	8-18-17 to 12-15-38	4.2	0.4	0.1	2.0	2.1
13	12-15-38 to 16-16-59	4.3	1.8	3.3	2.3	4.7
14	16-16-59 to 20-17-9	4.0	0.3	0.3	3.6	3.7
15	20-17-9 to 24-13-2	4.9	0.3	1.0	4.4	4.5
16	24-13-2 to 28-13-29	4.6	2.5	1.1	1.8	3.4
17	28-13-29 to 2-16-38	3.4	3.0	3.0	1.1	4.6
18	2-16-38 to 5-15-59	2.2				

Table 4. Interim definitive orbit for satellite 1959 α

Summary of certain position information for arcs extending from 1605 UT 17 February 1959 to 1604 UT 15 March 1959

Arc	Interval (d-h-m) UT	Standard deviation of fit, millirad	Coordinate differences and corresponding distances between points in adjacent books at transfer times			
			Longitude, nm at sea level	Latitude, nm at sea level	Height, nm	Radial distance, nm
1	18-05-30 to 25-05-01	1.7	2.01	0.35	2.03	3.30
2	24-15-28 to 03-13-50	1.5	0.57	0.25	1.32	1.51
3	03-13-50 to 10-15-34	1.4	0.11	0.10	0.67	0.69
4	10-15-34 to 15-16-04	1.04				

Table 5. Interim definitive orbit for satellite 1958 η

Summary of certain position information for arcs extending from 0530 UT eptember 18, 1959 to 1429 UT December 11, 1959

Arc	Interval (d-h-m) UT	Standard deviation of fit, millirad	Coordinate differences and corresponding distances between points in adjacent books at transfer times			
			Longitude, nm at sea level	Latitude, nm at sea level	Height, nm	Radial distance, nm
1	18-05-30 to 25-05-01	0.8	0.7	0.2	2.5	2.7
2	25-05-02 to 01-18-24	0.9	0.6	0.1	1.0	1.2
3	01-18-25 to 08-18-09	1.0	0.1	0.2	0.7	0.7
4	08-18-10 to 15-19-14	1.0	0.7	0.0	0.6	1.0
5	15-19-15 to 22-18-11	1.1	0.0	0.2	0.9	0.9
6	22-18-12 to 29-17-05	1.1	0.3	0.2	2.5	2.5
7	29-17-06 to 05-18-08	1.0	1.2	0.9	3.1	3.7
8	05-18-09 to 12-20-01	0.9	3.1	0.8	2.1	4.3
9	12-20-02 to 19-18-52	1.0	4.7	0.0	0.1	5.1
10	19-18-53 to 26-18-44	0.8	3.9	0.7	0.6	6.1
11	26-18-45 to 3-19-40	1.3	2.5	1.2	2.6	4.6
12	3-19-40 to 11-14-29	0.9				

Table 6. Interim definitive orbit for satellite 1959 ι

Summary of certain position information for arcs extending from 1540 UT October 13, 1959 to 1039 UT December 2, 1959

Arc	Interval (d-h-m) UT	Standard deviation of fit, millirad	Coordinate differences and corresponding distances between points in adjacent books at transfer times			
			Longitude, nm at sea level	Latitude, nm at sea level	Height, nm	Radial distance, nm
1	13-15-40 to 20-15-40	3.0	1.3	0.7	0.4	1.7
2	20-15-41 to 28-20-27	2.9	0.8	0.6	0.7	1.3
3	28-20-28 to 04-17-45	3.0	0.9	0.3	0.4	1.1
4	04-17-46 to 11-10-05	3.4	1.1	0.0	0.4	1.3
5	11-10-06 to 18-07-29	3.3	3.3	0.1	0.2	3.7
6	18-07-30 to 25-03-03	3.5	0.7	0.4	1.4	1.7
7	25-03-04 to 2-10-39	4.5				

REFERENCES

1. Herget, P., and P. Musen. "General Theory of Oblateness Perturbations," American Mathematical Society Symposium on Orbit Theory (1957).

2. Eckert, W., and D. Brouwer. "The Use of Rectangular Coordinates in the Differential Correction of Orbits," Astronomical Journal, Vol. 46, pp. 125–132 (1941).

NASA Computing Center Predictions

ROBERT W. BRYANT

Goddard Space Flight Center,
National Aeronautics and Space Administration,
Washington, D.C.

ABSTRACT

Predictions obtained from the general oblateness perturbations theory used at the NASA Computing Center are compared with observations. Sets of data are used and a plot of standard deviation of fit vs time from epoch is presented to indicate the mathematical model's adequacy for prediction work.

I. GENERAL DISCUSSION

The purpose of this paper is to exhibit the ability of the mathematical model used at the NASA Computing Center to predict accurately a satellite's position. The results given here should not be construed as the accuracy of predictions issued in the past by the Computing Center. For actual predictions which have been issued, other factors have entered to either improve or detract from the model.

The mathematical model referred to in this paper is the modified Hansen theory with second and fourth harmonics of the Earth's potential included. Also included is a seventh unknown (permitting acceleration of the mean anomaly) to account for the effect of drag.

The procedure used was the following:

1. Elements were obtained by differential correction.
2. Using these elements an orbit of extended duration was generated.
3. Observations were compared with the computed values and residuals were obtained.

In order to exhibit the model's ability as a function of a particular satellite the foregoing procedure was carried out for four of the six satellites for which interim definitive orbits have been generated and for 1958 β.

II. RESULTS

Table 1 gives the orbit elements of 1958 β which were used as starting values for an orbit of 6 weeks' duration (approximately 450 revolutions). Also given are the changes from the previous iteration of the differential correction leading to the elements and the standard deviation of fit.

Table 1. Orbit elements of 1958 β (epoch $108^d\ 12^h\ 27^m$)

Variable	Change	New values
M	−2.2850589,−08	+1.5166276,+00
a	+1.8784600,−08	+1.3617170,+00
e	−5.5488222,−09	+1.8978199,−01
i	−2.1671552,−06	+5.9775692,−01
w	+1.5147153,−08	+4.2526921,+00
Ω	+2.8122929,−08	+3.2916295,+00
N_2	+1.0263456,−13	+9.1189783,−09
Standard deviation of fit: +3.062,−04.		

Figure 1 contains a portion of the computer output for the residuals for satellite 1958 β. Specifically, it contains the first 6 pairs of Minitrack observations of the first week and the complete residual plots for l and m for the first week as plotted by the computer (Fig. 2 and 3). These are true residuals.

Figure 4 is a plot of mean l and m residuals for 3-day periods vs time for the whole 6 weeks. The trend of the l residuals is clearly evident. This trend is attributed to

```
LIMAPU  LONG 282 50 LAT  -11  46 HT    160     58  7  3 21  15 43
  L  OBS =-2.7632323,-03 CAL = -2.5603624,-03 RES = -2.0286993,-04 M =  1
  M  OBS =-2.9166426,-01 CAL = -2.9192272,-01 RES = +2.5845319,-04 M =  2

PANTIG  LONG 298 13 LAT   17   8 HT     16     58  7  3 23  57 53
  L  OBS =+1.1022031,-03 CAL = +7.7786590,-04 RES = +3.2433729,-04 M =  3
  M  OBS =+1.3215673,-01 CAL = +1.3253240,-01 RES = -3.7566386,-04 M =  4

OOMERA  LONG 136 46 LAT  -31   6 HT    524     58  7  4  1  22 21
  L  OBS =+6.5754353,-03 CAL = +7.2589454,-03 RES = -6.8351009,-04 M =  5
  M  OBS =-3.3674989,-01 CAL = -3.3712502,-01 RES = +3.7513300,-04 M =  6

HAVANA  LONG 277 28 LAT   22 52 HT    141     58  7  4  2  19 47
  L  OBS =-1.1542183,-02 CAL = -1.1262495,-02 RES = -2.7968874,-04 M =  7
  M  OBS =+1.6590942,-01 CAL = +1.6587984,-01 RES = +2.9588118,-05 M =  8

OOMERA  LONG 136 46 LAT  -31   6 HT    524     58  7  4  3 44 15
  L  OBS =+3.0099716,-02 CAL = +3.0361319,-02 RES = -2.6160245,-04 M =  9
  M  OBS =-2.6062886,-01 CAL = -2.6094408,-01 RES = +3.1521916,-04 M = 10

PANTIG  LONG 289 13 LAT   17   8 HT     16     58  7  4  7 31 33
  L  OBS =-4.3447727,-03 CAL = -4.6966180,-03 RES = +3.5184522,-04 M = 11
  M  OBS =+2.1481545,-01 CAL = +2.1480171,-01 RES = +1.3748183,-05 M = 12
```

Fig. 1. Residuals for 1958 β (computer sample)

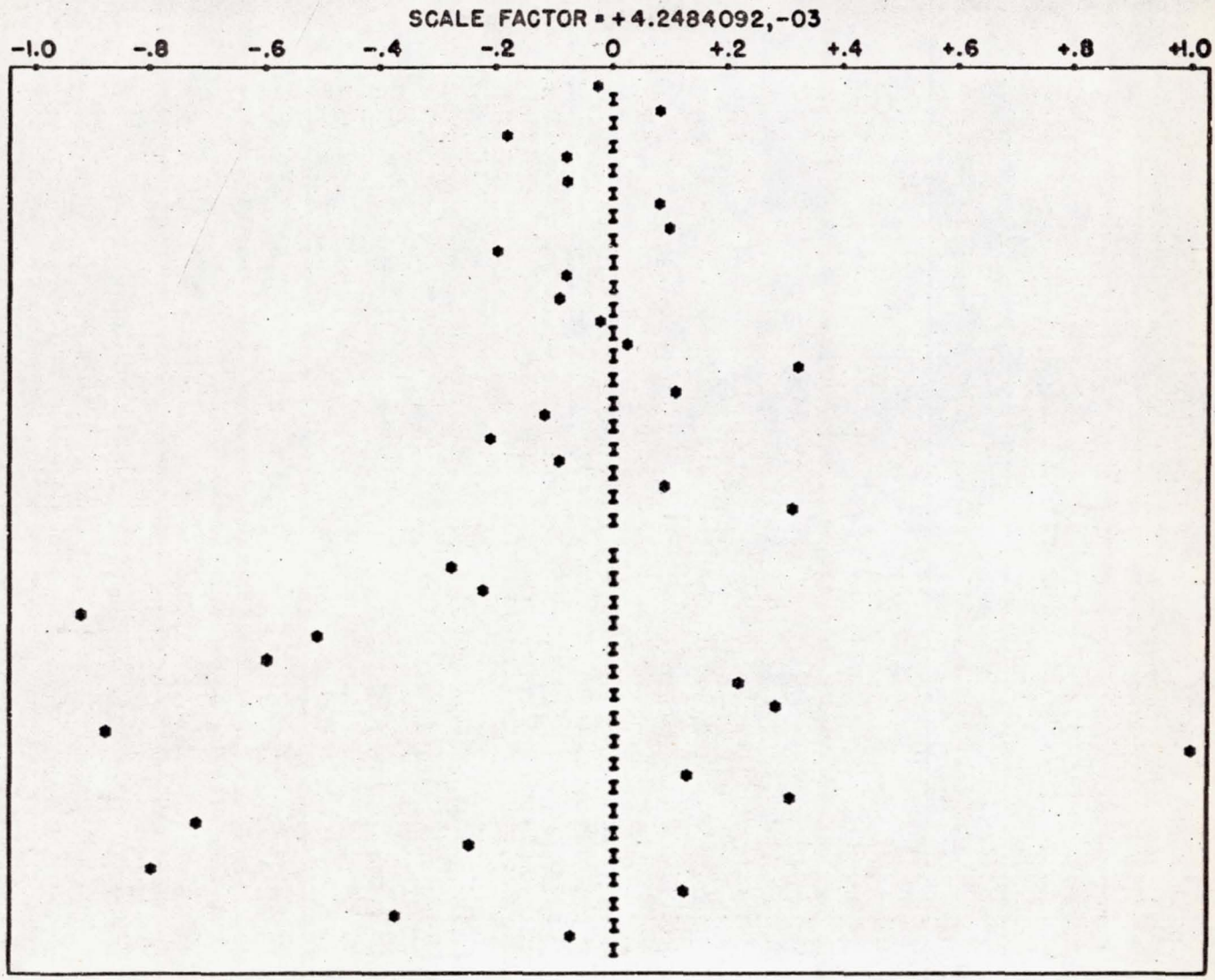

Fig. 2. Residual plot for *l*

the inadequacy in handling drag, which is accounted for in the theory being used only by a quadratic term in the mean anomaly. The effect is evident primarily in the *l*-residuals (l being the direction cosine with the east axis) because of the low inclination of 1958 β. It should be pointed out here that the residuals' being negative means that the observed satellite is behind the calculated satellite position, which is contrary to what would be expected from the effect of drag. The explanation is that the value of the seventh unknown, i.e.,

$$N_2 \text{ in } M = M_0 + n(1+N_2 t)t$$

as determined by the differential correction, is larger than it should be. The values of N_2 as determined on a weekly basis are 9.11898×10^{-8}, 6.8988×10^{-8}, 2.1499×10^{-8}, 2.1499×10^{-8}, 3.1746×10^{-8}, 1.5332×10^{-8}, and 1.3350×10^{-8}. It is easily seen that carrying the first throughout the other five weeks will give rise to the residual phenomenon observed. Figures 5 through 8 are residual plots for the satellites 1958 γ, 1958 ϵ, 1959 η, and 1959 ι.

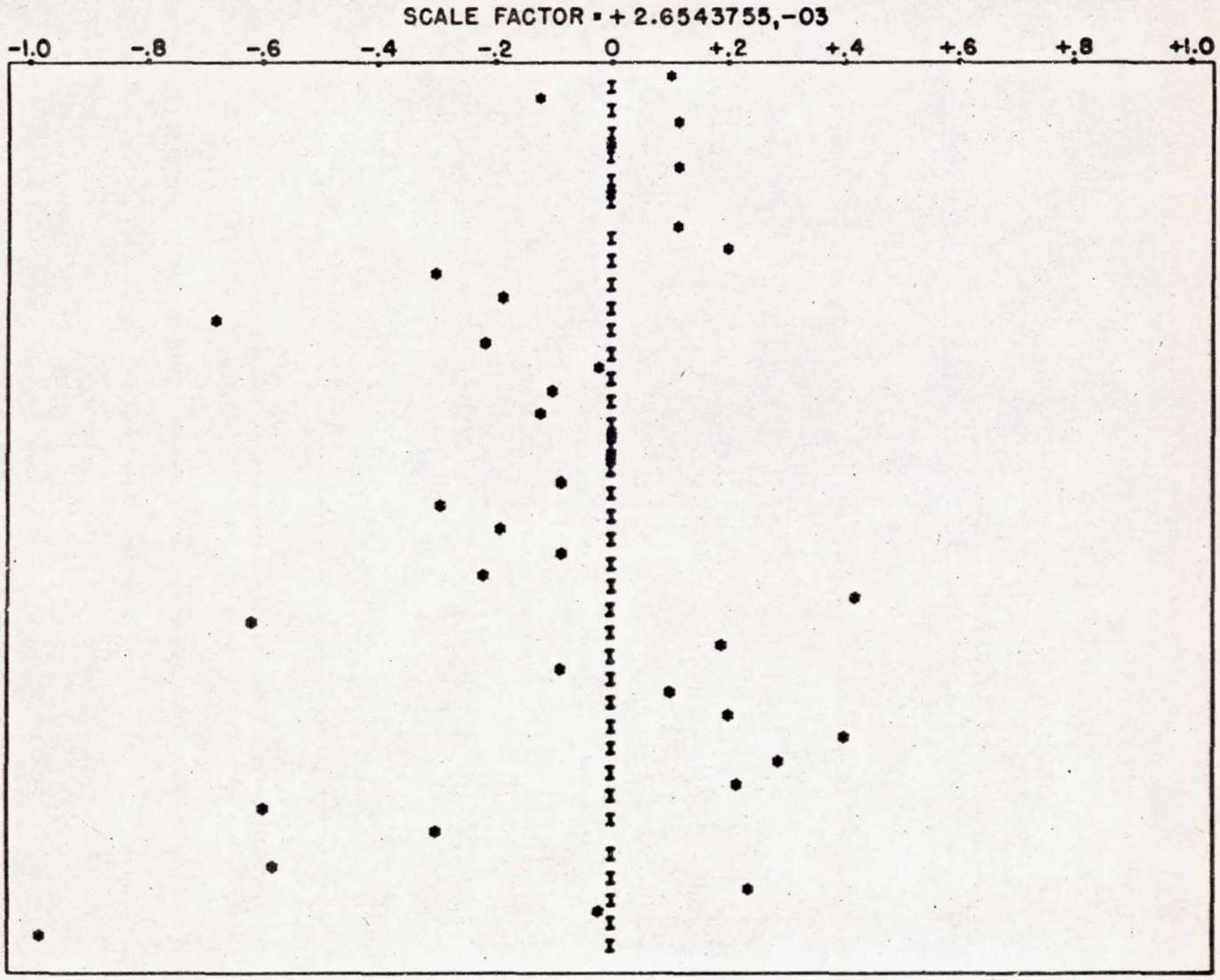

Fig. 3. Residual plot for m

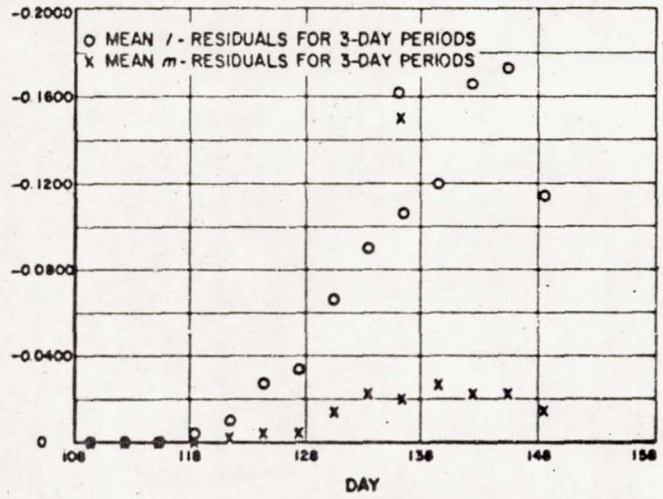

Fig. 4. Plot of mean *l* and *m* residuals for 3-day period

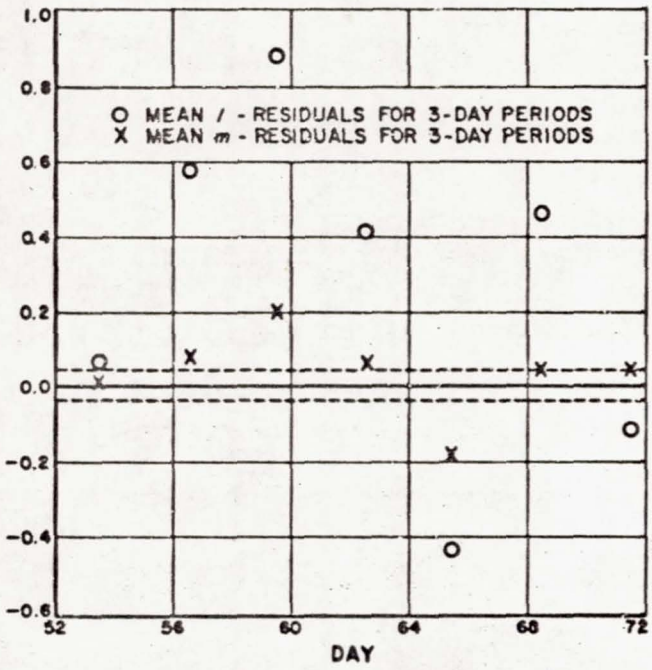

Fig. 5. Residual plot for 1958 γ

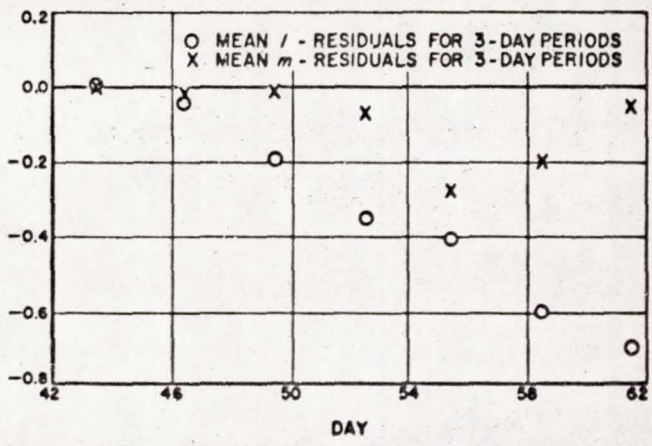

Fig. 6. Residual plot for 1958 ϵ

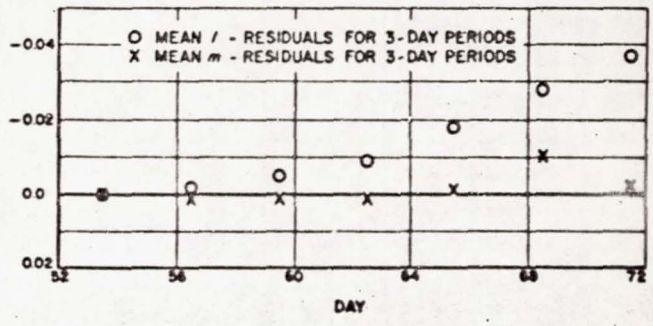

Fig. 7. Residual plot for 1959 η

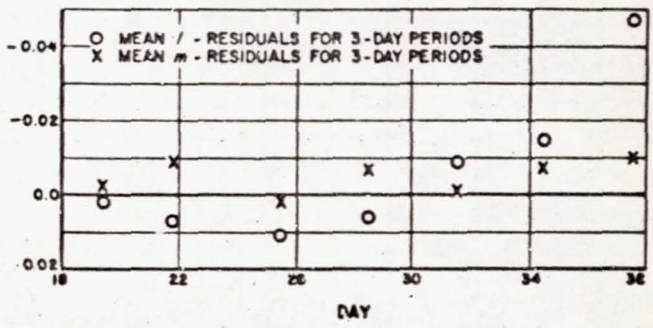

Fig. 8. Residual plot for 1959 ι

The Programming System for Orbit Determination at the IBM Space Computing Center

A. R. MOWLEM

International Business Machines Corp.,
Washington, D.C.

ABSTRACT

The discussion covers IBM's role in the tracking of Earth satellites and lunar probes. A description of the programming system is outlined as well as the various techniques used in the computation and prediction of satellite orbits and lunar trajectories from observational data. Consideration is also given to the data flow at the IBM Space Computing Center and its processing through the computer installed there.

I. INTRODUCTION

The purpose of this paper is to describe the programming system that has evolved at the IBM Space Computing Center. The Center has had a unique opportunity in working on a number of challenging problems in the fields of orbit determination, satellite tracking, etc. When the Center was opened, it was named the *Vanguard* Computing Center, since at that time this program was the Nation's only effort in the satellite field. IBM was interested in Project *Vanguard* because of its challenging aspects, since something of this nature had never been attempted previously, and also as a contribution to the International Geophysical Year. In June of 1956, IBM entered into a contract with the Naval Research Laboratory to do the computing for all the satellites that were to be launched during the International Geophysical Year. This was a big decision on the part of the NRL and IBM, since at that time one could not be sure that satellites would behave exactly the way they have or, indeed, that computers were suitable for orbital computation. It might be said that this effort was a leap into the future. As a matter of fact, much of the work that was done on Project *Vanguard* had a research characteristic. Since that time, we have seen the programming system that was developed being used for orbital calculations on the various satellites that have been launched. These range from the *Sputniks* to the *Vanguards* and the *Explorers*, as well as the lunar probes, both Russian and American. The only satellites for which the Space Computing Center did not

make any calculations were the *Discoverer* series, since the data for these were of a classified nature and, therefore, were not obtained at the Center.

Soon after the contract was signed, a Working Committee on Orbits was formed which consisted of many eminent astronomers and scientists, such as Dr. Paul Herget, Director of the Cincinnati Observatory, Dr. G. M. Clemence, Director of the Naval Observatory, and Dr. R. L. Duncombe, also of the Naval Observatory, together with Dr. Joseph Siry, who at the time headed the Theory and Analysis Branch of the Naval Research Laboratory and, at present, is Chief of the Theory and Analysis Staff, Goddard Space Flight Center, NASA, and is chairman of one of the sessions at this Seminar. This committee was responsible for the mathematical formulation of the problem which was turned over to IBM; IBM, in turn, was to convert the problem into machine language to be run on the 704 computer and, later, on the 709 when it was installed. A group of expert mathematicians and programmers at IBM was assigned to this project and formed an integral part of the Working Group on Orbits. This work resulted in one of the most comprehensive and accurate systems of programs that are being constantly used in production. To give you an idea of the size of the system, IBM has spent something on the order of about 25 man years on the project and about 50,000 instructions have been written specifically for the 704 and 709 computers.

Why are satellites useful? One reason is that experimental findings are a part of every satellite that has been launched. These findings have to do with the pressure and temperature of the atmosphere, the radiation around the Earth, and so on. However, if we could not determine the position of the satellite precisely in space, then these experimental measurements would be of little value because they could not be correlated with the satellite in space at a particular time. In fact, Dr. Van Allen used the calculations that were made at the *Vanguard* Computing Center in mapping out his radiation belts.

A second use of satellites is the more accurate determination of the shape of the Earth. *Vanguard I* was a satellite that was very suitable for this type of work because most of its orbit was in the upper regions of space and, therefore, little affected by the drag of the atmosphere. Its perigee was 400 miles and its apogee was around 2400 miles. Also, the satellite was spherical and would remain in orbit for a long period of time, about 200 years. The analysis of the motion of the satellite resulted in the determination that the shape of the Earth was more like a pear. Many NASA scientists were involved in this determination. In studying the motion of the satellite, Miss Ann Eckles noticed that whenever the perigee was in the southern hemisphere it was always lower than when the perigee was in the northern hemisphere, which led to the conclusion that there must be a greater land mass at the southern hemisphere exerting a greater gravitational attraction on the satellite than in the northern regions. The calculations for this determination were made at the Center, and the preciseness of these calculations is evident when we consider that the difference between the previously conceived shape of the Earth and the recently determined pear shape is only a matter of about 25 ft at some points and 50 ft at other points. Of course, there are many other uses of satellites, some of which will be mentioned later, but all of them depend primarily on knowing the position of the satellite precisely.

II. DATA FLOW

At this point it would be worth while to consider the flow of data at the Computing Center. Let us consider the *Vanguard* Project and the *Vanguard* satellite as representative of the satellite field in general. The tracking stations that are used are called Minitrack stations. They are aligned in a picket-fence fashion along North and South America. There are additional stations in Australia and South Africa. The reason for choosing such a picket fence is that one could be sure of obtaining at least one observation for each revolution of the satellite. The Minitrack stations receive radio signals from the satellite. These radio signals are then transmitted by radio or by teletype to a central collecting agency of the Naval Research Laboratory called the Control Center from which they are transmitted to the Space Computing Center by teletype. As a result of this teletype transmission, punched paper tape is produced which is then fed automatically into the IBM 047 to be converted into punch card form. The punch cards then become the observations which are fed into the computer. These observations, which are in the form of phase differences between two antennas separated by a measured baseline, are equivalent to direction cosines or elevation angles in the east–west or north–south directions. These observations are then fed into the 704 computer and, under the control of a master program, are processed through a series of computing cycles to produce predictions of the subsatellite position in longitude and latitude for every minute of time for a week or ten days in advance. These predictions can also come out in the form of punch cards from the computer. The prediction cards now go through a reverse process whereby they are converted through the IBM 063 into teletype tape and are transmitted back again to the Control Center, from which they are retransmitted to the various stations so that they can be alerted to the time of satellite passage and obtain good observations.

III. PROCESSING WITHIN THE COMPUTER

Observations of the satellite are made by the Minitrack stations for every second of time, so that for a passage of the satellite over a station there may be as many as 30 or 40 readings. These individual readings are smoothed parabolically and adjusted for various calibrations and corrections to give one reading for the entire passage over a station. If there are insufficient observations during any computing cycle, after the smoothing process the message can be split into say three parts to determine the "side lobes" so that there can be more observations for any particular passage of the satellite.

When a satellite is launched, the processing cycle can start in one of two ways, depending upon whether we have information during the launch phase. If we consider the *Vanguard* rocket as representative of other rockets, we note that it consists of three stages. The first two stages are used to power the rocket to an altitude of 140 miles and a speed of 11,000 miles per hour, at which time the coasting phase begins in order to reach orbital altitude and so that the third stage is aligned parallel to the surface of the Earth. When these conditions are fulfilled, the third stage powers the satellite into orbit with a final burst of speed. At Cape Canaveral the entire launching operation is monitored for safety purposes. There is a 709 impact predictor which is used for this purpose, calculating the impact point at any instant if the power is shut off. Radar data are fed into the computer at the rate of 10 per sec, and while the missile ascends in its trajectory, the computations are done in real-time, producing output at the same high-speed rate of 10 per sec. This calculation is continued into the coasting phase until the missile is considered to be out of range of populated areas. In addition to computing the impact point, the Cape Canaveral computer also calculates the position and the velocity of the rocket at any instant of time. A set of these values during

the coasting phase is transmitted to the Space Computing Center. During this phase the rocket assembly is actually in free flight although it does not have the necessary speed to orbit the Earth. These values, after being converted from the local to the inertial frame of reference, can then be used in a numerical integration program to determine the position and velocity at the instant of third-stage burnout. The integration is carried out with a time interval of 1 sec to the nominal time for injection of the satellite into orbit. The nominal contribution to the velocity from third stage is added vectorially to the velocity vector to determine the injection conditions. As a result, the numerical integration program can be run once again with these injection conditions to determine if the satellite has a chance of orbiting. These calculations are made very soon after launching and in advance of receipt of any observations which may take as long as 1½ hr to arrive at the Center. If it is determined that the satellite will orbit, predictions are computed for the stations along the launch path. These calculations are used to check the observation data when they come in, as well as to solve any "resolution" problems that the Minitrack stations may be encountering (which was the case with the Russian *Sputniks*). This whole process serves the purpose of arriving at a rough determination of **r** and **v** at injection. From this point on, observations, when received, can be used to refine the **r** and **v** and make good predictions.

Let us now consider a satellite for which there is no information concerning launching or injection conditions, such as in the case of the *Sputniks*. In this case we must use the observations themselves in order to make a rough determination of the **r** and **v** at burnout. For this purpose we have a circular orbit program which uses two widely spaced observations, an elliptic orbit program which uses three observations closely spaced in time, and another elliptic orbit program for four observations, the fourth being a redundant observation for greater accuracy. It is at this point that we could decide to split a Minitrack observation into several parts. All of these programs are based on Gaussian iteration techniques. In the case of the elliptic orbit program, three timed two-dimensional observations are necessary for determining the six constants of integrations of the three second-order differential equations that are the equations of motion. The basis of the iteration scheme is that for an elliptic orbit the radius vector at any time t_2 is some linear combination of the radius vectors at times t_1 and t_3.

Once the position and velocity vectors are known at injection we can proceed with the process of prediction and differential correction with the use of observations. This process is iterated until a refined set of these starting vectors is obtained, at which time the programming cycle is transferred to a second and more accurate technique involving oblateness perturbations, which will be described later. This first prediction process is the numerical integration of the equations of motion. The method used is sixth-order Cowell's integration, which is an accurate method as compared with other numerical integration techniques. Its principal disadvantage is the time it takes to set up a converged function table at the start of integration. This factor is, of course, of minor importance when predictions are being made for hours and days. The method itself is founded on the calculus of finite differences, which requires that over the range of the argument concerned, the function shall be continuous and shall have continuous derivatives of all orders. The function table is built 6 time steps backward and 6 forward around a reference position and velocity. At the start of integration the reference values for this function table are the injection conditions, and an iteration technique is used to produce convergence of the table. Once a converged function table is obtained, the process of integration involves a predictor–corrector technique for determining the position and velocity vector at each time step. This integration is carried out 3 times for all 3 components in the inertial frame of reference.

Having produced a "minute vector" tape containing predicted position vectors for every minute of time, the prediction cycle continues with a program which converts the inertial position vectors into a form more universally understood. This is called the "World Map macro-operation," which determines the predicted subsatellite longitude and latitude together with the altitude of the satellite for every minute of time for whatever period desired. Enclosed is a sample report (Fig. 1) which shows the various quantities in detail. In addition, if the satellite is passing over cities or observing stations, an alert is indicated with a twilight indication for the optical stations, together with the zenith angle and the time of meridian crossing.

Once predictions are complete and observations are received, we are in a position to improve the orbit by means of a differential correction program which will try iteratively to bring predictions into closer agreement with the observations by correcting the starting position and velocity vectors. This is a process which develops what is called an equation of condition for every observation quantity, i.e., two equations, one for l and the other for m, or one for each of the direction cosines. On the left side of each equation are given the partial coefficients, which show the contribution of the deviation between

```
WORLD MAP
  LAMBDA SUB ZERO = +2.5521128,+00      TAU SUB ZERO = +5.7151547,+00
                                  DREF = + 534
X                 Y                 Z
-0.3583863       -1.2984952        +0.1813887
                 LONGITUDE  LATITUDE                    HEIGHT IN
 DAY HR MIN      DEG.MI.SE.DEG.MI.SEC.                  KILOMETERS
  18  2 18   -  89  6 35 +21 37  4                      +2372.0859        TWILIGHT
1CHIGO  9  18 2  18 37.776  -57.0116   3499.2266    N
  18  2 19   -  86 52 56 +22 41 31                      +2433.6871        TWILIGHT
  18  2 20   -  84 39  5 +23 42 47                      +2493.7747        TWILIGHT
1ATLAN 13  18 2  20  6.127  -35.6544   2878.6721    N
1CINCI  7  18 2  20  3.861  -46.9805   3199.6603    N
  18  2 21   -  82 24 57 +24 40 52                      +2552.2549        TWILIGHT
CBDIAL 42  18 2  21 48.979  -10.5105   2629.9975    N
1MIAMI 12  18 2  21 59.114  - 0.7152   2608.3895    N
  18  2 22   -  80 10 30 +25 35 45                      +2609.0398        TWILIGHT
  18  2 23   -  77 55 41 +26 27 25                      +2664.0468        TWILIGHT
BPOINT 49  18 2  23 22.274  -36.1738   3094.0698    N
1WASHN 10  18 2  23 24.602  -37.1820   3121.6781    N
  18  2 24   -  75 40 31 +27 15 53                      +2717.2011        TWILIGHT
FTMONM 48  18 2  24 43.621  -37.6531   3209.7395    N
1NYORK  8  18 2  24 44.342  -38.7777   3240.7071    N
  18  2 25   -  73 24 57 +28  1  6                      +2768.4328        TWILIGHT
LINCON 47  18 2  25 50.713  -41.1192   3369.4160    N
  18  2 26   -  71  9  1 +28 43  6                      +2817.6764        TWILIGHT
PTRICO 44  18 2  27 47.017  +34.9140   3298.9467    N
  18  2 27   -  68 52 43 +29 21 52                      +2864.8718
  18  2 28   -  66 36  6 +29 57 25                      +2909.9639
  18  2 29   -  64 19 11 +30 29 44                      +2952.9020
  18  2 30   -  62  2  3 +30 58 49                      +2993.6385
  18  2 31   -  59 44 44 +31 24 42                      +3032.1311
  18  2 32   -  57 27 19 +31 47 23                      +3068.2399
  18  2 33   -  55  9 53 +32  6 53                      +3102.0 95
  18  2 34   -  52 52 29 +32 23 12                      +3133.7666
  18  2 35   -  50 35 14 +32 36 23                      +3162.9226
  18  2 36   -  48 18 14 +32 46 26                      +3189.6700
  18  2 37   -  46  1 33 +32 53 23                      +3213.9855
  18  2 38   -  43 45 16 +32 57 16                      +3235.8475
  18  2 39   -  41 29 31 +32 58  6                      +3255.2375
  18  2 40   -  39 14 22 +32 55 56                      +3272.1398

*LSPM2. LOCAL STATION PREDICTION MACRO-OPERATION                    07060358


                        LOCAL STATION PREDICTIONS

DREF=+206       T SUB 0=+0.0000000,-40       LAMBDA SUB 0=+3.1927978,+00
                                                YR.MN.DY.HR.MI.SE.MI.SE.INTERVAL
PANTIG   LONG  298 13 LAT  17  8 HT    16       58  6 14  1 57  0 59  0  5
 SL.RA. AZIMUTH ELEVATION
 KILOMTS.DEG.MI.DEG.MI.
   550    189 15  48  9      537    184 37  50 16      527    179 19  52 15
   519    173 22  54  1      513    166 45  55 29      510    159 34  56 35
   510    152  0  57 14      512    144 17  57 24      516    136 41  57  5
   523    129 28  56 20      532    122 49  55 13      544    116 48  53 48
   557    111 27  52 11      573    106 46  50 26      590    102 39  48 36
   609     99  4  46 45      630     95 55  44 53      651     93 10  43  4
   674     90 44  41 19      698     88 35  39 37      723     86 41  37 59
   749     84 59  36 26      776     83 28  34 57      803     82  6  33 33
   831     80 51  32 12


                                                YR.MN.DY.HR.MI.SE.MI.SE.INTERVAL
1SPAIN   LONG  353 47 LAT  36 27 HT     0       58  6 14  2 13  0 16  0  5
 SL.RA. AZIMUTH ELEVATION
 KILOMTS.DEG.MI.DEG.MI.
  1003    149 30  63 10     1012    145 43  62 23     1021    142 12  61 30
  1032    138 57  60 33     1043    135 58  59 33     1055    133 13  58 30
  1068    130 41  57 25     1082    128 22  56 19     1096    126 14  55 11
  1111    124 16  54  4     1127    122 28  52 56     1144    120 48  51 48
  1161    119 16  50 41     1179    117 51  49 34     1198    116 32  48 28
  1217    115 19  47 23     1236    114 11  46 19     1256    113  8  45 16
  1277    112  9  44 16     1298    111 14  43 14     1319    110 23  42 15
  1341    109 34  41 17     1364    108 49  40 20     1386    108  6  39 24
  1409    107 26  38 30     1432    106 48  37 37     1456    106 13  36 46
  1480    105 39  35 55     1504    105  7  35  6     1529    104 36  34 18
  1553    104  8  33 31     1578    103 40  32 45     1603    103 14  32  1
  1629    102 49  31 17     1654    102 26  30 34     1680    102  3  29 52
  1706    101 42  29 12
```

Fig. 1. World Map macro-operation

observed and computed values of direction cosines in each of the unknowns. The right-hand side shows the total differential or total deviation between observed and computed. The six unknowns in the equations are the corrections to the 3 components of position and the 3 components of velocity vectors. In equation form we have, essentially,

$$\frac{\partial l}{\partial x}dx + \frac{\partial l}{\partial y}dy + \frac{\partial l}{\partial z}dz + \frac{\partial l}{\partial \dot{x}}d\dot{x} + \frac{\partial l}{\partial \dot{y}}d\dot{y} + \frac{\partial l}{\partial \dot{z}}d\dot{z} = \delta l = (0 - C)$$

$$\frac{\partial m}{\partial x}dx + \frac{\partial m}{\partial y}dy + \frac{\partial m}{\partial z}dz + \frac{\partial m}{\partial \dot{x}}d\dot{x} + \cdots = \delta m = (0 - C)$$

Therefore, for every observation two equations are formed which are then solved by the least squares method to obtain the corrections dr and dv. It should be noted that the partials in the equations have explicit relationships. For the process to converge, deviations from computed quantities must not be too large; the very basis of the process is that the deviations must be differential. During the run, observations with large deviations can be removed from the solution. The technique of using punched cards for observations (which can be weighted according to how far away they are from the zenith) is a good one, since these form unit records and they can be easily removed or inserted at will. For convergence, the method also requires that the observations span only a few revolutions of the satellite. This process is especially useful shortly after launching. As we shall see, other means are available for longer-arc differential correction.

The process of differential correction and numerical integration is repeated until the corrections to the position and velocity vectors converge to a minimum, at which time the corrected values are used for prediction purposes in a final integration. The disadvantage, from an operational viewpoint, of the numerical integration technique is that when one is interested in the predicted quantities corresponding to the time of an observation, all the previous steps leading up to this point must be calculated. In addition, the step-by-step process is subject to cumulative errors due to rounding so that these prediction runs cannot be extended too far in time (for more than 4 days to a week). In spite of all of these factors, integration is very useful soon after launching and also during the last stages of a satellite's life, when the drag forces become appreciable upon re-entry. However, when the orbit is stabilized so that its changes from one revolution to the next are only minor, and when we have obtained a good set of reference vectors, we are in a position to substitute oblateness perturbation techniques for the integration and to obtain greater accuracy, longer arc extension, and operational ease.

The general oblateness perturbation (GOP) program has the advantage that it can be evaluated for any particular time in the orbit, given the orbital elements at a certain epoch. As a result, the process avoids cumulative errors. It has an additional operational advantage in that none of the intermediate steps, which are necessary in integration, are needed in developing the equations of condition in the differential correction process associated with this program. The disturbed mean anomaly which corresponds to time is used as the independent variable. This leads to simpler expressions and avoids the need for expansion into Taylor's series.

The whole GOP process is based on Hansen's lunar theory, which is being described by Dr. Peter Musen at this Seminar. Dr. Paul Herget, Director of the Cincinnatti Observatory, together with Dr. Musen developed this method for satellite tracking. This method treats the fixed elliptic reference orbit as a rigid body moving in inertial space under the influence of perturbing forces due to the oblateness of the Earth, and constrained only to have its focus at the center of the Earth. The coordinate system attached to this rigid body has its origin at the focus, its departure point at perigee. Any radius vector in this ellipse is represented by a two-dimensional vector, which can be transformed to the inertial frame of reference by a series of rotation matrices which are functions of the inclination of the orbit plane, the argument of perigee, and the longitude of the ascending mode. The semimajor axis and the eccentricity of this ellipse are fixed.

The procedure involves the use of Fourier series in the development of the perturbations. In Kepler's equation for the eccentric anomaly, the perturbation is applied in the form of an additive term to the mean anomaly (ΔM). This additive term is determined iteratively as a Fourier series in terms of the eccentric anomaly E and ω (the argument of perigee), and evaluated only for the fixed a, e, and i (the semimajor axis, the eccentricity, and the inclination). In the orbit plane which is considered fixed in space a perturbation is also applied in the radial direction ν in the determination of the predicted radius vector. This perturbation is also determined as a function of E and ω and evaluated only for the three elements. The program ends up with nine Fourier series which are functions of E and ω. For prediction purposes, these series can be evaluated for the times desired by determining the corresponding values of E, also iteratively through the

perturbed Kepler equation, and by inserting the remaining orbital element ω. Provision is made for drag by including another term in Kepler's equation, which becomes an additional unknown to solve for in the differential correction.

Now that we have developed our series we are in a position to go through a differential correction in order to bring predictions into close agreement with observations by determining the corrections to the six classical orbital elements (plus an additional one representing drag). This program is similar to the differential correction program that is used with numerical integration except that the partial coefficients of the equations of condition are in terms of the classical orbital elements. The Fourier series perturbations are brought in from tape and evaluated for the remaining orbital elements and, iteratively, through Kepler's equation for the values of E corresponding to the observation times. Equations of condition are then developed with the observed deviations on the right-hand side.

$$\frac{\partial l}{\partial a}da + \frac{\partial l}{\partial i}di + \frac{\partial l}{\partial e}de + \frac{\partial l}{\partial M}dM + \frac{\partial l}{\partial \theta}d\theta + \frac{\partial l}{\partial \omega}d\omega = \delta l = (0 - C)$$

Similarly,

$$\frac{\partial m}{\partial a}da + \frac{\partial m}{\partial i}di + \cdots + \frac{\partial m}{\partial \omega}d\omega = \delta m = (0 - C)$$

The condition equations are solved by the least square method to obtain the corrections to the orbital elements. The partials are once again explicitly stated and provision is made for removing bad observations.

The GOP process coupled with its own differential correction is used iteratively until the corrections to the elements are minimized. Operationally, this is conveniently done since the calculations are made only for the observations. The process is much more rapid, therefore, than the one involving integration. With a refined set of elements we can make refined predictions. The procedure applies for long arcs with great accuracy. In fact, this is the method that was used in making a hindsight analysis covering the orbit of *Vanguard I*. Observations covering a period of 90 days were fed into the system in one orbital run on the machine and differential corrections made. This analysis would have been impossible with integration. The study resulted in better determination of the oblateness terms including the evaluation of the third spherical harmonic, leading to the determination of the pear-shaped Earth by the NASA scientists working at the Space Center.

Previously, it was pointed out that in the rough determination of the elements shortly after launching, the differential correction technique associated with numerical integration has the limitation that the process converges for an arc of a few revolutions of the satellite. If during this arc we do not have sufficient observations to make the differential correction run, or if the few observations should span a longer arc with the elements still roughly determined, we can use a numerical technique to determine corrections to the elements. This process is unsophisticated but useful in that integrations are made with starting vectors slightly deviated from the reference set. This means that seven integrations are necessary—one for the reference set and one integration for each of the six deviated components of the position and velocity vectors. Only one component at a time is deviated while holding

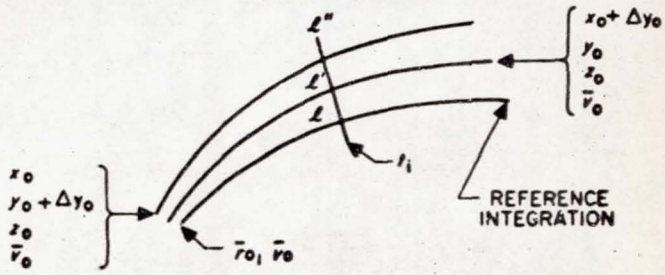

the remainder at the reference values. The basis of the process is that partial derivatives are approximated by differences, i.e.,

$$\frac{\partial l}{\partial x}\Big)_{t_i} \sim \frac{\Delta l}{\Delta x}\Big)_{t_i} = \frac{l - l'}{\Delta x_0}\Big)_{t_i}$$

Equations of condition are once again developed in terms of deviations to the position and velocity vectors with differences replacing derivatives as shown in this equation:

$$\left(\frac{l' - l}{\Delta x}\right)dx + \left(\frac{l'' - l}{\Delta y}\right)dy + \cdots = \delta l$$

and similarly for δm,

$$\left(\frac{m' - m}{\Delta x}\right)dx + \left(\frac{m'' - m}{\Delta y}\right)dy + \cdots = \delta m$$

The condition equations are solved, as before, by the least square method. With this technique, we must balance the need for sufficiently small deviations from the reference values in order to represent the derivatives accurately against the need for sufficiently large deviations to maintain computing accuracy in the determination of the differences.

Except for the oblateness perturbation programs, many of the above techniques have been used for lunar trajectories and space probes. The principal programs used were the integration and numerical differential correction programs with provision being made for the Moon and Sun potentials. In the case of *Lunik II* the programs verified the Russian announcement of impact with the Moon.

There is an additional program that is useful in making specific predictions for a station. These are in the form of azimuth, elevation, and slant range for the interval of passage over a station. A six-point Lagrangian interpolation technique is applied to the "minute vector" tape to determine these values which are punched on cards and transmitted by teletype through the Control Center and to the individual stations in order to make their observations.

The programming system has many flexibilities; for instance, numerical integration can go forward or backward, in single or double precision, with a minute or a second time step. The World Map program is equally at ease with polar and inclined orbits, determining latitude and meridian crossings, and with satellites launched in easterly or westerly directions. In the local station prediction program we have the means of applying zenith angle tolerances on the predictions and determining mutual visibility times among stations. The programs are in a constant state of flux with modifications being made to handle special requirements and new uses. For instance, the system is being amplified to handle the special requirements of Project *Echo*.

The design of the programming system was such that all of the parts were highly subroutinized. This meant that the system consisted of relatively small parts which could be woven together into large macro-operations as needed. As a result, modifications were easy to incorporate since macro-operations as a whole did not need to be changed. This method made it possible for a number of programmers to be working on various parts of the system relatively independently. It also made the conversion of the 704 programs for use on the 709 a much easier task since the essential changes had to do with the input-output subroutines. This meant that the changes could be localized to these sections without even touching the macro-operations themselves.

The programming system is tape-operated. A system tape is prepared with the various macro-operations written as individual records on the tape. These programs are called in by a set of control cards and then automatically executed. The first record on this system tape contains the control program which reads the control cards for the individual programs and spaces the tape to the proper program, loads it into memory, and executes it. In addition, the first record also contains the so-called utility programs consisting of input-output and number conversion routines common to all the macro-operations. The tape is arranged according to frequency of use and contains as many as 60 macro-operations. Other macro-operations which do not utilize much machine time or are not in frequent use are kept as running decks in card form.

The programming system is generally machine symbolic with little FORTRAN used. The reason for this was that at the time the project started the FORTRAN system was not complete, and also that there was need for double precision options for which FORTRAN was not suited at the time. However, increasing use is being made of FORTRAN with new programs, especially for the "attitude" programming system for Project *Tiros*. This is a whole new system being developed for a meteorological satellite that is to be launched in the near future. The purpose of the system is to determine the orientation of the satellite with respect to the surface of the Earth. This involves the use of the orbital tracking programs, and the two systems must be wedded together since the position of the satellite in space is necessary in the determination of the satellite attitude.

The conversion to the 709 not only involved changes of input-output compatibility but provision was also made to take advantage of the overlap feature of the 709, whereby reading and writing operations can be done simultaneously with computing. An effective reduction in machine time was realized in the programs that could take advantage of this feature.

The oblateness perturbation program with its prediction and differential correction procedures involved a great many operations on Fourier series. For this purpose a system of subroutines was devised for handling Fourier series operations such as the addition and subtraction, multiplication and division of Fourier series. In addition, operations such as integration and differentiation, evaluation and expansion of Fourier series as functions of various arguments were also developed. This set of routines probably constitutes the most complete and interrelated set of its kind. These routines have actually been submitted by IBM to the SHARE organization. The system of representation of the series in memory and their handling for the various operations was ingeniously devised by Dr. George Collins under the direction of Mr. D. A. Quarles, Jr., who was Chief Mathematician for IBM in the project.

While the system is primarily designed for Minitrack observations, other types of input can be handled. Certain generalized routines have been written and others are in process for handling a variety of data types and input formats including radar and doppler. This has become especially necessary since we have begun programming for Project *Echo*, which will launch a communications satellite into space, and for the attitude system of Project *Tiros*. The Space Center has also added Project *Mercury* to its many activities, and this is now consuming the major portion of the work being done. With this project a new aspect is injected into the field of orbit determination, and this is truly real-time computing for the tracking of the manned capsule.

The scope of this paper does not allow a highly mathematical presentation of the various techniques described but does serve the purpose of explaining the programming system as a whole. Once again I would like to recognize the efforts of Dr. Paul Herget in the over-all formulation, and of Dr. Peter Musen in the adaptation of Hansen's lunar theory. As a member of the Working Committee on Orbits, Dr. Joseph Siry has also been responsible to a major degree in the formulation, especially recently in the case of the *Echo* and *Tiros* projects. Dr. Siry has had invaluable assistance from Mr. R. W. Bryant, head of the Orbit Determination Section, Theory and Analysis Branch, National Aeronautics and Space Administration.

REFERENCES

1. Herget, P., The Computation of Orbits, Published privately, 1948.
2. Herget, P., and P. Musen. General Theory of Oblateness for Vanguard Satellites (unpublished memorandum presented in abstract form at the American Mathematical Society Symposium on Orbit Theory by Dr. Herget, April 14, 1957), March 23, 1957.

Western Satellite Research Network[1]

GARY A. McCUE and DAVID A. PIERCE

Aero-Space Laboratories, Missile Division,
North American Aviation, Inc.
Downey, Calif.

ABSTRACT

A brief history of Moonwatch is presented to demonstrate how an evolution in observing techniques led to the establishment of the Western Satellite Research Network, a small, unique group of Moonwatch teams. The network's development of advanced techniques and instrumentation for optical tracking of artificial Earth satellites is discussed. Use of these developments has helped these teams maintain an outstanding Moonwatch record, which is included in this report along with the network's functions and plans for the future.

I. INTRODUCTION

The Moonwatch project was organized as an integral part of the satellite program of the International Geophysical Year. A world-wide network of Moonwatch teams, designed to visually acquire and track IGY satellites, was established through the efforts of the Smithsonian Astrophysical Observatory (SAO). Trained observing talent was available within many amateur astronomer groups throughout the world, and SAO utilized this resource in forming Moonwatch teams. These teams established operational stations using equipment borrowed, donated, or constructed by team members. A series of ten or more low-power, wide-field telescopes, arranged with their overlapping fields positioned along the meridian, comprised the typical station's optical instrumentation.

[1]This report is prepared to present the development and accomplishments of The Western Satellite Research Network. This network of Moonwatch teams was established to observe artificial Earth satellites in support of the Smithsonian Astrophysical Observatory's Moonwatch Program. Network activities are coordinated and supported by North American Aviation's Aero-Space Laboratories.

Initially, Moonwatch observation of artificial satellites was visualized as a series of routine operations. This thesis might have held true if U. S. satellite launchings had proceeded according to schedule. *Sputnik I* ushered in the first of a series of major changes in Moonwatch observing techniques. *Sputnik's* 65-deg orbital inclination caused it to pass over most Moonwatch stations in a near north–south direction, seldom passing through a given Moonwatch team's meridian "fence" of telescopes. Thereafter, each new Russian or American satellite created additional problems that necessitated a gradual evolution to new and improved methods of satellite observation.

II. CHANGING MOONWATCH CONCEPT

The extreme brightness of *Sputniks I* and *II* created the illusion that all satellites might be easily observed —an illusion that lasted only until the first American satellite was orbited. Accurate predictions for the *Sputniks* were unnecessary, as these objects could be easily observed with the naked eye or with a low-power optical device having a large field of view. If predictions were 5 or 10 deg in error it made little difference, as the satellite was extremely conspicuous and immediately gave away its identity. Actually, the only prediction necessary was the approximate transit time of the satellite and the general area of the sky in which it would appear. For a large number of teams, making the observation consisted of merely recording the time and position with respect to the brighter stars. Optical instrumentation was not necessarily required; as a result, many teams abandoned efforts to improve observing techniques and instrumentation.

With the advent of faint satellites it became necessary to utilize astronomical telescopes. Conventional Moonwatch telescopes, lacking the penetration power necessary to view faint satellites, seldom allowed observation. Teams were forced to use larger and larger telescopes in order that satellites fainter than 9th or 10th magnitude would not escape observation.

Unfortunately, gains resulting from improved penetrating power were quickly offset by the small fields of the high-power telescopes. Small field instruments (less than 2-deg field diameter) required the use of very accurate predictions. Using the data provided by SAO or Space Track, an experienced person would spend at least an hour calculating each prediction. If the proper methods were used, if no calculation errors were made, and if the clouds blew away, the satellite was easily observed. The entire procedure was essentially repeated for each observation. As a result, much of the time of the average successful Moonwatch team was, and still is, spent making tedious routine calculations. Only a small percentage of time is devoted to actually observing satellites.

Today, the primary objective of Moonwatch—observation of every visible satellite transit—is still unfulfilled by the average team. Team members may lack time to make necessary calculations, or they may lose interest as a result of spending many hours performing this routine task. They may also be unskilled in the proper use of the necessary instruments and calculation methods. The typical team receives little if any assistance directed toward improving its observing skills. New developments that make satellite observing more and more difficult tend to overwhelm and discourage average teams. The resulting decline in morale may render useless the efforts of any given team.

However, a check of Moonwatch records shows that in spite of the above difficulties a few persistent teams are still going strong and are regularly observing faint satellites. In particular, a small group of teams comprising the Western Satellite Research Network (WSRN) has been consistently making over one-half of the nation's Moonwatch observations. In addition, WSRN teams have made many timely contributions to the Moonwatch project, including the acquisition of three lost satellites. The unique success of the WSRN can be attributed to a number of factors that are explained in the following pages.

III. WESTERN SATELLITE RESEARCH NETWORK

Early in 1958, several California Moonwatch teams saw the need for mutual assistance, inasmuch as they were having little or no success observing the distant, sub-naked-eye American satellites with their early Moonwatch equipment. It was thought that mutual efforts might be the best way to meet this new challenge. The teams arranged informal meetings to exchange ideas and devise methods of satellite tracking that would be especially applicable to the faint objects. Immediate effects of initial meetings were an increase in morale and interest. No longer were these teams on their own. They could now benefit from the mistakes, knowledge, and experience of other teams.

Since standard Moonwatch telescopes lacked the power necessary to permit observation of faint satellites, these teams began experimenting with their own astronomical telescopes. Use of astronomical telescopes having very small fields of view necessitated development of highly accurate prediction methods. An error of 1 deg or more in the predicted position meant that the observer, with a field of less than 2 deg, would miss the satellite entirely. Arthur Leonard, leader of the Sacramento Moonwatch team, developed a computation technique that yielded predictions having the necessary accuracy. However, his technique required at least an hour's computation with a desk calculator for each prediction. The teams successful in the use of this technique were still limited.

In July 1958, Gary McCue, leader of the Whittier Moonwatch Team, joined North American Aviation's Aero-Space Laboratories in Downey, California. He was assigned to aid the company's research programs in the field of orbit determination and satellite research. It happens that today's electronic digital computers can be readily adapted to solve problems involving routine computations such as predicting satellite transits. In early 1959 McCue announced that he had successfully programmed North American's IBM 709 computer to make individual station satellite predictions using Leonard's computation techniques. Precise predictions for each of the cooperating teams resulted. Since then, McCue has developed several other prediction programs which have proved very useful in such activities as searches for lost satellites. These programs will be discussed in some detail in this report.

On 17 July, 1959, representatives of the China Lake, Sacramento, San Jose, Walnut Creek, and Whittier Moonwatch teams held their third conference at Davis, California. The teams agreed to adopt "Western Satellite Research Network" as their official title. Though not represented at the conference, Albuquerque was to be a member of the newly formed network. Since then, the network has expanded to include teams at Spokane, Washington, and Rochester, New York. The location of WSRN teams is graphically illustrated by Fig. 1. Spokane extends WSRN boundaries to 48 deg north latitude, while Whittier is the southernmost team. Rochester, the newest addition, serves as the eastern outpost of this "western" network.

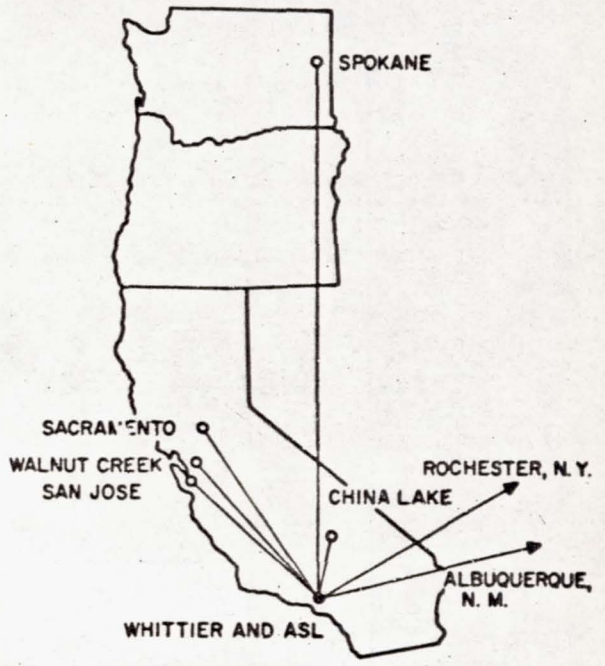

Fig. 1. Western Satellite Research Network

At the third conference, teams of the newly formed WSRN unanimously adopted the following objectives. The teams also agreed to participate in a number of activities designed to assure adequate support of the stated objectives.

Objectives:

1. Provide the Smithsonian Astrophysical Observatory with precision visual observations of artificial Earth satellites.
2. Conduct research pertaining to the mechanics of space vehicles.

Teams participating in network activities will endeavor to accomplish the objectives through the following means:

1. Consolidation of satellite tracking efforts.
2. Maintenance of an assured network of observers.
3. Incorporation of methods of making precision predictions.
4. Production and analysis of accurate data.
5. Assurance of rapid dissemination of observational data among network teams.
6. Maintenance of a radio communications network.
7. Interchange of ideas and methods.

North American Aviation's Aero-Space Laboratories (ASL) in Downey, California, serves as WSRN headquarters. ASL was established to conduct fundamental research in sciences related to flight within and beyond the Earth's atmosphere. As a natural consequence of its background and interests, ASL undertook sponsorship of WSRN activities on a limited basis. ASL coordinates the activities of the network and keeps teams supplied with individual station predictions for most of the visible satellites.

The predictions are based on current elements received from SAO or Space Track or derived by someone in the network. WSRN also generates its own elements for searches and other special projects. At ASL, the elements are coded for the computer and run in one of several prediction programs. Figure 2 illustrates a typical individual station prediction set that is sent to all WSRN teams. Information appearing at the beginning of the prediction set includes station and satellite identification, coded orbital parameters, and program control indicators. In Fig. 2, it is noted that the following information is given for each satellite transit over a given station: year day, transit time, angular altitude above the horizon, azimuth, height, slant range, right ascension, declination, height of the Earth's shadow, revolutions since epoch, and geocentric latitude of the subsatellite point. Depending upon the satellite's orbit, a meridian transit program and/or a culmination transit program may be used. These two programs compute the position of a given satellite as it crosses the observer's meridian and as it reaches a point near greatest angular altitude above the observer's horizon, respectively.

The polar satellites presented an interesting problem whose solution illustrated the need for up-to-date prediction schemes. It was immediately recognized that these high-inclination satellites seldom transited through a given station's meridian within view of the station. The culmination transit program, thought to be ideal for this situation, proved unsatisfactory because these satellites occasionally come into visibility above the horizon and then go into the Earth's shadow before reaching culmination. The solution adopted for this particular problem is a special latitude transit program developed to output a satellite's coordinates as it crosses a designated latitude. Thus, if a high-inclination satellite is known to be entering the shadow at 50 deg north latitude on its north–south transits, the program is scheduled to output the satellite's position as it crosses latitude 55 deg north. Thus, the teams are able to observe it just before it enters the shadow.

ASL's prediction programs are unique in that they also provide differential corrections upon the elements for each individual prediction. The two short lines following each full line in Fig. 2 have been termed differential corrections upon the standard elements. They represent the position of a satellite in a slightly different orbit leading or lagging the standard by a few minutes. Using these predictions, one can construct a graph indicating the angular altitude of the orbit's intersection with the meridian plane as a function of time. Thus, an observer can continuously point his instrument at the orbit, allowing observation of the satellite whether it is early, on schedule, or late.

In general, the differential corrections are computed to give positions for satellites running 5 minutes early or late. If an observer knows that the particular satellite is about 5 minutes ahead of the prediction, he sets to the corrected position and watches the satellite sail through the center of his field. The corrections can also be interpolated to cover almost all satellites not running right on the predictions. This method is especially powerful for observing a close satellite for which the Earth's rotation introduces considerable time-dependent parallax. The position of such a satellite's orbit may move several deg per minute, so that one observer with a small-field instrument will see an early or late satellite only if he is able to follow the orbit's movement in the sky.

Differential corrections are particularly useful to WSRN because member teams know exactly how the satellites are running with respect to predictions and can make the necessary adjustments. Each week the teams call ASL to report their observations and corresponding residuals with respect to the current set of predictions. The residuals are distributed to WSRN teams in a weekly newsletter that also contains other information pertinent to

```
 CHINA LAKE   GEOD.LONGITUDE=117.66300W  GEOD LATITUDE=35.65700N  GEOC.RADIUS=3959.1 MI.

---WESTERN SATELLITE RESEARCH NETWORK PREDICTIONS BY AERO-SPACE LABORATORIES  M.A.D.---

  1958 BETA ONE  SAO ELEMENTS OF 9 MAR 1960                    58021G07X

    31.00000      5508.64       -0.001  0.20678999-0.000002623     34.2590
 0.                 -0.              -1.57291773E-09   9.61415040E-02   3.10870609E 01
-0.                 -0.               1.76999998E-06   1.04013349E 01  -2.05549991E-01
-0.                 -0.              -5.02999991E-06  -2.84299999E 00   1.08229995E 01
-0.                 -0.               7.34999996E-06   4.15599996E 00   8.61929989E 01
 -1.    -1.    -1.     0.     84.00     90.00  83.44975  83.55513       0.          0.
  1.     1.     1.    -1.     1.    0.02083

     TRANSIT TIME     ALTITUDE  AZIMUTH  REF.HT.  SL.RANGE  RT.ASCEN.   DEC.   SHAD.HT.    REV.   GC.SLAT.
YEAR DAY   H  M   S   (DEG.)    (DEG.)  (ST.MI.)  (ST.MI.)   H  M      (DEG.)  (ST.MI.)    NO.     (DEG.)

 DO NOT FORGET TO CALL IN YOUR OBSERVATIONS...  SIGNED 709

MERIDIAN TRANSIT PREDICTIONS

 85.32024 12.29. 8.3  43.64    180.00   1301.45   1676.08  16. 0.42  -10.70    241.  566.18294  22.18
 85.32406 12.34.39.0  45.82    180.00                                              566.18664
 85.31641 12.23.38.0  41.48    180.00                                              566.17929

 86.47775 11.27.57.7  23.77    180.00   1010.90   1800.10  15.52.87  -30.58    857.  576.14258  16.14
 86.48156 11.33.27.1  25.83    180.00                                              576.14612
 86.47394 11.22.28.8  21.78    180.00                                              576.13909

 87.54084 12.58.48.7  63.60    180.00   1428.43   1543.89  17.27.93    9.26     79.  587.20033  26.20
 87.54465 13. 4.17.8  65.34    180.00                                              587.20384
 87.53704 12.53.20.0  61.82    180.00                                              587.19688

 88.49846 11.57.46.8  44.92    180.00   1142.13   1463.18  16.30.77   -9.42    425.  597.16103  23.79
 88.50226 12. 3.14.9  47.15    180.00                                              597.16441
 88.49467 11.52.19.2  42.70    180.00                                              597.15771

 JOB STATUS            4.       1.        1.        0.
```

Fig. 2. Set of WSNR satellite predictions (1958 β1 for China Lake Moonwatch Station)

network operations. Figure 3 is the 28 March 1960 newsletter. It lists the satellite, year and day of observation, time residual (R_t), and altitude number. For observations made from ASL's predictions, the element number listed in the newsletter is the last three digits of the identification number following the satellite designation on the prediction sheets. For example, China Lake's two sightings of 1958 $\beta 1$ (on days 85 and 88) were made from the

NOTICE TO WSRN TEAMS
28 March 1960

The Network reported 29 observations this week. Satellite deviations f. the mean predictions are:

Satellite	Day	R_t	R_{Alt}	As	Station	Element
58 α	84	78^s late	.30°S	180	Ch. Lk.	011
	85	86^s late	.35°S	180	Ch. Lk.	011
	86	91^s late	.43°S	180	Ch. Lk.	011
58 $\beta 1$	85	8.1^s early	.13°S	180	Ch. Lk.	007
	88	8.2^s early	.12°S	180	Ch. Lk.	007
59 $\alpha 1$	88	5.5^s early	.23°S	180	Ch. Lk.	SAO 9 Mar.
59 $\epsilon 2$*	88	1^m late	-	-	Sac.	Spacetrack 7
59 η	85	9.2^m early	.29°N	180	Sac.	008
59 i 1	83	10^s early	.5°N	180	Spokane	009
	84	8^s early	.29°N	000	Ch. Lk.	009
	87	12^s early	.3°N	000	Rochester	009

1958 $\delta 2$ - The expected fall-in for Sputnik III is April 2. Sacramento and Albuquerque are still listening to its broadcasts. It is hoped that these teams will report $\delta 2$'s time residuals on their ham net as other teams, who have been listening in, would like to know how it's running. Art Leonard indicates that the satellite is currently running very close to Spacetrack's predictions. More about this later this week in a special bulletin from Mr. Leonard.

*1959 $\epsilon 2$ - The northern teams in the Network ought to have some fun with this one. Art Leonard gives us the following facts: He has been following the satellite for two and three passes per night and expects to do so for several more weeks. The satellite should remain visible to us for about 2 months, and it's disappearing into the shadow at about 45°N on NS transits. He also indicates that Spacetrack's node is about 0.4° East of the satellite's actual node.

Gary ran culmination predictions for 59 $\epsilon 2$, and they all came out in the shadow. So we'll run it on a latitude transit program and have them out later this week.

WESTERN SATELLITE RESEARCH NETWORK

Fig. 3. WSNR Weekly Newsletter

predictions shown in Fig. 2. The newsletter lists element number 007 which corresponds with the identification number 58021007X found at the end of the third line of print on the prediction sheet. In some cases the newsletter lists the number of the SAO or Space Track bulletin from which the team calculated its own prediction. The residuals are especially appreciated by the Moonwatch teams in the northern latitudes. Knowing the exact time of a satellite's transit greatly reduces the amount of time the observers must wait hip-deep in snow at subzero temperatures.

The differential correction technique is also very useful for generating search ephemerides. Predictions are made from an orbit and differential corrections applied at intervals of about plus and minus 20, 40, and 60 minutes. These predictions give the orbit's position in the sky for a period of about two hours, as is illustrated in Fig. 4. The team then constructs a tracking schedule by plotting the data as shown in Fig. 5. This schedule is used to keep telescopes continuously bracketing the orbit's position of intersection with the meridian. Thus, when the lost satellite finally crosses the observer's meridian, his telescope is in the proper position to make an observation. In this case the predictions shown are those used in the recovery of 1958 ϵ during June 1959. The position where the satellite finally appeared is shown (triangle). This very efficient method requires only a few observers and telescopes for complete coverage of a great number of suspected orbits.

Some WSRN teams communicate daily via a ham radio network which supplements the weekly bulletin by transmitting up-to-date residuals and other urgent information. This radio network has proved very helpful to WSRN teams, and it is envisioned that it will eventually be expanded to serve teams in other parts of the United States. It will probably operate at a fixed time each day with one team directing the communications in a manner similar to existing ham radio networks.

The WSRN holds semiannual conferences (usually hosted by one of the network teams) wherein teams get together for a weekend to iron out problems and plan for future cooperation. At these conferences recent studies are presented and discussed, and new researches are planned for the coming months. Teams receive instruction concerning new methods and techniques which are currently being developed. The conferences are very helpful in streamlining the network and help to maintain a high level of interest among the teams. Some of the topics presented at past conferences are: "A Multiple Eyepiece Telescope for Satellite Observing," Jack Borde, Walnut Creek; "Use of an Analog Shadow Height Computer," Carroll Evans, Jr., China Lake; and "An Analytical Method for Accurately Predicting the Lifetime of Artificial Satellites," Gary McCue, Whittier. Outside scientists are also invited to participate in the conferences. At the last conference, Richard Davies, from Caltech's Jet Propulsion Laboratory, presented a talk entitled "The Search for Extraterrestrial Life," and Dr. David Bender of Aero-Space Laboratories discussed his recent studies in a talk entitled "The Earth's Shape and Its Effect on Satellite Orbits."

It should be clear by now that the Western Satellite Research Network is not comprised of conventional Moonwatch teams. A survey of the group's instrumentation is presented here to further this thesis. The Sacramento team has three permanently mounted telescopes: one 6-in., 68-power refractor and two 4-in., 40- and 53-power refractors. These instruments are mounted together with overlapping fields and form a vertical fan covering 2.9 deg. They may be moved in unison to different altitudes, but observations can be made only on the meridian. Sacramento also has ten apogee telescopes on portable mountings. The Whittier team currently uses a 12-in., F6 and an 8-in., F15 (reflecting telescope) to supplement four precision theodolite-mounted apogee telescopes. China Lake also uses apogee telescopes, three of which are mounted as precision theodolites. San Jose and Spokane use an 8-in. and a 6-in. reflecting telescope, respectively, as their deep penetration instruments. Walnut Creek uses several kinds of astronomical telescopes including a 10-in., F13 reflector. They also have six apogee telescopes to use on brighter satellites. Albuquerque (actually two teams) has one of the original Apogee Stations, so it is well equipped with apogee telescopes. Their telescopes, near-perfect seeing condition, and about 40 enthusiastic observers keep Albuquerque consistently near the top of the list of outstanding Moonwatch teams. Rochester, the network's newest addition, lists 23 observers and even more instruments ranging from three 12-in. and two 10-in. reflectors.

WSRN teams have found it absolutely necessary to use their high-power instruments to observe all but the brightest satellites. High power is important because it tends to enhance greatly the ratio of satellite brightness to field brightness. The importance of having a dark field when observing extremely faint satellites cannot be overemphasized. An observer with a small, low-power telescope can stare at the proper position night after night and miss the satellite simply because his instrument is incapable of penetrating "deep" enough. Several WSRN teams have

SACRAMENTO-E GEOD.LONGITUDE=121.7525W -GEOD.LATITUDE=38.549N GEOC.RADIUS=3958.14MI.

1958 EPSILON ART L. ELEMENTS OF JUNE 16.1959

JUN16.00000 =EPOCH

MON	DAY	TRANSIT TIME H M S	ALTITUDE (DEG.)	AZIMUTH (DEG.)	REF.HT. (ST.MI.)	SL.RANGE (ST.MI.)	RT.ASCEN. H M	DEC. (DEG.)	SHAD.HT. (ST.MI.)	REV. NO.	GC.SLAT. (DEG.)
JUN	26.	8.32.54.17	11.20	0.	254.68	858.95	6.40.79	62.66	167.	150.13033	50.08
	26.	8.43.20.07	11.93	0.							
	26.	8.58.58.59	13.30	0.							
	26.	9.19.51.55	15.78	0.							
	26.	8.22.35.72	10.62	0.							
	26.	8. 6.53.61	9.96	0.							
	26.	7.46. 3.80	9.46	0.							
JUN	26.	10.16.23.05	30.17	0.	330.22	592.79	8.24.55	81.62	148.	151.17677	45.40
	26.	10.26.56.46	35.09	0.							
	26.	10.42.46.48	43.13	0.							
	26.	11. 3.58.31	66.09	0.							
	26.	10. 5.54.67	26.29	0.							
	26.	9.50.11.11	21.79	0.							
	26.	9.29.14.14	17.49	0.							
JUN	27.	5.51.54.25	13.53	0.	176.12	580.02	4. 3.29	64.98	114.	163.06321	46.38
	27.	6. 2.21.93	12.18	0.							
	27.	6.18. 2.48	10.73	0.							
	27.	6.38.55.04	9.52	0.							
	27.	5.41.26.44	15.30	0.							
	27.	5.25.43.42	19.21	0.							
	27.	5. 4.41.26	29.44	0.							

Fig. 4. Search ephemerides used for recovery of 1958 ε *(Explorer IV)*

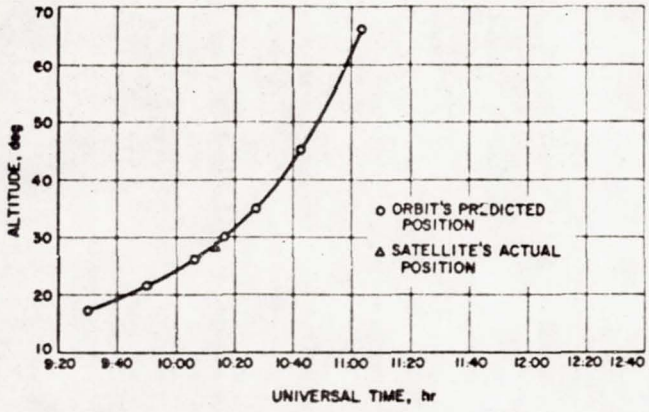

Fig. 5. Orbit tracking schedule used for recovery of 1958 ε *(Explorer IV)*

observed the "grapefruit," 1958 $\beta 2$. Observing small satellites at ranges of 2500 miles is routine with high-power instruments. To date the network's record is *Vanguard III*, 1959 η, tracked at over 3000 miles!

The observations are of consistent accuracy. Stopwatches, started as the satellite transits a cross-hair in the observer's field of view and stopped on WWV time signals, give a satellite's transit time to the nearest 1/10 second. Positions are measured to a few hundredths of a degree either with a precision theodolite or against a detailed star background. WSRN teams continually strive to maintain the best accuracy possible because if Moonwatch observations are to be useful to future work, consistent accuracy is an absolute necessity..

IV. ACHIEVEMENTS OF WSRN

What has been accomplished by the Western Satellite Research Network? With respect to quantity and quality of satellite observations, the results are outstanding. Figure 6 presents the results in graphical form. During the period from July 1959 to February 1960 the approximately 95 registered United States Moonwatch teams observed 1624 satellite transits. Of these 1624 transits, 879, or 54 percent, were contributed by the nine teams of the WSRN. A high was reached in the month of February 1960 when the network made 67 percent of the United States' Moonwatch observations. These statistics indicate that this small, unique group of Moonwatch teams, comprising about 9 percent of the nation's teams, is currently making well over one-half of the United States' Moonwatch observations.

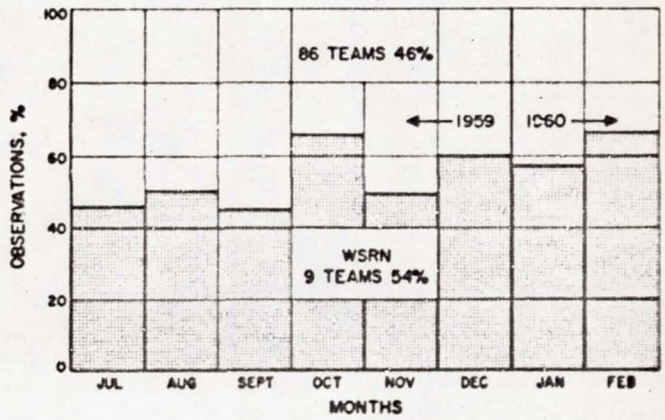

Fig. 6. Percentage of United States satellite transit observations made by WSRN

WSRN's accomplishments do not end with production of large numbers of high quality observations. One of the most challenging and rewarding feats in Moonwatch is the recovery of lost satellites. As a result of the persistent efforts of Arthur Leonard, the network has recovered three lost satellites. 1958 ϵ was acquired, lost and finally reacquired in June 1959. 1959 $\alpha 2$, the carrier rocket of *Vanguard II*, was finally recovered three weeks after launch, and 1958 $\beta 1$, the carrier rocket for *Vanguard I*, was recovered more than one year after it was lost at launch. Several important factors stand out as having been essential to the successful recovery of the satellites. Of course, the persistence of the teams involved in the searches was invaluable, but even more important was the use of up-to-date observing techniques, instrumentation, and computation schemes. One or two accurate observations quickly sent to the proper person (in these cases, Arthur Leonard) enabled the computation of revised orbital elements that were used to secure further observations. In the case of 1959 $\alpha 2$, two highly accurate observations (by Walnut Creek and Sacramento) were enough for Leonard to predict the satellite's next visible transit to within 3.8 seconds of time. A basic contribution to the success of the searches was the timely computation of predictions and search ephemerides using North American Aviation's computer, and the rapid distribution of this information to teams in the network.

The network plans to continue searching for lost satellites. Also under consideration as future research are techniques for refining a satellite's orbital elements to include some of the periodic effects of the pear-shaped Earth and atmospheric drag at high altitudes. Inclusion of these effects is expected to make it possible to predict, with a consistently high degree of accuracy, a satellite's position more than a month in advance.

V. CONCLUSION

WSRN has produced some outstanding and unusual results which have considerably augmented the nation's overall Moonwatch program. Several factors stand out as primary contributors to WSRN's success: Precise individual station predictions relieve the teams of much routine calculation, and make it possible for them to devote a maximum of time and effort toward development of the refined techniques and methods so necessary today. Also, more time is available for building the instrumentation necessary for acquiring faint satellites. Secondly, these teams were high quality teams from the start. They have been intensely interested in Moonwatch since its inception and are continually striving to further the project's objectives through their own efforts and through support of others interested in Moonwatch. A third contributing factor is that these teams are organized into an efficient network, and can benefit from a coordinated effort.

It is hoped that the network will soon be able to expand and extend its benefits to many other Moonwatch teams. Such an expansion would do much to further the nation's Moonwatch capabilities.

Differential Orbit Correct Experimentation with Satellites 1958 Alpha One and 1958 Epsilon[1]

L. G. WALTERS, G. B. WESTROM, C. T. VAN SANT,
R. H. GERSTEN, and G. L. MATLIN

Aeronutronic, a Division of Ford Motor Company,
Newport Beach, Calif.

ABSTRACT

A differential correction theory inclusive of special perturbations and based on variation of parameters has been developed for the determination of a geocentric orbit from observations. To achieve the utmost in computational efficiency and speed, the variant calculation procedure was discarded in favor of an analytic formulation of the differential expressions, relating observation residuals to parameter variations. The single ephemeris required for residual computation was numerically integrated by the variation-of-parameters method of special perturbations. The paper discusses the computational program and experimental results.

I. INTRODUCTION

A differential orbit correction procedure applicable to the low (including zero) to medium eccentricity geocentric satellite has been developed as a tool for the evaluation of earlier ephemerides produced for satellites 1958 $\delta 1$ and 1958 ϵ. This procedure accepts preliminary orbit parameters and topocentric observations of range or angle and yields the parameters of an improved orbit. The basic philosophy underlying this orbit correction procedure has been previously published.[2] For the application discussed here, two important departures were required, involving the extension of the differential formulae to (1) nonzero eccentricity and (2) topocentric observations of right ascension and declination or of altitude and azimuth.

[1]This research was sponsored by the Air Force Cambridge Research Center, C. R. D. (Space Surveillance System) under contract AF19(604)-5885.

[2]Walters, L. G., Van Sant, C. T., Enright, J. D., and Sashkin, L., "Differential Correct Experimentation with the Low-Eccentricity Geocentric Orbit," American Rocket Society Preprint 960-59. The proposal to employ differential correction with variation-of-parameters and the major part of the theoretical development are due to Samuel Herrick.

Differential orbit correction involves four steps:

1. Representation of the observations by an ephemeris computed from a preliminary set of orbit parameters.
2. Computation of observation residuals, or differences between observed quantities and their representation determined in (1) above.
3. Determination of differential cause and effect relationships between parameter variations (cause) and corresponding variations in the observed quantities (effect).
4. Solution for corrections to be applied to the preliminary orbit parameters by inversion of the system of equations assembled in steps (2) and (3), including least-squares reduction of overdetermination resulting from an excess of observations over orbit parameters to be corrected.

Each of these steps is discussed in the following paragraphs, followed by a discussion of the experimental results obtained from both simulated and actual observations.

II. EPHEMERIS COMPUTATION

The variation-of-parameters[3] method is employed for the ephemeris computation. This method is capable of high precision with outstanding efficiency and speed.[4] This efficiency is achieved by suppressing the dominant gravitation term in the Earth's potential by integrating parameters which, in the absence of perturbative effects, are constant. The familiar "elements" such as semimajor axis, eccentricity, time of perigee passage, etc., display this property as do the angular momentum and other derived parameters. Several patterns involving vector orbit parameters[5] were considered for this application.

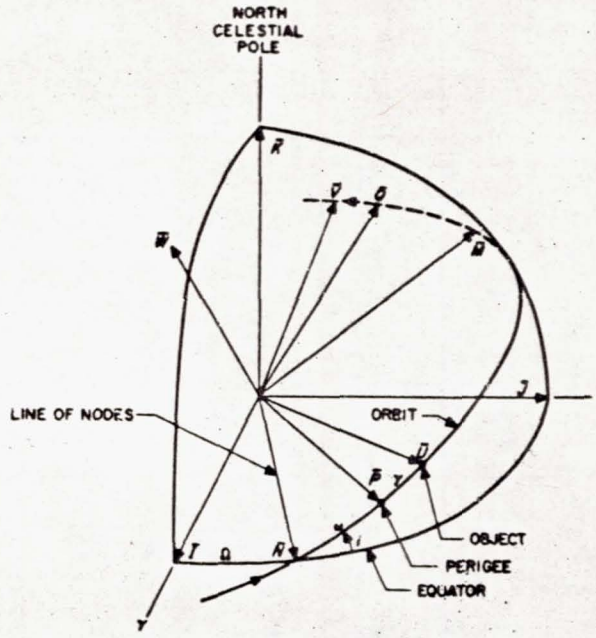

Fig. 1. Projection of orbit on celestial sphere, with orientation unit vectors and angles displayed

[3]An extensive discussion of the variation-of-parameters method will appear in the forthcoming book *Astrodynamics* by Samuel Herrick.

[4]A quantitative discussion of numerical orbit integration methods is published in a paper by Baker, Westrom, et al., "Efficient Precision Orbit Computation Techniques," American Rocket Society Preprint 869-59.

[5]The unit vectors P and Q lie in the orbit plane, at right angles to each other, with P directed to perigee and with $\mathbf{W} = \mathbf{P} \times \mathbf{Q}$ defining the sense of motion in the orbit (see Fig. 1). The quantities e and p denote the eccentricity and semilatus rectum of the osculating two-body orbit respectively.

A familiar pattern based upon the vectors $\mathbf{a} = e\mathbf{P}$ and $\mathbf{b} = e\sqrt{p}\,\mathbf{Q}$ deteriorates as the eccentricity approaches zero, whereas the formulation utilized in this orbit correction procedure and based upon $\mathbf{a}$ and $\mathbf{h} = \sqrt{p}\,\mathbf{W}$ remains valid.[6] In addition to the five quantities defined by $\mathbf{a}$ and $\mathbf{h}$ (their orthogonality implies that only five of the six components can be independently specified), the mean longitude L_e of the object at some epoch is also integrated. The mean longitude is the sum of the nodal longitude, argument of perigee and mean anomaly, and describes the mean position of the object along two spherical arcs on the celestial sphere. This seemingly unusual choice is made to preserve the identification of the object's mean position even for zero eccentricity and inclination. This variation-of-parameters procedure yields a satisfactory ephemeris for relatively-low-altitude satellites with integration intervals as large as 6 min.[7] The Adams–Bashforth numerical integration procedure is used to further enhance the computational efficiency of this ephemeris computation.

III. COMPUTATION OF OBSERVATION RESIDUALS

This step is trivial in concept, involving only the differencing of observed quantities from corresponding values determined by the ephemeris computation. Since the observations are taken at random, interpolation from this ephemeris is required; a four-point Everett's interpolation was utilized for this purpose.

IV. DETERMINATION OF DIFFERENTIAL RELATIONSHIPS

The determination of the differential relations relating observation residuals to parameter variations has been approached analytically rather than by variant calculation to further improve the computational efficiency of the procedure. Where the perturbations from two-body motion are small, as in the Earth satellite of modest lifetime, the analytic differentiation of two-body formulae gives a good approximation of the neighborhood properties of the actual orbit. The alternative variant calculation approach requires the integration of an additional ephemeris for each parameter undergoing correction, a substantial burden where as many as six parameters are corrected.

[6] The vector $\mathbf{h} = \sqrt{p}\,\mathbf{W}$ is the orbit angular momentum, and may be alternately defined by $\sqrt{\mu}\,\mathbf{h} = \mathbf{r} \times \dot{\mathbf{r}}$, where $\mathbf{r}$ and $\dot{\mathbf{r}}$ are the position and velocity of the object.

[7] The limitation on interval size was imposed by truncation error in the integration of drag and bulge perturbations, principally near perigee. Integration with respect to one of the anomalies will further improve the computational efficiency by providing more steps near perigee, less elsewhere.

The key to successful application of differential orbit correction is the selection of parameters which result in nearly linear differential expressions. The choice of eccentricity, for example, would lead to difficulty for nearly circular orbits, since by definition the eccentricity is nonnegative. Similar difficulty can be visualized with the perigee location, which becomes indeterminant for circular orbits. To avoid these pitfalls, the following choice of parameters was made:

a = semimajor axis

$a_{rN} = e\cos\omega$, $a_{tN} = e\sin\omega$ } where e and ω are the eccentricity and argument of perigee respectively

U_0 = mean argument of the object, measured from node

Ω = nodal longitude

i = inclination

The parameters a_{rN} and a_{tN} are components, along node and antinode directions, of the vector **a**, which is integrated in the ephemeris computation. The selection of parameters referred in this manner to the nodal direction, and of the nodal longitude itself, requires that the inclination be nonzero.*

In the derivation of the differential relationships, it is first necessary to relate the observation geometry to the selected parameters. This is accomplished with the aid of Fig. 2, which demonstrates the relationship of observer, geocenter, and object for topocentric observations. The observation $\boldsymbol{\rho}$, observatory location **R**, and object's position **r** are related by

$$\boldsymbol{\rho} = \mathbf{r} + \mathbf{R} = r\mathbf{U} + \mathbf{R} \tag{1}$$

where **U** is a unit vector directed along **r**, as shown in Fig. 1. Differentiation leads to

$$\Delta\boldsymbol{\rho} = \mathbf{U}\Delta r + r\Delta\mathbf{U} + \Delta\mathbf{R} \tag{2}$$

For the present analysis, the observatory location is assumed well known, i.e., $\Delta\mathbf{R}$ is assumed zero. The term Δr can be related to those parameters which describe the motion in the orbit plane, i.e., a, a_{rN}, a_{tN}, and U_0. This analysis is tedious, and only the results will be reported, in the following form:

$$\Delta r = R_u\,\Delta U_0 + R_a\frac{\Delta a}{a} + R_{rN}\,\Delta a_{rN} + R_{tN}\,\Delta a_{tN} \tag{3}$$

*This procedure behaves well even at inclination as low as 1 deg. An alternative procedure tailored to orbits of all inclination has been developed to consider equatorial satellites.

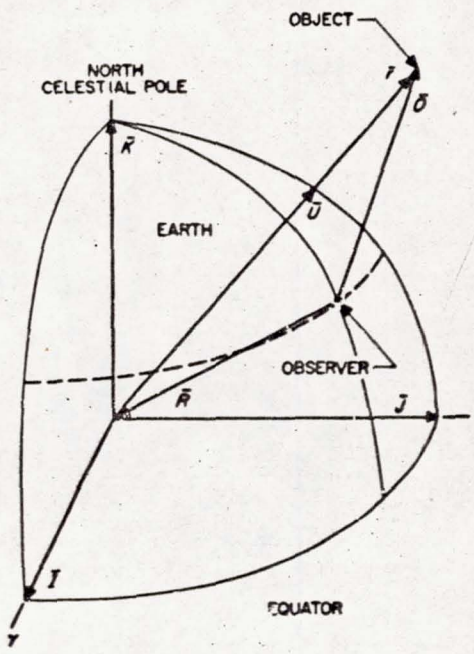

Fig. 2. Observational framework

This relationship was developed by differentiating the equations for the ellipse. Four coefficients, denoted by the R's, evolve in this development; these are:

$$R_u = \frac{a^2}{r}e\sin E \tag{4a}$$

$$R_a = r - \frac{3}{2}(U - U_0)R_u \tag{4b}$$

$$R_{rN} = \frac{a^2}{r}[a_{rN} - \cos(E+\omega)] \tag{4c}$$

$$R_{tN} = \frac{a^2}{r}[a_{tN} - \sin(E+\omega)] \tag{4d}$$

In these expressions, E denotes the eccentric anomaly; other terms have been defined.

The remaining ΔU term involves those parameters defining orbit-plane orientation as well as the object's position in its plane. Referring angles to node, a procedure which preserves the orientation even when perigee is indeterminate, the vector **U** and its derivative follow:

$$\mathbf{U} = \mathbf{N}\cos u + \mathbf{M}\sin u \tag{5}$$

$$\Delta\mathbf{U} = \Delta\mathbf{N}\cos u + \Delta\mathbf{M}\sin u + \Delta u\,(\mathbf{M}\cos u - \mathbf{N}\sin u) \tag{6}$$

Reference to Fig. 1 will clarify this usage; in particular the angle u, the "argument of the latitude," is the sum of

two angles, the argument of perigee ω and the true anomaly v. M and N can be expressed in terms of Ω and i; their derivatives are:

$$\Delta N = M\,\Delta\Omega\cos i - W\,\Delta\Omega\sin i \tag{7a}$$

$$\Delta M = -N\,\Delta\Omega\cos i + W\,\Delta i \tag{7b}$$

The final step involves an expression for Δu. This is derived in two parts, involving $\Delta\omega$ and Δv, and added to give the form:

$$r\Delta u = U_u\,\Delta U_0 + U_a\frac{\Delta a}{a} + U_{rN}\,\Delta a_{rN} + U_{vN}\,\Delta a_{vN} \tag{8}$$

The four partial derivatives, the U's, assume the form given in Eq. 9a through 9d:

$$U_u = \frac{a^2}{r}\sqrt{1-e^2} \tag{9a}$$

$$U_a = -\frac{3}{2}(U - U_0)\,U_u \tag{9b}$$

$$U_{rN} = \frac{a^2}{r}\left[\left(1+\frac{r}{a}\right)\sin(E+\omega) + a_{rN}\,e\sin E\,\frac{e^2-(1+\sqrt{1-e^2})\,e\cos E}{\sqrt{1-e^2}\,(1+\sqrt{1-e^2})} - \frac{a_{vN}}{1+\sqrt{1-e^2}}\right] \tag{9c}$$

$$U_{vN} = \frac{a^2}{r}\left[-\left(1+\frac{r}{a}\right)\cos(E+\omega) + a_{vN}\,e\sin E\,\frac{e^2-(1+\sqrt{1-e^2})\,e\cos E}{\sqrt{1-e^2}\,(1+\sqrt{1-e^2})} + \frac{a_{rN}}{1+\sqrt{1-e^2}}\right] \tag{9d}$$

Special care has been taken to arrange terms so that no computational singularities are encountered for small eccentricity. For example, all terms involving trigonometric functions of either the anomalies or perigee location can be arranged with coefficients of e. The dominant term for low and zero eccentricity involves the well-defined angle $E + \omega$. Thus no computational hazards are encountered for any eccentricity below, say, 0.9, including zero. These expressions complete the description of $\Delta\rho$ in terms of the selected orbit parameters.

The description of $\Delta\rho$ in terms of observation residuals requires a description of the observer's geometry. For topocentric right ascension α and declination δ measurements, the unit vector triad **L**, **A**, and **D** defined in Table 1 describes the observation geometrically.

Table 1. Components of L, A, D in equatorial-equinox system (see Fig. 1)

x—component	y—component	z—component
L $\cos\delta\sin\alpha$	$\cos\delta\cos\alpha$	$\sin\delta$
A $-\sin\alpha$	$\cos\alpha$	0
D $-\sin\delta\cos\alpha$	$-\sin\delta\sin\alpha$	$\cos\delta$

Differentiation of the expression $\rho = \rho\mathbf{L}$, and substitution of components of **A** and **D**, where possible, leads to the form:

$$\Delta\rho = \mathbf{L}\,\Delta\rho + \mathbf{A}\,\rho\cos\delta\,\Delta\alpha + \mathbf{D}\,\rho\Delta\delta \tag{10}$$

This completes the description of the differential relationships between orbit parameter and observation. By forming dot products of Eq. (2) and (10) with **L**, **A**, and **D**, direct linear relationships appear between the observation residuals and the selected orbital parameters. The orbit quantities appearing in these equations are defined from the ephemeris computation.

This development has been restricted to topocentric angle and range observations. Where other observed quantities are involved, such as range rate or altazimuth measurements, similar considerations will yield the desired differential relations.

V. SOLUTION FOR PARAMETER CORRECTIONS

The final step in the differential correction procedure involves identification of observation residuals with appropriate coefficients in the linear correction equation. As the number of observed quantities exceeds the number of parameters being corrected, a least squares procedure is used to weight the results statistically. The final matrix inversion procedure determines the solution to the system of linear correction equations; this solution is a set of corrections to be applied to the parameters used for the preliminary orbit correction. In addition the root-mean-square value of the residuals is calculated; this quantity is indicative of the quality of the observations and of the resulting orbit, as will be demonstrated in subsequent experimentation.

VI. EXPERIMENTATION WITH SIMULATED OBSERVATIONS

Prior to attempting an orbit correction based upon actual data observed under field conditions, simulated observations generated with an ephemeris program were employed. This procedure affords the following advantages:

1. Greater flexibility in the choice of observation pattern is available.
2. The quality of the observations can be controlled.
3. Since the parameters utilized in generating the observations are known, a means of assessing the mode of convergence and intrinsic error in the determination is available.

Illustrative of the value of simulated experimentation in gaining confidence in the behavior of a correction program is the example discussed here. An ephemeris for an object in an orbit similar to that of 1958 δ 1 was integrated and observations simulated for several stations which were capable of "seeing" the object. These observations and a new set of parameters were entered into the correction program; the new parameters were modified from those used to generate the observations by amounts leading to rms residuals of approximately 280 miles. Several iterations of the correction procedure followed, and at each step the rms value of the residuals, given by

$$\left[\frac{\sum(\rho\Delta\alpha\cos\delta)^2+\sum(\rho\Delta\delta)^2}{n}\right]^{\frac{1}{2}}$$

was calculated. These values, tabulated in Table 2 below, converge slowly at first, then dramatically as the residuals become small and the linear relationships employed for the correction equations become more valid.

Table 2. RMS residuals

Iteration	Earth radii	Miles (approx.)
1	0.082,410,894	284
2	0.013,880,485	48
3	0.000,636,049	2
4	0.000,006,293	0.02

In practice, this convergence in the residuals would be limited by the quality of the data employed as well as the ability of the ephemeris program to represent and integrate the gravitational and nongravitational environment. The stationary value approached by the residuals is indicative of the quality of the orbit determination. As long as the residuals continue to diminish, the orbit analyst is wise to continue the iterative determination process.

Since the orbit analyst has, in this simulated exercise, knowledge of the parameters which generated his observations, the *means* by which convergence took place in each parameter (if at all) can be studied for various distributions of observation data. He is privileged to observe, for example, how observations taken only near the antinode fail to determine the nodal longitude precisely, even though a good ephemeris in the vicinity of the antinodes is obtained. Observations near the antinodes, for example, fail to distinguish between cause and effect due to, say, nodal longitude and argument of the object measured from the node, if these parameters are corrected, whereas their sum is well determined. Considerable tradeoff in the poorly determined parameters is possible when the distribution of observations is poorly "conditioned," or, in other words, incapable of distinguishing between cause and effect between two or more parameters. This situation leads to a nearly-zero matrix in the process of inverting the correction equations, and the whole determination process may often diverge.

VII. EXPERIMENTATION BASED UPON DATA FOR 1958 DELTA ONE

Satellite 1958 δ1 was the rocket case for one of the larger Russian satellites and, due to its size, readily observed. Voluminous observation data are available from almost every conceivable source. While much good data are available, the observation opportunities offered the casual observer led to the inclusion of large amounts of data of dubious quality.

Beginning with all available data and a preliminary orbit roughly approximating the true orbit (say with rms residuals of 1000 miles or so) the residuals were examined before any correction was attempted. In this way, observations of the wrong satellite or observations from a station whose location was incorrectly transmitted or whose timing or observation was in error could be discarded. This process was repeated later in the correction process to delete observations leading to excessive residuals. The orbit determined from available data for 1958 δ1, screened in this manner from the abundant supply, led typically to an rms residual of approximately 6 miles.

An unusual opportunity to experiment with 6-parameter differential correction from data obtained at a single station (Pic Midi, France) over a short interval (13 min, day 199) was available. These observations were recorded at very short intervals; for experimentation purposes, 29 were selected at random and processed. Residuals were reduced to the order of 5 miles in this process, without triggering instability anticipated from such a short span of observations.

VIII. EXPERIMENTATION BASED UPON DATA FOR 1958 EPSILON

In contrast to the large mass of data available on 1958 δ1, the small size of 1958 ε restricted its observation to the serious observer, and only a few observations of uniformly good quality were available. 1959 day 127 was typical; only thirteen observations over a period of 504 minutes were reported. Beginning with a preliminary orbit where root-mean-square residuals were approximately 1400 miles, it was possible to reduce these to 5 miles by successive application of the differential correction procedure.

IX. SUMMARY

This paper describes the research and experimentation undertaken at Aeronutronic with a differential correction procedure designed for satellite orbit determination. The experimentation included, in addition to the activities discussed above, an extensive evaluation of truncation error in the numerical integration of the ephemeris as well as the description of drag perturbations on these objects. Since the computational procedures were discharged on International Business Machines 650 equipment, every effort to achieve high computational efficiency was required. The combination of analytical expressions for differential correction with a variation-of-parameters ephemeris program is established as a very powerful tool for differential orbit correction.

Lunar Vehicle Orbit Determination[1]

C. TROSS

Aeronutronic, a Division of Ford Motor Co.
Newport Beach, Calif.

ABSTRACT

A highly efficient special perturbation procedure for lunar vehicle ephemeris prediction is developed. The basic method employed is the procedure known to astronomers as Encke's method. With this procedure it is possible to calculate the ephemeris for a ballistic Earth–Moon trajectory with only 15 integration steps, yet maintaining precision everywhere along the orbit to within ½ mile while considering all pertinent perturbation effects such as terrestrial bulge, Sun and Moon attraction, and atmosphere drag. By increasing the number of integration steps this procedure can yield accurate ephemerides to virtually any degree providing a sufficient number of digits are carried in the calculation.

I. INTRODUCTION

Orbit determination techniques for satellite, lunar, and interplanetary vehicles have received much consideration, especially in recent months. Perhaps the most frequently employed method whereby such orbits are determined is a procedure generally known as Cowell's method. This is a method through which the equations of motion, Section II, are integrated directly to obtain total velocity and position at any epoch. Although this procedure yields adequate results, it is very costly in computer time requirements. In seeking another procedure which is less demanding of computer time and one with which higher precision over a very long ephemeris can be attained, a procedure known to astronomers as Encke's method, Section III, was precipitated. Further pursuit indicated that Encke's method is very well suited for lunar vehicle orbit determinations With Encke's method the user may incorporate all desired and significant perturbations. For example, an Encke method which considers the solar, lunar, and terrestrial perturbations can determine a 3-day lunar trajectory with only 15 integration steps, so that the error at impact on the lunar surface is less than ½ mile[2]. In contrast, the same calculation with Cowell's method

[1]This work was supported in part by the United States Air Force under Contract AF33(616)-6005.

[2]By increasing the number of integration steps this procedure can yield accurate ephemerides to virtually any precision, providing that a sufficient number of digits are carried in the calculation. For example, a 3-day ephemeris has been calculated with errors less than 100 ft at impact, yet only 50 integration steps were required.

required 190 integration steps. Encke's superiority over Cowell's method is thus clearly demonstrated. This method achieves its speed by calculating only departures from a two-body orbit. In a moderately perturbed medium such as that which a lunar vehicle is exposed to during the major portion of its flight, the true orbit resembles a two-body orbit rather closely. Only as a vehicle approaches the immediate proximity of the Moon do perturbations become large so that the departures from a two-body orbit increase. It has been found (Ref. 1) that on the Moon's surface the true orbit deviates from a two-body orbit by ½ and 2 g-radii for vehicles whose transit times are 1 and 4 days, respectively.

In this paper Encke's method is developed and the overall problem of lunar vehicle orbit determination is discussed.

II. EQUATIONS OF MOTION

A. The Basic Equations

The motion of a small particle or space vehicle near a large celestial body can be approximated by the two-body equations of motion which, in an inertial frame of reference, can be written in component form as:

$$\ddot{x} = -m\frac{x}{r^3} \qquad (x \to y, z) \tag{1}$$

The two-body equations of motion can be solved in closed form and therefore are frequently employed in feasibility studies. Unfortunately, a two-body representation of a vehicle's motion within close proximity to the Earth ignores such effects as the Earth's bulge and lunar, solar, and planetary attractions. For high-precision work some or all of these perturbative forces must be considered, so that these effects must be incorporated into the equations of motion.

The complete form of the equations of motion for a vehicle in close proximity to the Earth can be written as follows:

$$\ddot{x}_{1,e} = -m_1\frac{x_{1,e}}{r_{1,e}^3} + \sum_{i=2}^{n} m_i\left(\frac{x_{i,1}}{r_{i,1}^3} - \frac{x_{i,e}}{r_{i,e}^3}\right)$$
$$- J'm_1\frac{x_{1,e}}{r_{1,e}^5}(1 - 5U_z'^2) - H'm_1\frac{x_{1,e}z_{1,e}}{r_{1,e}^7}(3 - 7U_z'^2)$$
$$- K'm_1\frac{x_{1,e}}{6r_{1,e}^7}(3 - 42U_z'^2 + 63U_z'^4) + \frac{\partial\phi_2}{\partial x'}\frac{\partial x'}{\partial x} + \cdots \tag{2a}$$

$$\ddot{y}_{1,e} = -m_1\frac{y_{1,e}}{r_{1,e}^3} + \sum_{i=2}^{n} m_i\left(\frac{y_{i,1}}{r_{i,1}^3} - \frac{y_{i,e}}{r_{i,e}^3}\right)$$
$$- J'm_1\frac{y_{1,e}}{r_{1,e}^5}(1 - 5U_z'^2) - H'm_1\frac{y_{1,e}z_{1,e}}{r_{1,e}^7}(3 - 7U_z'^2)$$
$$- K'm_1\frac{y_{1,e}}{6r_{1,e}^7}(3 - 42U_z'^2 + 63U_z'^4) + \frac{\partial\phi_2}{\partial y'}\frac{\partial y'}{\partial y} + \cdots \tag{2b}$$

$$\ddot{z}_{1,e} = -m_1\frac{z_{1,e}}{r_{1,e}^3} + \sum_{i=2}^{n} m_i\left(\frac{z_{i,1}}{r_{i,1}^3} - \frac{z_{i,e}}{r_{i,e}^3}\right)$$
$$- Jm_1\frac{z_{1,e}}{r_{1,e}^5}(3 - 5U_z'^2) + H'm_1\frac{3}{5r_{1,e}^5}\left(1 - 10U_z'^2 + \frac{35}{3}U_z'^4\right)$$
$$- K'm_1\frac{z_{1,e}}{6r_{1,e}^7}(15 - 70U_z'^2 + 63U_z'^4) + \frac{\partial\phi_2}{\partial z'}\frac{\partial z'}{\partial z} + \cdots \tag{2c}$$

where

- x_{ij} distance from body i to body j along x axis $(x \to y, z)$
- r_{ij} $\sqrt{x_{ij}^2 + y_{ij}^2 + z_{ij}^2}$
- m_i mass of body i
- J' coefficient of the second harmonic in the Earth's gravitational potential
- H' coefficient of the third harmonic in the Earth's gravitational potential
- K' coefficient of the fourth harmonic in the Earth's gravitational potential
- U_z' z/r or $\sin\delta$, where δ is the geocentric declination of the object
- $\partial\phi_2/\partial x'$ second lunar harmonic (bulge) term $(x' \to y', z')$

and subscripts refer to the indicated bodies:

0 vehicle
1 Earth
2 Moon
3 Sun
4 to n other perturbative bodies such as planets

The first term in Eqs. (2), i.e.,

$$m_1 \frac{x_{1,0}}{r_{1,0}^3}$$

and the corresponding terms in y and z describe the two-body motion of a vehicle whose mass is negligible, moving under the influence of the Earth's gravitational field only.

The second term, which involves

$$\sum_{i=2}^{n}$$

is a sum of the planetary, solar, and lunar perturbations.

The third, fourth, and fifth terms, i.e., those involving J', H', and K', are the perturbations due to the Earth's bulge.

B. The Lunar Bulge Effects

The last term is the second-order bulge harmonic of the Moon. Although these terms are quite small, they have an effect on lunar vehicles when the Moon is approached and should, therefore, receive consideration. If triaxial symmetry is assumed, then the accelerations of a point in space referred to a selenocentric coordinate system whose z' axis is along the rotational axis of the Moon and whose x' and y' axes lie in the plane of the Moon's equator, the x' axis being directed toward the Moon's prime meridian and the y' axis completing the right-hand coordinate system, take the form:

$$\frac{\partial \phi_2}{\partial x'} = \frac{-3}{2r_{2,0}^4}(U'_{x'}, C)\left[\frac{C-A}{C}(1-5U_{x'}'^2)+\frac{B-A}{C}(1-5U_{y'}'^2)\right]$$

$$\frac{\partial \phi_2}{\partial y'} = \frac{-3}{2r_{2,0}^4}(U'_{y'}, C)\left[\frac{C-A}{C}(1-5U_{x'}'^2)+\frac{B-A}{C}(3-5U_{y'}'^2)\right]$$

$$\frac{\partial \phi_2}{\partial z'} = \frac{-3}{2r_{2,0}^4}(U'_{z'}, C)\left[\frac{C-A}{C}(3-5U_{x'}'^2)+\frac{B-A}{C}(1-5U_{y'}'^2)\right]$$

where

A moment of inertia about the x' axis
B moment of inertia about the y' axis
C moment of inertia about the z' axis

and $U'_{x'}$, $U'_{y'}$, and $U'_{z'}$ are the direction cosines of the radius vector to the point in space referred to the lunar equatorial coordinate system. It is possible to transform this selenocentric system to a terrestrial system by a suitable rotation matrix.

Experimentally determined values (Ref. 2) for the ratios of the moments of inertia are:

$$\frac{C-A}{C} = 0.6296 \times 10^{-3} \pm 2.7 \times 10^{-6}$$

$$\frac{B-A}{C} = 0.2081 \times 10^{-3} \pm 9.0 \times 10^{-7}$$

These values of the ratios of the moments of inertia yield an upper bound to the size of the bulge perturbations close to the surface of the Moon. The acceleration is less than 1.3×10^{-5} Earth g at the Moon's surface.

C. Perturbation Effects

A convenient frame of reference for lunar vehicles has been found to be a geocentric equatorial system in which the x-axis is directed towards the vernal equinox, the z-axis is directed towards the Earth's North Pole, and the y-axis lies in the Earth's equator plane and completes the right-hand coordinate system.

In Section IV of this paper methods for the numerical evaluation of Eqs. (2) will be considered, but before doing so it will be of interest to analyze the perturbative effects that various members of the solar system have upon a lunar vehicle.

The second term in Eqs. (2), as was stated above, is a sum of planetary, solar, and lunar perturbations. Maximum values for the differential accelerations of some of the more important bodies have been determined (Table 1) by considering the following simplified configuration for the planets: Jupiter, Mars, and the Moon

Table 1. Solar system and terrestrial perturbations on lunar vehicles

Perturbing object	Acceleration relative to the geocenter in Earth g		
	At Earth	At 32 radii	At Moon (64 radii)
Earth	1.0	0.1×10^{-3}	0.2×10^{-3}
Second terrestrial harmonic	0.6×10^{-3}	0.6×10^{-7}	0.4×10^{-8}
Fourth terrestrial harmonic	0.7×10^{-4}	0.7×10^{-12}	0.1×10^{-4}
Moon	—	0.1×10^{-4}	0.16
Sun	—	0.16×10^{-8}	0.33×10^{-8}
Venus	—	0.15×10^{-8}	0.30×10^{-8}
Mars	—	0.25×10^{-11}	0.5×10^{-11}
Jupiter	—	0.2×10^{-10}	0.4×10^{-10}
Centrifugal force due to precession	—	—	0.3×10^{-4}

are assumed to be located at opposition and Venus is assumed to be located at inferior conjunction. The distance from any planet to Earth is then easily determined by the appropriate subtraction or addition of its mean distance from the Sun and the Earth's mean distance. From Table 1 it will be observed that planetary perturbations are so small that they may well be ignored even in very high precision lunar trajectory determinations.

The next three terms are the second, third, and fourth-order harmonics of the bulge of the Earth which are functions of J', H', K' and r; the coefficients are related to the DeSitter constants for which the following numerical values are adopted:

$$J' = 1623.41 \times 10^{-6}$$
$$H' = 6.04 \times 10^{-6}$$
$$K' = 6.37 \times 10^{-6}$$

Table 2 gives maximum acceleration caused by the three terrestrial harmonics as functions of r. From this table it is seen that the bulge harmonics of the second order would perhaps have to be carried through the entire calculation for a precision orbit, whereas the fourth-order harmonic quickly becomes negligible after the vehicle is 8 Earth radii away from the geocenter and the third harmonic after 16 Earth radii.

Since the equations of motion as written apply to a nonrotating system of axes, the question of the axes rotating slowly due to precession and nutation is next considered. The coordinate system is tied to the vernal equinox, which moves about 50″ per year due to precession. The centrifugal acceleration at the distance of the Moon (approximately 64 Earth radii) is then about 1.4×10^{-17} radii/min^2 (see Table 1).

The maximum Coriolis force due to precession at the surface of the Earth with a velocity of 7 miles per second amounts to 5×10^{-13} g.

Reference 3 gives positions of the Sun referred to the mean equinox of 1950.0. However, the vernal equinox will have rotated about 500″ in 10 years. The precessional displacement for the Sun will be 2.4×10^{-5} times the perturbational terms of the Sun, which can be seen to be small. The nutational terms are of even a lesser order of magnitude and can be neglected. The largest of the short-period nutational terms gives rise to a maximum acceleration of 2×10^{-15} g. Thus, it can be concluded that no compromise in precision is encountered in assuming the reference frame to be inertial rather than rotating.

Table 2. Effect of terrestrial bulge for $V_z' = 1$

r, g-radii	$\frac{4J'}{r^3}$	$\frac{4H'}{r^3}$	$\frac{4K'}{r^3}$
1	6.493×10^{-3}	2.416×10^{-3}	3.616×10^{-3}
2	2.029×10^{-4}	7.550×10^{-5}	2.825×10^{-4}
4	6.341×10^{-6}	2.359×10^{-6}	2.207×10^{-5}
8	1.982×10^{-7}	7.373×10^{-8}	1.724×10^{-6}
16	9.908×10^{-9}	3.686×10^{-9}	2.155×10^{-7}
32	1.935×10^{-10}	7.200×10^{-11}	1.052×10^{-8}
64	6.048×10^{-12}	2.251×10^{-12}	8.221×10^{-10}

III. SPECIAL PERTURBATIONS

The equations of motion as presented in Section II may be integrated as they stand. Such a procedure is generally called Cowell's Method and is straightforward, but it is very demanding of computer time especially when the integration is to be advanced over a long time period. It is therefore desirable to search for procedures which will simplify and especially shorten the computational burden.

More than a century ago the German astronomer J. F. Encke developed a special perturbation procedure which is computationally very efficient. Encke developed his method for planetary orbit calculations, but it has been found to be especially well-suited for the orbit determination of bodies in a slightly perturbed medium such as that in which a lunar vehicle will find itself. Encke begins by noting that a celestial body in orbital motion deviates only slightly from two-body motion. Consequently, it would appear much more desirable to integrate the differential accelerations from a two-body orbit rather than the total acceleration as required in Cowell's method. In fact, it has been shown that for lunar vehicle orbit determination a total of 15 integration steps suffices for the complete trajectory determination, maintaining integrity in all parameters so that integration errors at lunar distance are less than ½ mile.

If this same problem were evaluated by direct integration, i.e., Cowell's method, 190 integration steps would be needed to obtain the same integrity.

A. Development of Encke's Method

When the central force field is known it is possible to determine a two-body orbit for a space vehicle from its position and velocity vectors. Thus, a two-body orbit which osculates with the true orbit can be determined. Let it be assumed that the true position vector $\mathbf{r}$ of the vehicle at time t is known. Furthermore, let it be assumed that a hypothetical vehicle travels along a two-body osculating orbit whose position vector corresponding to time t can be specified by $\mathbf{r}_e$. The difference in position between the vehicle on the actual orbit and the hypothetical vehicle on the osculating two-body orbit can be written as

$$\begin{cases} \xi = x - x_e \\ \eta = y - y_e \\ \zeta = z - z_e \end{cases} \tag{3}$$

The differential acceleration can be expressed by

$$\begin{cases} \ddot{\xi} = \ddot{x} - \ddot{x}_e = -\mu\left(\dfrac{x}{r^3} - \dfrac{x_e}{r_e^3}\right) + \ddot{\bar{x}} \\ \ddot{\eta} = \ddot{y} - \ddot{y}_e = -\mu\left(\dfrac{y}{r^3} - \dfrac{y_e}{r_e^3}\right) + \ddot{\bar{y}} \\ \ddot{\zeta} = \ddot{z} - \ddot{z}_e = -\mu\left(\dfrac{z}{r^3} - \dfrac{z_e}{r_e^3}\right) + \ddot{\bar{z}} \end{cases} \tag{4}$$

where $\ddot{\bar{x}}$ is the total perturbation component, such as acceleration due to the Earth's bulge, drag, thrust, and all accelerations due to bodies other than the central body upon which the osculating orbit is determined. Equations (4) may also be written as

$$\ddot{\xi} = \frac{\mu}{r_e^3}\left[x_e - (r_e/r)^3 x\right] + \ddot{\bar{x}}$$

or, introducing $x_e = x - \xi$, $(x \to y, z;\ \xi \to \eta, \zeta)$

$$\begin{cases} \ddot{\xi} = \dfrac{\mu}{r_e^3}\left\{\left[1 - r_e/r)^3\right] x - \xi\right\} + \ddot{\bar{x}} \\ \ddot{\eta} = \dfrac{\mu}{r_e^3}\left\{\left[1 - (r_e/r)^3\right] y - \eta\right\} + \ddot{\bar{y}} \\ \ddot{\zeta} = \dfrac{\mu}{r_e^3}\left\{\left[1 - (r_e/r)^3\right] z - \zeta\right\} + \ddot{\bar{z}} \end{cases} \tag{5}$$

If the true orbit follows the osculating orbit very closely, then r_e is very nearly equal to r and the quantity $1 - (r_e/r)^3$ approaches zero, whence significance is lost. This difficulty is overcome by expanding $1 - (r_e/r)^3$ in a series. Now:

$$\begin{aligned} r^2 &= x^2 + y^2 + z^2 \\ &= (x_e + \xi)^2 + (y_e + \eta)^2 + (z_e + \zeta)^2 \\ &= r_e^2 + 2\left[(x_e + \tfrac{1}{2}\xi)\,\xi + (y_e + \tfrac{1}{2}\eta)\,\eta + (z_e + \tfrac{1}{2}\zeta)\,\zeta\right] \end{aligned} \tag{6}$$

so that

$$(r/r_e)^2 = 1 + 2q$$

or

$$(r_e/r)^3 = (1 + 2q)^{-3/2}$$

where

$$q = \left[(x_e + \tfrac{1}{2}\xi)\,\xi + (y_e + \tfrac{1}{2}\eta)\,\eta + (z_e + \tfrac{1}{2}\zeta)\,\zeta\right]/r_e^2$$

Through a binomial expansion

$$(1 + 2q)^{-3/2} = 1 - \frac{3}{2}(2q) + \frac{\left(-\frac{3}{2}\right)\left(-\frac{5}{2}\right)}{2!}(2q)^2 + \cdots$$

so that

$$\begin{aligned} 1 - (r_e/r)^3 &= 1 - (1 + 2q)^{-3/2} \\ &= 3q\left(1 - \frac{5}{2!}q + \frac{5\cdot 7}{3!}q^2 - \frac{5\cdot 7\cdot 9}{4!}q^3 + \cdots\right) \\ &= f(q) \end{aligned} \tag{7}$$

from which the Encke expression can be rewritten as:

$$\begin{cases} \ddot{\xi} = \dfrac{\mu}{r_e^3}\left[f(q)\,x - \xi\right] + \ddot{\bar{x}} \\ \ddot{\eta} = \dfrac{\mu}{r_e^3}\left[f(q)\,y - \eta\right] + \ddot{\bar{y}} \\ \ddot{\zeta} = \dfrac{\mu}{r_e^3}\left[f(q)\,z - \zeta\right] + \ddot{\bar{z}} \end{cases} \tag{8}$$

B. Perturbation Components

In Eqs. (4), the perturbation components $\ddot{\bar{x}}, \ddot{\bar{y}}, \ddot{\bar{z}}$ are employed. For geocentric orbits in close proximity to the Earth, these terms include the gravitational effects of the Sun and Moon and the bulge terms of the Earth's potential field. The perturbation components are:

$$\begin{aligned} \ddot{\bar{x}} = \sum_{i=2}^{3} m_i\left(\frac{x_{i,1}}{r_{i,1}^3} - \frac{x_{i,0}}{r_{i,0}^3}\right) - J'm_1\frac{x_{1,0}}{r_{1,0}^5}(1 - 5U_z'^2) \\ - H'm_1\frac{x_{1,0}z_{1,0}}{r_{1,0}^5}(3 - 7U_z'^2) - K'm_1\frac{x_{1,0}}{6r_{1,0}^7} \\ \times (3 - 42U_z'^2 + 63U_z'^4) + \frac{\partial\phi_2}{\partial x} + \cdots \end{aligned} \tag{9a}$$

$$\begin{aligned} \ddot{\bar{y}} = \sum_{i=2}^{3} m_i\left(\frac{y_{i,1}}{r_{i,1}^3} - \frac{y_{i,0}}{r_{i,0}^3}\right) - J'm_1\frac{y_{1,0}}{r_{1,0}^5}(1 - 5U_z'^2) \\ - H'm_1\frac{y_{1,0}z_{1,0}}{r_{1,0}^5}(3 - 7U_z'^2) - K'm_1\frac{y_{1,0}}{6r_{1,0}^7} \end{aligned}$$

$$\times (3 - 42U_z'^2 + 63U_z'^4) + \frac{\partial \phi_2}{\partial y} + \cdots \tag{9b}$$

$$\ddot{z} = \sum_{i=2}^{3} m_i \left(\frac{z_{i,1}}{r_{i,1}^3} - \frac{z_{i,0}}{r_{i,0}^3} \right) - J'm_1 \frac{z_{1,0}}{r_{1,0}^5}(3 - 5U_z'^2) + H'm_1 \frac{3}{5r_{1,0}^4}\left(1 - 10U_z'^2 + \frac{35}{3}U_z'^4\right) - K'm_1 \times \frac{z_{1,0}}{6r_{1,0}^7}(15 - 70U_z'^2 + 63U_z'^4) + \frac{\partial \phi_2}{\partial z} + \cdots \tag{9c}$$

where terms with subscript 2 refer to the Moon and those terms with subscript 3 to the Sun.

The remaining terms used in Eqs. (7), (8), and (9) are fully discussed in Section II.

C. Eccentric Anomaly as Independent Variable

Thus far the Encke method has been developed with time as the independent variable. In the reference orbit epoch calculation it is necessary to evaluate Kepler's equation:

$$M = E - e \sin E = n(t - t_0) \tag{10}$$

If time is the independent variable, then it is necessary to solve the transcendental equation for E. Although this is quite possible and causes no analytical difficulty, it is a time-consuming calculation. Therefore, it would be desirable to have the eccentric anomaly E for the independent variable so that Kepler's equation could be solved for t, this being somewhat faster calculation. The change in independent variables requires a reinvestigation of the Encke formula, which is given in the form:

$$\ddot{\xi} = \frac{\mu}{r_c^3}[f(q)x - \xi] + \ddot{x} \tag{11}$$

$$(\xi \to \eta, \zeta \text{ and } x \to y, z)$$

Since

$$\frac{d\xi}{dt} = \frac{d\xi}{dE}\frac{dE}{dt}$$

$$\frac{d^2\xi}{dt^2} = \frac{d}{dt}\left(\frac{d\xi}{dE}\right)\frac{dE}{dt} + \frac{d\xi}{dE}\frac{d^2E}{dt^2} = \frac{d}{dE}\left(\frac{d\xi}{dE}\right)\left(\frac{dE}{dt}\right)^2 + \frac{d\xi}{dE}\frac{d^2E}{dt^2}$$

$$\frac{d^2\xi}{dt^2} = \frac{d^2\xi}{dE^2}\left(\frac{dE}{dt}\right)^2 + \frac{d\xi}{dE}\frac{d^2E}{dt^2}$$

Solving for $d^2\xi/dE^2$ yields

$$\frac{d^2\xi}{dE^2} = \left(\frac{d^2\xi}{dt^2} - \frac{d\xi}{dE}\frac{d^2E}{dt^2}\right)\left(\frac{dt}{dE}\right)^2 \tag{12}$$

Since

$$\frac{dE}{dt} = \frac{\sqrt{\mu}}{r_c\sqrt{|a|}} \tag{13}$$

and

$$r_c = a(1 - e\cos E) \quad \text{for } a > 0$$
$$r_c = a(1 - e\cosh E) \quad \text{for } a < 0 \tag{14}$$

we have

$$\left(\frac{dt}{dE}\right)^2\frac{d^2E}{dt^2} = \frac{-ae\sin E}{r_c} \quad \text{for } a > 0$$
$$\left(\frac{dt}{dE}\right)^2\frac{d^2E}{dt^2} = \frac{-ae\sinh E}{r_c} \quad \text{for } a < 0 \tag{15}$$

Substituting Eqs. (11) and (15) into Eq. (12) yields the desired Encke formula with E as independent variable.

$$\frac{d^2\xi}{dE^2} = \frac{ae\sin E}{r_c}\frac{d\xi}{dE} + \frac{a}{r_c}[f(q)x - \xi] + \frac{r_c^2 a\ddot{x}}{\mu} \quad \text{for } a > 0$$
$$\frac{d^2\xi}{dE^2} = \frac{ae\sinh E}{r_c}\frac{d\xi}{dE} + \frac{a}{r_c}[f(q)x - \xi] + \frac{r_c^2 a\ddot{x}}{\mu} \quad \text{for } a < 0 \tag{16}$$
$$(\xi \to \eta, \zeta \text{ and } x \to y, z)$$

D. Rectification

The reference orbit is chosen as an osculating two-body orbit. Osculation occurs only at one epoch. As the body moves away from this epoch, perturbations cause the body to depart from the reference orbit. As these departures become large, integration step size shrinks, thereby slowing down the numerical advancement of the solution. This difficulty is easily eliminated by determining a new reference orbit when the terms ξ, η, ζ become large.[3]

As the lunar vehicle approaches the immediate proximity of the Moon, the two-body geocentric reference orbit deviates very rapidly from the true orbit so that very frequent rectifications become necessary. When the vehicle is about 4 g-radii from the Moon, the Moon's influence on the vehicle is more significant than the Earth's. Consequently, a coordinate transformation should be performed from geocentric to selenocentric coordinates, and the two-body reference orbit is determined as a selenocentric orbit. This transformation only alters the perturbative components, $\ddot{x}, \ddot{y}, \ddot{z}$, in Encke's expression and all other parameters such as r, x, y, z, ξ, η, ζ, r_c, x_c, y_c, and z_c are referred to the Moon's center. At the time the transformation from geocentric to selenocentric coordinates is made, the vehicle is so distant from the Earth that the third and fourth harmonic terms of the terrestrial bulge have an insignificant effect on the vehicle so that the corresponding terms may be dropped from the calculations.

[3]Experimentation has shown that the integration step size shrinks considerably when perturbation displacements, i.e. $(\xi^2 + \eta^2 + \zeta^2)^{\frac{1}{2}}$, become larger than ½ g-radius. Rectification is recommended at that point for lunar vehicle orbit calculations.

IV. EPHEMERIDES

In Section II it was shown that, for high-precision lunar trajectory determinations, planetary perturbations may be ignored so that it is only necessary to consider those perturbations due to the Earth, Moon, and Sun. For accurate perturbation calculations it is necessary that the position of the perturbing body be known at any epoch during the vehicle's transit. The coordinate system chosen is geocentric so that the Earth is fixed in this coordinate system and the Moon and Sun move around the Earth. In this section a discussion will be presented to illustrate the means by which positions of these bodies can be determined.

A. The Lunar Ephemeris

The most accurate method by which the instantaneous position of the Moon can be obtained is through evaluation of Brown's trigonometric series. Extensive efforts are made, especially by the U. S. Naval Observatory, to evaluate Brown's series to obtain a very accurate lunar ephemeris. Results of these calculations are published yearly in *The American Ephemeris and Nautical Almanac* (Ref. 4). Unfortunately, Brown's series is so complex[4] that it is too demanding of computer time and space to be useful in direct application. Consequently, the lunar ephemeris as published by the U. S. Naval Observatory should be employed and the lunar positions obtained by interpolation. *The American Ephemeris and Nautical Almanac* supplies the Moon's right ascension α, declination δ, and horizontal parallax π. The rectangular geocentric position of the Moon, as required by the equations of motion, is obtained from these quantities:

$$\begin{aligned} x_{1,2} &= \csc \pi \cos \alpha \cos \delta \\ y_{1,2} &= \csc \pi \sin \alpha \cos \delta \\ z_{1,2} &= \csc \pi \sin \alpha \end{aligned} \tag{17}$$

The right ascension and declination are tabulated in *The American Ephemeris and Nautical Almanac* at hourly intervals and horizontal parallax at 12-hr intervals. In order to obtain position coordinates of the Moon at any epoch, the Lagrangian 6-point interpolation formula has been found to be an efficient and accurate method for interpolation in the lunar ephemeris. It was found that this interpolation will result in errors of less than ¼ mile at the Moon's distance when a 12-hr ephemeris is employed.

[4]The complete series is composed of about 1450 terms, the coefficients of which are series expressions in themselves. A complete discussion of Brown's series can be found in Ref. 5.

B. The Solar Ephemeris

Although the Sun's apparent motion as viewed from an inertial geocentric coordinate system is much slower than the Moon's, an accurate representation of this motion is vital for high-precision work. Again *The American Ephemeris and Nautical Almanac* supplies the necessary solar position data. By experimentation it was found that 1-day solar ephemeris data are adequate if used together with a 6-point Lagrangian interpolation formula, thus yielding the same precision as was obtained for the lunar ephemeris.

C. Ephemerides and the Vernal Equinox

The intersection of the equator and ecliptic through which the Sun moves when crossing the equator from south to north is defined as the vernal equinox, or first point of Aries. This point of intersection is continually shifting due to the retrograde motion of the equator along the ecliptic. There are two motions inherent in this shifting, one of which is known as precession[5] and the other as nutation.[6] The "mean equinox" is a fictitious equinox whose position is that of the vernal equinox with the effect of nutation removed. The position of the mean equinox at any epoch is known as the mean equinox of that date.

In *The American Ephemeris and Nautical Almanac* the right ascension and declination of the Moon are referred to the true equator and equinox or true equinox. The solar ephemeris is given in rectangular coordinates in two tables. One is referred to the mean equator and equinox of the beginning of the listed year and the other is referred to the mean equator and equinox of 1950.0. If both solar and lunar ephemerides are required, as they are in high-precision lunar vehicle orbit determinations, it is vitally important that they be referred to the same equinox. Therefore, either the lunar ephemeris must be referred to the equinox used in the solar ephemeris or the solar ephemeris must be referred to the true equator and equinox. The latter transformation has been chosen so that both ephemerides are referred to the true equator

[5]Precession causes the equinox to retrograde along the ecliptic at a uniform rate.

[6]Nutation is the periodic displacement of the equinox from its mean position as defined by precession.

and equinox although either would be acceptable for the problem at hand.

The rectangular coordinates of the Sun are referred to the geocenter as origin and the mean equator and equinox of the year 1950.0, with the x axis directed towards the vernal equinox in the mean equatorial plane, the z axis directed toward the north celestial pole, and the y axis in the mean equator plane completing the right-hand system. These equatorial rectangular coordinates may be referred to any other equinox by the formulae:

$$\begin{bmatrix} X \\ Y \\ Z \end{bmatrix} = \begin{bmatrix} X_x & Y_x & Z_x \\ X_y & Y_y & Z_y \\ X_z & Y_z & Z_z \end{bmatrix} \begin{bmatrix} X_0 \\ Y_0 \\ Z_0 \end{bmatrix} \tag{18}$$

where X_0, Y_0, Z_0 are the rectangular equatorial coordinates referred to the equinox of 1950.0 and X, Y, Z are the rectangular equatorial coordinates referred to any other equinox. The terms (cf. Table 3) in the transformation matrix (18) are determined through the following series (Ref. 3):

$$X_x = 1 - 2.9697 \times 10^{-4} T^2 - 13 \times 10^{-8} T^3$$

$$Y_x = -X_y = -2.234988 \times 10^{-2} T - 6.76 \times 10^{-6} T^2 + 2.21 \times 10^{-6} T^3$$

$$Z_x = -X_z = -9.71711 \times 10^{-3} T + 2.07 \times 10^{-6} T^2 + 96 \times 10^{-8} T^3 \tag{19}$$

$$Y_y = 1 - 2.4976 \times 10^{-4} T^2 - 15 \times 10^{-8} T^3$$

$$Y_z = Z_y = -1.0859 \times 10^{-4} T^2 - 3 \times 10^{-8} T^3$$

$$Z_z = 1 - 4.721 \times 10^{-5} T^2 + 2 \times 10^{-8} T^3$$

where $T = (t - 1950.0)$, in centuries, and t is the epoch desired.

Table 3. Typical values which may be employed in the transformation matrix of Eq. (18)

	1959.0	1960.0	1961.0
X_x	0.99999759	0.99999703	0.99999641
X_y	−0.00201150	0.00223501	−0.00245851
X_z	−0.00087450	0.00097167	0.001^4883
Y_x	−0.00201150	−0.00223501	−0.00. ^51
Y_y	0.99999798	0.99999750	0.99999698
Y_z	0.00000088	0.00000109	0.00000131
Z_x	−0.00087450	−0.00097167	−0.00106883
Z_y	−0.00000088	−0.00000109	−0.00000131
Z_z	0.99999962	0.99999953	0.99999943

V. REFERENCE ORBIT

Through Encke's method, as described in Section III, orbits can be calculated as deviations from two-body orbits. In order to relate these deviations to positions in inertial space the two-body problem or reference orbit must be solved. Fortunately, the two-body problem can be solved analytically. The reference orbit must be a conic section which is completely specified by any six independent orbital elements.

This section will illustrate how inertial coordinates may be obtained from orbital elements. Let it be assumed that the following six orbital elements are given:

Time of perigee passage T

Period P

Orbit inclination i

Right ascension of ascending node Ω

Argument of perigee ω

Eccentricity e

The mean motion of the body can be calculated immediately from the relation

$$n = \frac{2\pi}{P} \tag{20}$$

The semimajor axis is obtained from

$$a = \left(\frac{k}{n}\right)^{2/3} \tag{21}$$

where the value of the geocentric gravitational constant is $k_e = 0.07436574$ g-radii$^{3/2}$/min (Ref. 6). The mean anomaly is calculated from

$$M = n(t - T) \tag{22}$$

and then Kepler's equation is solved for the eccentric anomaly

$$M = E - e \sin E \tag{23}$$

The parameter p is calculated from

$$p = a(1 - e^2)$$

It is convenient to define a rectangular coordinate system in which the x_ω axis is directed toward perigee along the semimajor axis of the orbit and y_ω is directed along the semilatus rectum. Then the coordinates of the vehicle in the orbit plane are

$$\left.\begin{aligned} x_\omega &= a(\cos E - e) \\ y_\omega &= a\sqrt{1 - e^2}\,\sin E \end{aligned}\right\} \text{for } a > 0 \tag{24}$$

$$r = a(1 - e \cos E)$$

$$\dot{x}_\omega = -\frac{\sqrt{|a|}}{r} \sin E \tag{25}$$

$$\dot{y}_\omega = \frac{\sqrt{p}}{r} \cos E$$

Two convenient unit vectors can be used to replace the orientation elements i, Ω, and ω. The unit vector **P** is directed along the semimajor axis toward perigee and **Q** is in the direction of the velocity vector when the object is at perigee. These quantities are illustrated in Fig. 1. Then,

$$\begin{aligned} P_x &= \cos\omega \cos\Omega - \sin\omega \sin\Omega \cos i \\ P_y &= \cos\omega \sin\Omega + \sin\omega \cos\Omega \cos i \\ P_z &= \sin\omega \sin i \end{aligned} \tag{26}$$

and

$$\begin{aligned} Q_x &= -\sin\omega \cos\Omega - \cos\omega \sin\Omega \cos i \\ Q_y &= -\sin\omega \sin\Omega + \cos\omega \cos\Omega \cos i \\ Q_z &= \cos\omega \sin i \end{aligned} \tag{27}$$

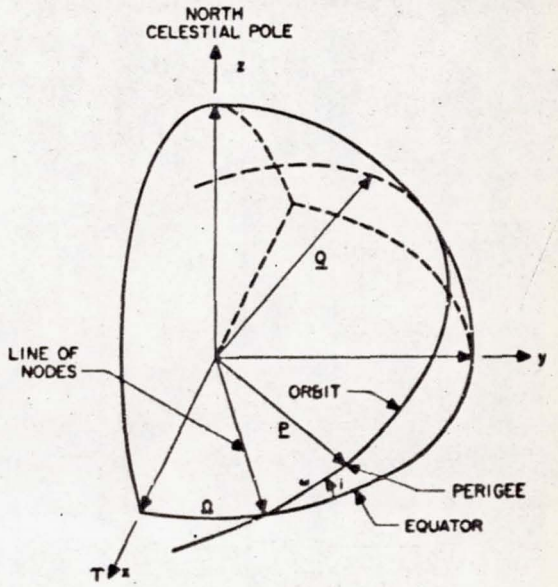

Fig. 1. Projection of Orbit on Celestial Sphere

The inertial rectangular coordinates are now found by

$$\begin{bmatrix} x \\ y \\ z \end{bmatrix} = \begin{bmatrix} P_x & Q_x \\ P_y & Q_y \\ P_z & Q_z \end{bmatrix} \begin{bmatrix} x_\omega \\ y_\omega \end{bmatrix} \tag{28}$$

and

$$\begin{bmatrix} \dot{x} \\ \dot{y} \\ \dot{z} \end{bmatrix} = \begin{bmatrix} P_x & Q_x \\ P_y & Q_y \\ P_z & Q_z \end{bmatrix} \begin{bmatrix} \dot{x}_\omega \\ \dot{y}_\omega \end{bmatrix} \tag{29}$$

The x axis is in the equator plane directed to the vernal equinox, and the z axis to the terrestrial north pole, and the y axis completes the right-hand system.

Thus it has been shown that it is possible to obtain inertial position and velocity coordinates from six orbit elements T, P, i, Ω, ω, e. Other sets of six independent elements could have been chosen equally well to achieve the desired orbit.

VI. COLLECTION OF FORMULAE FOR COMPUTATION PURPOSES

In the event that the reader's appetite has been sufficiently whetted so that he may want to try out Encke's Method on a lunar orbit determination, all pertinent equations have been collected to facilitate the programming of this problem for an automatic computer.

It will be assumed that the vehicle's position and velocity are known in an altazimuth system i.e.,

- s velocity, g-radii/k_e^{-1}-min
- r distance from geocenter, g-radii
- ϕ latitude, rad
- λ longitude, rad, measured positive to the west
- A azimuth heading, rad, measured positive to the east from the north
- γ elevation angle, rad
- θ_{0R} Greenwich sidereal time or hour angle of the vernal equinox at Greenwich, rad

This initial position and velocity are considered as exact so that an ephemeris can be calculated based on these initial conditions.

A. Loading the Ephemeris

The positions of the Moon and Sun must be made available in addition to the vehicle's position. Perhaps the best way in which this can be achieved is by reading a portion of the respective ephemerides from *The American Ephemeris and Nautical Almanac* into the computer, ensuring, of course, that the portion chosen is sufficient to cover the vehicle's entire transit. The lunar ephemeris is given in spherical coordinates as horizontal parallax π, declination δ, and right ascension α, and the Sun's ephemeris is given in rectangular coordinates. Since the lunar ephemeris is used only to the extent of obtaining inertial positions of the Moon it may be desirable to subject the lunar ephemeris to a transformation to bring these points into rectangular inertial coordinates, thereby eliminating the conversion each time the ephemeris is consulted. The following transformation should be employed to place the Moon's ephemeris into inertial rectangular coordinates in g-radii:

$$\begin{aligned} x_{1,2} &= \csc\pi \cos\alpha \cos\delta \\ y_{1,2} &= \csc\pi \sin\alpha \cos\delta \\ z_{1,2} &= \csc\pi \sin\delta \end{aligned} \qquad (30)$$

It is important to remember that the solar ephemeris is referred to the equinox of 1950.0, whereas the lunar ephemeris is referred to the true equinox. Consequently, the transformation equation (18) should be applied to the solar ephemeris upon read-in. As was pointed out in Sections IV A and IV B it is sufficient to supply 12-hr data for the lunar ephemeris and 24-hr data for the solar ephemeris.

B. Reference Orbit Element Determination

The following set of equations can be used to obtain the orbit elements based upon the given parameters:

The radial velocity, in g-radii/k_e^{-1}-min, is obtained by

$$\dot{r} = j \sin\gamma \qquad (31)$$

The magnitude of the semimajor axis a, in g-radii, the parameter p, in g-radii, and the eccentricity e are obtained from:

$$a = \frac{r}{2 - j^2 r} \qquad (32)$$

$$p = (rj - \cos\gamma)^2 \qquad (33)$$

$$e = \sqrt{\left(\frac{p}{r} - 1\right)^2 + \dot{r}^2 p} \qquad (34)$$

The true anomaly v is found by:

$$\sin v = \frac{\dot{r}\sqrt{p}}{e}, \qquad \cos v = \frac{p - r}{er} \qquad (35)$$

and the mean-motion n, in radians/min, is found by

$$n = \frac{k_e}{|a|^{3/2}} \qquad (36)$$

The eccentric anomaly E, in radians, is obtained from

$$\begin{aligned} E &= \tan^{-1}\frac{r\dot{r}\sqrt{a}}{a - r} \qquad \text{for } a > 0 \\ E &= \log_e\left[\frac{a - r}{ea} + \frac{r\dot{r}}{e\sqrt{|a|}}\right] \qquad \text{for } a < 0 \end{aligned} \qquad (37)$$

The mean anomaly M, in radians, is found by

$$\begin{aligned} M &= E - \frac{r\dot{r}}{\sqrt{a}} \qquad \text{for } a > 0 \\ M &= \frac{r\dot{r}}{\sqrt{|a|}} - E \qquad \text{for } a < 0 \end{aligned} \qquad (38)$$

and the hour angle of the vernal equinox for the sub-latitude position is found by

$$\theta = \theta_{GR} - \lambda \tag{39}$$

Thus far, all the elements of the reference orbit have been obtained, but its orientation in inertial space remains to be determined. The following unit vectors are defined to aid in the orientation of the reference orbit.

It will be found that a unit vector **U** directed along the position vector **r** will be useful:

$$\begin{aligned} U_x &= \cos\phi \cos\theta \\ U_y &= \cos\phi \sin\theta \\ U_z &= \sin\phi \end{aligned} \tag{40}$$

Another unit vector **S** directed along the velocity vector is given by:

$$\begin{aligned} S_x &= B_1 \cos\alpha - B_2 \sin\alpha \\ S_y &= B_1 \sin\alpha + B_2 \cos\alpha \\ S_z &= \sin\gamma \sin\phi + \cos\gamma \cos A \cos\phi \end{aligned} \tag{41}$$

where

$$\begin{aligned} B_1 &= \sin\gamma \cos\phi - \cos\gamma \cos A \sin\phi \\ B_2 &= \cos\gamma \sin A \end{aligned}$$

The unit vector **V** is defined as a vector in the direction of motion in the orbit plane and therefore perpendicular to **U**:

$$\begin{aligned} V_x &= \frac{\dot{r} S_x - r\dot{r} U_x}{\sqrt{p}} \\ V_y &= \frac{\dot{r} S_y - r\dot{r} U_y}{\sqrt{p}} \\ V_z &= \frac{\dot{r} S_z - r\dot{r} U_z}{\sqrt{p}} \end{aligned} \tag{42}$$

These unit vectors can be related to the unit vectors **P** and **Q**, where **P** is directed along the semimajor axis, and **Q** along the semilatus rectum, and both lie in the orbit plane.

$$\mathbf{P} = \mathbf{U} \cos v - \mathbf{V} \sin v \tag{43}$$

$$\mathbf{Q} = \mathbf{U} \sin v + \mathbf{V} \cos v \tag{44}$$

Finally, the time of perigee passage T in minutes is given by

$$T = -\frac{M}{n} \tag{45}$$

Here it is assumed that the initially given point is supplied at time zero, so that T is measured with respect to this zero time point.

Thus, the reference orbit is completely determined.

C. Epoch Calculation

So that the vehicle's position can be determined at any epoch the two-body position must be determined in accordance with the independent variable. In Section III C it was demonstrated that there exists a one-to-one relation between time t and the eccentric anomaly E, Eq. (10). Choosing E as the independent variable permits solving Kepler's equation the "easy way," thereby conserving computer time. Consequently, E will be assumed to be the independent variable in the following discussion.

The epoch calculation is designed to yield the two-body position of the vehicle according to the value E at any instant.

Although the time is not actually needed for the calculation, it is desirable to have this value available for the ephemeris look-up, since it is physically more meaningful than E. The time, in minutes, is obtained from:

$$\begin{aligned} t &= \frac{1}{n}(E - e \sin E) \qquad \text{for } a > 0 \\ t &= \frac{1}{n}(-E + e \sinh E) \quad \text{for } a < 0 \end{aligned} \tag{46}$$

The two-body radial distance of the vehicle from the geocenter, in g-radii, is obtained from:

$$\begin{cases} r_e = a(1 - e \cos E) & \text{for } a > 0 \\ r_e = a(1 - e \cosh E) & \text{for } a < 0 \end{cases} \tag{47}$$

The rectangular position coordinates, in g-radii, in the orbit plane are obtained from:

$$\begin{aligned} x_w &= a(\cos E - e) && \text{for } a > 0 \\ y_w &= a\sqrt{1 - e^2} \sin E && \text{for } a > 0 \\ x_w &= a(\cosh E - e) && \text{for } a < 0 \\ y_w &= -a\sqrt{e^2 - 1} \sinh E && \text{for } a < 0 \end{aligned} \tag{48}$$

where the x_w axis is directed towards perigee and y_w along the semilatus rectum.

From Eq. (48) and the unit vectors **P** and **Q**, the vehicle's position in geocentric inertial coordinates is obtained:

$$\begin{bmatrix} x_e \\ y_e \\ z_e \end{bmatrix} = \begin{bmatrix} P_x & Q_x \\ P_y & Q_y \\ P_z & Q_z \end{bmatrix} \begin{bmatrix} x_w \\ y_w \end{bmatrix} \tag{49}$$

where the x_e-axis is directed to the vernal equinox, the z_e-axis is directed to the Earth's north pole, and the y_e-axis completes the right-hand system.

Here, a very simple check on Eqs. (47), (48), and (49) exists:

$$r_e = \sqrt{x_e^2 + y_e^2 + z_e^2} = \sqrt{x_\omega^2 + y_\omega^2} \tag{50}$$

The rectangular velocity coordinates, in g-radii/k_e^{-1}-min, in the orbit plane are determined from:

$$\begin{aligned}
\dot{x}_\omega &= \frac{-\sqrt{a}\sin E}{r_e} && \text{for } a > 0 \\
\dot{y}_\omega &= \frac{\sqrt{a(1-e^2)}\cos E}{r_e} && \\
\dot{x}_\omega &= \frac{-\sqrt{|a|}\sinh E}{r_e} && \text{for } a > 0 \\
\dot{y}_\omega &= \frac{\sqrt{|a(1-e^2)|}\cosh E}{r_e} &&
\end{aligned} \tag{51}$$

Again employing the unit vectors **P** and **Q** and the results from Eq. (51), the vehicle's velocity in inertial coordinates is obtained:

$$\begin{bmatrix} \dot{x}_e \\ \dot{y}_e \\ \dot{z}_e \end{bmatrix} = \begin{bmatrix} P_x & Q_x \\ P_y & Q_y \\ P_z & Q_z \end{bmatrix} \begin{bmatrix} \dot{x}_\omega \\ \dot{y}_\omega \end{bmatrix} \tag{52}$$

Thus, all required orbit elements are obtained.

D. Initial Conditions

Theoretically, the initial perturbative displacements are zero because the reference orbit is chosen as an osculating orbit. In the process of calculating rectangular coordinates for position and velocity, however, rounding errors are encountered which may cause the initial perturbations to differ slightly from their nominal value. It is therefore desirable to calculate the initial perturbative displacements by the following:

$$\begin{aligned}
\xi_0 &= r_e U_x - x_e & \lambda_0' &= \left(\frac{d\xi}{dE}\right)_0 = (\dot{x} - \dot{x}_e) r_e \sqrt{|a|} \\
\eta_0 &= r_e U_y - y_e & \Omega_0 &= \left(\frac{d\eta}{dE}\right)_0 = (\dot{y} - \dot{y}_e) r_e \sqrt{|a|} \\
\zeta_0 &= r_e U_z - z_e & \psi_0 &= \left(\frac{d\zeta}{dE}\right)_0 = (\dot{z} - \dot{z}_e) r_e \sqrt{|a|}
\end{aligned} \tag{53}$$

where

$$\begin{aligned}
\dot{x} &= S_x \dot{s} \\
\dot{y} &= S_y \dot{s} \\
\dot{z} &= S_z \dot{x}
\end{aligned} \tag{54}$$

E. Lunar and Solar Ephemeris Look-Up

Prior to entering the derivative evaluation, the Moon's position corresponding to the time t as obtained by Eq. (46) should be determined. In Section IV A it was pointed out that a 6-point Lagrangian interpolation will yield sufficient integrity in both lunar and solar ephemerides when 12- and 24-hr data are used, respectively.

F. The Differential Equations

Before the differential equations of motion are written, the following terms should be evaluated:

$$x_{2,0} = x_{1,0} - x_{1,2} \qquad x \to y, z \tag{55}$$

$$x_{3,0} = x_{1,0} - x_{1,3} \qquad x \to y, z \tag{56}$$

$$r_{2,0} = \sqrt{x_{2,0}^2 + y_{2,0}^2 + z_{2,0}^2} \tag{57}$$

$$r_{3,0} = \sqrt{x_{3,0}^2 + y_{3,0}^2 + z_{3,0}^2} \tag{58}$$

$$U_z' = \frac{z_{1,0}}{r_{1,0}} \tag{59}$$

The three perturbative terms may now be written:

$$\begin{aligned}
\ddot{x} = {} & m_2\left(\frac{x_{2,1}}{r_{2,1}^3} - \frac{x_{2,0}}{r_{2,0}^3}\right) + m_3\left(\frac{x_{3,1}}{r_{3,1}^3} - \frac{x_{3,0}}{r_{3,0}^3}\right) \\
& - J' \frac{x_{1,0}}{r_{1,0}^5}(1 - 5U_z'^2) + H' \frac{x_{1,0} z_{1,0}}{r_{1,0}^5}(-3 + 7U_z'^2) \\
& - K' \frac{x_{1,0}}{6r_{1,0}^7}(3 - 42U_z'^2 + 63U_z'^4)
\end{aligned} \tag{60}$$

$$\begin{aligned}
\ddot{y} = {} & m_2\left(\frac{y_{2,1}}{r_{2,1}^3} - \frac{y_{2,0}}{r_{2,0}^3}\right) + m_3\left(\frac{y_{3,1}}{r_{3,1}^3} - \frac{y_{3,0}}{r_{3,0}^3}\right) \\
& - J' \frac{y_{1,0}}{r_{1,0}^5}(1 - 5U_z'^2) + H' \frac{y_{1,0} z_{1,0}}{r_{1,0}^5}(-3 + 7U_z'^2) \\
& - K' \frac{y_{1,0}}{6r_{1,0}^7}(3 - 42U_z'^2 + 63U_z'^4)
\end{aligned} \tag{61}$$

$$\begin{aligned}
\ddot{z} = {} & m_2\left(\frac{z_{2,1}}{r_{2,1}^3} - \frac{z_{2,0}}{r_{2,0}^3}\right) + m_3\left(\frac{z_{3,1}}{r_{3,1}^3} - \frac{z_{3,0}}{r_{3,0}^3}\right) \\
& - J' \frac{z_{1,0}}{r_{1,0}^5}(3 - 5U_z'^2) + H' \frac{3}{5r_{1,0}^5}\left(1 - 10U_z'^2 + \frac{35}{3}U_z'^4\right) \\
& - K' \frac{z_{1,0}}{6r_{1,0}^7}(15 - 70U_z'^2 + 63U_z'^4)
\end{aligned} \tag{62}$$

where

$$\begin{aligned}
J' &\quad 1.62341 \times 10^{-3} \\
H' &\quad 6.04 \times 10^{-6}
\end{aligned}$$

$$K' \quad 6.37 \quad \times 10^{-6}$$
$$m_2 \quad 1.22888 \times 10^{-7}$$
$$m_3 \quad 332488$$

and, finally, the differential equations take the following form:

$$\frac{d\xi}{dE} = \lambda' \tag{63}$$

$$\frac{d\eta}{dE} = \Omega \tag{64}$$

$$\frac{d\zeta}{dE} = \psi \tag{65}$$

$$\frac{d\lambda'}{dE} = \frac{ae\sin E}{r_e}\lambda' + \frac{a}{r_e}[f(q)\,x_{1,0} - \xi] + r_e^3 a\ddot{\bar{x}} \quad \text{for } a > 0 \tag{66a}$$

$$\frac{d\lambda'}{dE} = \frac{ae\sinh E}{r_e}\lambda' + \frac{a}{r_e}[f(q)\,x_{1,0} - \xi] + r_e^3 a\ddot{\bar{x}} \quad \text{for } a < 0 \tag{66b}$$

$$\frac{d\Omega}{dE} = \frac{ae\sin E}{r_e}\Omega + \frac{a}{r_e}[f(q)\,y_{1,0} - \eta] + r_e^3 a\ddot{\bar{y}} \quad \text{for } a > 0 \tag{67a}$$

$$\frac{d\Omega}{dE} = \frac{ae\sinh E}{r_e}\Omega + \frac{a}{r_e}[f(q)\,y_{1,0} - \eta] + r_e^3 a\ddot{\bar{y}} \quad \text{for } a < 0 \tag{67b}$$

$$\frac{d\psi}{dE} = \frac{ae\sin E}{r_e}\psi + \frac{a}{r_e}[f(q)\,z_{1,0} - \zeta] + r_e^3 a\ddot{\bar{z}} \quad \text{for } a > 0 \tag{68a}$$

$$\frac{d\psi}{dE} = \frac{ae\sinh E}{r_e}\psi + \frac{a}{r_e}[f(q)\,z_{1,0} - \zeta] + r_e^3 a\ddot{\bar{z}} \quad \text{for } a < 0 \tag{68b}$$

where

$$q = \frac{1}{r_e^2}\left[\xi\left(x_e + \frac{1}{2}\xi\right) + \eta\left(y_e + \frac{1}{2}\eta\right) + \zeta\left(z_e + \frac{1}{2}\zeta\right)\right]$$

and

$$f(q) = 3q\left(1 - \frac{5}{2!}q + \frac{5.7}{3!}q^2 - \frac{5.7.9}{4!}q^3 + \cdots\right)$$

The differential Eqs. (63) to (68) may now be evaluated numerically by any numerical procedure such as the Adams-Bashforth, Milne, Runge-Kutta, etc.

G. Terminal Epoch Calculation

In Section VI F the differential equations of motion were set up and evaluated to obtain the departures of the true orbit from the reference orbit. It is now necessary to determine the true rectangular position and velocity coordinates of the vehicle. Vehicle position coordinates are obtained from

$$x_{1,0} = \xi + x_e$$
$$y_{1,0} = \eta + y_e$$
$$z_{1,0} = \zeta + z_e$$

Vehicle velocity coordinates are obtained from

$$\dot{x}_{1,0} = \dot{x}_e + \frac{\lambda'}{r_e\sqrt{|a|}}$$

$$\dot{y}_{1,0} = \dot{y}_e + \frac{\Omega}{r_e\sqrt{|a|}}$$

$$\dot{z}_{1,0} = \dot{z}_e + \frac{\psi}{r_e\sqrt{|a|}}$$

REFERENCES

1. Aeronutronic, a Division of Ford Motor Company. Free Flight Trajectory for a Lunar Mission, by A. Liu and C. Tross. Newport Beach, Calif., March 6, 1959 (Publication U-329a).
2. Aeronutronic, a Division of Ford Motor Company. The Lunar Potential, by I. Alexandrov. Newport Beach, Calif., December 12, 1958 (Publication 377).
3. Planetary Coordinates for the Years 1960–1980. London, Her Majesty's Stationery Office, 1958.
4. U.S. Naval Observatory. The American Ephemeris and Nautical Almanac. Washington, D.C., U.S. Government Printing Office.
5. U.S. Naval Observatory. Improved Lunar Ephemeris 1952–1959. Washington, D.C., U.S. Government Printing Office, 1954.
6. Baker, R. M. L., S. Herrick, and C. G. Hilton. "Gravitational and Related Constants for Accurate Space Navigation," in Proceedings of the VIII Astronautical Congress, Vienna, Spring, 1958.

BIBLIOGRAPHY

University of California at Los Angeles. Efficient Precision Orbit Computation, by R. M. L. Baker and others. June 11, 1959 (Astrodynamical Report No. 3).

Brower, D. "A New Determination of the Solar Parallax from the Parallactic Inequality in the Moon's Longitude," Bulletin Astronomique, Vol. 15, 1950.

Brower, D. "Comments on the Masses of the Inner Planets," Bulletin Astronomique, Vol. 15, 1950.

Brower, D., and A. E. Lilley. "The Solar Parallax and the Hydrogen Line," American Astronomical Society, Toronto Meeting, August, 1959.

Brower, D. "On the Accumulation of Errors in Numerical Integration," Astronomical Journal, Vol. 46, p. 149, 1937.

Collatz, L. "Numerische Behandlung von Differentialgleichungen," Springer Verlag, 1951.

Davis, R. J., F. L. Whipple, and J. B. Zirker. "The Orbit of a Small Earth Satellite," in Scientific Uses of Earth Satellites, edited by J. A. Van Allen, University of Michigan Press, 1956.

De Sitter, W. "On the System of Astronomical Constants," Astronomical Institute Bulletin of Netherlands, Vol. 8.

Aeronutronic, a Division of Ford Motor Compa y. Coordinate Systems for Lunar Vehicle Orbits, by C. G. Hilton and S. Herrick. Newport Beach, Calif., August 8, 1958 (Publication U-245).

Herrick, S. Astrodynamics and Rocket Navigation. New York, D. Van Nostrand, to be published.

Jeffreys, H., and B. Swirler. Methods of Mathematical Physics. Cambridge, University Press, 1956.

Lass, H. Vector and Tensor Analysis. New York, McGraw-Hill, 1950.

Army Ballistic Missile Agency. Analysis of Computational Accuracy of Lunar Probe Decks in Use at ABMA, by W. E. Miner. Huntsville, Ala. (Report DA-TN-16-59).

Moulton, R. F. An Introduction to Celestial Mechanics, 2nd ed. New York, Macmillan, 1956.

Eckels, A., and J. A. O'Keefe. "The Gravitational Field of the Earth," to be published.

Smart, W. M. Spherical Astronomy, 4th ed. Cambridge, University Press, 1956.

Aeronutronic, a Division of Ford Motor Company. Astronomical Constants and Their Importance in Lunar Trajectory Determination, by C. Tross. Newport Beach, Calif., September, 1959 (Publication U-626).

Walters, L. G. "Lunar Trajectory Mechanics," Journal of the Institute of Navigation, Vol. 6, Spring, 1958.

Aeronutronic, a Division of Ford Motor Company. The Influence of the Earth's Potential Field on a Nearly Circular Satellite, by S. Herrick and L. G. Walters. Newport Beach, Calif., January 9, 1959 (Publication U-326).

Bruton, R. H., K. J. Craig, N. G. Roman, and B. S. Yaplee. "Radar Echoes from the Moon at a Wave Length of 10 cm.," Proceedings of the IRE, Vol. 46, January 1958.

Remarks on the Programming System of Project Space Track

E. W. WAHL

Air Force Cambridge Research Center, Hanscom Field,
Bedford, Mass.

ABSTRACT

Programming development at Project Space Track is discussed in general terms. This discussion includes the special problems of data input, utilization of subroutines for achieving data conformity, kinds of basic programs available and desirable, and adaptation of output routines to specialized user requirements.

I. INTRODUCTION

For more than two years Project Space Track has been active in the field of satellite orbit determination and prediction. With the growing number of satellites and the improvement of methods, an increasingly complex system of computations had to be put together. Finally, Space Track, in December 1959, acquired its own 709 computing system which started operation on January 11, 1960. We are now in the process of integrating our computing system to achieve the most satisfactory solution to our mission as far as computing is concerned, and I will try to explain to you in a few general remarks our programming philosophy.

I will be using the name "Space Track" frequently in my talk; actually the name has, by now, only historical significance. Our program officially is known now as the Electronic Support System 496L and its nerve center is the National Space Surveillance Control Center (NSSCC). Its mission, in the broadest sense, is the surveillance and cataloguing of all space vehicles from the time they attain orbit until their eventual decay or possible loss in deep space. Parts of this system are: (1) the observation (sensor) network, about which we will talk here only incidentally; (2) the communications system and the network control function, which also are not directly relevant to our discussion; and (3) the Computing Center at the NSSCC. Here, observations and, in cases of U.S. satellites, also initial orbital elements are reviewed, data reduction methods are applied, and, finally, predictions and other information are produced and compiled for dissemination through communication lines.

II. DISCUSSION

The efficiency of this computer operation hinges to a large extent on two things: (1) the use of automatized equipment to minimize the time loss from the actual time of observation to the instant when the prediction becomes possible, and (2) the interplay of programs used inside the computing facility, minimizing the actual processing time within the computer. We are currently working on both problems, and while we are still some time away from a satisfactory solution we can now see rather clearly at least the problems and, in some cases, preliminary solutions. Let me therefore indicate some of these problems and their possible solutions in these two areas.

When Space Track started out, as a two-man operation, we just attempted to learn the first steps in this game. Initially, we concerned ourselves with the straightforward system of data reduction and prediction which, I believe, is familiar to all of you; it has been referred to frequently in the various publications of Space Track and basically goes back to the work done by Jacchia and others at the Smithsonian Astrophysical Observatory. In the course of the last two years, we built up this system and increased our computing capability by utilizing, finally, a 610 (small-scale computer) in-house and a 650 system on the base, and rented time on a locally available 709. We also expanded our reduction programs to include such data as radar observations, doppler and interferometer data, Minitrack and Microlock observations, and, finally, TLM-18 data. In the orbital computation field we built up a limited capability in orbit improvement (by means of radar data), a first-pass capability using radar runs, and, finally, orbital improvement systems, one of which has been described by Dr. Walters in a previous talk.

This, however, is just the raw material. We also used a system which will allow us to use these programs in the most efficient manner. In order to do so, we plan to eventually develop a "master executive program," which will not only initiate the proper programs at the right time but also allow assignment of priorities to particular observations, satellites, or requests. This will certainly take some time to develop, but in the meantime we are developing a smaller-scale version of this system to fill our immediate needs. Our current system combines automatic features with command decisions by a human operator and/or a "duty analyst" who is responsible for the proper initiation of scheduled and unscheduled prediction procedures, etc.

The organization of the programs into a synthesized system obviously starts by breaking the various programs down into their basic components and then, block-fashion, rebuilding the whole program structure in such a way that, with a minimum of computer time, the necessary job can be accomplished. As you all know, there are, in the data reduction as well as in orbital computation, quite a number of equations, program steps, etc., which occur over and over again—solution of the Kepler equation, coordinate transformations, etc. After a while, it frequently becomes a matter of writing certain bridging subroutines to build up a program from these little blocks. Extensive use can also be made of the various subroutines in the Share system.

However, in order to come to a near real-time capability—and this ultimately has to be our goal—we have to go one step further. We have to automatize the system as far as possible, from the observer on down through the computer, back into the output channels to the users. This is now being implemented, maximum use being made of the computer in streamlining the total operation.

As I said, it has to start at the observing site. We are introducing a special coding system which is designed (1) to be compatible with regulations governing TWX transmission practices, and (2) to minimize the time needed for transmission as much as possible. Since Space Track is using—and I believe strongly that, at least now, this is our chief strength—all kinds of observations from a wide variety of instruments and therefore of different accuracies, a large number of code forms are being introduced, out of which the observer, under guidance from us, selects the most appropriate code to be used for his particular type of transmission. An incoming data message therefore will consist of a series of five digit groups on TWX (up to 12 per message). As of now, these messages are received in our Communications Center, retransmitted into the computer area, and then automatically punched into standard (fixed format) punch-cards, using the IBM 047 tape-to-card converter. Currently under development for Project Mercury is a real time channel, which will allow the direct acceptance of TWX data from up to 32 TWX channels into the 709 or 7090, and we are watching this development closely and hope, by fall of this year, to install this "black box" on our computer to automatize data input nearly completely.

The next step, the transcription of data into machine format (the so-called standard observation card) is done

by subroutines in the 709 which are called up by using the code number which is the first word in each message. At the same time, a redundancy check is performed to eliminate transmission errors. Finally, we perform a preliminary data reduction using the standard observation format. In this reduction we compute, with the current orbital elements already available in the machine (core or tape), a simple reduction to time and right ascension of the node (at the start of that revolution in which the observation was obtained), check the deviations Δt and ΔRA and, if they do not exceed a preset value, finally incorporate the particular observation in the "data file" on a magnetic tape. Once a day this tape is dumped into punchcards (off-line) and the "good" observations are then sorted into their particular slots according to satellite and time. In addition to the actual observation in the data file, we also record the values Δt_n, ΔRA_n, which, in effect, compare the observations to the current predictions —since predictions were based upon the same orbital elements against which these values had been computed. By examining the deviations (e.g., by plotting the Δt vs revolution N) one will become aware of systematic deviations which, in turn, will then be used to initiate element improvement methods to arrive at better elements and thus better predictions.

This more-or-less automatic system of data reduction and acceptance occupies the computer only for an extremely short time; in fact, to receive, in this manner, 100 observations and to process them up to the transcription into the data file is a matter of seconds. (Data reduction alone, to obtain Δt, ΔRA, for 100 observations with off-time output lasts only 1½ seconds.) We will probably make this data acceptance of the computer completely automatic by using the in–output system with the interrupt feature in such a way that any program can be interspersed with this routine. One tentative plan is to allot about 16K of the core to permanent storage of all constants and routines necessary for this reduction and to utilize the remainder of the memory for transient storage of other programs. This would eliminate tape access time and speed up the reduction process even more.

Let us recapitulate: Data acceptance from stations in coded format is fast becoming a completely automatic process; it includes, in addition to decoding and conversion into standard format, a self-checking routine which eventually lets only "good observations" appear in the data file. Under normal circumstances this system will accept about 80 to 90% of the incoming data as being correct and useful for further calculations. What happens to the rest? Obviously, we cannot utilize apparently "wrong" data directly. These data are thrown out of the computer with the appropriate remark as to why they were rejected and are then checked in the Data Control Group where "human computers" will make an attempt to rectify errors, if possible, and, in doubtful cases, even may contact the observer for clarification. This, however, happens only after the machine has already tried to find the error. One likely error obviously is the assigning of an observation to the wrong object—these things in the sky unfortunately have no names attached. If, in the reduction check, the deviations are too large, the machine will attempt to find another satellite for which the observation is better reduced, i.e., comes close to the prediction according to its elements. If so, the machine will use the observation with this object; however, in the data file this will also be noted. This latter procedure is qui necessary since, in some of our sensor systems, a reliable identification of the object is not very easy (e.g., a "fence crossing" only gives an analog signal, and it is only possible to assign a specific satellite by knowing that, at this particular spot and time, this satellite "should" be observed). In such cases, the 709 will make the identification.

If, however, the observation is otherwise all right but no satellite can be found, the 709 is programmed to reject this observation by kicking it out and by stopping—a notification to the operator that an unknown object has appeared. Then this datum is transferred into a special "new object file," and once sufficient data are accumulated the operator, in conference with the duty analyst, will start the operation of attempting a new initial orbit determination.

In normal operation, however, the next step would be the routine issuing of predictions, etc. There are two cases to discuss: (1) The case in which satellite elements in the 709 are still satisfactory. In this case, using these elements, one goes upon command into the procedure of computing a new bulletin, which entails (a) the proper updating of the elements to the new epoch, (b) the computation of the equatorial crossing times and longitudes, and (c) the obtaining, if necessary, of a new "grid," i.e., the values for reducing equatorial crossings to other latitudes and the heights of the satellite above the Earth's surface. (2) The case in which the comparison of the previous predictions with the observations has shown that systematic deviations have started to build up (this, at the moment, is determined subjectively by the duty analyst, but will later on be done automatically by the 709). In this case, in short intervals of time (i.e., every three days or so), a partial element correction is performed by least-squaring of the Δt values (automatically from the Δt vs

N on the data file data); once every ten days to two weeks (or more frequently if desirable), a complete differential correction of the elements is performed. After the better elements have been obtained, the prediction process as in (1) is performed.

The program routines necessary for these steps are kept on tapes to be used in conjunction with data file tapes or, in some cases, with punchcards. It is obvious that at the moment, with relatively few satellites in orbit, these processes can be initiated by human decision. Later, the scheduling of such operations certainly will be under control of the executive program, where this program will initiate the new prediction routines according to either schedule or need, as given by buildup of deviation observed minus deviation computed.

In addition to these routine, or general, predictions (they are issued for general consumption), we have to give to some of our sensors more detailed information such as look angles or fence crossing times. These are either routine (i.e., for a given sensor a certain number of satellites will be computed routinely to obtain all possible passes) or they may be made upon special requests.

All prediction data are computed in the 709 from the elements stored in the core, from data (observations) on tape, and from programs usually also available on tapes. If it is a routine matter, for example, the operator will attempt to compute all bulletins due, in sequence, so that they have to read in the program only once from tape into the memory; he then will compute all requested look angles and, finally, all fence crossing times. Such a sequence, at the moment, takes anywhere from ½ to 3 hr, depending upon the total number of predictions necessary. All machine output is recorded on tape, and only monitoring comments are typed out on-line to avoid unnecessary delays. At suitable intervals, the tape containing results is switched off-line and punchcards are obtained. These are then transformed into teletype tape using the IBM 063 (in fact, since this machine is very slow, we use two such machines in parallel), and, finally, the tape is sent up to the Communications Center for transmission. In case of look angles for specific stations, we patch the TWX transmitter at the 709 directly into the TWX channel and transmit directly from the Computer to the station; only addresses, etc., are added at the Communication Center while patching the lines together.

It is obviously premature to give you any estimates here about the speed with which we are operating in this system. In many cases, the data reduction speed (which is quite high) has no relationship to the prediction speed, since predictions are done on a scheduled routine as far as possible. However, I can tell you at least one thing: In case of a normal launch, say a *Discoverer*, our data reduction of initial data, the obtaining of orbital elements, and the computing of a bulletin, have been so fast that, in the last few launches, our bulletin was ready for transmission well before the moment when the DOD did announce successful launch. Since our predictions are (a) unclassified and (b) go also to overseas addresses, we are not allowed to issue bulletins before the launch is officially announced—but in all cases we were able to issue the first bulletin within minutes of this announcement.

I hope that, from my account, you have obtained an indication of how the NSSCC computations are operating. Let me repeat once more this fact: We have developed this system from small beginnings, and even now our 709 system has been in operation just about six weeks. Quite obviously, our system, as I have described it, is still full of inadequacies and will be changed quite drastically in some respects. It is also not yet in full operation, but we can see at least some of the problems and our operation is attempting to give preliminary answers.

Our strength, but also our difficulty lies in the fact that while we are developing better methods we still are charged with the responsibility to perform now, to be at all times operational and, while developing a "good" system, we have to produce here and now. This is quite a problem at times, but let me assure you—it is also great fun and my colleagues and I enjoy it immensely.

Smithsonian Astrophysical Observatory Differential Orbit Improvement Program[1]

G. VEIS and C. H. MOORE

Smithsonian Astrophysical Observatory,
Cambridge, Mass.

ABSTRACT

The differential corrections program employed at the Smithsonian Astrophysical Observatory for orbit improvement presently employs the standard equatorial elliptic elements. Mean elements over a single revolution are defined. Variations of these mean elements produced by secular long-period and drag terms are represented by convenient series developments in time. These terms may be treated as input or output.

Short-period perturbations are included to the first order and are applied to the reference orbit at the time of the individual observation.

Due to the large number of parameters required to represent the orbit, the program is generally used in a series of successive approximations. Individual determinations are run for about one week's observations with assumed coefficients for the higher order terms in the secular expansions.

The program is extremely rapid and flexible, allowing corrections of any selected parameters.

The program cannot be employed for cis-lunar orbits.

[1]This writeup of DOI is intended to provide enough relevant details to serve as a reference adequate for normal usage. It is not self-contained, but assumes a familiarity with typical applications and experience in interpreting the input and output formats. Special applications are often possible with only minor changes in the program. However, the only reference of any value in such a case is the program listing.

The program is presently coded for an 8K 704 with optional use of 8K magnetic drums for additional storage.

Appreciable changes are planned in the next few months which will result in a program that will not correspond to the details of this description.

I. INTRODUCTION

The program referred to at Smithsonian as the "Differential Orbit Improvement Program" was designed in the fall of 1958 by Dr. George Veis as an outgrowth of his dissertation concerning geodetic applications of Earth satellites. The program was originally intended to provide determinations of improved station positions on the basis of satellite observations. However, as the program evolved, emphasis shifted from purely geodetic applications until, as presently coded for an SK 704, it is used for routine processing of observations. In that capacity it produces the input for Smithsonian's prediction programs and forms the basis for most analytical examinations which utilize satellite observations.

One of the problems encountered at Smithsonian, which the program must be able to handle adequately, concerns the types of observations available. Efforts at Smithsonian are directed chiefly to obtaining optical observations. Good optical observations require photographs, the main source of which are the twelve Baker-Nunn camera stations located in various parts of the world. The cameras differ from ordinary telescopic cameras in that they can track satellites at the relatively high angular velocities required and thus obtain good photographs of faint satellites. Two qualities of observations are obtained from these cameras. Immediately available are measurements of the films made at the stations with angular accuracies of a few minutes of arc. Several weeks later, more precise measurements of the films are made in Cambridge, with accuracies of a few seconds of arc. For the brighter satellites, visual observations are provided by Moonwatch teams, with accuracies of about one-half degree, and occasionally photographs are obtained from more conventional astronomical telescopes. Minitrack observations are sometimes used to supplement the optical observations of those satellites whose transmitters are still operating and whose ranges and positions are occasionally obtained from radar stations. Diversified observations are thus available, all characterized by the fact that they are observations of position, as distinct from observations of velocity (i.e., doppler slopes or range rates).

Among the problems introduced by this variety of observations is the fact that a fairly complex input routine must be provided to read and distinguish between the various types. The differing accuracies require that each observation be considered in the light of its accuracy; i.e., it must be weighted in some manner prior to its consideration. This is done by assigning nominal accuracies to each type of observation, or perhaps to each station, depending upon the accuracy of the observing equipment used and previous statistical determinations of resulting accuracies, where available. To minimize internal complications due to the fact that observations may refer to one of several coordinate systems, all observations are converted to a sidereal system; ranges are invariant, but directions are expressed as direction cosines and positions in rectangular coordinates. Thus, internally there are only three distinct types of observations, all referred to the same coordinate system.

To treat the precise measurements of the Baker-Nunn observations adequately, it was necessary to accurately define the coordinate system to which they are referred. The system eventually chosen was the customary sidereal system, referred to the equinox of 1950 and the equator as of the date of the observation. The chief consideration in defining this system was that the orbits of close Earth satellites are more likely to follow the instantaneous equator of the Earth than an inertial equator which is independent of the motion of the Earth. The equinox was left at 1950 to allow a simple expression for sidereal time. This system may be more precisely defined by the matrices used to rotate a coordinate system with a different equinox and equator from that defined, but these will not be given here.

This, then, is the information the program has available to it and the framework in which it must work. The information desired comprises orbital elements which are consistent with the observations available and are to be determined on the basis of minimizing the weighted squares of the residuals of the observations. The orbital elements employed by the program are the elliptical elements: argument of perigee, right ascension of the ascending node, inclination, eccentricity and mean anomaly, referred to a convenient epoch. Mean motion is determined as the time derivative of mean anomaly and is used to compute the semimajor axis of the orbit, with the additional assumption of an ellipsoidal Earth. These are "mean" elements in the sense that they represent the orbit over an entire revolution. Those perturbations which have no net effect upon the elements after a revolution (short-period perturbations: period less than the period of the satellite) are computed from theoretical expressions and used to convert the mean elements to instantaneous osculating elements at any point of the orbit. At present, short-period perturbations include only the effect of the second harmonic in the expansion of the Earth's potential; however, in the near future the effect of

atmospheric drag as characterized by a restriction in the vicinity of perigee will be included.

The basic philosophy of the program is phenomenological in the sense that only significant observed variations in the orbital elements will be considered, rather than whatever variations one expects. The use of short-period perturbations is not quite consistent with this approach; however, it is required by the characteristics of optical observations. In order to obtain an optical observation, two conditions must be fulfilled: the satellite must be illuminated by the Sun, or provided with a light, and the station must be in the Earth's shadow. These conditions are normally met only at two limited regions of the orbit, with the result that all observations must be made within these regions; hence observations well distributed along the orbit are rarely obtained. A direct treatment of these observations results in the determination of osculating elements, which will change irregularly as the zones of visibility change. The definition of mean elements and the application of perturbations are intended to avoid this difficulty.

Secular and long-period perturbations of the orbital elements are included in the following way: Each of the five orbital elements is expressed as a function of time utilizing a combination of a polynomial, sine terms and an asymptotic function which is useful near demise. Thus, in reality it is not the orbital elements that define the orbit of the satellite, but rather the parameters of the expressions representing the time variation of the elements. It is these parameters that are read and treated as variables by the program and for which improved values are ultimately obtained. This approach is particularly useful in representing the mean anomaly which is subject to irregular variations resulting from fluctuations in the drag produced by the atmosphere of the Earth. An expression commonly used is a quadratic polynomial which defines a constant acceleration. However, a higher order polynomial or sine terms are often used to provide a better fit over a longer interval of time. Any of the parameters used to define the orbital elements may be treated as variable, allowing assumptions made concerning the variation of the elements to be conveniently verified.

Considerable effort has been put into making the program as simple to use as possible. The input has been simplified, the output has been minimized and labeled, and the internal operation of the program has been made completely automatic. Thus, relatively little experience is required to use the program, which is a considerable advantage both for routine and special purpose applications. The input includes a specification of the expressions to be used to represent the orbital elements, approximate values of the parameters used in these expressions, and an indication of which parameters are to be treated as variables. The only other inputs are the observations themselves, which are available on standard observation cards, and the coordinates of the stations that made the observations. The program examines the observations, computes corrections to the orbital parameters, and re-examines the observations, repeating the process until convergence is attained. The output ultimately produced includes an indication of the process of convergence, the final corrected values of the orbital parameters and their standard deviations, and the residuals of the observations referred to the final orbit.

The sequence of operations of the program is as follows: The program reads the orbital elements, station coordinates, and observations and converts the observations to the defined sidereal system. The osculating elements are computed for each observation by evaluating the expressions for the mean elements at the time of the observation and adding the perturbations. The position of the satellite and the partial derivatives of position with respect to the orbital parameters to be varied are computed from the osculating elements. The position of the station is determined and the position of the satellite relative to the station. A pseudo-observed position is then computed by employing the computed range with the observed direction or the computed direction with the observed range as necessary. This allows a uniform treatment of the various types of observations in the following computations. The pseudo-observed and computed positions are then compared and the observation rejected if the disagreement is too large. If the observation is retained, there results a set of equations expressing corrections to the orbital parameters in terms of residuals and partial derivatives of position expressed in rectangular, sidereal coordinates. A matrix rotation is then performed to rotate the residuals to the original observed coordinate system, at the same time reducing the number of equations to the number of variables actually observed. That is, three equations with rectangular residuals might be reduced to two equations with residuals expressed in terms of altitude and azimuth, or whatever is appropriate. These equations are added to a set of similar equations resulting from other observations and will ultimately be solved by the techniques of least squares.

The contribution of each observation to the least squares solution is weighted by the inverse square of the assumed accuracy of the observation. After all observations are considered, the standard deviation of an observation so weighted is computed. This method is

employed in two ways. Observations will be rejected if their weighted residual is greater than three times the standard deviation as determined by the previous iteration. Moreover, after all observations have been considered in the present iteration, residuals of an observation will be compared with the current standard deviation, and if any observations are rejected at this stage, the standard deviation will be recomputed from the remaining observations and this process repeated until no further observations are rejected. This technique has the effect of forcing a more normal distribution upon the residuals of the observations and is remarkably effective in locating bad observations before effecting a solution and improperly correcting the orbital parameters.

The standard deviation is also used to define convergence of the iterations. A change of less than a tenth of one percent in the standard deviation between successive iterations is required for convergence.

The speed of the program is an essential characteristic in determining the extent to which it can be employed. The coding was intended to produce as efficient a program as possible, and to date that efficiency has given the following results. Observations may be read at a rate of 10 per second. They are examined and their contributions to the least squares solution computed at a rate of 2 per second. (The time required to actually obtain the corrections to the parameters is negligible.) If an average run is considered as consisting of 50 observations with perhaps 7 variables, it would require about 4 iterations for convergence or about 2 minutes of machine time. A longer run employing perhaps 500 observations and 10 variables might require 10 iterations or about 45 minutes of machine time. The length of such a run is not unreasonable if one considers that with the volume of observations used by Smithsonian, 500 observations might cover a period of 6 months. The increase in the number of iterations required results both from the added difficulty of identifying the bad observations and the additional degrees of freedom in the least squares solution.

Some typical applications of the program might be useful to illustrate the sort of results which may be obtained. Specific examples of satellites, however, will be avoided.

The major routine application of the program is in obtaining orbital elements which may be extrapolated for prediction purposes. The expressions for the elements used in making predictions are usually rather simple, rarely involving more than a quadratic polynomial and perhaps a sine term. Since the secular and periodic variation of the elements has usually been previously determined, only the constant terms of the polynomials and the first and second derivatives of mean anomaly are varied. This results in a total of 7 variables. Predictions are normally made a week in advance, utilizing the elements determined from the previous 2 weeks' observations. Using the program in this way, orbital elements suitable for predictions may be conveniently, indeed automatically, obtained. The program is also used on a daily basis to compare the observations that have been obtained with the predictions from which they resulted in order to keep track of the accuracy of the predictions. This is done by examining the residuals of the observations from the prediction orbit as printed out by the program when no parameters are varied. If these residuals exceed a tolerable maximum before new predictions would normally be prepared, corrective action can be taken.

The program may also be used in an analytical sense to determine values of the orbital parameters, utilizing observations over a specific interval of time. For instance, observations covering an interval of 6 months might be used to determine secular variations or amplitudes of periodic variations which would be poorly determined over a shorter interval. The program is fast enough to make such applications feasible. An alternate examination over extended intervals utilizes a special feature of the observation input whereby observations covering a specified interval of time are read and the elements determined at the center of the interval. Then observations covering an interval equal in duration but displaced in time from the previous are used and the elements evaluated at another epoch. Thus, the elements can be determined successively on the basis of observations centered about the epoch. The observations for successive determinations may overlap if necessary to provide enough observations to permit a determination of the elements. Such techniques have been used successfully in determining definitive orbits, which for well-behaved satellites may cover intervals some months in duration.

The program may also be used in two ways with reference to the originally intended geodetic applications. The position of a station may be varied in addition to the orbital parameters. If, for instance, observations are available from a station located on an island, the position of the station, hence the position of the island, might be varied and determined more accurately than before. Moreover, if there are groups of stations whose relative positions are accurately known, the positions of the groups may be varied relative to one another. That is, a group of stations may be treated as a unit and the same correction made to the position of each station. Thus, if there are several stations on the island, their relative positions will not be changed, but the position of the island may

be varied. By the same approach, the relative positions of continents may be varied.

There is an additional possibility of varying the shape of the Earth. Irregularities in the Earth's potential result in periodic variations in the orbital elements. Such periodic variations may be included in the expressions for the elements and the parameters of the expressions treated as variables. If the presence of such effects can be determined from the observations available, this should be evident from the resulting values of the parameters and their standard deviations.

The results of geodetic investigations so far have not produced improvements in the accuracies with which the positions of stations are known, but they have suggested some irregularities in the Earth's potential. The limitation has been in the agreement attainable between observations and computed positions. However, improved treatment of precise Baker-Nunn observations with residuals reduced to less than 20 seconds of arc provide a hopeful basis for improved results.

This completes a brief description of Smithsonian's Differential Orbit Improvement Program. Modifications which are planned in the near future include the addition of short-period perturbations due to drag at perigee, an increase in the number of stations and observations that may be used, and an appreciable increase in the speed of the program. A more detailed description of the program, heavily weighted toward describing input and output conventions but containing a complete description of the coordinate system and the equations used, is available through Smithsonian.

II. INPUT

The input deck serves two distinct purposes:

1. It specifies the station coordinates, observations, and orbital elements the program is to use.
2. Through code numbers it controls the operation of the program. Appreciating the flexibility thus provided is essential for effective utilization of the program.

The input deck consists of BCD cards of which columns 1–72 are interpreted. It may be read at the on-line card reader or from a BCD tape previously prepared at an off-line card-tape unit. The input unit is determined by Sense Switch 1:

SS1 Down: on-line card reader
Up: tape 4

Initially, and when necessary thereafter, the program refers to the input deck for instructions. These instructions take the form of a code number punched in the first column of a card (command card). Other information may be punched on the card but is interpreted later.

The code numbers and meanings are:

0 (or blank)—stop
1—read station coordinates
2—read orbital elements
3—read observations and improve orbit
4—improve orbit
5—restore original orbit
6—read stations to be varied
7—select output unit
8—skip *n* of every *n* + 1 observations read

The action initiated by each of these codes will be considered in detail. The description serves as a reference as well as an explanation, so information is included that is usually unnecessary.

0 (or blank)—stop

This causes the normal program stop (*HTR* 13241 in 13260). Thus, if input is from tape, a blank card should be the last record, while if input is at the on-line card reader, three blank cards should terminate the input deck

(an extra two to feed in the first). Pressing start causes the program to look for another command card.

The instruction *TRA* 13241 may be executed manually from any portion of the program (unless the machine is already reading input) to force the program to look for another command. This will usually result in losing the orbital elements already in memory, though no other damage is possible. To guarantee retaining the orbital elements, *TRA* 17145 will restore the original orbit, print out the residuals of the observations, and then look for another command.

1—read station coordinates

The cards which follow contain the station coordinates to be read into core memory. The command is terminated upon encountering a blank card. Station coordinates may be read at any time so long as they precede the observations with which they are to be used. They replace any coordinates previously in memory.

A station coordinate card is defined as containing the following information:

1. Station number (a positive, nonzero, decimal integer less than 10,000).
2. The geodetic rectangular coordinates of the station (megameters) in the order x, y, z.
3. The latitude of the station (radians).

These four data are read from columns 1–48 of the card and should follow the conventions of the variable field input routine (see description). Thus, only the order and mode of the numbers are significant. The rest of the card is ignored.

Storage is available for 100 stations (7 data per station). If more than 100 stations are included in a deck, the first 100 will be retained. The stations must be in ascending numerical order by station number. To reduce search time, as few stations as possible should be used.

2—read orbital elements

Any title which appears in columns 25–72 of the command card is printed, and the following cards are interpreted as a set of orbital elements.

The first card contains the element identification code. This consists of (1) a description of the functions used to describe each orbital element and (2) the parameters of these functions which are to be treated as variables. The following conventions are employed:

The orbital elements are assumed to be in the order ω, Ω, i, e, M. The functions (of time) used to express each may include polynomials of degree 0–7 inclusive:

$$\sum_{0}^{7} P_i (t - t_0)^i \qquad \text{(coded } P0, \ldots, P7\text{)}$$

sine:

$$S_0 \sin [S_1 + S_2 (t - t_0)] \quad \text{(coded } S\text{)}$$

exponential:

$$E_0 e^{E1 (t - t_0)} \qquad \text{(coded } E\text{)}$$

hyperbolic function:

$$H_0 (H_1 - t)^{H2} \qquad \text{(coded } H\text{)}$$

The sum of any combination of functions may be chosen to represent each element provided that a polynomial is included. The program recognizes a polynomial as beginning to define the next element; hence, it must appear first.

The code representation of each function is followed by a code digit for each parameter in the function. If this digit is 1 the parameter will be treated as a variable. If this digit is 0 the parameter will be treated as a constant. The digits refer to the parameters in the order they appear in the definitions above.

Any of the parameters may be varied, in any combination save that in a polynomial; if a coefficient of a term of given degree is to be varied, all coefficients of terms of lower degree must be varied also.

As a sample, the element identification code (*P*2100 S100 *P*2110 S011 *P*01 *P*100 *E*10 *P*111 *H*111 S000) indicates:

ω:	quadratic polynomial	vary constant
	+ sine	vary amplitude
Ω:	quadratic polynomial	vary constant, derivative
	+ sine	vary phase, frequency
i:	constant polynomial	vary constant
e:	linear polynomial	(vary nothing)
	+ exponential	vary amplitude
M:	linear polynomial	vary constant, derivative
	+ hyperbolic function	vary all three parameters
	+ sine	(vary nothing)

The following limitations are inherent or defined by storage limitations: A total of 5 to 25 functions may be employed containing a maximum of 72 parameters, of which 0 to 23 are variable. (The maximum of 23 variables includes station coordinates.)

The code words (one function/word) are punched in columns 1–72 with at least one blank between words (extra blanks are ignored). The code is assumed complete upon encountering blanks in columns 1–6 or 66–72. If 2 cards are necessary, a word in the first must end in columns 66–72, whereupon the interpretation will continue with the next card. If the last word ends in columns

66–72, a blank card must be provided to terminate the interpretation.

After reading and deciphering the element identification code, the program interprets the following cards as containing:

1. The epoch—the reference time for the expressions describing the orbital elements (t_0). It is composed of 2 decimal fractions: day number (Julian day number $-2{,}400{,}000.5$) and fraction of day (UT).
2. The parameters which define the elements in the order specified by the element identifications code. The units for ω, Ω, i are degrees, those for M are revolutions, those for the argument of a sine are degrees. The unit of time is days.

These are read according to the conventions of the variable field input routine (see description) and only the order is important. A blank card terminates the input, whereupon the program prints the initial orbital elements, identifying each element and function as instructed by the element identification code, and looks for its next command.

Several options are available in the element input. If a blank card is substituted for the element identification code, the code already in the machine will be retained unchanged. The program will proceed to read in different parameters (including epoch).

If no parameters (or epoch) are read (blank card immediately follows terminated element identification code) the existing parameters will be retained, but the new identification code will be applied. The elements will not be printed.

3—read observations and improve orbit

Any title appearing in columns 25–72 is printed. Four decimal fractions may appear in columns 3–24 (see below). The cards which follow are interpreted as observations. They may be treated in 3 ways:

1. A maximum of 155 observations are read and stored in core memory (8K). A blank card terminates the observation input, and control is transferred to the main computation loop. (Magnetic drums are not referred to.)
2. A maximum of 628 observations are read and stored on drums 4–1. Input is terminated either by a blank card or the 628th observation and control transferred to the main computation loop. If 628 observations were used, after completing the element improvement, control is returned to the observation input. Ultimately, the input is terminated by a blank card.
3. n_2 days of observations are read into core (maximum of 155 observations) and control is transferred to the main computation loop. After completing the element improvement, the first n_1 days of observations are deleted and an additional n_1 days read. Ultimately the input is terminated by a blank card. More than 155 observations per interval cause hopeless confusion; input must be reinitiated from a new "3" card to continue. The observations must be in chronological order, since the times of the observations define the observation to be used. The order is immaterial in cases (1) and (2), however.

Cases (1) and (2) are identical, except that drums are not referred to if the conditions for (1) are met. Cases (2) and (3) are distinguished by the numbers punched in columns 3–24 of the "3" card (variable field conventions). If columns 3–24 are blank, the values read from the previous "3" card will be retained (they are initially zero in a cleared machine).

For case (2) the decimal fractions n_3 and n_4 may be specified:

n_3: integral portion of the epoch to which the improved elements are to be referred. If n_3 is zero, then (1) if n_4 is nonzero, the mean of the times of the observations will be employed as epoch; (2) if n_4 is zero (or blank) the above mean, truncated to an integer, will be employed.

n_4: fractional portion of epoch. If it is not punched, it is considered zero.

For case (3) the decimal fractions n_1, n_2, n_3 (n_4) must be specified:

n_1: (integer) number of days to be deleted from and added to the previous interval to define the next.

n_2: number of days of observations to be included in each interval.

n_3: integral portion of the first epoch desired (the n_2 day interval will be centered about it); n_1 is added to the epoch of the previous interval to determine the epoch of the next.

n_4: fractional portion of epoch. If it is not punched, it is considered zero.

Observations may be read at any time with the following restrictions:

1. The station coordinates to be used must have previously been read. If a station is required whose coordinates have not been furnished, the observation will be omitted and a remark to that effect printed.

2. The orbital elements with which the observations are to be used must have previously been read. (The times of the observations are referred to the epoch of the elements, which may be relocated internally. Hence observations preceding a set of elements refer to the wrong epoch.)

The consequences of entering the main computation loop are described below. From there, control either returns to the observation input or proceeds to seek another command.

The observation cards have a fixed format described in the following pages. The interpretation of this format has been built into the program in such a way that changes involve the coding rather than a format statement. Any appreciable modification would require considerable reprogramming.

4—improve orbit

This transfers control to the main computation loop, the same transfer that concludes the observation input. There, each observation is compared with the orbit, the orbital elements are corrected, and the results (residuals for each observation and improved elements) are printed.

This command would be used, for instance, after a change in the parameters to be treated as variables. An automatic transfer would not follow (as in the case of observation input), so it would have to be initiated.

5—restore original orbit

Normally, after improving the orbital elements, the corrected parameters are used as the initial orbit for successive improvements (i.e., successive sets of observations). Occasionally it might be preferable to return to the original orbit rather than trust the improvement.

If columns 7–12 of the command card are nonblank, the original orbit will be restored after each improvement, just as it is if no improvement is possible (i.e., iterations fail to converge). The original orbit is defined as the orbit in the machine at the time the command is executed, or any orbits read after the command.

The command may be read at any time. To cancel the command, a "5" card with columns 7–12 blank will restore the program to its normal operation.

6—read stations to be varied

The following cards contain the numbers of the stations whose coordinates are to be varied. A maximum of 56 numbers (decimal integers, variable field conventions) may be used, input being terminated by a blank card. Only nonzero integers are considered station numbers, zeros being used to separate groups of stations whose coordinates are being varied as a unit (i.e., varying the position of a continent). If individual stations are being varied independently, their numbers must be separated by zeros.

If no station numbers are read (blank card immediately follows command card) no stations will be varied. The station numbers may be read at any time, provided the coordinates for the stations referred to have previously been read. After completing the input, the stations and their coordinates are printed to furnish a check of the input and a comparison for the corrected coordinates printed later.

With each group of stations to be varied, 3 variables (x, y, z) are associated, so at least 3 observations must be available for each group or a singular matrix will result. A maximum of 23 variables (including orbital parameters) is imposed by storage limitations.

The program will continue to vary the station coordinates until instructed otherwise. However, the coordinates themselves remain unchanged in memory (although a correction is computed and employed) so that corrected coordinates are not used for successive sets of observations.

7—select output unit

Tape 2 is the normal output unit for the considerable output which the program produces. This command may be executed at any time to select another output unit, allowing output to be put on different tapes or printed (punched) on-line. The decimal address of the unit desired is punched in columns 3–6 of the command card.

Any comment punched in columns 7–72 of the command card will be printed on-line to help identify the output or to locate the position of the program within a large input deck.

8—skip n of every $n + 1$ observations read

To cover a large interval in time which includes more than 628 observations, it is useful to be able to exclude observations without destroying their order by sorting.

This command reads the number (n) of tape records (observations) the program is to skip between observations; n is a decimal integer punched in columns 3–6 of the command card. Several restrictions are apparent:

1. Observation input must be from tape (Tape 4).
2. $n + 1$ blank cards must terminate the observation input, since it would be difficult to predict which blank card will be read (the skipped records are not examined). This may leave n blank cards for the

computer to encounter when it seeks its next command, each of which will cause the normal program stop (which may be overcome by pressing start).

Other commands may be defined as the need arises. Program constants may be conveniently altered in this way. All that is required is to store the constant in the proper place, since the variable field input routine will translate any number in columns 1–23 of the command card.

The commands may be executed in any order (with a few restrictions) and, by utilizing this generality, complex input decks may be formed which can yield more information or induce more certain convergence than would otherwise be obtained.

III. OUTPUT

PKEDIT is used to prepare and print the output. Floating point numbers are printed with the sign of the exponent and a 2-digit exponent (of a power of 10) followed by the sign of the fraction and a normalized fraction ($0.1 \leq |f| < 1$). Thus, the decimal point is understood to precede the first digit of the fraction.

The output is designed for a 120-character tape record to be printed with program control. It is possible to print (or punch) the output on-line; however, this produces a 72-column record with no spacing control, which is difficult to interpret.

Output may occur at three stages of the program: during input, during computation, and upon completion.

During input, the command cards might produce the following output:

0—stop: (none)

1—read station coordinates: (none)

2—read orbital elements:

Program title and any title punched in columns 25–72 of the command card.

The initial orbital parameters, interpreted and labeled as specified by the element identification code. The elements are labeled:

argument of perigee *W*
right ascension of the ascending node *ND*
inclination *I*
eccentricity *E*
mean anomaly *M*

The functions are labeled:

polynomial *P0*–*P7*
sine *SN*
exponential *EX*
hyperbolic function *HY*

Each function is followed by its parameters in the order and with the units specified by the definition (see Section II). The parameters are printed as 8-digit floating point numbers. If a parameter is to be varied, it will be followed by a 2-digit floating point zero, which will eventually correspond to the standard error of the parameter.

3—read observations and improve orbit:

Program title and any title punched in columns 25–72 of the command card (printed whenever the observation input routine is entered).

If an observation refers to a station whose coordinates are not in memory:

OMITTED OBSERVATION (observation no.)
MISSING STATION (station no.)

4—improve orbit: (none)

5—restore original orbit: (none)

6—read stations to be varied:

Title

Station number and coordinates (megameters) of each station to be varied. Groups of stations to be varied as a unit are separated by a heading, with stations within a group listed beneath the heading.

7—select output unit:

Any comment punched in columns 7–72 of the command card. Printed at the on-line printer.

8—skip *n* of every *n* + 1 observations read: (none)

During the computation the results of each iteration are printed including:

Heading.
Iteration number.
Standard error of an observed quantity[2] σ.
Number of observations used (an observation defined as an input record).
Corrections applied (added) to the current values of the variables.[3]

If SS2 is down, the iteration number σ and the number of observations are also printed at the on-line printer to allow monitoring the convergence of the iterations. (With few observations, the printer cycle time becomes an appreciable fraction of the time required for an iteration.)

If the program cannot obtain a solution, the reason is printed and the program continues:

NO OBSERVATIONS: the program read too few or rejected too many observations to permit a solution (fewer equations than variables).

ECC. OUT OF RANGE: the eccentricity was outside the range $0 \leq e < 1$ due either to input error or to an excessive correction applied by the program.

SINGULAR MATRIX: input error or lack of observations from a station being varied resulted in a singular matrix.

NOT CONVERGING: 21 iterations were completed without converging to a solution (about 5 iterations should suffice). Convergence is defined as a change of less than 0.1% in successive values of σ.

DIVERGING: 3 successive iterations resulted in increasingly large values of σ. Apparently the iterations will not converge.

Upon converging to a solution the program prints: (1) the elements of the variance–covariance matrix (as 2-digit floating point numbers) interrelating the errors of the variables; (2) the order and units corresponding to the corrections applied each iteration (suppressed if SS3 is down); (3) the final corrections to the positions of the stations that were varied (megameters), followed by the corrected station coordinates in the same format as the original coordinates.

The program title and title from the observation input are printed as a heading followed by: (1) number of observations and σ from the last iteration; (2) standard error in the orbital longitude [$\Delta(\omega + M)$, deg]; (3) instantaneous values of the orbital elements [$\omega, \Omega, i, e, M, (n)$] evaluated at epoch; (4) semimajor axis and perigee (megameters) evaluated at epoch, epoch specified by the observation input; (5) corrected values of the orbital parameters in the same format as used for their initial values.[4]

The program title and title from the observation input, and the residuals of the individual observations (suppressed if SS3 is down) are printed under a heading followed by: (1) observation number (if negative the observation was rejected and no residuals are available); (2) station number; (3) time of observation (day and fraction UT); (4) mean anomaly at the time of observation (revolutions); (5) differential residual in mean anomaly (O–C; revolutions; as a differential expression it is valid only if small, i.e., less than 10^{-2} revolutions); (6) positional error (megameters; the distance between observed and computed positions of the satellite); (7) precision of observations (seconds; expected accuracy of the observation, as determined from the position precision index); (8) differential residual in observed quantities[5] (O–C; angles, sec; range, megameters).

If no solution is obtained (no variables are specified, or trouble occurs), the residuals of the observations are printed (regardless of the position of SS3) referred to the original orbit. This provides a qualitative evaluation of the agreement between orbit and observations. After printing the residuals, the program either returns to the observation input or seeks its next command.

[2]The units refer to the position precision assigned each observation. If $\sigma < 1$, the agreement between orbit and observations is better than the precision of the observations would lead one to expect. If $\sigma > 1$, the orbit leaves residuals in the observations σ times those expected from the accidental scatter of the observations.

[3]The units are the same as the units of the input, save that degrees are everywhere replaced by radians. The corrections are printed as 4-digit floating point numbers in the order: (1) corrections to station coordinates (in the order x., y., z.) in the order in which the groups were listed; (2) orbital parameters in the order they appeared in the input.

[4]Each parameter that was varied is followed by its standard error (a 2-digit floating point number) in the same units as the parameter.

[5]Labeled columns identify each quantity: *DEC* ($\Delta\delta$), *RA* ($\cos\delta\Delta\alpha$), *ALT* (Δh), *AZ* ($-\cos h\Delta Z$), *L* (Δl), *M* (Δm), *R* (Δr); as differential expressions they are valid only if small, i.e., less than 1000" or less than 0.001.

IV. METHOD

The procedure followed in obtaining improved values of the orbital parameters is outlined in this section. A list of the equations involved is included to provide a more detailed description. However, reference must be made to the program listing to determine how the computer implements the process.

Basically, the observed position of the satellite is compared with the position computed from the orbital elements. The partial derivatives of position with respect to the orbital parameters are computed and a system of equations formed. Corrections to the parameters are found by solving these equations by the method of least squares. The corrected parameters are used to repeat the process until no further corrections result.

Some relevant details are as follows: Within the observation input routine, an observation is converted from the observed coordinate system to the rectangular sidereal system. If the position was observed, the coordinates are used; if only direction was observed, the direction cosines are used; if only range was observed, it is used.

Within the main computation loop each observation is handled as follows: The orbital elements are evaluated at the time of the observation. The short-period perturbations due to the second harmonic term in the expansion of the Earth's potential are computed. This is done the first and third iterations only; however, the perturbations are stored and applied each iteration (they are insensitive to small changes in the orbital elements). They are treated as first-order differential corrections, the error made in neglecting their squares (approximately 10^{-6}) imposing a limit of approximately 10 meters on the accuracy of the satellite position.

The rectangular coordinates of the satellite are computed and the position of the station at the time of observation subtracted to give the computed position (relative to station).

The observed position is determined from the computed position and the observation as follows: (1) position as observed; (2) direction as observed and computed, range used to determine position; and (3) range as observed and computed, direction used to determine position.

Use is made of a fictitious observed position to permit uniformity in the treatment of various observations. The observation may be rejected if the observed and computed positions (properly weighted) differ by more than $3\sigma'$ (3 times the standard error of an observation) from the previous iteration.

A matrix is formed expressing the residuals (in rectangular coordinates) of the position as linear combinations of the corrections required in the orbital parameters. The coefficients of the matrix are the partial derivatives of the position with respect to the orbital parameters. These are computed by multiplying the partial derivatives of the position with respect to the orbital elements (computed from analytical expressions) by the partial derivatives of the elements with respect to their parameters (functions of time). (If $x(b)$ represents position (x) as a function of the orbit (b), an expansion about the approximate orbit (b_o) yields:

$$x(b) = x(b_o) + \frac{\partial x}{\partial b}\Delta b$$

Since the orbit is a function of the parameters (p)

$$x(b) - x(b_o) = \frac{\partial x}{\partial b}\frac{\partial b}{\partial p}\Delta p$$

To avoid correlations introduced by using rectangular coordinates, the resulting matrix is multiplied by a matrix which rotates the coefficients to the original coordinate system of the observation. In the process the number of residuals is reduced to the number originally observed: 3 for position, 2 for direction, 1 for range.

Conceptually, the resulting matrix is appended to a set of similar matrices from other observations, and the completed system of equations solved by the method of least squares. Storage restrictions require, however, that the contribution of each observation to the normal matrix of the least squares solution be computed immediately.

After all the observations have been examined, the standard error of an observation (σ') is computed from the residuals of the observation (Δx).* A procedure is initiated in which the residual of each observation is compared with $3\sigma'$. If any observations are rejected, σ' is recomputed and the process repeated until no further observations are rejected. This is an effective and highly efficient method of recognizing bad observations; however, it is abandoned as the iterations converge to a solution since it induces instability and blocks further

*$\sigma' = \sqrt{\Sigma \Delta x^2/(N-1)}$, where N is the number of observations.

convergence. The rejected observations are re-examined and their contribution removed from the normal least squares matrix.

The matrix is inverted, the corrections to the orbital parameters computed and applied, and the standard error of an observed quantity (σ) computed.[1] If σ differs by less than 0.1% from its value in the previous iteration, the solution has been obtained. Otherwise, the observations are re-examined with the corrected orbital parameters.

When station coordinates are varied, the only modification is that the partial derivatives of position with respect to station position are placed in the initial matrix. The corrections to station position are not applied to the stored station coordinates, but are added during the computation of the station position for each observation.

Difficulties which might prevent a solution are described in Sections III and V. The few tests which may detect machine errors merely skip the offending observations.

V. OPERATION

There are three distinct types of problems to which the Differential Orbit Improvement (DOI) program can apply. They may be described in terms of the results desired:

1. Orbital elements which can be extrapolated for prediction purposes.
2. A detailed description of the variations of the orbital elements.
3. Expressions which provide reasonable representations of the elements over an extended period of time (months or years).

Each of these will be considered in detail and the techniques which have proven useful and the problems encountered described.

The extrapolation of an orbit requires a method for predicting how the orbital elements are going to change. At present the assumption is made that they will continue to change in the near future as they have in the recent past. The major difficulty arises with irregular variations (such as atmospheric drag) which cannot be anticipated. Presumably, predictable variations can be included in expressions for orbital elements. Since irregular effects cannot be predicted, one can do no better than extrapolate their current effects and accept resulting limitations on accuracy and range of extrapolation.

A simple, effective technique using this philosophy and the DOI program suggests:

1. Prepare a set of expressions for the orbital elements which take into account those predictable variations deemed important. The expressions should not be needlessly complicated in order to facilitate rapid evaluation. Reasonable expressions for prediction purposes would probably not include more than a cubic polynomial and a sine term (due perhaps to the third harmonic in the expansion of the Earth's potential).
2. Determine which parameters should be varied to provide a good fit over the period of interest. Normally this will not include more than the coefficients of the polynomials, and perhaps not all of those.
3. Fit those parameters to the most recent observations available extending back a time twice that over which predictions are desired. The range of observations used is arbitrary, but twice that to be predicted appears to introduce a reasonable amount of smoothing.
4. Use the resulting parameters as the prediction orbit.

Since effects have been ignored which will eventually become important, it is necessary to keep track of the accuracy of the predictions and to determine when they should be changed. An effective method is to check observations against the predictions which produced

[1] $\sigma = \sqrt{\Sigma \Delta x^2/(N-n)}$, where N is the number of observed quantities (average 2 per observation) and n is the number of variables.

them by comparing the observations with the prediction orbit. If no parameters are varied, DOI will print the residuals of the observations against the input orbit. When these residuals exceed a tolerable maximum, new predictions should be prepared. If the new observations are run and compared in this manner each day, a continuous check can be kept on the accuracy of the predictions.

Since it is usually the mean anomaly that suffers the greatest irregular perturbation and hence is largely responsible for prediction errors, a residual in mean anomaly is printed with the observation residuals. If this is plotted against the time of the observation, another criterion is available for assessing the accuracy of the prediction elements: the extent to which the mean anomaly has drifted from its predicted value.

To determine in detail how the orbital elements vary, it is useful to determine them at short intervals (say 2 days). Usually in a short interval there are insufficient observations to provide a good determination. That is the reason for the Type 3 observation input. From a given epoch a specified range (say 6 days) of observations may be used to determine mean elements at the epoch (mean in the sense that they are averaged over the range used). Moving the epoch ahead by the interval selected (2 days) and dropping and adding the same range of observations will permit an equivalent evaluation at the new epoch. This may be repeated without sorting or selecting observations, providing a practical procedure for obtaining detailed results. Plotting the elements thus obtained against time allows a determination of the expressions useful in describing the elements as well as a picture of the actual variation of the elements. For instance, an expected periodic variation might be so masked by observational scatter that there would be no advantage in including it in a prediction orbit.

For definitive orbits over extended intervals of time, the ability of the program to handle large numbers of observations is invaluable. The procedure just outlined may be employed to give approximate expressions for the input orbit. In particular, the mean anomaly must be fitted rather accurately (less than 10^{-2} revolutions) so that the position of the satellite may be computed fairly accurately. This requires the introduction of functions merely to fit a curve, with no theoretical significance. Sine terms have proven convenient, as there are usually periodic fluctuations present.

With an input orbit obtained, observations may be used covering the period of interest and the parameters improved. If too many observations are available, only every nth may be read, thus covering a larger range without sorting the input. It is suggested that a minimum of time be spent fitting the approximate expressions to be employed as input orbit, since the program is very effective, especially with polynomials, in fitting the parameters, given only a crude approximation. At present some difficulty has been encountered in fitting sine terms over these large intervals, but it is probable that the difficulty lies in the analysis, rather than in the program.

Occasionally, the observation selection function of the program will decide that all the observations are bad. Or perhaps the iterations will fail to converge, a common difficulty being indecision on the part of the program as to which observations to use. Usually such failures are the result of faulty input. If this is not the case, the only advice possible is to remark that since the program cannot treat the problem as stated, the problem must be changed. That means changing either the observations or the input orbit. The former is usually both preferable and more effective. Adding or deleting 10% of the observations usually changes the situation sufficiently to avoid any instability. Sometimes slight changes in the input elements will permit convergence along a different, smoother path. Such difficulties are to be expected, but are fairly easy to get out of. Unexpected stops within the program have invariably been due to input error, which recurs with distressing frequency.

One major application of the program relates to geodetic determinations. Toward this end the station coordinates have been included as variables. The problem thus far has been to obtain sufficiently good agreement between observations and orbit to produce an improvement in the accuracy with which the stations are known. The general technique is to use a limited range of observations (approximately 10 days), determine a good (the best possible) orbit, then vary the stations desired. Eventually both stations and elements can be varied and the best fit determined. The ability to vary groups of stations as a unit promises facility in determining relative positions of continents. Recent improvements in the accuracy of the treatment of photo-reduced Baker-Nunn observations (with residuals reduced to approximately 20 sec) promise a breakthrough in this effort.

Another geodetic application has been the search for a short-period perturbation (diurnal) indicative of a triaxial Earth. The approximate amplitude and phase of the sine term expected are introduced in the elements and varied to seek the magnitude and position of a bulge, presumably in Africa. Examination of the resulting values and their standard errors is indicative of the plausibility of the hypothesis, or to some extent its ability to be substantiated from the information available.

VI. EQUATIONS

The following equations provide a description of the details relevant in the program. They are intended as a guide in following the Smithsonian Astrophysical Program listing and as a reference in deciding exactly what the program does.

A considerable portion of the program is concerned with referring observations to the rectangular, sidereal coordinate system (equinox: 1950, current equator). Observations referred to a local coordinate system require only that the expression for sidereal time be appropriate. Observations referred to the sidereal system must be first corrected to epoch 1950, then corrected for the nutation of the equator since 1950. This is accomplished by the matrix rotations P_1 and P_2, respectively.

A. Treatment of Observations

The treatment of each type of observation is outlined as follows with the input format and coordinate rotation appended:

RA, DEC (α, δ)

Convert to directional cosines

$$l = \cos\delta\cos\alpha$$
$$m = \cos\delta\sin\alpha$$
$$n = \sin\delta$$

Rotate to defined sidereal system[8]

$$\mathbf{l}_0 = P_2 P_1 \mathbf{l}$$

L, M, N (l, m, n)

Correct for refraction (optional)

$$h = \sin^{-1} n$$
$$z = \cos^{-1}\frac{m}{\cos h}$$

Continue as with (z, h)

AZ, ALT (z, h)

Correct for refraction (optional)

$$h = h + k\cot h$$

where $k = -0.0015$ radio, -0.00029 visual

Convert to directional cosines

$$l = \cos h\sin z$$
$$m = \cos h\cos z$$
$$n = \sin h$$

[8]See Section VIB for definitions of matrices P_2 and P_1.

Rotate to defined sidereal system[9]

$$\mathbf{l}_0 = A\mathbf{l}$$

Range (r)

Observed in conjunction with direction

$$\mathbf{x}_0 = r\mathbf{l}_0$$

Observed alone

$$r_0 = r$$

B. Definition of Coordinate System

The matrices used in the coordinate transformations are defined as follows (T_0 refers to equinox of 1950, current equator):

1. Rotation from equinox T_0 to equinox T:[10]

$$P_1 = \begin{cases} -\sin\kappa\sin\omega & -\cos\kappa\sin\omega & -\cos\omega\sin\nu \\ +\cos\kappa\cos\omega\cos\nu & -\sin\kappa\cos\omega\cos\nu & \\ \sin\kappa\cos\omega & \cos\kappa\cos\omega & -\sin\omega\sin\nu \\ +\cos\kappa\sin\omega\cos\nu & -\sin\kappa\sin\omega\sin\nu & \\ \cos\kappa\sin\nu & -\sin\kappa\sin\nu & \cos\nu \end{cases}$$

in which

$$\kappa = [0.11171334\cdot10^{-3} + 0.67743016\cdot10^{-6}(T_0 - 1900)] \times (T - T_0) + 0.14655918\cdot10^{-9}(T - T_0)^2$$

$$\omega = [0.11171334\cdot10^{-3} + 0.67743016\cdot10^{-6}(T_0 - 1900)] \times (T - T_0) + 0.53087098\cdot10^{-9}(T - T_0)^2$$

$$\nu = [0.97189871\cdot10^{-4} - 0.41369151\cdot10^{-6}(T_0 - 1900)] \times (T - T_0) - 0.20687000\cdot10^{-9}(T - T_0)^2$$

2. Rotation from equator 1950 to equator T:[11]

$$P_2 = \begin{pmatrix} 1 & 0 & -\psi\sin E_0 \\ 0 & 1 & \Delta E \\ \psi\sin E_0 & -\Delta E & 1 \end{pmatrix}$$

in which

$$\psi = \psi_1 T + \psi_3\sin A_1 + \psi_4\sin 2A_1 + \psi_5\sin A_2 + \psi_6\sin A_3$$
$$\Delta E = E_2\cos A_1 + E_4\cos 2A_1 + E_5\cos A_2 + E_6\cos A_3$$
$$A_1 = 0.211408241 - 0.924219906\cdot10^{-3}T$$
$$A_2 = 3.49349291 + 0.344055813\cdot10^{-1}T$$
$$A_3 = 2.24736972 + 0.459943057\cdot T$$
$$\psi_1 = 0.668643158\cdot10^{-6}$$

[9]See Section VIB for definition of matrix A.

[10]Angles are in radians, time in years.

[11]Error in matrix elements is less than 10^{-6}; T must be less than 41 yr. Angles are in radians; time in days since Jan. 1.0, 1950.

$\psi_3 = -0.835314579 \cdot 10^{-4}$
$\psi_4 = 0.101229097 \cdot 10^{-5}$
$\psi_5 = -0.616101225 \cdot 10^{-5}$
$\psi_6 = -0.977384380 \cdot 10^{-6}$
$E_0 = 0.409206212$
$E_3 = 0.446455222 \cdot 10^{-4}$
$E_4 = -0.436332313 \cdot 10^{-6}$
$E_5 = 0.267035375 \cdot 10^{-5}$
$E_6 = 0.436332313 \cdot 10^{-6}$

3. **Sidereal time θ:**

$\theta = 0.277987616 + 1.00273781191\,(T - \text{Jan } 1.0, 1950)$ revolutions

4. **Rotation from local [12] coordinates to sidereal coordinates:**

$$\mathbf{l} = A\mathbf{l}$$

where

$\mathbf{x}_s(t)$ = sidereal coordinates of station
$\mathbf{x}_{s0}$ = geodetic coordinates of station
ϕ = astronomic latitude of station (altitude of north celestial pole)

$$\mathbf{x}_s = \begin{pmatrix} \cos\theta & -\sin\theta & 0 \\ \sin\theta & \cos\theta & 0 \\ 0 & 0 & 1 \end{pmatrix} \mathbf{x}_{s0}$$

$$k = \sqrt{x^2 + y^2}$$

$$A = \begin{pmatrix} -\frac{y}{k} & -\frac{x\sin\phi}{k} & \frac{x\cos\phi}{k} \\ \frac{x}{k} & -\frac{y\sin\phi}{k} & \frac{y\cos\phi}{k} \\ 0 & \cos\phi & \sin\phi \end{pmatrix}$$

VII. OBSERVATION FORMAT

Input format of the observation cards is as follows:[13]

Identification Group

Card Column	Content
1–4	satellite identification (ignored)
5–9	5-digit observation no.
10	(ignored)
11–14	4-digit station number

Time of Observation Group

Card Column	Content
15	year minus 1957
16–17	month
18–19	day
20–21	hour (UT)
22–23	minute
24–29	second (4 decimal places)

[12] x = east; y = north; z = vertical.

[13] Blank is equivalent to zero; plus signs may not be punched.

Observation Group[14]

Card Column
30–48

Observation Code Group

Card Column	Content
49	time precision index (ignored)
50–51	position precision index
52	observation type
53	equinox index (*RA DEC* only)
54	instrument description (ignored)

Range Group (when position observed)

Card Column	Content
55–59	range (km) (4 decimal places)
60	exponent of power of 10 multiplying range
61–80	station abbreviation (ignored)

[14] See sequence at end of card format.

Observation Group

Card Column 52	Card Column	Content
0		*RA DEC*
	30	blank
	31–32	hr of *RA*
	33–34	min of *RA*
	35–39	sec of *RA* (3 decimal places)
	40–42	sign, deg of *DEC*
	43–44	min of *DEC*
	45–48	sec of *DEC* (2 decimal places)
1		*AZ ALT*, corrected for refraction
2		illegal
3		*AZ ALT*, uncorrected for refraction
	30–32	deg of *AZ*
	33–34	min of *AZ*
	35–39	sec of *AZ* (3 decimal places)

Observation Group

Card Column 52	Card Column	Content
	40	blank
	41–42	deg of *ALT*
	43–44	min of *ALT*
	45–48	sec of *ALT* (2 decimal places)
4		*LM*, corrected for refraction
5		*LM*, uncorrected for refraction
	30	sign of *L* (blank, minus)
5	31–38	*L* (8 decimal places)
	39	(ignored)
	40	sign of *M* (blank, minus)
	41–48	*M* (8 decimal places)
6		range (megameters)
	30–38	range (6 decimal places)
	39–48	(ignored)

VIII. OBSERVATION LOOP

The major portion of the program is concerned with processing the observations and preparing the equations of condition. This is done once per observation per iteration. The eventual matrix inversion and application of computed corrections completes each iteration.

Evaluate orbital elements (b)

$$\omega = \omega(t)$$
$$\Omega = \Omega(t)$$
$$i = i(t)$$
$$e = e(t)$$
$$M = M(t)$$
$$n = \dot{M}(t)$$

Compute position of satellite

$$a = \left(\frac{k}{n^2}\right)^{\frac{1}{3}}\left[1 + \frac{1}{3}\frac{J}{p^2}\sqrt{1-e^2}\left(-1 + \frac{3}{2}\sin^2 i\right)\right]$$

where

$$p = \left(\frac{k}{n^2}\right)^{\frac{1}{3}}(1-e^2)$$

$$E = M + e\sin E$$

$$\sin v = \frac{\sqrt{1-e^2}}{1-e\cos E}\sin E \qquad \cos v = \frac{\cos E - e}{1-e\cos E}$$

$$l = \omega + v$$

Compute short-period perturbations (see "expressions for short-period perturbations," page 183)

Apply perturbations

$$\Omega = \Omega + \delta\Omega$$
$$\sin i = \sin i + \delta i \cos i$$
$$\cos i = \cos i - \delta i \sin i$$
$$\sin l = \sin l + \delta l \cos l$$

$$\cos l = \cos l - \delta l \sin l$$
$$R = a(1 - e\cos E) + \delta R$$

Compute rectangular coordinates ($\mathbf{x}$)

$$x = R(\cos l \cos\Omega - \sin l \cos i \sin\Omega)$$
$$y = R(\cos l \sin\Omega + \sin l \cos i \cos\Omega)$$
$$z = R(\sin l \sin i)$$

Compute position relative to station ($\Delta\mathbf{x}_s$: computed correction to station position)

$$\mathbf{x}_0 = \mathbf{x} - \mathbf{x}_s - \Delta\mathbf{x}_s$$
$$r_c = |\mathbf{x}_c|$$

Compute error of position

If position observed

$$\Delta\mathbf{x} = \mathbf{x}_0 - \mathbf{x}_c$$

If direction observed

$$\Delta\mathbf{x} = r\mathbf{l}_0 - \mathbf{x}_c$$

If range observed

$$\Delta\mathbf{x} = \frac{r_0 - r_c}{r_c}\mathbf{x}_c$$

Reject observation if $|\Delta\mathbf{x}| > 3\sigma_{i-1}$

(σ_{i-1}: Standard deviation of $|\Delta\mathbf{x}|$ as computed the previous iteration)

Set up equations of condition [$\Delta\mathbf{x} = (\partial\mathbf{x}/\partial\mathbf{b})\,\Delta\mathbf{b}$].

$$\frac{\partial x}{\partial \omega_k} = f_k[R(-\sin l\cos\Omega - \cos l\cos i\sin\Omega)]$$

$$\frac{\partial y}{\partial \omega_k} = f_k[R(-\sin l\sin\Omega + \cos l\cos i\cos\Omega)]$$

$$\frac{\partial z}{\partial \omega_k} = f_k[R\cos l\sin i]$$

$$\frac{\partial x}{\partial \Omega_k} = f_k[-y]$$

$$\frac{\partial y}{\partial \Omega_k} = f_k[x]$$

$$\frac{\partial z}{\partial \Omega_k} = 0$$

$$\frac{\partial x_1}{\partial i_k} = f_k[z\sin\Omega]$$

$$\frac{\partial y}{\partial i_k} = f_k[-z\cos\Omega]$$

$$\frac{\partial z}{\partial i_k} = f_k[R\cos i\cos l]$$

$$\frac{\partial \mathbf{x}}{\partial e_k} = f_k\left[\frac{\mathbf{x}}{R}\left(\frac{ae\sin^2 E}{1 - e\cos E} - a\cos E\right) + \frac{\partial \mathbf{x}}{\partial v}\left(\frac{\sin v}{1 - e\cos E} + \frac{\sin v}{1 - e^2}\right)\right]$$

$$\frac{\partial \mathbf{x}}{\partial M_k} = f_k\left[\frac{\mathbf{x}}{R}\left(\frac{2\pi ae\sin E}{1 - e\cos E}\right) + \frac{\partial \mathbf{x}}{\partial v}\left(\frac{2\pi\sin v}{\sin E(1 - e\cos E)}\right)\right] + f_k^*\left[-\frac{2}{3}\frac{\mathbf{x}}{n}\right]$$

$$\frac{\partial \mathbf{x}}{\partial v} = \frac{\partial \mathbf{x}}{\partial \omega}$$

See following for tabulation of f_k, f_k^*

k	f_k	f_k^*
P_0	1	0
P_1	t	1
P_2	t^2	$2t$
•		
•		
•		
P_n	t^n	nt^{n-1}
S_0	$\sin(S_1 + S_2 t)$	$S_2\cos(S_1 + S_2 t)$
S_1	$S_0\cos(S_1 + S_2 t)$	$-S_0 S_2\sin(S_1 + S_2 t)$
S_2	$S_0 t\cos(S_1 + S_2 t)$	$S_0\cos(S_1 + S_2 t) - S_0 S_2 t\sin(S_1 + S_2 t)$
E_0	$e^{E_1 t}$	$E_1 e^{E_1 t}$
E_1	$E_0 t e^{E_1 t}$	$E_0 e^{E_1 t} + E_0 E_1 t e^{E_1 t}$
H_0	$(H_1 - t)^{H_2}$	$-H_2(H_1 - t)^{H_2 - 1}$
H_1	$H_0 H_2(H_1 - t)^{H_2 - 1}$	$-H_0 H_2(H_2 - 1)(H_1 - t)^{H_2 - 2}$
H_2	$\ln(H_1 - t)\,H_0(H_1 - t)^{H_2}$	$-H_0(H_1 - t)^{H_2 - 1} - \ln(H_1 - t)\,H_0 H_2(H_1 - t)^{H_2 - 1}$

Rotate equations of condition to observed coordinates

$[\Delta \mathbf{l} = \mathbf{C}\Delta\mathbf{x} = \mathbf{C}(\partial x/\partial b)\,\Delta\mathbf{b}]$

If *RA*, *DEC* observed (α, δ)

$$\begin{pmatrix} d\delta \\ \cos\delta\, d\alpha \\ \frac{dr^*}{r} \end{pmatrix} = C \begin{pmatrix} dx \\ dy \\ dz \end{pmatrix}$$

$$C = \frac{1}{r}\begin{pmatrix} -\frac{zx}{rk} & -\frac{zy}{rk} & \frac{k}{r} \\ -\frac{y}{k} & \frac{x}{k} & 0 \\ \frac{x}{r} & \frac{y}{r} & \frac{z}{r} \end{pmatrix} \qquad k = \sqrt{x^2 + y^2}$$

If L, M, N observed (l, m, n)

$$\begin{pmatrix} dl \\ dm \\ \frac{dr^*}{r} \end{pmatrix} = C \begin{pmatrix} dx \\ dy \\ dz \end{pmatrix}$$

$$C = \frac{1}{r}\begin{pmatrix} -\frac{y_s}{k} & \frac{x_s}{k} & 0 \\ -\frac{x_s \sin\phi}{k} & -\frac{y_s \sin\phi}{k} & \cos\phi \\ \frac{x}{r} & \frac{y}{r} & \frac{z}{r} \end{pmatrix} \qquad k = \sqrt{x_s^2 + y_s^2}$$

If *AZ*, *ALT* observed (z, h)

$$\begin{pmatrix} dh \\ -\cos h\, dz \\ \frac{dr}{r} \end{pmatrix} = C \begin{pmatrix} dx \\ dy \\ dz \end{pmatrix}$$

Omit dr/r if range not observed.

$$C = \frac{1}{r}\begin{pmatrix} -\frac{nl}{k} & -\frac{nm}{k} & k \\ -\frac{m}{k} & \frac{l}{k} & 0 \\ l & m & n \end{pmatrix} A^T$$

$$\begin{pmatrix} l \\ m \\ n \end{pmatrix} = A^T \begin{pmatrix} x \\ y \\ z \end{pmatrix} \qquad k = \sqrt{l^2 + m^2}$$

If range observed (r)

$$\frac{dr}{r} = \frac{1}{r}(x\,dx + y\,dy + z\,dz)$$

Print out residuals if iteration completed

Weight and normalize equations of condition
(σ': assumed accuracy of observation)

$$\frac{1}{\sigma'}\Delta\mathbf{l} = \frac{1}{\sigma'}C\,\Delta\mathbf{p}$$

$$C^T\frac{1}{\sigma'^2}\Delta\mathbf{l} = C^T\frac{1}{\sigma'^2}C\,\Delta\mathbf{p}$$

$$(\Delta\mathbf{x} = D\,\Delta\mathbf{p})$$

Return for next observation

Final computation

Reject observations

Compute standard deviation of $|\Delta x/r|_i$ (1)

$$\sigma_i = \sqrt{\frac{\sum_1^n \left|\frac{\Delta\mathbf{x}}{r}\right|_i^2}{n-1}}$$

If $\left|\frac{\Delta\mathbf{x}}{r}\right|_i > 3\sigma$

Repeat observation

Repeat from (1)

Repeat computation loop removing rejected observations from normal equations

Solve normal equations $(\Delta\mathbf{x} = D\,\Delta\mathbf{b})$

$$\mathbf{b} = \mathbf{b}_0 + D^{-1}\Delta\mathbf{x}$$

Repeat if $\frac{\sigma_i - \sigma_{i-1}}{\sigma_i} > 0.001$

Print results

Orbital elements

Repeat computation loop for observation residuals (Included in the observation output is residual in mean anomaly, revolutions)

$$\mathbf{T} = \frac{\frac{\partial\mathbf{x}}{\partial M}}{\left|\frac{\partial\mathbf{x}}{\partial M}\right|}$$

If position observed

$$\delta x = \Delta\mathbf{x}\cdot\mathbf{T}$$

If direction observed

$$\delta x = \frac{\Delta\mathbf{x}\cdot\mathbf{T}}{1 - \left(\frac{\mathbf{x}\cdot\mathbf{T}}{r}\right)^2}$$

If range observed

$$\delta x = \frac{r\,|\Delta\mathbf{x}|}{\mathbf{x}\cdot\mathbf{T}}$$

$$\Delta M = \frac{\delta\tau}{\left|\frac{\partial\mathbf{x}}{\partial M}\right|}$$

Expressions for short-period perturbations

$$\delta L = \frac{J}{p^2}\left[\frac{1}{2}\left\{\sin(2\omega+2v)\left(-1+\frac{7}{6}\sin^2 i\right)+e\left[\sin(2\omega+v)\left(-1+\frac{5}{3}\sin^2 i\right)+\frac{\sin(2\omega+3v)(-1+\sin^2 i)}{3}\right]\right\}\right.$$
$$-\left\{\frac{1}{3}\left(-1+\frac{3}{2}\sin^2 i\right)\left[(1-\sqrt{1-e^2})\sin v\cos v+\frac{2\sin v\left[(1-\sqrt{1-e^2})-\tfrac{1}{2}e^2\right]}{e}\right]\right.$$
$$\left.\left.+(v-M+e\sin v)\left(-2+\frac{5}{2}\sin^2 i\right)\right\}\right]$$

$$\delta R = \frac{1}{3}\frac{J}{p}\left[\left(-1+\frac{3}{2}\sin^2 i\right)\left(1-\frac{1-e\cos E}{\sqrt{1-e^2}}+\frac{(1-\sqrt{1-e^2})\cos v}{e}+\frac{1}{2}\cos(2\omega+2v)\sin^2 i\right)\right]$$

$$\delta\Omega = \frac{J}{p^2}\cos i\left[-(v-M+e\sin v)+\frac{1}{2}\left\{\sin(2\omega+2v)+e\left[\sin(2\omega+v)+\frac{1}{3}\sin(2\omega+3v)\right]\right\}\right]$$

$$\delta i = \frac{1}{2}\sin i\left(\frac{J}{p^2}\cos i\right)\left\{\cos(2\omega+2v)+e\left[\cos(2\omega+v)+\frac{1}{3}\cos(2\omega+3v)\right]\right\}$$

$$p = \sqrt[3]{\frac{GM}{n^2}}(1-e^2)$$

$$a = \sqrt[3]{\frac{GM}{n^2}}\left[1+\frac{1}{3}\frac{J}{p^2}\sqrt{1-e^2}\left(-1+\frac{3}{2}\sin^2 i\right)\right]$$

DISCUSSION

C. H. MOORE: One other thing I might mention before I close is the fact that these orbital elements have been criticized because they fail for zero inclination and zero eccentricity. The equations we use are not singular for either case. I agree that the problem becomes less determinate; you don't know the position of the node if the inclination is zero, and you don't know the position of perigee if the eccentricity is zero, but the program itself will not fail in that case. If you try to vary such parameters under such conditions you may get large standard deviations; the argument of perigee might be determined to within one revolution, but the program itself won't fail. That is the contention I want to make. I've never tried it; it never occurred to me that it would be necessary to try. I think I shall and see just what does happen.

J. V. BREAKWELL: You indicated that you discovered a periodicity due to the third harmonic by considering rather short periods of time in which your number of parameters is reduced so that you don't have too many extra parameters involving slow rates. I would think it would be a rather good moral lesson if you put too many of these things in and didn't find out too much. In other words, it is very difficult to get determinations of these except over a very long period of time, when the drag will probably hurt you.

My second question concerns throwing out observations beyond three sigma. I'm not quite sure what this means. Suppose that you have some pretty accurate camera observations and you've got a pretty accurate orbit and then you don't get pictures for four or five days. Then you get a picture and tie it in with the previous orbit. It is so far off that even though it is remote it is outside 3 standard deviations of its own estimate, since a camera picture is supposed to be very good. Do you throw that picture out?

C. H. MOORE: As it happens, it usually does get thrown out.

J. V. BREAKWELL: Well it seems to me that you're penalizing it. The method I described yesterday might not apply to an individual camera picture, but it says that if you have a host of camera pictures after three or four days, you measure their own standard deviation by measuring, so to speak, a local sigma rather than a sigma associated with the smoothed data and only use that to throw observations out.

C. H. MOORE: Yes, but we don't have a set of measurements; we don't have a local fit.

J. V. BREAKWELL: From Baker-Nunn you get a series of points across the sky.

C. H. MOORE: Not in practice. From the camera station we get a single point. Three weeks later we'll get photo-reduced observations that may include a set of points. But that is useful only for analysis. For predictions there is too much time lost in processing.

J. V. BREAKWELL: In your program you might throw that one out, and that might be the one you should be hanging onto. If automatized in the machine it would be unfortunate. I think the procedure I described gets around this issue and could be automatic.

H. F. MICHIELSEN: It isn't very clear to me why the angles and direction cosines are replaced by positions using the computed range. Is there any advantage in this, or is it impossible to use the angles directly?

C. H. MOORE: It is not impossible, but computationally it is simpler to deal with positions, for you can simply subtract the sum of the positions of the station and the (assumed) observation from the computed position. Otherwise, for each type of observation you have to go through a different process to determine the computed value of the observed quantity, say right ascension, subtract the observed right ascension from it, and then deal with that residual. This way we can treat all the observations equivalently up to the point where we perform a matrix rotation to obtain the final residuals.

H. F. MICHIELSEN: I can see that; but I was wondering if you could use only angles, the right ascension and declination for instance, and work with these instead of working with the position which requires that you use a computed range. Your input is partly observed and partly computed, and it would seem to me that this confuses the program.

C. H. MOORE: I understand your confusion. The residuals we eventually use are independent of range, and the residual in range is identically zero, since observed and computed range were identical. Any confusion that might result from assuming we knew the range is lost at that point by throwing away the irrelevant equation representing an error in range.

J. V. BREAKWELL: I think what it amounts to is that the residual in range is weighted zero in the smoothing procedure.

H. F. MICHIELSEN: In the bulletins, especially of 1958 δ2, I noticed that the coefficients in the polynomials of the right ascension of the node and the argument of perigee, for instance, are many times exactly the same for many weeks, which would indicate that they are not evaluated every time. Are you solving the equations for all or only part of the parameters?

C. H. MOORE: During the routine runs which are made, the five elements are varied and the first and second derivatives of mean anomaly. However, if the differences are not significant, the orbit cards are not repunched, and the slight resulting error is neglected. That probably is not the best attitude, but it is the one that exists.

E. W. WAHL: I think that in this particular case something else should be mentioned. Smithsonian is using visual observations and you know that, naturally, the periods of visibility very strongly influence the use of this method. You have at certain times a satellite visible in the morning, passing on the ascending node, and you will get, for a week or so, a concentration of observations over the United States, or this particular area, and you get observations of only one part of the orbit. After a certain time, especially with δ, it happens that you have no visual observations at all for two or three weeks. This is when the predictions have to stay put. Usually, when you use only visual observations your observations indicate that you can't make any corrections; therefore, your equations are bad after a while.

This is very frequently the reason for the difference between the bulletins of Smithsonian and Space Track. We are using, in addition to visual data, doppler data which, especially with δ, help us over these periods of weeks when the satellite is not visible. At times of visual coverage, I agree perfectly that your method is better than ours, in which we use a rough polynomial fit. However, at the moment when the satellite is no longer being observed, we start slowly catching up. You will find also in the Smithsonian bulletin, I think, that, at certain times, as visibility starts up again, you start rather violent changes in your coefficients, and then you home in very fast and have very good predictions again. This is simply in the nature of the case that you have this part of the orbit only, because the other part, for example, is in daylight. This is sometimes rather tricky.

Technical Aspects of Satellite Tracking on IBM Computers at Smithsonian Astrophysical Observatory in Cambridge, Massachusetts

JOHN P. ROSSONI

IBM Corporation, Federal Systems Division Space Systems, Cambridge, Mass.

ABSTRACT

The Smithsonian Astrophysical Observatory is responsible for the visual acquisition and optical tracking of artificial Earth satellites as well as for the communication of observational data, orbital predictions, and flight analyses to the scientific community. As early as 1956, a complete data processing procedure had to be devised to handle the operations from the time they were received to the time the predictions were sent out. This paper attempts to describe some technical aspects of this procedure as it was developed, without entering into the details of the tracking programs which comprise its main body.

I. INTRODUCTION

The Smithsonian Astrophysical Observatory at Harvard University, Cambridge, Massachusetts, is responsible for the visual acquisition and optical tracking of artificial Earth satellites, as well as for the communication of observational data, orbital predictions and flight analyses to the scientific community. Dr. Fred L. Whipple, director of the Astrophysical Observatory, acts as Project Director. Dr. J. Allen Hynek, Associate Director of the Observatory,[1] is in charge of the operation of the Optical Tracking Program, which includes three major activities:

[1]Resigned from this position as of January 1, 1960.

1. Project Moonwatch, directed by Mr. Leon Campbell, Jr., who operates and coordinates the activities of some 220 visual observing stations in the United States and abroad. The groups of amateurs who man these stations are volunteers devoted to the work of acquiring a satellite when it first goes into orbit and of recording the final stages of its flight. Their observations are essential in the early and final stages of satellite flight, although the precision of their measurements is somewhat limited by the simple equipment used. For example, the position–time date of a Moonwatch observation has an accuracy of about 1 deg of arc and 1 sec of time.
2. A world-wide network of 12 precision photographic stations, set up by Dr. K. G. Henize[3], which provide the most accurate visual observations (up to 2 sec of arc and 1/1000 sec of time).
3. A Computation Center and an Analysis & Research Center under the direction of Mr. C. W. Tillinghast and Dr. C. Whitney which receive and process the data transmitted by the visual and photographic stations and, in turn, supply the stations with orbital predictions.

A communications staff supervised by Mr. C. M. Peterson links these three aspects of the program and provides the vital channels for world-wide transmission of data.

As early as 1956, a complete data processing procedure had to be devised to handle the operations from the time that observations were received to the time that predictions were sent out. The procedure was the result of close teamwork between Smithsonian scientists and IBM personnel. This paper will attempt to describe some technical aspects of this procedure as it was developed, without entering into the details of the tracking programs which compose its main body. The procedure was concerned primarily with the organization of the flow of data, the development of a comprehensive 704 system flexible enough to suit the major aspects of optical satellite tracking, and the establishment of machine procedures capable of efficiently handling all data processing requirements.

II. INPUT

The organization of the flow of data consists in collecting observations from the different sources, organizing them in well-ordered files, and providing the necessary input to the different programs at various stages of the computation. The files of data must also lend themselves to various groupings and sorting procedures for publication purposes. There are two main files of data: (1) the observations and (2) the station coordinates. Both are kept on IBM cards, keypunched in standard formats, one for the observations and one for the station coordinates. Besides these, there are elements, constants, and parameters which are involved in certain calculations and which change from time to time and are keypunched, when needed, on separate cards.

The "standard format-card" for the station data was simple to achieve, since only one system of geodetic coordinates was used for all stations as reference frame. A unique format for all incoming observations was more difficult to achieve because of the different reference systems used by the various observers and because of the difference in observing equipment used. The final format of an observation card was planned to accommodate the highest foreseeable accuracy in measurements and to include the two reference systems most widely used in optical tracking: right ascension–declination and altitude–azimuth. Observations from Minitrack, radar, and other electronic sensors are converted to these systems by the programs using them.

At the Smithsonian, the teletyped messages received from observers all over the world are screened and then

[3]Now at Northwestern University, Evanston, Ill.

keypunched on IBM cards. Each observation is tagged by serial numbers identifying, among other things, the observing station. This "station number" appears also on the station coordinates cards, so that cross-referencing, matching, and sorting between an observation card and a station card are possible on both the 704 computer and the smaller electric accounting machines such as sorters and collators.

For processing purposes, the pair "observation-station" forms a complete datum relating an observed point in the sky with an observing point on the Earth. Thus two cards are necessary to process one datum when the input to a program is from cards read on-line. This method of input seemed only a stop-gap at the beginning of the operation, under the pressure of the first *Sputniks*, and yet it is still in use today, having proven to be very flexible, extremely easy to use in the preparation of any kind of production runs, and simple enough to be taught in a few minutes to new personnel. It is the safest approach to rapid preparation of runs combined with accurate filing. It works well on the computer when a limited number of observations have to be processed per run. In cases where most of the station coordinates are needed, as in the subsatellite programs, the station data are written on magnetic tape. This is done also when a great number of observations are to be processed, as in postflight analysis of a satellite lifetime. In general, a binary-coded decimal tape is prepared off-line.

The file of observations is organized in order of satellite and, within each satellite, in order of time of observation.

Usually, the input to a program consists of the latest observations received, plus a number of constants and parameters specifying, for instance, orbital characteristics, limits, like intervals of time, etc. These constants are keypunched separately, while the observation cards are chosen from the main files and are paired with the station coordinate cards; this constitutes the data check.

Periodically, the Smithsonian publishes in its *Special Reports* a list of all the observations received and an up-dated catalog of the tracking stations. These lists are prepared by a single run of cards through the 407 accounting machine. The printouts are then reproduced by a photo-offset procedure for publication.

III. PROCESSING

The basic input data are processed on the IBM 704 by a series of programs which have been organized into a system.

The routine operations consist, in general, in the determination of an initial orbit on the basis of the first three good observations available, in the subsequent differential corrections procedures applied as observations are received, and in the prediction of future passes. There are a number of programs for each one of these three main phases to fit the various requirements of the Smithsonian scientific investigations. Almost all the programs undergo constant revision and updating, and when the new version is ready, it must supersede the obsolete one without causing any delay in the system. This is a characteristic peculiar to a system that has to serve a tracking organization: it must be revised randomly and sometimes drastically, and therefore it should be flexible; yet it must be operative at any time. Therefore, its components should be fixed and well integrated. These requirements were met by a simple procedure which enabled the revision of binary tapes off-line.

At the beginning of the actual tracking, in the fall of 1957, the few programs in existence were kept as decks of binary cards and read on-line when needed. Outputs were generally written on magnetic tapes to be printed off-line later. Only during launching or re-entry phases was the output printed on-line for fast access to information.

As the number of programs increased and the processing operation took on a more routine aspect, a system could be developed to use the machine more efficiently. The most important program decks used daily were written on a magnetic tape in separate files, one program to a file. Files were designated by the order in which they were written, starting from the beginning of the tape. When needed, a program was loaded in core memory by a call card, read on-line. The card looked for a specific file by skipping over the unwanted ones; the number of skips to be made was keypunched on the card. Each program on tape had a separate call card.

This method helped to save machine time in reading programs into core memory, but presented two disadvantages: (1) it had to start always from the beginning of the tape, and therefore time was wasted in rewinding, and (2) it became impractical when too many programs were on the tape, because the search for the last program could take as much time as if it were read on-line from a deck of binary cards. The waste of time was alleviated by rewinding the tape while the program just called into memory was running. This overlap was obtained by inserting a few instructions at the end of each program in order to start the rewinding of the tape just before the transfer to the first instruction of the program took place. Thus the program tape was always left ready for use. The second inconvenience was somewhat reduced by keeping on the master program tape only those programs used almost daily and writing the others on a separate tape.

Further improvements could be made to such an elementary approach if the programs themselves could be integrated into a system; for instance, most of the programs used the same share subroutines, not only for the mathematics but for the utilities, like input–output, etc. These subroutines are part of each program. For instance, assuming there are ten programs written on tape all using the same input–output subroutine, this one would be written ten times, thus increasing the length of tape to be skipped in searching. It would be sensible to collect together the subroutines common to most programs and read them in fixed locations in core memory as a single package every time the tape is used. (In general the program tape reads into core several programs during normal processing.) But this concept implies certain restrictions on the programmers, because they have to give up a portion of memory to make space for the subroutines, would be forced to use only certain subroutines, and would be compelled to refer to them by absolute addresses. It also leads to higher concepts, like Compool, or common pool of information, and other techniques which transcend the scope of this brief exposition. However, it should be evident that the elementary system we started with is susceptible of great development only if coordination is achieved at the programming level and, even higher, at the planning stage of the entire system.

Going back to our simple program tape, it may be of interest to describe how its maintenance was carried out independently of the on-line operations. By maintenance is meant the revisions necessary to up-date the programs, make changes in the order in which they follow one another, insert new ones, etc. However small the change, the entire tape has to be written again. The operation may become a costly one if done on-line and frequently, because there are many tapes to be maintained and up-dated, such as utility tapes, special subroutines tapes (developed especially for Smithsonian use), etc.

To prevent redoing a whole tape on-line, the maintenance operation was shifted to the off-line equipment. This was accomplished by adopting the columnar-binary cards rather than the row-binary cards for keeping files of programs. Columnar-binary (or Chinese-binary) cards are formed by punching into a card binary instructions, or "words," column by column instead of row by row. This is actually the format obtained every time that a binary-written tape is punched on the off-line punch equipment (possible if the punch is equipped with a special switch). A binary-written tape is obtained as a by-product of every assembly or compilation of a program. The same columnar-binary format may be read on the off-line equipment to write a binary tape, provided that a simple modification is made to the 714 or 759 reader and a specially wired board is used (see Share Reference Manual, Section 3.10-13 for the wiring diagram).

Let us now see, as an example, the steps through which a program would be processed to be incorporated into a binary tape by using only off-line equipment. First of all the program has to be assembled. This operation produces not only the usual row-binary deck of cards, but also leaves a binary tape. Generally this tape is not used, but in our example it will be punched off-line, thus yielding a columnar-binary deck of cards. This deck is identical to the row-binary one, except for the mode in which it is punched. Two operations must now be performed on the columnar-binary deck to prepare it for incorporation into the program tape. The transfer card must be removed and substituted with another one containing the "rewind tape" instructions; the transfer address is punched in columnar form into this card, and a dummy transfer card added at the end of the deck. Then the initial part of the deck must be preceded by a simple set of instructions to

cause the self-loading of the entire file from tape into memory and the transfer to the correct location. Both these operations are done by placing sets of prepunched cards in front and at the end of the deck, after punching the transfer addresses in the last cards added. Now this deck is ready to be read off-line for the creation of a binary tape, provided that the equipment has the special features installed and the appropriate board for reading columnar-binary cards is used. The deck now has provision for self-loading into memory and for rewinding the tape after it has been read from the deck.

When all the programs are treated this way, a program tape can be prepared off-line and a complete file of columnar-binary decks is available, which gives at a glance the composition of the binary tape. This is an advantage in itself, since it is readily accessible for verification in case of doubtful tape performance. Now any changes to the program tape are reduced to card handling; if a program has to be added or discarded, the decks are rearranged, new call cards issued, and the tape written off-line, without disturbing the processing on the machine. When a program needs minor changes, these can be key-punched in columnar-binary form and the corrections added or substituted in the card deck. Only for major changes in a program, too involved to be key-punched, is a reassembly necessary. In any event, the machine is used only for that program, not for the entire tape, which is always written off-line.

The call-card method could be further improved if a single card were used to start several programs in succession. This implies that the programs themselves must have provisions for calling the next program into core memory, or, better, any other one of a choice of programs, depending on the partial results of the calculations performed. Attention is being given to this area because it may lead to an almost automatic processing system. The use of macro-instructions is contemplated, which would partially substitute call cards.

Recently a program has been developed at Smithsonian by Dr. G. Veis, the Differential Orbit Improvement Program. It performs the differential correction of the orbit until a refined orbit is achieved for prediction purposes. It is widely used at Smithsonian. Since this program is fully described in the preceding paper (Moore–Veis), reference is made thereto for further details.

IV. OUTPUT

The final result of all the processing consists mainly of the prediction of future satellite passes over particular sites or the time of parallel crossings. The output is generally printed off-line from a tape.

Of a certain interest is the method used to send predictions to the Baker-Nunn precision optical tracking cameras. The camera settings have to be prepared ahead of time for tracking. To do this, the arc to be described by the satellite in its course must be set on the tracking mechanism, along with the rate of tracking. Then the instrument is pointed to the position in the sky where tracking is to begin. Finally the time at which the operation should begin is specified. All this information is given to the cameras by setting a number of dials.

The program for sending predictions to the Baker-Nunn cameras computes all the necessary data, then translates them into a set of coded numbers which can be applied directly to the dials on the cameras by the operators. The program prints out the celestial positions and time of tellite passage in usual astronomical units and the translation of these in appropriate camera settings in units referring to dials and knobs on the cameras. Alongside,

it prints the same information grouped in coded blocks suited to teletype transmission. A check is carried and printed for each line to be transmitted.

This information has to be read from the machine printouts by the teletype operators to transmit it on their circuits. Since this human intervention causes a certain delay and extra work, Smithsonian is exploring the possibility of avoiding it by having the computer punch a paper tape ready to be fed into the teletypes. Special equipment is contemplated for this purpose.

A study along the same lines is being done for the input to the computer from the teletypes. The objective is to have the observation cards punched directly from the paper tape produced by the teletypes. In this case the equipment is readily available, since paper tape to card punch are standard machines. The problem lies in the standardization of the messages received, and involves the observers rather than the methods of machine processing at Smithsonian. Therefore, it is only mentioned here.

The operation of the Smithsonian Computing Center is now on a routine basis. Satellite observations coming from all parts of the world are received at Smithsonian Astrophysical Observatory and evaluated. The most reliable ones are forwarded to the 704 calculator for processing. Results are analyzed and when predictions are computed, they are sent to the Communications Center, where they are forwarded to all interested people throughout the world.

Some aspects of the data processing system developed at Smithsonian Astrophysical Observatory have been briefly outlined. The system grew out of the necessity of the moment and is always under development. The future trend points to more automatic procedures, relying on the speed and accuracy of the equipment used.

DISCUSSION

J. P. ROSSONI: One of the outstanding examples in automatic procedures is being developed for Project Mercury by IBM. A device capable of interrogating 32 teletypes is being built now, so that the messages coming in on the teletypes will go directly into core memory. An interrupt signal is provided with this device which tells the computer when a message has arrived. The signal is recognized by an executive program, a monitor, which is always in core memory. When a signal arrives, the monitor program interrupts the processing, records the situation in the computer at that moment, takes care of the data that have arrived, and then re-establishes the situation in the computer as it was before the interruption and resumes the processing. The executive routine and the monitor that are built now for the Mercury Project are, to my knowledge, the most outstanding ones in the field at present.

C. A. LUNDQUIST: You mentioned the Mercury Project. I was curious to ask just what the approach is in Mercury, the computation scheme?

J. P. ROSSONI: We have planned on a real time operation with no human intervention except interrogation of the computer via one of the teletypes which are scanned by the multiplexer device. Predictions will be sent on a signal provided by an internal clock to the different stations during the flight. Programs are being developed now so that they can be integrated with one another, mostly run by macro-instructions, being called in by the monitor at different times.

C. A. LUNDQUIST: Is this Hansen's method approach or what?

J. W. SIRY: No, it is numerical integration and differential corrections, like one of the three that I mentioned the other day, similar to one of the types of systems used in the *Vanguard* project. Owing to the short orbital flight, the disadvantages of numerical integration are not important.

J. P. ROSSONI: I may go a little further and say that there is going to be a table of the positions and velocity

vectors kept in memory at all times. Actually, it is at an interval of 1 minute for a total of 300 points, which would cover over 3½ hours. The way the table is updated is by means of differential corrections as soon as a set of observations comes in from the radar. The orbit itself is computed on the basis of a sliding arc technique which was developed by Dr. Herget. That is, when we have a return of observations from one radar, then only the observations which were within a certain interval Δ_t will be taken into consideration, not all around the orbit, because of the uncertainty of the drag. As new observations are expected, then we shift what is called an anchor point, that is, the point of closest approach to the nearest station, and this is also reduced to the nearest integral minute. It is from that minute that the new values of r and v are computed, and the integration is carried on forward and backward. The table is always kept in memory so that it is available for the predictions which may be requested at any moment by an interruption from the clock.

E. W. WAHL: John, I think it may be interesting to some of the people here to tell a little more about the multiplexer, the real time package of the Mercury system, because it will have quite a good use for people who need real time input-output from teletype in handling data arriving at the computer.

(Dr. Wahl described the manner in which the Data Communication Channel is used at the 709 installation of the National Space Surveillance Control Center in Bedford, Massachusetts. A detailed description of the Data Communication Channel IBM 7281, Model I, may be available in the future from the IBM Space Center, 615 Pennsylvania Avenue N. W., Washington, D. C.)

Tracking a Passive Satellite by the Doppler Method

P. B. RICHARDS

Space Sciences Laboratory, General Electric Co.,
Missiles and Space Vehicles Dept.,
Philadelphia, Pa.

ABSTRACT

Two methods are described for predicting the orbit of a passive (nontransmitting) Earth satellite from measured values of the doppler shift of radio signals transmitted from a station on the surface of the Earth. The difficulty of this problem lies in the fact that initial conditions are unknown, unlike the case of a friendly satellite which can transmit its position, or a friendly ballistic missile whose launch and burnout conditions are known.

One method employs a numerical procedure for minimizing the sum of squares of the errors between doppler observations and range rates computed from assumed initial conditions. The method consists of fitting a complete second-degree polynomial in the six variables used as initial conditions to the sum of squares in the neighborhood of a minimum. The location of the minimum of the sum of squares is found. This process is continued until convergence is reached.

The second method is a geometrical approach designed to give the initial approximation for the numerical procedure. It is based on the fact that integration of the doppler equation determines time-dependent ellipsoids whose intersections lie on the trajectory of the satellite. The required constant of integration is computed from conditions at time of closest approach.

I. INTRODUCTION

In connection with the application of radio-doppler methods to satellite tracking, the Ballistics Research Laboratory, Aberdeen Proving Grounds, asked GE's Space Sciences Laboratory to investigate the problem of orbit determination of a passive (nontransmitting) Earth satellite using doppler data alone during one pass of the

vehicle.[1] The following discussion is a brief summary of initial thinking on this problem.

Mathematically, the problem is as follows: Given the doppler differential equation

$$\dot{\rho}_T + \dot{\rho}_R = D(t) \tag{1}$$

where $D(t)$ is measured, and subscripts T and R denote transmitter and receiver, respectively, solve

$$\ddot{\mathbf{r}} = -\mu \frac{\mathbf{r}}{r^3} \tag{2}$$

consistent with (1).

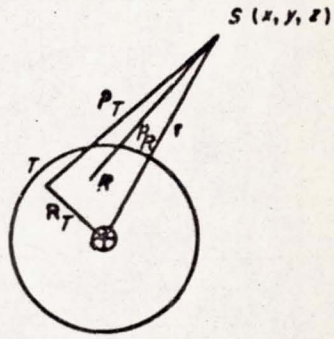

Sketch 1

II. METHODS OF SOLUTION

Two methods have been investigated for solving the problem: a numerical procedure and a geometrical approach. The numerical procedure will be described first.

The measured information $D(t)$ is related to the solution of the vector equation of motion (2) as follows (see Sketch 1):

$$\boldsymbol{\rho}_T = \mathbf{r} - \mathbf{R}_T$$

or

$$\boldsymbol{\rho}_T = \hat{i}(x - X_T) + \hat{j}(y - Y_T) + \hat{k}(z - Z_T)$$

$$\dot{\boldsymbol{\rho}}_T = \hat{i}(\dot{x} - \dot{X}_T) + \hat{j}(\dot{y} - \dot{Y}_T) + \hat{k}(\dot{z} - \dot{Z}_T)$$

$$\dot{\rho}_T \equiv \frac{\boldsymbol{\rho}_T \cdot \dot{\boldsymbol{\rho}}_T}{\rho_T} =$$

$$\frac{(x - X_T)(\dot{x} - \dot{X}_T) + (y - Y_T)(\dot{y} - \dot{Y}_T) + (z - Z_T)(\dot{z} - \dot{Z}_T)}{\sqrt{(x - X_T)^2 + (y - Y_T)^2 + (z - Z_T)^2}} \tag{3}$$

A similar expression is obtained for $\dot{\rho}_R$. Since the solution $x(t)$, $y(t)$, $z(t)$ of (2) is unique, corresponding to a particular set of initial conditions $x(t_0)$, $y(t_0)$, $z(t_0)$, $\dot{x}(t_0)$, $\dot{y}(t_0)$, $\dot{z}(t_0)$, any numerical procedure would consist of 5 steps:

1. Select values of the initial conditions.
2. Solve (2) for $x(t)$, $y(t)$, $z(t)$.
3. Compute $\dot{\rho}_T + \dot{\rho}_R$ for each transmitter-receiver pair at times corresponding to measured values $D(t)$.
4. Compare computed values of $\dot{\rho}_T + \dot{\rho}_R$ with measured $D(t)$.
5. Iterate steps 1–4 until doppler equation is satisfied.

The difference between numerical techniques lies in the method of comparing the computed values with the measured data.

Here we define the comparison function to be

$$Q(\alpha_1, \alpha_2, \cdots, \alpha_6) = \sum [D - (\dot{\rho}_T + \dot{\rho}_R)]^2 \tag{4}$$

where $\alpha_1 = x(t_0)$, $\alpha_2 = y(t_0)$, $\alpha_3 = z(t_0)$, $\alpha_4 = \dot{x}(t_0)$, $\alpha_5 = \dot{y}(t_0)$, $\alpha_6 = \dot{z}(t_0)$,

the summation extending over all time observations at all station pairs. The problem is to determine the set $(\alpha_1, \alpha_2, \cdots, \alpha_6)$ that minimizes Q. If we look at the α's as

[1]Work supported by contract No. DA-36-034-509-ORD-3046-RD.

coordinates of a six-dimensional space, each point in this space determines a point Q on a hypersurface. By the definition of Q, Eq. (4) this hypersurface must have a minimum. To locate this minimum we approximate the hypersurface, in the neighborhood of the minimum, by a quadratic surface in the six independent variables,

$$P(\alpha_1, \alpha_2, \cdots, \alpha_6) = b_0 + \sum_{i=1}^{6} b_i \delta_i + \tfrac{1}{2}\sum_{i=1}^{6} a_{ii}\delta_i^2 + \sum_{j>i} a_{ij}\delta_i\delta_j$$

$$\delta_i(\alpha_i) = \frac{\alpha_i - \alpha_i^{(l)}}{h_i^{(l)}}$$

where $\alpha_i^{(l)} = l$th approximation to the solution, $h_i^{(l)}$ is a nonnegative real number, $h_i^{(l)} > E_i$ = admissible error. To evaluate the coefficients in P, we equate P and Q at 28 points in the neighborhood of the minimum. These points are reached in an orderly fashion by constructing a rectangular six-dimensional lattice about the point selected as the lth approximation. Once the form of P is determined, this quadratic is minimized through the relations $\partial P/\partial\alpha_i = 0$, $i = 1, 2, \cdots, 6$ and a new approximation to the location of the minimum of Q is found.

A sample calculation of this procedure, in which calculated values were compared to a simulated computer trajectory, is shown in the table below. A total of thirty doppler measurements were used, ten at each of three transmitter-receiver pairs. Convergence to the true solution occurred in 15 minutes of IBM 704 computation.

	First Approximation	True Solution
$x(t_0)$	1.55×10^7 ft	1.5494123×10^7 ft
$y(t_0)$	1.55×10^7	1.5494122×10^7
$z(t_0)$	4.00×10^6	$-3.0957031 \times 10^{-1}$
$\dot{x}(t_0)$	1.95×10^4 ft/sec	1.4066537×10^4 ft/sec
$\dot{y}(t_0)$	-1.78×10^4	-1.2355931×10^4
$\dot{z}(t_0)$	0	-1.8683510×10^4

The geometrical approach is based on the direct integration of the doppler differential equation (1), $\rho_T + \rho_R = D(t)$. The integral of the term on the right between the fixed time t_0 and an arbitrary time t is simply the area $A(t)$ under the doppler S curve (see Sketch 2).

Sketch 2

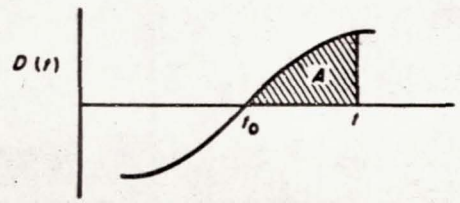

Integrating the term on the left we obtain

$$\rho_T(t) + \rho_R(t) = A(t) + \rho_T(t_0) + \rho_R(t_0) = 2a(t) \qquad (5)$$

which indicates that at a given time t, the satellite lies on an ellipsoid (see Sketch 3) of semimajor axis $a(t)$, with foci at T and R, the locations of the transmitter and receiver.

Sketch 3

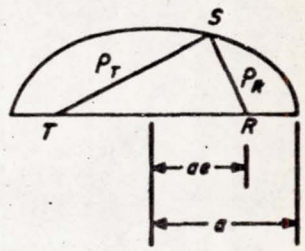

Since T and R are known locations, the eccentricity of the ellipsoid is obtained from the expression

$$oe = \frac{TR}{2}$$

Thus the ellipsoid is completely determined once the constant of integration $\rho_T(t_0) + \rho_R(t_0)$ is known. The intersection of simultaneous ellipsoids generated by three transmitter–receiver pairs will determine position vectors and hence the trajectory of the satellite. The problem is to determine $\rho_T(t_0) + \rho_R(t_0)$ for each transmitter–receiver pair, and this may be done in the following manner:

The doppler equation (1) can be written in vector form as

$$\frac{\rho_T \cdot \dot{\rho}_T}{\rho_T} + \frac{\rho_R \cdot \dot{\rho}_R}{\rho_R} = D(t) \qquad (6)$$

or, since $\rho_T = \rho_R = \mathbf{v}$, the satellite velocity,

$$\mathbf{v} \cdot \left(\frac{\rho_T}{\rho_T} + \frac{\rho_R}{\rho_R}\right) = D(t) \qquad (7)$$

Define the vector

$$\mathbf{p}(t) = \tfrac{1}{2}\left[\frac{\rho_T \rho_R}{1 - \left(\frac{TR}{\rho_T + \rho_R}\right)^2}\right]^{1/2}\left(\frac{\rho_T}{\rho_T} + \frac{\rho_R}{\rho_R}\right) \qquad (8)$$

Then

$$|\mathbf{p}| = p(t) = \tfrac{1}{2}(\rho_T + \rho_R) \qquad (9)$$

Equation (1) can now be written

$$\dot{p}(t) = \frac{D}{2} \qquad (10)$$

or

$$\frac{\mathbf{p}\cdot\dot{\mathbf{p}}}{p} = \frac{D}{2} \tag{11}$$

If we define the time of closest approach t_0 to be the time at which $\rho_T + \rho_R$ is minimum, then, from (7) and (8),

$$\mathbf{v}_0 \perp \mathbf{p}_0 \tag{12}$$

and from (11)

$$\dot{\mathbf{p}}_0 \perp \mathbf{p}_0 \tag{13}$$

where zero subscripts denote values at t_0.

All that these expressions imply is that the vectors $\mathbf{v}_0$ and $\dot{\mathbf{p}}_0$ lie in a plane perpendicular to $\mathbf{p}_0$. The vector $\mathbf{p}(t)$ must in general have the form

$$\dot{\mathbf{p}}(t) = a(t)\,\boldsymbol{\rho}_T + b(t)\,\boldsymbol{\rho}_R + c(t)\,\mathbf{v} \tag{14}$$

where a, b, and c are scalar variables, for the vectors $\boldsymbol{\rho}_T$, $\boldsymbol{\rho}_R$, and $\mathbf{v}$, in general, constitute a basis in three-dimensional space.

The vector $\dot{\mathbf{p}}(t)$ may be interpreted as a fictitious velocity, for if we hold the base of $\mathbf{p}(t)$ fixed at the origin of a three-dimensional vector space, the locus of the end point of $\mathbf{p}(t)$ will be a fictitious trajectory. We take as origin of this vector space the base of $\mathbf{p}_0$, i.e., $\mathbf{p}$ at closest approach. This point will be in the plane of $\boldsymbol{\rho}_T$ and $\boldsymbol{\rho}_R$ on the normal to the actual trajectory at the point of the trajectory where $\rho_T + \rho_R$ is a minimum, and at a distance along this normal equal to ½ this minimum value of $\rho_T + \rho_R$. In the vector space there will be a sphere of radius $p_0 = \frac{1}{2}(\rho_T + \rho_R)_{min}$ such that the fictitious trajectory and the true trajectory are both tangent to this sphere at the point of closest approach (see Sketch 4). Elsewhere, both trajectories are exterior to the sphere.

Sketch 4

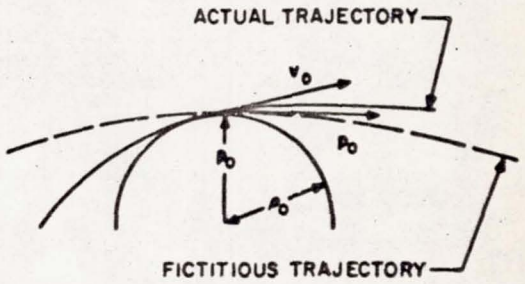

If now we assume that $\dot{\mathbf{p}}$ is constant ($=\dot{\mathbf{p}}_0$) in the neighborhood of closest approach t_0, we can write, in this neighborhood,

$$\mathbf{p}(t) = \mathbf{p}_0 + \dot{\mathbf{p}}_0(t - t_0) \tag{15}$$

Then, using (13)

$$p^2(t) = p_0^2 + |\dot{\mathbf{p}}_0|^2(t - t_0)^2 \tag{16}$$

and

$$\dot{p}(t) = \frac{|\dot{\mathbf{p}}_0|^2(t - t_0)}{\sqrt{p_0^2 + |\dot{\mathbf{p}}_0|^2(t - t_0)^2}} \tag{17}$$

From (10) we see that knowledge of three points on the doppler curve will yield the parameters p_0, $|\dot{\mathbf{p}}_0|$, and t_0, where $p_0 = \frac{1}{2}[\rho_T(t_0) + \rho_R(t_0)]$ is the constant of integration we want.

Lunar and Interplanetary Trajectory Determination Activities at General Electric[1]

V. G. SZEBEHELY

Space Sciences Laboratory,
General Electric Company,
Philadelphia, Pa.

ABSTRACT

Application of a lunar trajectory program to the determination of the orbit of the Russian Automatic Interplanetary Station (1959 θ1, or *Lunik III*) is described. Perigee distances are computed and re-entry predictions as well as the effect of the close Moon approaches on the trajectory are discussed. Programs to solve a two-point boundary value problem in a force field representing interplanetary mission conditions are used to find initial conditions for an Earth–Venus trajectory.

I. TRAJECTORY DETERMINATION OF THETA ONE

The computer program used in connection with attempts to determine the trajectory of 1959 θ1 is a Runge–Kutta–Gill type integration of the restricted four-body problem. Cowell's method is programmed including the gravitational effects of the Earth, Moon, and Sun. Oblateness effects are considered; drag effects, however, are excluded. The variable intervals of the integration are selected automatically. Near the singularities the integration steps are approximately 500 times shorter than at the farthermost parts of the trajectory. The average orbital period of 1959 θ1 is approximately 16 days, corresponding to 2 minutes of IBM 704 computer time. Further details on the program are given in Ref. 1 and 2; at this point only a few results of special interest will be described.

The input data consisted of *Tass*-released times and corresponding angular coordinates around the first apogee following the vehicle's first close approach to the Moon. (In what follows, perigee and apogee will refer to the vehicle's orbit relative to the Earth.) Using these data points a trajectory was computed from burnout to the

[1]This work was performed under the joint auspices of the U. S. Air Force, Cambridge Research Center, Wright Air Development Center, and the General Electric Company.

seventh perigee. The perigee distance was found to be approximately a linear function of the number of revolutions, i.e.,

$$p = -4.5\,n + 50.5, \qquad 1 \leqq n \leqq 7$$

where p is the perigee distance measured from the center of the Earth in 10^3 km and n is the number of revolutions.

The first perigee occurring on October 18, 1959 is at 46,000 km; the period for the first seven revolutions is about 16 days and the seventh perigee distance is 19,000 km, occurring on January 21, 1960. Another close Moon approach occurs after the seventh perigee. The time rate of change of the perigee distance for the first seven perigee revolutions is

$$\dot{p}_1 = -4.5 \times 10^3 \frac{\text{km}}{\text{revolution}}$$

which is changed to

$$\dot{p}_2 = -12 \times 10^3 \frac{\text{km}}{\text{revolution}}$$

after this close approach. The computed first close approach to the Moon occurs on October 6, 1959 at 6732 km; the second occurs on January 24, 1960 at 50,545 km. After this second close approach the orbit is greatly changed, and the eighth, ninth, and tenth perigee distances are 6760 km, 6730 km, and 5830 km, respectively. The last one indicates re-entry on March 8, 1960.

An opportunity for comparison with Russian predictions was offered regarding the seventh perigee. The difference between the Russian prediction and our prediction of the seventh perigee distance was approximately 1.4%; the error in time was less than 1%. By changing only the magnitude of the initial velocity vector one can eliminate the time error in the seventh perigee, but considering the crude input data such exercises are of limited significance. Nevertheless, it is interesting to observe that, because of the existence of the second close approach to the Moon, the part of the trajectory after this approach shows extreme sensitivity to small changes introduced prior to the close approach. Matching, for instance, the Russian prediction regarding the seventh perigee results in a re-entry date of late April. In other words, a 1% epoch change prior to the close approach will result in approximately 30% change in the lifetime of the vehicle.

Trajectory and especially re-entry predictions using nominal initial conditions are quite meaningless considering the two close approaches to the Moon. In fact, using the best available observational data[2] the predicted perigee locations and times could not be verified by sightings.

[2]The cooperation of Dr. C. Whitney of the Smithsonian Astrophysical Observatory is acknowledged regarding the securing of the observational input data.

II. INITIAL CONDITIONS FOR AN EARTH–VENUS FLIGHT

In general terms the problem might be formulated as follows: In a time and position dependent force field, $f_i(x_1, x_2, x_3, t)$, with $i = 1, 2$, and 3, two four-dimensional vectors, $x_i^{(1)}$ and $x_i^{(2)}$ are prescribed with the coordinates $x_1^{(1)}, x_2^{(1)}, x_3^{(1)}, t^{(1)}$ and $x_1^{(2)}, x_2^{(2)}, x_3^{(2)}, t^{(2)}$. Find the velocity vector at the first point which will result in a trajectory going through the second point. (It is remarked that this problem does not necessarily have a solution.)

The interplanetary trajectory program in use furnishes the initial conditions, i.e., the components of the velocity vector at the first point as the result of an iterative procedure. The first approximation is obtained by the conventional two-body technique whereby the orbit of the vehicle is first established in the gravitational field of the Sun alone; then this trajectory is matched with a hyperbolic escape trajectory considering the Earth's gravitational field alone. Refinements regarding the effects of non-coplanar planet orbits and of the utilization of the Earth's rotation are included in the technique without any special difficulty.

The second approximation is obtained by first computing the elements of the error matrix; i.e.,

$$G_{ik} = \frac{\partial x_i}{\partial j_k}$$

where x_i is the position vector at $t^{(2)}$ and j_k is the initial velocity vector. The inverse of G_{ik} will furnish then the second approximation for the initial velocity by using

$$j_k = j_k + G_{ki}^{-1} \Delta x_i$$

where j_k is the second approximation of the initial velocity vector, j_k is the first approximation of the initial velocity vector. G_{ki}^{-1} is the inverse of the error matrix, and Δx_i is the vector connecting the vehicle and the target at $t^{(2)}$.

This technique might be modified by recomputing the elements of G_{ik} at every step of the iterative procedure. Whether using one set of values for the error matrix will give faster convergence than using recomputed values depends on the case under consideration.

The experience obtained with a 107-day transfer orbit indicates that, if one of the conditions of the problem is relaxed, the use of the same G_{ik} elements is strongly favored as compared to the use of the recomputed elements. The condition to be relaxed is the time of arrival, since if a hit trajectory is to be established, the precise arrival time is of little significance. For the above-mentioned transfer orbit the miss distance using the first approximation of the initial condition was slightly above 1%. The second approximation resulted in slightly less than 1%, and the third approximation in 0.01%. The final trajectory was obtained by the next approximation giving an intercept 2 hr earlier than prescribed.

It is of interest to note that the first approximation and final value of the initial velocity vector differed only by 0.6% regarding magnitude. The directional changes of the initial velocity vector during the iteration process are more significant.

REFERENCES

1. Michaels, J. E., M. Wachman, and A. Petty. "Lunik III Trajectory Predictions," Astronautical Sciences Review, April 1960.

2. Wright Air Development Center. Generalized Interplanetary Trajectory Study, by J. E. Michaels and others. Wright-Patterson Air Force Base, Dayton, Ohio, April 1960.

A Computer Program for First-Order Error Propagation in Satellite Orbit Prediction

PETER SWERLING

The RAND Corporation,
Santa Monica, Calif.

ABSTRACT

A program for the IBM-704 computer has been written which computes the first-order errors in estimation of satellite orbital parameters as a function of observation errors. One may input a specification of an arbitrary observation network and Earth satellite orbit, a description of the errors in each type of observation, for each observation site, and a data smoothing method from a fairly broad class of possible smoothing methods. The output consists of the first-order errors in prediction of satellite position and velocity components at any specified time. These may be described either statistically or nonstatistically.

I. INTRODUCTION

The program to be described is written for the IBM-704 computer.[1] Its purpose is not to provide precision predictions of satellite orbits, but rather to compute the errors in predicted orbits which result from observation errors. The program will therefore be of use in the evaluation of the tracking and prediction capabilities of various types of satellite observation networks.

[1]The program was written by B. W. Boehm, of the RAND Numerical Analysis Division.

II. DESCRIPTION OF THE PROGRAM

In order to compute error propagation, a specific data smoothing method or class of methods must first be assumed. We suppose that a satellite orbit is completely determined by a finite number of parameters called elements. In the program in its present form, these elements are taken to be six in number and are assumed to be components of position and velocity, at some specified time, in an inertial reference frame. Let us call those elements x_0, y_0, z_0, v_{x0}, v_{y0}, v_{z0}. We suppose the data to be smoothed so as to give estimates $\hat{x}_0, \cdots, \hat{v}_{z0}$ of these quantities.

Let all the observations which are to contribute to the element estimates be lumped together and indexed with the index μ ($\mu = 1, \cdots, N$ where N is the total number of individual observations to be processed). The value of the μth observation will be denoted by F^μ.

If there were no observation error, the values of these observations would be completely determined as functions of the elements and of the times of observation t_μ:

$$F^\mu = f^\mu(x_0, \cdots, v_{z0}; t_\mu) \tag{1}$$

When there are observation errors E^μ, the values of the observations are

$$F^\mu = f^\mu(x_0, \cdots, v_{z0}; t_\mu) + E^\mu \tag{2}$$

Here, the f^μ are assumed to be known functions.

It is assumed that the estimates $\hat{x}_0, \cdots, \hat{v}_{z0}$ are obtained by minimizing, with respect to $\hat{x}_0, \cdots, \hat{v}_{z0}$, the quantity

$$Q = \sum_{\mu,\nu=1}^{N} \eta_{\mu\nu} [F^\mu - f^\mu(\hat{x}_0, \cdots, \hat{v}_{z0}; t_\mu)] \times [F^\nu - f^\nu(\hat{x}_0, \cdots, \hat{v}_{z0}; t_\nu)] \tag{3}$$

where $(\eta_{\mu\nu})$ is a symmetric positive definite matrix. (It is assumed that $N \geq 6$.)

In the program in its present form, $(\eta_{\mu\nu})$ is always taken to be diagonal, so that the class of data processing methods is actually assumed to consist of minimizing

$$Q = \sum_{\mu=1}^{N} \eta_{\mu\mu} [F^\mu - f^\mu(\hat{x}_0, \cdots, \hat{v}_{z0}; t_\mu)]^2 \tag{4}$$

This method, minimization of a quadratic form in residuals (usually a weighted sum of squares of residuals), is a standard numerical analysis technique for estimating a finite number of parameters from observed data, and has long been used in connection with orbits of astronomical bodies.

It may also be interpreted as a maximum likelihood method of estimation, provided (1) that the errors E^μ are Gaussian and (2) that the matrix $(\eta_{\mu\nu})$ is chosen to be the inverse covariance matrix of the errors E^μ. Since frequently neither of these conditions is satisfied, it is good not to overemphasize the maximum likelihood interpretation.

It is clear that if $E^\mu = 0$, all μ, then $\hat{x}_0 = x_0, \cdots, \hat{v}_{z0} = v_{z0}$ will minimize Q, since Q will be zero with these values of $\hat{x}_0, \cdots, \hat{v}_{z0}$. Provided the functions f^μ are reasonably well-behaved, the errors $\hat{x}_0 - x_0, \cdots, \hat{v}_{z0} - v_{z0}$ will depend linearly on the errors E^μ, provided the latter are sufficiently small:

$$\begin{aligned}
\hat{x}_0 - x_0 &= \sum_{\mu=1}^{N} \Gamma_1^\mu E^\mu \\
\hat{y}_0 - y_0 &= \sum_{\mu=1}^{N} \Gamma_2^\mu E^\mu \\
&\vdots \\
\hat{v}_{z0} - v_{z0} &= \sum_{\mu=1}^{N} \Gamma_6^\mu E^\mu
\end{aligned} \tag{5}$$

Formulas for Γ_i^μ may be obtained from Ref. 1.

The program computes these first-order errors in estimated position and velocity components at any given time instant.

The first-order error computation has the advantage that the first-order errors may be computed without actually minimizing Q. Thus, all questions as to the particular method used to minimize Q, how fast a given iteration process converges, or whether it converges, are avoided. It is merely assumed that somehow the quantities $\hat{x}_0, \cdots$ that minimize Q have been found, and the first-order errors $\hat{x}_0 - x_0, \cdots$ are then calculated.

However, further research is needed on the question of how large the errors E^μ may be while the first-order error equations still give reasonably good approximations to the actual errors.

Once the first-order errors in $\hat{x}_0, \cdots, \hat{v}_{z0}$ have been obtained, one may then compute the first-order errors in

any equivalent set of parameters (such as the osculating elliptic elements); this cannot, however, be accomplished in the program as it now stands (except that first-order errors in position and velocity components at different time instants may be calculated).

In order to utilize the program, one first specifies a satellite orbit. This is done by specifying the true values of $x, \cdots, v_z$ at some specified time.

The next thing that must be specified is the observation network. Th' 's described by specifying:

1. The locations (i.e., x, y, z coordinates at a specified time) of the observation sites.
2. The type of observations taken at each site. Six types of observations may be specified: range, range rate, azimuth, elevation, right ascension, declination.
3. The minimum elevation angle at each site for valid observations. Also, for azimuth observations, a maximum elevation angle is specified.
4. The rate at which observations are taken at each site.

Next, the observation errors must be described. 'r these purposes, two categories of observation error are distinguished: "random" and "systematic." Random errors are defined to be statistically independent—i.e., all the "random" components of E^μ, $\mu = 1, \cdots, N$, are defined to be mutually independent. All other errors are "systematic."

The random errors are specified by stating their standard deviations or variances; specifically, let the variance of the random component of E^μ be denoted by ϕ_μ. These variances may be functions of the relative positions of the satellite and the observation site: specifically, ϕ_μ is of the form[a]

$$\phi_\mu = a\rho^b + c(\cos\beta)^d \tag{6}$$

where a, b, c, d are specified (differently) for each observation site and each type of observation; ρ and β are, respectively, range and elevation at the time t_μ with respect to the observation site from which the μth observation is taken.

The systematic error components are treated in a nonstatistical way: they are merely specified as a set of numbers. Let δ^μ be the systematic component of E^μ. Then, we may specify

$$\delta^\mu = a'\rho^{b'} + c'[\cos(\beta + e')]^{d'} \tag{7}$$

[a]The notations used here do not coincide with those used in the program input or printout.

where a', b', c', d', e' are specified separately for each observation site and each type of observation.

It might be well to mention at this point the subject of timing errors. The program assumes that the times t_μ are known without error. Of course, timing errors may always be reduced to equivalent systematic errors in the observations. However, these equivalent systematic errors would be functions of position which will not in general be described by functions of the form given in Eq. (7).

We next specify the weights η_μ. At present, these are specified to be of the form

$$\eta_\mu = \frac{1}{a''(\delta^\mu)^2 + b''\phi_\mu + c''} \tag{8}$$

where a'', b'', c'' are specified separately for each site and each type of observation.

The calculation of the functions f^μ and their partial derivatives, which enter into the formulas for Γ_1^μ, is done by numerical integration from the prescribed initial conditions; the partial derivatives are obtained by differencing. The force field is assumed to be that of an oblate Earth (using just the J-term); also, simple atmospheric drag models may be included. However, it is presently assumed that the J-term and the drag parameters are known quantities; thus, these terms are included to give more accurate values of the functions f^μ and their partial derivatives, and not for the purpose of augmenting the number of parameters to be estimated from the data.

The outputs of the program are as follows: since a first-order error analysis is being used, it is possible to say that a certain component of the output errors is due to the random component of observation error, and another component due to the systematic:

$$\hat{x}_0 - x_0 = (\hat{x}_0 - x_0)_{random} + (\hat{x}_0 - x_0)_{systematic} \tag{9}$$

where

$$(\hat{x}_0 - x_0)_{random} = \sum_{\mu=1}^{N} \Gamma_1^\mu (E^\mu)_{random} \tag{10}$$

$$(\hat{x}_0 - x_0)_{systematic} = \sum_{\mu=1}^{N} \Gamma_1^\mu (E^\mu)_{systematic} \tag{11}$$

and similarly for the other prediction errors.

The random errors in predicted quantities are specified by a covariance matrix (r_{ij}), where $i, j = 1, \cdots, 6$. Here the index $i = 1$ refers to error in $\hat{x}_0$, $i = 2$ to error in

$\mathcal{G}_0, \cdots, i = 6$ to error in $\hat{v}_{x_0}$. Also, covariance matrices for the random prediction errors may be computed for any set of specified prediction times.

The systematic prediction errors are specified as a set of numbers $s_i, i = 1, \cdots, 6$; they may also be computed for any set of specified prediction times.

III. PRESENT AND FUTURE PLANS FOR USE OF THE PROGRAM

We are presently using this program to provide inputs to whatever studies require information of the type provided. It is difficult to summarize results of the runs which have so far been made, since one feature of this type of work seems to be that the results depend very strongly on the particular type of observation network assumed, the particular type of errors assumed, etc. On the basis of runs made so far, the following qualitative conclusions seem to emerge:

1. It is most important not to neglect systematic observation errors. If random and systematic observation error components are taken to be roughly equal, the systematic parts of the prediction errors begin to dominate decisively at fairly modest data acquisition rates (for example, in many of the runs this occurred at data rates of roughly one per second, with total N of about 400).
2. If it is desired to predict future prediction errors from errors in position and velocity components at some initial time, it is important to take into account the relationships which exist between the initial error components.

Suppose one knows the errors in initial position and velocity components resulting from the smoothing of a given collection of data and desires to use this knowledge to calculate errors in predicted position or velocity components at some future time (assuming that the predictions are made without any additional observational data). An erroneous picture of future error buildup would be obtained by estimating the effect of each initial error component separately, and then, say, calculating the square root of the sum of squares. The reason for this is that smoothing the original collection of data may impose rather strong relationships between the errors in position and velocity components at a given point.

Thus, to obtain a correct picture of future errors, it is necessary, when dealing with random errors, to utilize the full covariance matrix (r_{ij}), or, when dealing with systematic errors, to utilize complete sets $s_1, \cdots, s_6$, which result from the smoothing of a given collection of data.

The error program is capable of extension in several ways. For example,

1. If the force fields of the Sun and Moon were included in the numerical integration of the orbit, the program could without further alteration be applied to lunar orbits and, to some extent, to interplanetary orbits. Of course, the range of validity of first-order error predictions would be more limited in such cases.
2. The list of unknown parameters could be extended; for example, some of the drag parameters or Earth-gravity parameters might be regarded as unknowns to be estimated from the data.

Whether or not such extensions of the program are carried out depends to a considerable extent on whether a demand exists for such increased capabilities.

In addition, the functions describing the random and systematic components of observation error and the functions describing the weights, presently given by Eqs. (6), (7), and (8), can be modified if such modification should prove desirable. This can be done on a moment's notice.

REFERENCES

1. Swerling, P., "First Order Error Propagation in a Stagewise Smoothing Procedure for Satellite Observations," The Journal of the Astronautical Sciences, Vol. 6, No. 3, Autumn 1959.

Blank Page

ADDENDUM A

Seminar Attendees

Aichele, D.
Army Ballistic Missile Agency,
Computation Laboratory,
Huntsville, Ala.

Asderian, O.
Lockheed Aircraft Corp.,
Missiles Systems Division,
Palo Alto, Calif.

Beck, W.
Jet Propulsion Laboratory,
Pasadena, Calif.

Berger, W. J.
Aeronutronic Systems, Inc.,
Newport Beach, Calif.

Boughton, E. M.
Space Technology Laboratories, Inc.,
Los Angeles, Calif.

Breakwell, J. V.
Lockheed Aircraft Corp.,
Missiles Systems Division,
Sunnyvale, Calif.

Bronstein, L. M.
Jet Propulsion Laboratory,
Pasadena, Calif.

Bryant, R. W.
Goddard Space Flight Center,
Silver Spring, Md.

Buckingham, J. R.
Space Technology Laboratories, Inc.,
Los Angeles, Calif.

Cain, D. L.
Jet Propulsion Laboratory,
Pasadena, Calif.

Carr, R. E.
Jet Propulsion Laboratory,
Pasadena, Calif.

Conte, S. D.
Space Technology Laboratories, Inc.,
Los Angeles, Calif.

Coyle, R. J.
National Security Agency,
Washington, D. C.

Culver, J.
Convair Astronautics,
San Diego, Calif.

Cutting, E.
Jet Propulsion Laboratory,
Pasadena, Calif.

Des Jardins, P. R.
North American Aviation, Inc.,
Aero Space Laboratories,
Downey, Calif.

Eimer, M.
Jet Propulsion Laboratory,
Pasadena, Calif.

Fearey, J. P.
Jet Propulsion Laboratory,
Pasadena, Calif.

Fisher, D.
Goddard Space Flight Center,
Anacostia Naval Station,
Washington, D. C.

Frank, W.
Thompson-Ramo-Wooldridge, Inc.,
Canoga Park, Calif.

Gabler, R. T.
The RAND Corporation,
Santa Monica, Calif.

Hamilton, T.
Jet Propulsion Laboratory,
Pasadena, Calif.

Hanson, J. W.
Computation Center,
University of North Carolina,
Chapel Hill, North Carolina

Hanson, S. J.
Space Technology Laboratories, Inc.,
Los Angeles, Calif.

Heftman, K.
Jet Propulsion Laboratory,
Pasadena, Calif.

Herrick, C.
Convair Astronautics,
San Diego, Calif.

Herrick, S.
University of California at Los Angeles,
Los Angeles, Calif

Hibbs, A. R.
Jet Propulsion Laboratory,
Pasadena, Calif.

Hiroshige, Y.
Jet Propulsion Laboratory,
Pasadena, Calif.

Holdridge, D.
Jet Propulsion Laboratory,
Pasadena, Calif.

Hoover, W.
Jet Propulsion Laboratory,
Pasadena, Calif.

Hudson, H.
Jet Propulsion Laboratory,
Pasadena, Calif.

Johnson, M.
Jet Propulsion Laboratory,
Pasadena, Calif.

Kizner, W.
Jet Propulsion Laboratory,
Pasadena, Calif.

Kurtz, F.
Army Ballistic Missile Agency,
Aeroballistics Laboratory,
Huntsville, Ala.

Lass, H.
Jet Propulsion Laboratory,
Pasadena, Calif.

Leger, R. M.
Convair Astronautics,
San Diego, Calif.

Lesh, F.
Jet Propulsion Laboratory,
Pasadena, Calif.

Lorell, J.
Jet Propulsion Laboratory,
Pasadena, Calif.

Lundquist, C. A.
Army Ballistic Missile Agency,
Research Projects La' oratory,
Huntsville, Ala.

Marioni, J. D.
Lockheed Aircraft Corp.,
Missiles Systems Division,
Sunnyvale, Calif.

Matlin, G. L.
Aeronutronic Systems, Inc.,
Newport Beach, Calif.

McCormick, C. W. B.
Space Technology Laboratories, Inc.,
Los Angeles, Calif.

McCue, G. A.
North American Aviation, Inc.,
Downey, Calif.

Mercer, R. J.
Space Technology Laboratories, Inc.,
Los Angeles, Calif.

Michielsen, H. F.
Lockheed Aircraft Corp.,
Missiles Systems Division,
Palo Alto, Calif.

Mickelwait, A.
Space Technology Laboratories, Inc.,
Los Angeles, Calif.

Moe, O. K.
Space Technology Laboratories, Inc.,
Los Angeles, Calif.

Moore, C. H.
Smithsonian Astrophysical Observatory,
Cambridge, Mass.

Morrison, D. D.
Space Technology Laboratories, Inc.,
Los Angeles, Calif.

Mowlem, A. R.
International Business Machines,
Federal Systems Division,
Washington, D. C.

Muhleman, D.
Jet Propulsion Laboratory,
Pasadena, Calif.

Musen, P.
Goddard Space Flight Center,
Silver Spring, Md.

Naumann, R. J.
Army Ballistic Missile Agency,
Research Projects Laboratory,
Huntsville, Ala.

Noton, M.
Jet Propulsion Laboratory,
Pasadena, Calif.

Oslund, K.
Jet Propulsion Laboratory,
Pasadena, Calif.

Parkinson, R. W.
Aeronutronic Systems, Inc.,
Newport Beach, Calif.

Peabody, P. R.
Jet Propulsion Laboratory,
Pasadena, C .

Petty, C. M.
Lockheed Aircraft Corp.,
Missile Systems Division,
Sunnyvale, Calif.

Pierce, D. A.
North American Aviation, Inc.,
Downey, Calif.

Pines, S.
Republic Aviation Corp.,
Long Island, N. Y.

Pitton, A. R.
Space Technology Laboratories, Inc.,
Los Angeles, Calif.

Premo, D.
Goddard Space Flight Center,
Anacostia Naval Station,
Washington, D. C.

Richards, P. B.
General Electric Co.,
Missiles and Space Vehicle Dept.,
Philadelphia, Pa.

Ricupito, J. R.
Aeronutronic Systems, Inc.,
Newport Beach, Calif.

Roddy, R.
Army Ballistic Missile Agency,
Huntsville, Ala.

Rossoni, J. P.
International Business Machines Corp.,
Cambridge, Mass.

Routh, D. W.
Space Technology Laboratories, Inc.,
Los Angeles, Calif.

Scott, J.
Jet Propulsion Laboratory,
Pasadena, Calif.

Shucker, S.
Radio Corporation of America,
Moorestown, N. J.

Siry, J. W.
National Aeronautics and Space Administration,
Washington, D. C.

Smith, O. K.
Space Technology Laboratories, Inc.,
Los Angeles, Calif.

Speer, F.
Army Ballistic Missile Agency,
Aeroballistics Laboratory,
Huntsville, Ala.

Sperling, H. J.
Army Ballistic Missile Agency,
Aeroballistics Laboratory,
Huntsville, Ala.

Swerling, P.
The RAND Corp.,
Santa Monica, Calif.

Szebehely, V. C.
General Electric Corp.,
Missiles and Ordnance Systems Dept.,
Philadelphia, Pa.

Tillinghast, C. W.
Smithsonian Astrophysical Observatory,
Cambridge, Mass.

Titus, J.
Space Technology Laboratories, Inc.,
Los Angeles, Calif.

Tross, C.
Aeronutronic Systems, Inc.,
Newport Beach, Calif.

Van Sant, C. T.
Aeronutronic Systems, Inc.,
Newport Beach, Calif.

Wahl, E. W.
Cambridge Research Center,
Space Track Operations Branch,
Hanscom Field, Bedford, Mass.

Walters, L. G.
Aeronutronic Systems, Inc.,
Newport Beach, Calif.

Westlake, P.
Jet Propulsion Laboratory,
Pasadena, Calif.

Westrom, G.
Aeronutronic Systems, Inc.,
Newport Beach, Calif.

Whitney, C. A.
Smithsonian Astrophysical Observatory,
Cambridge, Mass.

Williams, W.
Bendix Systems Division,
Ann Arbor, Mich.

Wong, L.
Space Technology Laboratories, Inc.,
Los Angeles, Calif.

Yagi, F.
Jet Propulsion Laboratory,
Pasadena, Calif.

ADDENDUM B

Ephemeris Tapes

Nearing completion is a joint STL-JPL planetary coordinate project. Its aims are (1) to produce, mostly from U.S. Naval Observatory ephemerides, geocentric and heliocentric planetary coordinates and appropriate differences on IBM 704–709 magnetic tapes for easy, rapid interpolation, and (2) to write the various subroutines to read, interpolate, copy, print, and punch from the tapes.

All coordinates are rectangular coordinates referred to the mean equator and equinox of 1950.0, and are in au except for the geocentric lunar coordinates in Earth-radii. Virtually all bodies are tabulated on each tape. Specifically, the Sun, Moon, and planets (except Mercury) are on the geocentric tape at daily intervals for the period 1960–1980. On the heliocentric tape, the Earth and Earth–Moon barycenter and the planets are tabulated as before at 4-day intervals for the period 1960–2000.

The master tapes will be most economically used as a basic source from which all or selected portions may be (1) copied onto other working tapes, (2) printed on- or off-line, or (3) punched on-line. Programs for both the 704 and 709 are or will be available to accomplish these functions.

The principal subroutines are those which read and interpolate in the tapes. The subroutines will be available in the SCAT, SAP, and FORTRAN languages. The interpolation subroutine uses Everett's formula, and the derivatives thereof, to form interpolated positions and velocities from the tabulated positions and differences.

For further information concerning the tapes and subroutines write to R. J. Mercer, Space Technology Laboratories, Inc., Los Angeles, Calif., or R. H. Hudson, Jet Propulsion Laboratory, Pasadena, Calif.

ADDENDUM C

Seminar Papers Not Published in Proceedings

The following papers presented at the seminar are not available for publication in these Proceedings: "STL Orbit Determination and Prediction Programs," J. Titus, Space Technology Laboratories; "Evaluation of STL Programs on the Basis of *Explorer VI* Experience," L. Wong, Space Technology Laboratories; "Experimental Results Using Orbit Determination Program," M. Boughton, Space Technology Laboratories; "Orbit Determination at NASA Space Computing Center," J. W. Siry, National Aeronautics and Space Administration; "Hansen's Method of Perturbations and Its Limitations," P. Musen, Goddard Space Flight Center; "The Present *Discoverer* Orbit Code," J. V. Breakwell, F. Druding, and R. M. Gray, Lockheed Missile Systems Division.